THE UNIVERSITY *of* EDINBURGH

Ion channels and electrical excitability in native murine anterior pituitary corticotrophs

ZHI LIANG, B.sc, M.sc

THESIS PRESENTED FOR THE DEGREE OF DOCTOR OF PHILOSOPHY

THE UNIVERSITY OF EDINBURGH

March 2012

Declaration

I hereby declare that this thesis was composed by me and the work contained therein is my own, except where explicitly stated otherwise, at the Centre for Integrative Physiology, University of Edinburgh. No part of this thesis has been submitted for any other degree or qualification.

Zhi Liang

March 2012

Acknowledgements

Firstly, I would like to thank my supervisors, Professor Michael Shipston. My thesis would not complete without all your guidance, support and patience. I am deeply grateful for your invaluable help. Special thanks to Dr Iain Rowe for leading me into the electrophysiological world. Educating me, encouraging me and always helping me fix every little problem through all my recordings. Specially, the lowing voice talking joke make me laugh until now. Many thanks for Heather McClafferty, Lijun Tian and all the Shipston lab members for their help and support during my study.

Specially, I would like to thank Dr. Lie Chen, for all these years accompanying in experiments and life. I am very grateful for your teaching and helping. I will remember all the moments we spent together.

I also thank my mum and my grandparents for their love and understanding, and also my best friend Liting for her encourage and support.

And, Jingwei always for being there for me, I couldn't have this done without you.

Abstract

As a central component of the hypothalamic-pituitary-adrenal (HPA) axis, the anterior pituitary corticotrophs play an important role in the regulation of HPA axis function and the neuroendocrine response to stress. Pituitary corticotrophs integrate stress-induced stimulatory signals (CRH and AVP) from the brain together with the negative feedback control from circulating glucocorticoid hormones to coordinate adrenocorticotrophin hormone (ACTH) secretion. Previous studies have classified pituitary corticotrophs as both endocrine and electrically excitable cells with a number of ion channels and signaling pathways implicated in the control of their electrical properties and ACTH secretion. However, the mechanisms involved in native corticotrophs are poorly understood partly due to the current limitations of identifying physiological intact corticotrophs.

To address the electrophysiological properties of native murine corticotrophs, a lentiviral transduction system was developed, using a minimal pro-opiomelanocortin (POMC) promoter to drive the expression of enhanced yellow fluorescent protein (eYFP), to allow highly efficient and specific labeling and identification of corticotrophs *in vitro*. This approach, with patch clamp electrophysiological investigations, revealed metabolically intact native murine corticotrophs displayed spontaneous action potentials with highly heterogeneous firing patterns including single spikes and variable "pseudo plateau bursting" action potentials. The resting membrane potential of native murine corticotrophs was maintained by a TTX-resistant background sodium conductance. Physiological concentrations of

CRH/AVP rapidly depolarized native murine corticotrophs resulting in a sustained increase in the frequency of action potentials. Native murine corticotrophs express multiple outward potassium conductances with two major components mediated by intermediate-conductance calcium-activated (SK4) potassium channels and A-type potassium channels. Inhibition of SK4 channels with TRAM-34 lead to an increase in corticotroph excitability with firing pattern transition from single spikes to "pseudo plateau bursting". When A-type potassium channels were blocked, the afterhyperpolarization amplitude of single spikes was decreased in some corticotrophs. In native murine corticotrophs, outward potassium current carried by large conductance calcium- and voltage- activated potassium (BK) channels was very low, which is in contrast with that in the mouse pituitary adenoma cell line (AtT20 cell line).

Corticotroph cells from wild type (WT) mice and mice with a genetic deletion of the BK channel (BK-/-) were compared. The only potassium current that showed significant difference between WT and BK-/- corticotrophs was carried via the barium-sensitive inwardly rectifying (K_{ir}) potassium channel. However, the blockage of K_{ir} channels displayed no clear effect on corticotroph cell electrical excitability. Similar heterogeneous spontaneous firing patterns were found in WT and BK-/- corticotrophs.

Taken together, the lentiviral-mediated expression of eYFP, driven by a minimal POMC promoter, provides an efficient method to identify physiological intact native

murine anterior pituitary corticotrophs. These findings demonstrate that native murine anterior pituitary corticotrophs are spontaneous excitable cells that display significant heterogeneity of firing patterns. Results also reveal an important role of a background TTX-insensitive sodium conductance in controlling spontaneous and CRH/AVP evoked action potentials. Furthermore, an unexpected role for SK4 calcium-activated potassium channels in corticotroph excitability was revealed. In all, these studies give new insight into the physiology of corticotroph excitability and ACTH secretion, and provide the basis for understanding the roles of these ion channels in HPA axis function.

List of figures:

Chapter One: Anterior pituitary corticotrophs and the hypothalamic-pituitary-adrenal (HPA) axis

Chapter Two: Materials and Methods

Chapter Three: Potassium channels in native murine pituitary corticotrophs

Chapter Four: The role of potassium channels in spontaneous action potentials of native murine pituitary corticotrophs

Chapter Five: Regulation of spontaneous and CRH/AVP-evoked excitability by a background sodium conductance

Chapter Six: Summary and Conclusion

List of tables:

Chapter Two: Materials and Methods

Abbreviations

4-AP	4-Aminopyridine
ACTH	adrenocorticotropic hormone
AHP	afterhyperpolarization
AL	anterior lobe
AVP	vasopressin
$BaCl_2$	barium chloride
BK channel	large-conductance voltage- and calcium-activated potassium channel
BK-/- mice	mice with the deletion of the pore exon of α–subunit of BK channel
BSA	albumin solution from bovine serum
$[Ca^{2+}]_i$	cytosolic free Ca^{2+} concentration
cAMP	cyclic adenosine 3', 5'-cyclic monophosphate
$CaPO_4$	calcium phosphate
Ca_v channel	voltage-gated calcium channel
CMV	cytomegalovirus
CRH	corticotropin-releasing hormone
DAG	diacylglycerol
ddH_2O	double distilled water
DMEM	Dulbecco's Modified Eagles Medium
DMSO	dimethyl sulfoxide
DNAse I	Deoxyribonuclease I

ER	endoplasmic reticulum
eYFP	enhanced yellow fluorescent protein
FBS	foetal bovine serum
FIV	feline immunodeficiency virus
GFP	green fluorescent protein
GH	growth hormone
GΩ	gigaohm
GPCRs	G protein-coupled receptors
HBSS	Hank's Buffered Salt Solution
HEK	Human Embryonic Kidney
HEPES	4-(2-hydroxyethyl)-1-piperazineethanesulfonic acid
HIV	human immunodeficiency virus
HPA	hypothalamic-pituitary-adrenal
IP3	inositol-1,4,5-trisphosphate
ITS	insulin-transferrin-sodium
K_{ca} channel	calcium-activated potassium channel
K_{ir} channel	inwardly rectifying potassium channel
K_v channel	voltage-gated potassium channel
LB	lysogeny broth
LHPA	limbic-hypothalamic-pituitary-adrenal
MA	matrix
mp	medial parvocellular
MW	molecular weight
NA	Norepinephrine analogue

Na_b channel	background sodium channel
Na_v channel	voltage-gated sodium channel
NLS	nuclear localization sequence
$NMDG^+$	N-Methyl-D-glucamine
OT	oxytocin
PBS	phosphate buffered saline
PCR	polymerase chain reaction
PGK	phosphoglycerate kinase
PIP_2	phosphatidylinositol 4, 5 bisphosphate
PKA	protein kinase A
PKC	protein kinase C
POMC	proopiomelanocortin
PR	protease
PRL	prolactin
PVN	parvocellular nucleus
RMP	resting membrane potential
rPOMC	rat POMC
RRE	reverse response element
RT	room temperature
RTC	reverse transcription complex
SIV	simian immunodeficiency virus
SK4 channel	intermediate-conductance voltage- and calcium-activated potassium channel
SK channel	small-conductance voltage- and calcium-activated

	potassium channel
TEA	tetraethylammonium chloride
Tm	melting temperature
TM	transmembrane
TRAM-34	1-[(2-Chlorophenyl) diphenylmethyl]-1H-pyrazole
TRH	thyroid-releasing hormone
TrpC	canonical transient receptor potential
TTX	tetrodotoxin
TU	transduced unit
UV	ultraviolet
VGCI	voltage-gated calcium influx
VSV	vesicular stomatitis virus
VSV-G	vesicular stomatitis virus glycoprotein
WT	wild type

Contents

Chapter Two: Materials and Methods

Chapter Four: The role of potassium channels in spontaneous action potentials of native murine pituitary corticotrophs

Chapter Five: Regulation of spontaneous and CRH/AVP-evoked excitability by a background sodium conductance

Chapter Six: Summary and Conclusion

Chapter One:

Anterior pituitary corticotrophs and the hypothalamic-pituitary-adrenal (HPA) axis

1.1 Stress and its importance

Stress is a nebulous concept referring to the consequences of an inadequate response to psychological or physical demands from the actual environment or imagination, which disrupts the homeostasis of organisms (Selye, 1956; Sullivan, 1995). The demand elements that lead to stress are termed as stressors, which can be psychological from cognition or emotion like bad judgement, contempt, worry, isolation and agitation, or physical changes such as injury or diseases causing pain and infections (Sullivan, 1995). Stress is proposed as a major factor underlying many psychiatric diseases including a wide range of severe dysfunctions like depression, schizophrenia and other anxiety disorders, which evoke organisms to display abnormal behaviours like drug, alcohol addiction or suicide resulting in physical damage or even death (Sullivan, 1995).

In particular, chronic stress is emphasized as a key element leading to many problems. In a long-term stress environment, children showed significant developmental growth retardation due to the down-regulation of growth hormone (GH) secretion from pituitary gland (Gibbs & Vale, 1982). For adults, sustained stress causes memory and learning deficits due to a constant exposure of the brain to high levels of glucocorticoids, which impair hippocampal function and may lead to the death of brain cells (Lee, Ogle & Sapolsky, 2002). Chronic stress also has the potential in impairing the immune system and increasing the susceptibility to infections, neoplastic diseases or autoimmune diseases like lupus erythematosus (Connor & Leonard, 1998). Furthermore, high levels of stress have adverse effects

on the metabolic and cardiovascular systems leading to a wide variety of human disorders including obesity and hypertension (McEwan, 1983). For example, when female monkeys were exposed to high levels of stress, an accumulation of visceral fat was observed (Park, 2009).

Stress is a global epidemic and is getting more and more severe in today's high-speed modern lifestyle (Jones & Rees, 2002). Stress has been suggested as a major risk factor for many health problems and diseases, and to avoid these, stress must be managed. For humans, some people can simultaneously handle many stressors very well, while some others are not able to. Mild psychological stress management disorder may be resolved slowly by psychological strategies. However, in severe stress management disable or psychiatric related conditions, stress has to be controlled by drugs clinically. As a result, understanding the physiological systems that stress activates and how the human body regulates the stress response can give insights into how stress-induced conditions may be alleviated and thus improve human health.

1.2 The stress axis/HPA axis

From microorganisms to human beings, all organisms have evolved mechanisms to handle dramatic changes triggered by internal and external stressors from their environments (Sullivan, 1995). In mammals, the hypothalamic-pituitary-adrenal (HPA) axis (also known as the limbic-hypothalamic-pituitary-adrenal (LHPA) axis)

carries out the functions in mediating the response to stressors (Kudielka & Kirschbaum, 2005). The HPA axis is the major neuroendocrine system regulating the stress response through feed forward and feedback interactions between the hypothalamus, anterior pituitary gland and adrenal glands (Figure 1.1).

Various stress inputs to the brain are integrated and transferred to the parvocellular nucleus (PVN) of the hypothalamus in the medial parvocellular (mp) division of the brain (Sullivan, 1995; Kudielka & Kirschbaum, 2005). In mpPVN, the neuroendocrine neurons synthesize corticotropin-releasing hormone (CRH) and vasopressin (AVP) and release them from the external terminals of the median eminence into the portal blood (Sullivan, 1995; Jessop, 1999). Both CRH and AVP reach corticotrophs via portal circulation. Once CRH and AVP activate to their receptors on the anterior pituitary corticotroph cell membrane, different G protein-coupled receptors (GPCRs)-triggered signalling pathways are activated, cyclic adenosine monophosphate (cAMP) working by activating protein kinase A (PKA) pathway for CRH and D-myo-inositol-1,4,5-trisphosphate (IP3)/protein kinase-C (PKC) pathway for AVP. Then, adrenocorticotropic hormone (ACTH, also known as corticotropin) and the related peptides, like β-endorphins originating from the common precursor proopiomelanocortin (POMC) are released from the stimulated corticotrophs into the peripheral circulation (Sullivan, 1995; Jessop, 1999). When ACTH reaches the adrenal cortex of the adrenal gland, it activates the adrenal cortex (cells in the middle cortical layer) to biosynthesize and secrete glucocorticoids, corticosterone in rodents and cortisol in primates, which functionally reduce the metabolic demands caused by stressors in the body (Sullivan, 1995; Hatzinger, 2000).

Figure 1.1
The hypothalamic–pituitary–adrenal (HPA) axis

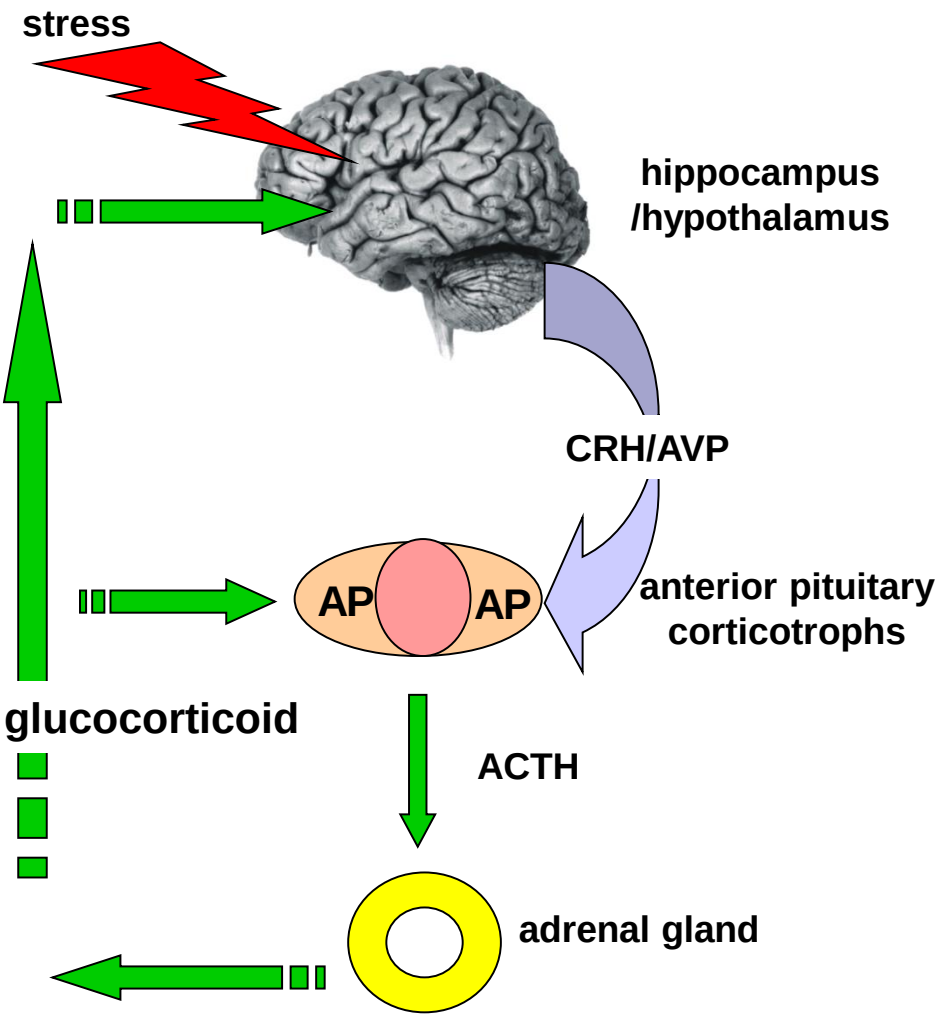

Figure 1.1 The hypothalamic–pituitary–adrenal (HPA) axis. The HPA axis is the major neuroendocrine system regulating the stress response through feed forward and feedback interactions between the hypothalamus, anterior pituitary gland and adrenal glands. Stress stimulates the release of corticotropin-releasing hormone (CRH) and vasopressin (AVP) from the hypothalamus that stimulates ACTH secretion from pituitary corticotrophs. For negative feedback, glucocorticoid released from adrenal gland in response to ACTH inhibits hormone secretion both from pituitary corticotrophs and the hypothalamus.

Theses steroids have extremely wide effects on various systems throughout the body by regulating specific intracellular ligand-activated receptors to control gene expression (Sullivan, 1995; Jessop, 1999; Kudielka & Kirschbaum, 2005).

Because of the highly efficient and broad effects, excess glucocorticoid levels are very harmful to organisms, so the level of glucocorticoids is strictly and optimally maintained (Sullivan, 1995; Jessop, 1999). Glucocorticoids thus regulate their own production in a variety of negative feedback mechanisms via their receptors in the hypothalamus and the anterior pituitary gland to suppress the CRH and ACTH production and release, and also reduced the mRNA cleavage of POMC into ACTH and related peptides (Sullivan, 1995; Jessop, 1999). With ACTH secretion depressed, glucocorticoid biosynthesis reduces and the negative feedback process completes.

1.3 Anterior pituitary corticotrophs-the central 'hub' of the HPA axis

1.3.1 Hypothalamic regulation of corticotrophs: stimulation by CRH and AVP

ACTH secretion from anterior pituitary corticotrophs is evoked and regulated by several secretagogues, while CRH and AVP are the primary hormones *in vivo*. CRH is the most efficient secretagogue to trigger corticotroph ACTH secretion. In addition,

other secretagogues like AVP and oxytocin (OT) are weaker stimuli to induce ACTH secretion but may synergise with CRH (Sullivan, 1995).

In response to stress, CRH, a 41-amino acid peptide hormone is released by mpPVN neurons of the hypothalamus and carries the major function of regulating pituitary corticotrophs electrical activity, ACTH secretion and POMC gene transcription (Jessop, 1999). Based on previous studies, ACTH release is closely associated with elevation of cytosolic Ca^{2+}. In conjunction with patch-clamp technique monitoring exocytosis, via the changes of membrane capacitance during ACTH secretion, with a fluorescent Ca^{2+} ion indicator to measure cytosolic Ca^{2+} concentration at the same time, CRH-induced ACTH secretion has been shown to be a Ca^{2+}-dependent exocytosis process. ACTH secretion can be stimulated both by extracellular Ca^{2+} entry via voltage-gated calcium channels or intracellular Ca^{2+} release from the inositol 1,4,5-trisphosphate (IP3)-sensitive stores (Tse & Lee, 2000). Although both extracellular Ca^{2+} entry and intracellular Ca^{2+} release generated a spatial Ca^{2+} gradient elevating a 3 fold higher local $[Ca^{2+}]_i$ near the exocytic sites than the mean $[Ca^{2+}]_i$, it could not account for the high efficacy of CRH, or adenosine 3', 5'-cyclic monophosphate (cAMP), in triggering ACTH release from rat corticotrophs (Tse & Lee, 2000). Further investigations show cAMP membrane-permanent analogues mimics the membrane depolarization, and increases in action potential frequency and intracellular elevation of $[Ca^{2+}]_i$ induced by CRH (Kuryshev, Childs & Ritchie, 1995b). In the AtT20 corticotroph cell line, a PKA specific inhibitor inserted in membrane reduces CRH-induced ACTH release CRH (Kuryshev, Childs & Ritchie, 1995b). These observations revealed that CRH activated L-type calcium channels

through stimulating the adenylyl cyclase and cAMP-dependent protein kinase A (PKA) pathway, and the phosphorylated PKA opened Ca_v channels allowing Ca^{2+} entry causing membrane depolarization and evoking action potentials in silent corticotrophs or increasing the firing frequency in spontaneously active corticotrophs that directly related with ACTH release (Guerineau *et al.*, 1991; Tse & Lee, 2000; Kuryshev, Childs & Ritchie, 1995b). In other endocrine cells, like lactotrophs, melanotrophs and pancreatic β-cells, intracellular cAMP increased the amplitude of action potentials or the rate of exocytosis stimulated by depolarization (Tse & Lee, 2000). Endocytosis must occur to compensate the cell plasma membrane after exocytosis. In rat corticotrophs, Ca^{2+}-induced exocytosis is followed by a 'slow' endocytosis, which is weakly Ca^{2+}-independent (Lee & Tse, 2001). However, there is a high Ca^{2+} affinity sensor involved in the endocytosis, so intracellular Ca^{2+} may mediate the efficacy of endocytosis directly (Lee & Tse, 2001). The high Ca^{2+} affinity 'slow' endocytosis may contribute to maintaining continuous cycles of exocytosis and endocytosis in the pituitary corticotrophs during sustained ACTH release (Lee & Tse, 2001) (Figure 1.2).

Various ion channels expressed in pituitary corticotrophs are proposed as the direct or indirect targets of CRH in the regulation of corticotroph electrical excitability in electrophysiological studies. In addition to the important role of CRH-activated calcium channels in the cAMP-dependent PKA signalling cascade leading to cell depolarization and hormone release, the inhibition of background potassium channels also appeared to contribute to CRH-mediated excitability. Potassium channels contribute to the membrane repolarization, which would normally show negative

Figure 1.2
The regulation of anterior pituitary corticotrophs by CRH and AVP

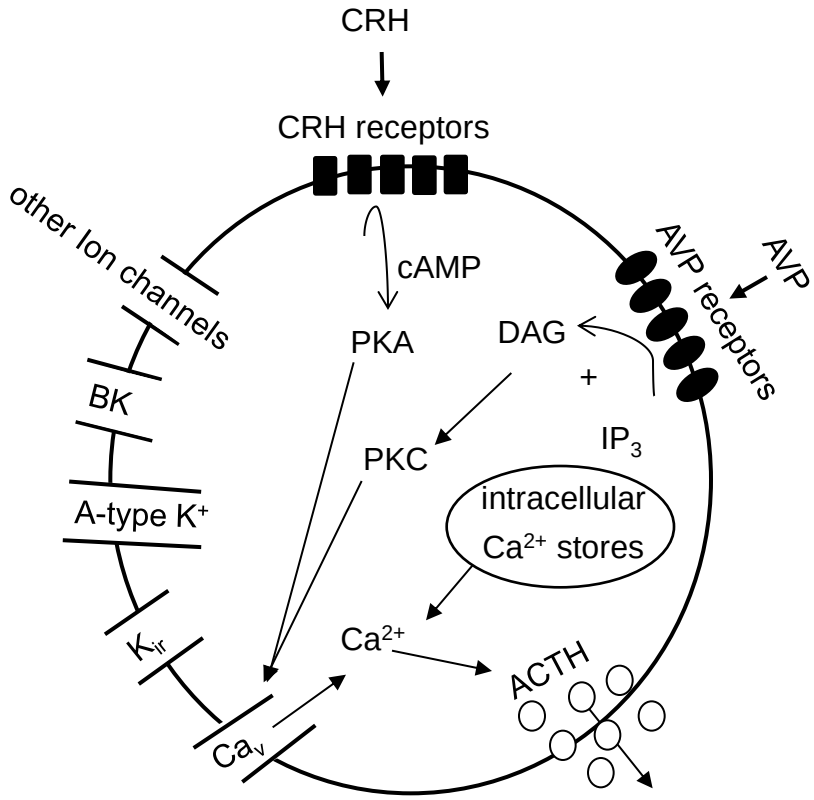

Figure 1.2 The regulation of anterior pituitary corticotrophs by CRH and AVP. CRH mediates the activation of cyclic adenosine monophosphate (cAMP)-protein kinase A (PKA) pathway, and AVP mediates the hydrolysis of phosphatidylinositol bisphosphate to inositol triphosphate (IP_3) and diacylglycerol (DAG) via phospholipase C (PLC). These signalling pathways stimulate ACTH secretion by increasing intracellular calcium (Ca^{2+}) concentrations through activation of voltage-gated Ca^{2+} (Ca_v) channels and inhibition of K^+ channels.

feedback to limit the duration of action potentials and control Ca2+ entry. Inhibiting these K+ channels could lead to a constant membrane depolarisation activating voltage-gated Ca2+ influx (VGCI), followed by a sustained [Ca2+]i elevation (Tse & Tse, 1998). Results from AtT20 pituitary corticotroph cells revealed that CRH significantly inhibited large conductance voltage- and calcium-activated potassium channels (BK channels) upon the activation of PKA signalling pathway promoting cell depolarization and ACTH release (Shipston et al., 1999). In rat corticotrophs, where Kir conductance was responsible for maintenance of the resting membrane potential, CRH-induced Kir inhibition exerted some effects, but not account for all of CRH-evoked membrane depolarization and firing frequency enhancement (Kuryshev et al., 1997) (Figure 1.2).

On the molecular level, CRH plays a role in mediating POMC mRNA level transcription via cyclic cAMP coupled CRH receptors in pituitary corticotrophs (Suda *et al.*, 1988; Sullivan, 1995). POMC is a peptide precursor gene encoding 241 residues. With an orderly series of tissue-specific enzymes cleavage at eight potential sites in the post-translation processing, the precursor POMC may result in ten peptides with various biological functions. POMC gene is mainly expressed in the pituitary gland, specifically in anterior lobe (AL) pituitary corticotrophs and all intermediate lobe pituitary cells. In pituitary corticotrophs, there are four cleavage sites of precursor POMC encoding ACTH, the opioid β-endorphin 1-31 and three copies of the active core of melanocortin (α, β, and γ-MSH) as the five major biological peptides (Sullivan, 1995; Slominski *et al*., 2000). Research on primary

pituitary cells showed both CRH and cAMP increased the rate of POMC gene transcription in anterior pituitary cells (Gagner, 1987).

In addition to CRH, the secretion of ACTH in anterior pituitary corticotrophs is also activated by other secretagogues, such as AVP. AVP is co-localized and co-released with CRH from mpPVN. Although AVP alone is a weak trigger for corticotroph ACTH secretion, its synergistic effect with CRH significantly enhances the release of ACTH from pituitary corticotrophs (Sullivan, 1995; Jessop, 1999). In human pituitary adenoma cells, AVP is proposed to extend the duration and the amplitude of action potentials by activating L-type voltage-gated calcium channels (Tse & Lee, 1998). In male rat corticotrophs, AVP evokes a biphasic ACTH release (Tse & Lee, 1998). The initial transient phase of AVP-induced ACTH release is related with the elevation of $[Ca^{2+}]_i$ from IP3-sensitve stores via a GTP binding protein-coupled phosphoinositide pathway and the calcium signal also stimulates apamin-sensitive, small conductance voltage- and calcium-activated channels (SK channels) leading to membrane hyperpolarization (Tse & Lee, 1998). The plateau phase of AVP-evoked ACTH release involves an extracellular Ca^{2+} influx via L-type voltage-gated calcium channels activated by the PKC pathway (Tse & Lee, 1998). In corticotrophs, AVP stimulates the translocation of PKC and its activity at the plasma membrane leading to repetitive cell excitability and ACTH release through elevating $[Ca^{2+}]_i$ (Tian, Philp & Shipston, 1999; Ozawa & Sand, 1986).

Although CRH and AVP are the two main secretagogues stimulating ACTH secretion from anterior pituitary corticotrophs, oxytocin and catecholamines are also able to trigger ACTH release (Sullivan, 1995). In rat corticotrophs, norepinephrine analogue (NA) leads to $[Ca^{2+}]_i$ oscillations depending on the adrenergic receptors and a G-coupled phosphoinositide pathway, which periodically activates apamin-sensitive SK channels (Tse & Tse, 1998). Through releasing intracellular Ca^{2+} from IP3-sensitive stores, NA triggers the weak exocytosis of a small pool of ready releasable granules released from rat pituitary corticotrophs (Tse & Tse, 1998).

1.3.2 Glucocorticoid negative feedback regulation

An important physiological function of adrenal glucocorticoids is the rapid suppression of CRH-induced ACTH secretion from anterior pituitary corticotrophs through negative feedback to maintain glucocorticoids in an optimal concentration to avoid harm from over-production. The early action (10 minutes to 3 hour) of glucocorticoids to inhibit anterior pituitary corticotroph ACTH release depends on the activation of intracellular type II glucocorticoid receptors, the synthesis of new mRNA and protein including the calcium-binding protein calmodulin (Gagner & Drouin, 1987; Shipston, 1995).

In animals including humans, glucocorticoids, the downstream products of the HPA axis, are characteristically released in rapid approximately hourly hormone bursts by the adrenal gland called ultradian rhythm (Lightman *et al.*, 2008; Sarabdjitsingh *et al.*, 2010). These ultradian glucocorticoids oscillations increase in advancing

amplitude of the active phase, leading to a circadian secretion pattern (Walker, Terry and Lightman, 2010; Sarabdjitsingh *et al.*, 2010). Not only the classic circadian rhythm, but also the ultradian pulses of discrete pulsatile glucocorticoids secretion characterize the activity of the HPA axis in response to stress (Walker, Terry and Lightman, 2010). Oscillatory changes of glucocorticoid levels are essential for the maintenance of proper homeostasis and the reactivity to a stressor. The pulse amplitude, frequency, and phase of glucocorticoid ultradian oscillations are all associate variables in regulating the acute adaptation of the HPA axis.

The pulse characteristics of glucocorticoid ultradian rhythmicity can signally be mediated by various physiological conditions. Pathological dysfunctions of the HPA axis produce altered ultradian patterns, and the disorganization of glucocorticoid pulsatility is suggested relevant with a number of stress-related psychiatric and metabolic diseases (Walker, Terry and Lightman, 2010). On molecular level, the transcriptional regulation of glucocorticoid responsive genes biologically meaningfully responds to these rapid fluctuations as a "gene pulsing" (Walker, Terry and Lightman, 2010; Sarabdjitsingh *et al.*, 2010; Scheff *et al.*, 2012).

The interaction of glucocorticoids release oscillation with physiological responses to stress is a major area that has not been totally investigated. Nowadays, a post hoc analysis in female rat in different phases of the glucocorticoid endogenous ultradian cycle has indicated during the ascending phase the acute stress evoked much greater HPA responsiveness. While when the stress was coincided in a falling phase, there

was a significantly smaller response, no greater than a basal pulse recorded. It suggested these alternate secretion and inhibition phases of generating basal HPA axis activity are a critical determinant in acute stress responses (Windle *et al.*, 1998; Sarabdjitsingh *et al.*, 2010).

Glucocorticoid early negative feedback of CRH-stimulated ACTH secretion in AtT20 cells was dependent on newly synthesised proteins that prevented the PKA and PKC-mediated inhibition of BK channels (Shipston, Kelly & Antoni, 1996; Shipston *et al.*, 1999; Tian, Philp & Shipston, 1999). Recent studies also support a role for BK channels that in native mouse pituitary corticotrophs with genetic deletion of BK channel, the CRH and AVP-induce ACTH secretion is enhanced (Brunton *et al.*, 2007). In contrast, investigations from native rat anterior pituitary cells suggest glucocorticoids-induced inhibition of ACTH release was dependent upon regulation of the synthesis of new mRNA and protein, but not BK or SK channels (Lim, Shipston & Antoni, 1998). Kv1.5 voltage-gated potassium channel subunits have been implicated in early glucocorticoid action in somatotrophs, but not in AtT20 corticotrophs (Shipston, Kelly & Antoni, 1996).

1.3.3 Previous studies on anterior pituitary corticotrophs

In the HPA axis, anterior pituitary corticotrophs operate as a central 'hub' in the control of HPA axis functions by integrating upstream signals from the hypothalamus and responding to the negative feedback from the adrenal gland that provide an optimal range of ACTH concentration in the circulation. Anterior

pituitary corticotrophs are characterised as both electrically excitable and endocrine cells, the same as other cell populations in the anterior pituitary (Stojilkovic, Tabak & Bertram, 2010). Previous research has established the mechanism of ACTH secretion regulation stimulated by CRH and AVP as well as ACTH output cessation by glucocorticoids mainly based on a variety of tumour cell models including mouse anterior pituitary corticotroph tumour cell line AtT20 cells and human pituitary corticotroph tumour cells (Pennington, Kelly & Antoni, 1994; Shipston, Kelly & Antoni, 1996; Takano *et al.*, 1996; Surprenant, 1982; Mollard *et al.*, 1987).

However, we poorly understand which ion channels control membrane excitability, as well as how calcium ion channel coupled to Ca^{2+}-dependent ACTH release from native anterior pituitary corticotrophs (Kuryshev *et al.*, 1997). A big challenge is the limitation of distinguishing live native corticotrophs from other sub-populations of anterior pituitary cells. There are five classes of pituitary cells located in the anterior pituitary: somatotrophs (growth-hormone (GH)-releasing cells, ~50% of the total anterior pituitary cells), lactotrophs (Prolactin (PRL)-releasing cells, ~15%), corticotrophs (ACTH-releasing cells, ~15%), thyrotrophs (thyroid-releasing hormone (TRH)-releasing cells, ~10%) and gonadotrophs (luteinizing hormone/follicle stimulating hormone-releasing cells, ~10%) (Childs *et al.*, 1988). Several approaches have been developed to identify corticotrophs including: 1) labelling corticotrophs by biotinylated CRH peptide (Childs, Marchetti & Brown, 1987), 2) labelling corticotrophs by ACTH secretion in haemolytic plaque assay (Lee & Tse, 1997), 3) *post hoc* ACTH immunohistochemistry staining or responsiveness to CRH or AVP of fixed recorded corticotrophs (Brunton *et al.*, 2007), 4) enriching corticotrophs

following cell volume enlargement by high doses of CRH stimulus followed by centrifugation (Kuryshev *et al.*, 1997). In most publications, the main approach is pre-treating rat anterior pituitary cells with high concentrations of 10-100 nM CRH with 20-100 nM AVP, and the CRH-responsive corticotrophs are enlarged and distinguished from other sub-populations of small unstimulated pituitary cells by counterflow centrifugation (Guerineau *et al.*, 1991). However, the CRH concentration used to pre-treat corticotrophs are supramaximal that is several orders of magnitude (typically 10-100 nM CRH) higher than the physiological levels in the portal circulation (Sheward & Fink, 1991). It has been reported that CRH stimulates corticotrophs leading to membrane depolarization and evokes firing of action potentials, so these pre-stimulated corticotrophs are unlikely to reflect the normal basal physiological properties, which may affect further investigations. A recent investigation of corticotrophs was based on an animal model of transgenic mice with constitutive expression of green fluorescent protein (GFP) driven by the POMC promoter in the corticotrophs, but no analysis of spontaneous electrical excitation was given (Lee *et al.*, 2011). The systematic analysis of spontaneous electrical excitability of native anterior pituitary corticotrophs in the absence of secretagogues is thus still limited by the lack of a routine technique to isolate corticotrophs. In this thesis I exploit a new approach to specifically label native mouse anterior pituitary corticotrophs to allow routine electrophysiological analysis.

1.4 Ion channels and control of corticotroph excitability

1.4.1 Ion channels implicated in corticotroph excitability

Studies on mouse AtT20 pituitary corticotrophs and native rat pituitary corticotrophs reveal different hypothalamic hormones trigger the elevation of $[Ca^{2+}]_i$ through Ca^{2+} entry by voltage-dependent calcium channels and/or release from IP3 intracellular stores, which leads to cell depolarization and ACTH secretion in pituitary corticotrophs (Tse & Lee, 2000). The cytosolic Ca^{2+} signals mediate diverse cellular functions of pituitary corticotrophs associated with various ion channels and signalling pathways. The most efficacious ACTH secretagogues, CRH mediates the inhibition of background K^+ channels via PKA/PKC signalling pathway, which also contribute to a constant membrane depolarisation which activated voltage-gated Ca^{2+} entry, followed by a sustained $[Ca^{2+}]_i$ elevation (Tse & Tse, 1998).

As electrically excitable cells, both the electrically activity and ACTH release of anterior pituitary corticotrophs triggered by CRH and AVP are thought to be regulated by controlling multiple different ion channels. The original corticotroph electrical model was a Hodgkin-Huxley-type model (1952) initially built upon four ionic currents: 1) a high-threshold voltage-gated L-type calcium current allowing Ca^{2+} influx during cell depolarization, 2) a low-threshold voltage-gated T-type calcium current which is rapidly inactivated, 3) a voltage-gated potassium current, mainly controlling repolarization, 4) a Ca^{2+}-gated potassium current, together with leak current represent for the rest of the non-specific ionic currents (Shorten *et al.*, 2000). Later on, 1) P-type calcium current modulating the firing frequency

(Kuryshev, Childs & Ritchie, 1995a), 2) TTX-sensitive sodium current (Kuryshev, Childs & Ritchie, 1996), 3) a non-selective cation current (Shorten *et al.*, 2000) and inward-rectified potassium channels (K_{ir} channels) responsible for maintaining the resting membrane potential (Kuryshev *et al.*, 1997) were suggested to be included into the original corticotroph model. The modified Hodgkin-Huxley-type model suggests a dual modulation of CRH on voltage-gated calcium channels and K_{ir} channels. In this model, CRH increased L-type calcium current is believe to sufficiently generate repetitive action potential, as well as CRH inhibited K_{ir} current increases the firing frequency and $[Ca^{2+}]_i$ transients (LeBeau *et al.*,1997).

1.4.1.1 Voltage-gated Na^+ channels (Na_v channels):

Voltage-gated Na^+ channels consist of a large α-subunit associated with β-subunits and other regulatory proteins. The expression of α-subunit alone is sufficient to produce a functional Na_v channels, and different β-subunits alter physiological properties of Na_v channels including the modulation of channel gating (Isom, 2001). There are nine genes coding the α-subunit of Na_v channels in mammals, named $Na_v1.1$-$Na_v1.9$ (Catterall, Goldin & Waxman, 2005). α-subunit consists of four homologous domains, termed I-IV, forming the ion pore, which selectively conducts Na^+ ion. Each homologous domain contains six transmembrane (TM) regions, labelled S1-S6 (Figure 1.3A). The voltage-gated sensor of Na_v channels is located in the highly conserved S4 region (Catterall, Goldin & Waxman, 2005). After stimulation by a transmembrane voltage change, the positive amino acids regions move toward the extracellular membrane side and open the ion permeable pore (Yu

& Catterall, 2003). The pore contains a selectivity filter made of negatively charged amino acid residues, which attracts the positive charged Na^+ ion and keeps out the negative charged ions such as Cl^- ion. The pore consists of two regions. The extracellular portion contains the "P-loops" between S5 and S6 including the tetrodotoxin (TTX) binding site, which is 0.3-0.5 nm wide and is the narrowest part of the pore (Yu & Catterall, 2003). This constricted structure is just large enough to allow a single Na^+ ion or with a water molecule associated to pass through (Yu & Catterall, 2003). The larger K^+ ion cannot fit through this area, and other differently sized ions also cannot interact with the negatively charged glutamic acid residues lining in the pore (Yu & Catterall, 2003). The cytoplasmic portion is formed by the combined S5 and S6 regions of the four repeated domains including the phosphorylation sites by protein kinase (Catterall, 2000b). The region linking domains III and IV shows an important function in rapid inactivating of Na_v channels (Yu & Catterall, 2003). There are also TTX-insensitive Na_v channel with α-subunit $Na_v1.5$, $Na_v1.8$ and $Na_v1.9$ (Yang *et al.*, 2008). The expression of TTX-sensitive and -resistant Na_v channels have been widely studied in major endocrine pituitary cells. Electrophysiological investigation reveals both TTX-sensitive and -insensitive Na^+ current components are found in melanotrophs, and TTX-sensitive Na_v channels also found in gonadotrophs from different species and biotinylated labelled rat corticotrophs, but not in cultured human pituitary adenoma cells (Stojilkovic, Tabak & Bertram, 2010; Guerineau *et al.*, 1991; Marchetti, Childs & Brown, 1987). Na_v channels are also found expressed in lactotrophs, somatotrophs and GH_3 cells. Thus, Na_v channels are proposed to be native to all endocrine pituitary cells (Stojilkovic, Tabak & Bertram, 2010).

Figure 1.3
Structures of ion channels pore-forming subunits

A

Na_V channels / Ca_V channels

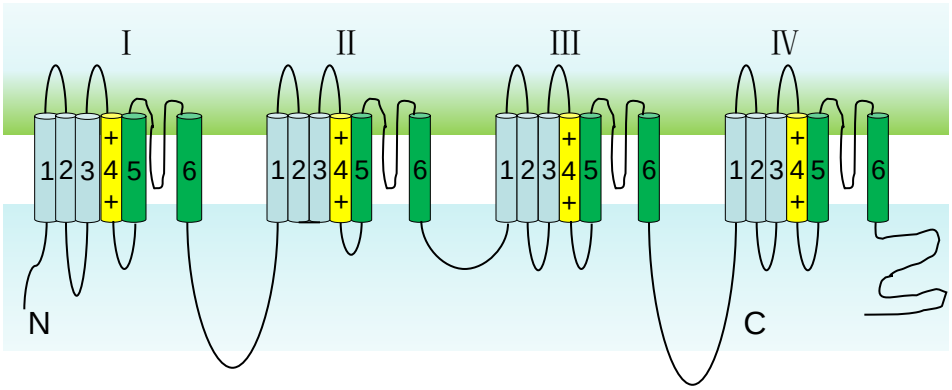

B

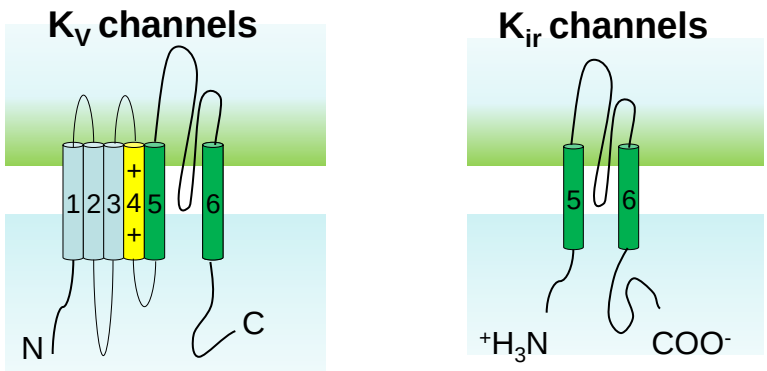

Figure 1.3 Structures of ion channels pore-forming subunits. α-helices are represented as cylinders and the extracellular and intracellular chains of amino acids as continuous lines. **A**, model of voltage-gated Na^+ (Na_v) channels and voltage-gated Ca^{2+} (Ca_v) channels. **B**, model of voltage-gated K^+ (K_v) channels and inwardly rectifying K^+ (K_{ir}) channels. The positive charged S4 domain represents the voltage sensor, and the loop between S5 and S6 domains line the channel pore. K_v and K_{ir} subunit assemble as tetramers.

Na_v channels both open and close more quickly than most K^+ channels, and thus contribute to the influx of positive charge (Na^+) during the upstroke of action potentials in many cell types either alone or together with Ca_v channels in some cells (Catterall, 2003). In electrically excitable cells like nerve, muscle and neuroendocrine cells, the major role of Na_v channels is generating the depolarization upstroke of the action potentials and maintains the spike amplitude (Sankaranarayanan & Simasko, 1996; Kwiecien *et al.*, 1998). In the majority of pituitary cells, the inhibition of Na_v channels shows no significant effect on generation of spontaneous action potentials. TTX did not abolish spontaneous or CRH-induced firing or influence the firing frequency in rat pituitary corticotrophs, only with an inhibition of the rapid initial component of the action potentials in most pituitary cells (Kuryshev, Childs & Ritchie, 1996). However, in some pituitary lactotrophs cells with high level of Na_v channel expression, TTX abolished their basal hormone secretion (Van Goor, Zivadinovic & Stojilkovic, 2001). Different functions of TTX-sensitive Na_v channels in the electrical excitability of pituitary cells are associated with their status at the resting membrane potential. The inability of TTX-sensitive Na_v channels to control electrical excitability and hormone secretion in most pituitary cells is most likely due to more than 90% of TTX-sensitive Na_v channels being inactivated at the resting membrane potential *in vitro* (Stojilkovic, Tabak & Bertram, 2010). In gonadotrophs, GnRH removed the steady inactivation status of TTX-sensitive Na_v channels and then induced transient membrane depolarization contributing to action potentials (Tse & Hille, 1993; Heyward, Chen & Clarke, 1995; Van Goor, Zivadinovic & Stojilkovic, 2001; Van

Goor, Li & Stojilkovic, 2001). Overall, TTX-sensitive Na_v induced-action potentials are not essential for hormone secretion from anterior pituitary cells.

1.4.1.2 Voltage-gated Ca^{2+} channels (Ca_v channels):

There are two major electrophysiological groups of Ca_v channels found in excitable cells, one is high-voltage-activated Ca_v channels only activated by a strong membrane depolarization, including L-, N-, P/Q-, and R-type Ca^{2+} channels with different biophysical and pharmacology properties. The other group is low-voltage-activated Ca_v channels that require less depolarization for activation but need a strong membrane hyperpolarization to drag them out of their inactivation status. They are thus named as transient or T-type Ca_v channels (Marchetti, Childs & Brown, 1987; Catterall, 2000a).

Ca_v channels consist of five subunits: a large α_1-subunit and four smaller ancillary subunits: α_2, β_{1-4}, γ and δ with several functions including channel gating modulation (Catterall, 2000a). Four homologous domains construct an α_1-subunit forming the ion conducting pore permeable to Ca^{2+} ions, and each domain contains six transmembrane regions (S1-S6) including a "P-loop" between S5 and S6, the S4 voltage sensor, as well as the gating machinery and regulation sites by intracellular messengers and signalling pathways such as multiple PKA phosphorylation sites (Catterall, 2000a) (Figure 1.3A). Although the pore is also slightly permeable to Na^+ ion, its permeability to Ca^{2+} ion is about 1000-fold greater than to Na^+ ion under normal physiological conditions.

Both T-type and L-type functional Ca_v channels have been recorded in various pituitary cells, including gonadotrophs, somatotrophs, lactotrophs, melanotrophs and corticotrophs from different species (Bosma & Hille, 1992; Van Goor, Zivadinovic & Stojilkovic, 2001, Wen *et al*., 2008). In neuroendocrine cells, influx of Ca^{2+} through T-type Ca_v channels contributes to cell depolarization, but are not sufficient to produce global intracellular Ca^{2+} concentration $[Ca^{2+}]_i$ elevation required for generating action potential. This is because T-type Ca_v channels are rapidly inactivated (McCobb & Beam, 1991). At the same time, L-type Ca_v channels help to maintain cell depolarization for a period of time until $[Ca^{2+}]_i$ is high enough to trigger Ca^{2+}-dependent secretion (Stutzin *et al*., 1989; Kuryshev, Childs & Ritchie, 1995a; Kwiecien *et al*., 1998).

Electrophysiological studies on Ca_v channels in a variety of pituitary corticotrophs explain their functions in more detail. Fluorescent intracellular Ca^{2+} labelling by indo-1 combined with electrophysiological patch-clamp recording suggested Ca^{2+}-dependent action potentials resulted in a significant transient $[Ca^{2+}]_i$ elevation and ACTH secretion in human tumoral corticotrophs, which suggested that ACTH-secretion from anterior pituitary corticotrophs is mainly dependent on extracellular Ca^{2+} influx and Ca^{2+} released from the intracellular store, the same as other secretory cells discussed above (Kuryshev, Childs & Ritchie, 1996; Guerineau *et al*., 1991). Since Ca^{2+} is critical for hormone secretion, Ca^{2+}-dependent action potentials are the targets of secretagogues to trigger hormone secretion from pituitary cells. In rat anterior pituitary corticotrophs, CRH, (Bu)2 cAMP (dBucAMP) and forskolin (the cAMP enhancer) all induce a long lasting cell depolarization triggering firing of

action potentials in silent cells or enhance the firing frequency of spontaneous active cells, which was dependant on the elevation of the frequency and amplitude of the transient $[Ca^{2+}]_i$ via Ca_v channels (Kuryshev, Childs & Ritchie, 1995b). The PKA inhibitor, H-89, did not stop CRH-stimulated depolarization but eliminated the increase of firing frequency and also limited Ca^{2+} entry to some extent (Kuryshev, Childs & Ritchie, 1995b). This inhibitor totally abolished dBucAMP and forskolin-induced $[Ca^{2+}]_i$ elevation and membrane depolarization indicating their activation are primarily mediated by PKA.(Kuryshev, Childs & Ritchie, 1995b).

In anterior pituitary corticotrophs, Ca^{2+} enters mainly through two Ca_v calcium channels, L-type Ca_v channels and T-type Ca_v channels as for other pituitary cells (Marchetti, Childs & Brown, 1987). In cultured human pituitary adenoma cells, AVP increased the amplitude and duration of action potentials, and enhanced the transient afterhyperpolarization of each spike (Mollard *et al.*, 1991). At the same time, the amplitude of L-type calcium current also showed enhancement by AVP, leading to Ca^{2+} influx, which suggests L-type calcium channels are associated with AVP-induced Ca^{2+}-dependent ACTH secretion from corticotrophs, and L-type calcium currents are also related to maintaining the amplitude and duration of action potentials, while AVP shows no effect on T-type calcium current (Mollard *et al.*, 1991). In rat anterior pituitary corticotrophs, Ca^{2+} entry is primarily dependent on CRH-induced action potentials through the activation of L-type calcium channels, with some help of P-type calcium channels in regulation. The L-type calcium channel inhibitor nifedipine not only stopped spontaneous and CRH-induced action potentials, but also abolished transient $[Ca^{2+}]_i$ (Kuryshev, Childs & Ritchie, 1996).

However, it did not abolish CRH-induced membrane depolarization and basal cytosolic Ca^{2+} levels (Kuryshev, Childs & Ritchie, 1996). In different human pituitary adenoma cells, the high threshold calcium current is largely from L-type calcium channels, while in rat anterior pituitary corticotrophs there are two more high threshold calcium channels responsible for the Ca^{2+} current, P-type calcium channels and a third undefined Ca^{2+} subtype (s) (Kuryshev, Childs & Ritchie, 1995a). ω-agatoxin-IVA, a P-type calcium channel blocker, reduced the firing frequency and decreased the CRH-induced $[Ca^{2+}]_i$ elevation. After applying L-type and P-type calcium channels blockers, membrane depolarization was still detected although cytosolic Ca^{2+} was reduced. P-type calcium channels are mainly responsible for the partial $[Ca^{2+}]_i$ elevation independent of action potentials (Kuryshev, Childs & Ritchie, 1996). Gonadotrophs also display similar voltage-gated calcium channels based Ca^{2+} entry mechanism during hormone stimulus (Marchetti, Childs & Brown, 1987).

1.4.1.3 Inwardly rectifying K^+ channels (K_{ir} channels):

Inwardly rectifying potassium (K_{ir}) channels allow K^+ ion influx into cells under strong hyperpolarization more negative that Ek and outward K^+ flow is inhibited by strong depolarization, which is different from the majority of K^+ channels typically responsible for cell repolarization following action potential (Stojilkovic, Tabak & Bertram, 2010). K_{ir} channels are globally expressed in a variety of cells, including leukocytes, neurons, cardiac, kidney and endocrine cells and play an important function in regulating cell activity and establishing cell resting membrane potential (Stojilkovic, Tabak & Bertram, 2010). There are 15 members in the K_{ir} channel

family divided into three groups depending on their regulation by different intracellular messengers, G-proteins and ATP (Stanfield, Nakajima & Nakajima, 2002). There is a long cytoplasmic pore in the structure of K_{ir} channels, which is critical for inward rectification and its gating properties that are regulated by G-proteins and phosphatidylinositol 4, 5 bisphosphate (PIP_2) Stanfield, Nakajima & Nakajima, 2002) (Figure 1.3B). G protein-regulated K_{ir} channels are widely expressed in endocrine pituitary cells, like lactotrophs, somatotrophs and AtT20 pituitary corticotroph cells, while other group of K_{ir} channels also have been detected in rat pituitary cells and GH3/B6 mammosomatotrophs by RT-PCR (Wulfsen *et al*., 2000).

In rat pituitary corticotrophs, the rapidly activated inward potassium current component is insensitive to TEA and 4-AP potassium channels blockers, but can be partially inhibited by Ba^{2+} suggesting the current component may be contributed by K_{ir} channels. K_{ir} current is mainly responsible for maintaining a negative resting membrane potential. When CRH is applied to rat corticotrophs, Kir channels are inhibited leading to membrane depolarization resulting in enhanced membrane excitability and ACTH release (Kuryshev *et al.*, 1997). This is consistent with when K_{ir} channels are selectively blocked by Ba^{2+}, cells were partly depolarized and the firing frequency increased (Kuryshev *et al.*, 1997). However, the PKA inhibitor, H-89 significantly decreased CRH-induced firing frequency in spontaneously active cells but not CRH-induced depolarisation (Kuryshev, Childs & Ritchie, 1995b).

1.4.1.4 Voltage-gated K^+ channels (K_v channels):

According to previous electrophysiological research, there are at least four functional K_v channel families recorded in electrically excitable cells (Stojilkovic, Tabak & Bertram, 2010). The first two subfamilies are the fast activating delayed rectifier K_v channels expressed in neurons and muscle cells with their role in modulating short action potentials, and the slow delayed rectifier K_v channels expressed in cardiac cells which are functional in cell repolarization (Stojilkovic, Tabak & Bertram, 2010). A-type K_v channels are the third classification. A-type K_v channels are fast and transiently activated in the subthreshold range of the resting membrane potential, rapidly inactivate and quickly recover from inactivation (Hille, 2001). A-type K_v channels play a role in firing frequency regulation in cardiac and other electrically active cells. 4-Aminopyridine (4-AP) selectively blocks A-type K_v channels at millimolar concentration and normally is used as the specific blocker for A-type K_v channels, although 4-AP also inhibits delayed rectifier at micromolar concentration (Hille, 2001). The fourth class of K_v channels are EAG channels, including eag, eag-like (elk), and eag-related (erg) with broad expression in cardiac, neuroendocrine, smooth muscle and neuroblastoma cells and are specifically inhibited by E-4031 (Stojilkovic, Tabak & Bertram, 2010). Erg K_v channels are responsible for maintaining the resting membrane potential in several cell types (Schwarz & Bauer, 2004).

α-subunits forming the ion conductance pore of K_v channels are grouped into 12 classes based on different sequence homology of the hydrophobic transmembrane

cores, named as K_v1-12, and β-subunits are auxiliary proteins associated with α-subunits that modulate the electric activity of K_v channels (Pongs *et al.*, 1999) (Figure 1.3B). A-type K_v channels are most likely formed by K_v1.4, 3.3, 3.4 and 4.1-4.3 (Gutman *et al.*, 2005; Maffie & Rudy, 2008). K_v channels exert their function in conjunction with Ca_v channels to modulate action potentials and hormone release. In turn, changes in hormonal and physiological status modulate the expression of K_v channels dynamically and alter the cell excitability of pituitary cells over the time scale of several hours (Pongs, 1992; Yellen, 2002; Armstrong & Hille, 1998).

The expression of delayed rectifier K_v channels is detected in GH cells, native rat lactotrophs and somatotrophs and gonadotrophs from a variety of species (Stojilkovic, Tabak & Bertram, 2010). In GH_3 cells, the inhibition of delayed rectifier K_v channels broadens the duration of APs and elevated the amplitude of spontaneous transient $[Ca^{2+}]_i$ (Sankaranarayanan & Simasko, 1998). In frog melanotrophs, increasing expression of delayed rectifier K_v channels prevents action potentials, while in native rat lactotrophs causes no change on action potentials (Mei *et al.*, 1998). A-type K_v channels are also widely expressed in most pituitary cells. Rat lactotrophs and gonadotrophs show clearly higher expression of A-type K_v channels than somatotrophs, while ovine somatotrophs display a high level of A-type K_v channels expression, which may be functional in action potentials and hormone secretion regulation (Chen *et al.*, 1994). In other anterior pituitary cells, the role of A-type K_v channels in cell excitability is not very clear, for A-type K_v channels show no participation in spike generation in rat lactotrophs, which may because the channels are inactivated at resting membrane potential (Sankaranarayanan &

Simasko, 1998). Investigation of A-type current in the mouse corticotroph tumour cell line AtT20/D16-16 revealed its role in early glucocorticoid feedback (Pennington, Kelly & Antoni, 1994). Selective enhancement of the A current by dexamethasone, shown here to require synthesis of new protein, is one of the mechanisms proposed whereby glucocorticoids exert inhibitory control on ACTH secretion.

1.4.1.5 Calcium-activated K^+ channels (K_{ca} Channels):

Electrophysiological studies have revealed three classes of K_{ca} channels based on the channel conductance: small-conductance K_{ca} channels (SK channels), intermediate-conductance K_{ca} channels (SK4 channels) and high-conductance big K_{ca} channels (BK channels). SK channels and SK4 channels are mainly activated by $[Ca^{2+}]_i$ elevation based on voltage-gated Ca^{2+} influx (VGCI) and release from intracellular stores with little voltage dependence (Latorre *et al*., 1989; Petersen and Maruyama, 1984). Calmodulin constitutively bound to the C terminus of each α-subunit forms the high-affinity Ca^{2+} sensor of SK channels (Latorre *et al*., 1989). SK channels are well documented in the majority of pituitary cells from different species. In gonadotrophs, the main function of SK channels is to generate oscillatory hyperpolarization resulting from periodic Ca^{2+} released from the ER triggered by the activation of GnRH receptors through the PKC signalling pathway, while in corticotrophs SK channels are stimulated by AVP (Tse, Tse & Hille, 1995). In GH3 cells, SK channels are activated by high frequency action potentials, extension of APs by K_v channels blockers or Ca^{2+} release from intracellular stores, and activated

SK channels are responsible for the after-spike hyperpolarization (Tse & Lee, 1998). In native pituitary cells, transient voltage gated-calcium influx (VGCI) cannot stimulate SK channels suggests that SK channels are localised next to intracellular Ca^{2+} release sites and only activated by Ca^{2}-mobilizing receptors, sustained VGCI and Ca^{2+}-dependent Ca^{2+} release (Stojilkovic, Zemkova & Van Goor,2005).

In contrast, BK channels are voltage-activated K^{+} channels and Ca^{2+} ion modulates its open probability (Kaczorowski *et al.,* 1996). The ion pore of BK channels is constructed with four repeated $K_{ca}1.1\alpha$-subunits with six transmembrane domains similar to K_v channels, an additional transmembrane segment S0 at the N terminus and the cation binding sites at the C terminus of α-subunits as Ca^{2+} sensor (Wei *et al.*, 2005). β-subunits are responsible for modulating the gating properties of BK channels (Fakler & Adelman, 2008; Hou, Heinemann & Hoshi, 2009). RNA alternative splicing produces numerous BK channel splice variants with distinct channel properties (Chen, 2005). BK channels are rapidly activated during cell depolarization due to the complexes formed with Ca_v channels, which provides an efficiency way in controlling BK channel activity during Ca^{2+} influx and also facilitates spike repolarization limiting action potential-dependent Ca^{2+} entry through Ca_v channels (Stojilkovic, Tabak & Bertram, 2010). BK channels also decrease the frequency of action potential-driven $[Ca^{2+}]_i$ transients by slowing down depolarization. In some cells, the activation of BK channels stimulates or enhances action potentials generation due to their role in easing Na_v and Ca_v channels from inactivation, and in some pituitary cells, BK channels show a function in producing "pseudo-plateau bursting" of action potentials (Stojilkovic, Tabak & Bertram, 2010).

BK channels also interact with K_{ir} channels in cell repolarization in the downstroke of action potentials. The higher expression of BK channels in somatotrophs and lactotrophs than gonadotrophs shows longer spike duration, bigger spike amplitude and stronger extracellular Ca^{2+}-induced Ca^{2+} transients instead of a limitation of action potential-dependent Ca^{2+} influx (Van Goor, Li & Stojilkovic, 2001). These results reveal BK channels had a paradoxical effect on prolonging membrane depolarization resulting in different firing patterns and facilitating Ca^{2+} entry into different pituitary cells (Van Goor, Li & Stojilkovic, 2001).

In some pituitary cells, BK channels also play a role in modulating the patterns of action potentials. In some somatotrophs, the inhibition of BK channels changes the bursting action potentials to large-amplitude single spikes, which reveals BK channels are critical in generating bursting (Stojilkovic, Tabak & Bertram, 2010). This role is consistent with mathematical modelling. When a hyperpolarizing BK-like current component is added into the model with single spikes, it converts single spike to bursting firings. When more BK-like current was added, the spike size and firing frequency of bursting decreased more, and the downstroke of the spikes during bursting is less repolarized and cannot reach the previous membrane potentials (Van Goor, Li & Stojilkovic, 2001; Tsaneva-Atanasova *et al*., 2007; Stern *et al*., 2008). Thus, the spikes of bursting form a depolarised plateau of bursting. When sufficient $[Ca^{2+}]_i$ activates more BK channels far away from Ca_v channels, $[Ca^{2+}]_i$ is reduced by Ca^{2+}-ATPase, and a new burst begins (Van Goor, Li & Stojilkovic, 2001). If BK channel current is a fast activated component, it also reduces the amplitude or broadens the duration of single spikes in pituitary cells and neurons (Van Goor, Li &

Stojilkovic, 2001). However, due to various expression levels of BK channels, the distance between BK channels and Ca_v channels in different pituitary cells, BK channels lose the function of converting firing patterns in some pituitary cells and neurons (Stojilkovic, Tabak & Bertram, 2010). BK channels exert the function in abolishing action potentials instead of converting firing patterns in GH_3 cells (Lang & Ritchie, 1990). Based on mathematical modelling, A-type K^+ current with similar properties as inactivating BK channels which reduce the spike amplitude and the activation of delayed-rectifying K^+ current also have the role in changing firing patterns (Chatterjee *et al*., 2009).

BK channels have been reported to dominate the membrane conductance of mouse pituitary AtT20 corticotrophs (Shipston *et al*., 1999). Increasing evidence suggests that BK channels exert a functional role in the signalling pathways regulating the control of ACTH secretion from the anterior pituitary corticotrophs by changing their cellular excitability. BK channels work as an important negative feedback regulator of VGCI in AtT20 mouse pituitary corticotroph tumour cells. During CRH-induced ACTH secretion, CRH exerts a PKA-mediated inhibition of BK potassium channels. BK channels are also inhibited by the PKC signalling pathway to achieve PKC-mediated Ca^{2+} influx resulted in a sustained ACTH release in response to AVP (Tian, Philp & Shipston, 1999). The inhibited BK channels lose their repolarizing function, which resulted in maintained cell depolarization and action potentials. In rat GH_4C1 pituitary cells, BK channels also acted as fast and efficient negative inhibitors of VGCI (Shipston & Armstrong, 1996).

In early glucocorticoids negative feedback, glucocorticoids prevent the PKA-mediated BK channel inhibition through activating a protein-synthesis-dependent signalling cascade (Tian, Philp & Shipston, 1999). Glucocorticoid-induced proteins render BK channels resistant to PKA inhibition which is crucial for glucocorticoid early inhibition on ACTH secretion (Tian, Philp & Shipston, 1999). Different from AtT20 cells, BK channels are not the target of early glucocorticoid inhibition in rat anterior pituitary cells although, the rapid newly synthesised RNA and proteins control membrane potential to inhibit CRH-induced ACTH secretion (Lim, Shipston & Antoni, 1998). Although BK channels would be predicted to contribute to membrane hyperpolarization, which would negatively feedback to limit the duration of action potentials and the control of Ca^{2+} entry, there is no direct evidence in native rat corticotrophs (Van Goor, Li & Stojilkovic, 2001). Female mice genetically deficient in the pore-forming BK channel α-subunit respond with a reduced ACTH and corticosterone secretion *in vivo* in response to acute restraint stress. At the level of the pituitary, deletion of the BK channel increased CRH-induced ACTH release *in vitro* suggesting the stress hyporesponsiveness seen *in vivo* is not due to a pituitary defect. Indeed, CRH expression and neuronal activation in the PVN and ACTH peptide content in the pituitary were reduced as well (Stojilkovic, Tabak & Bertram, 2010).

In turn, the endocrine outputs of HPA axis potently regulate the expression, function and splicing of BK channels in pituitary corticotrophs, suggesting an intimate link between them (Brunton *et al.*, 2007; Shipston *et al.*, 1999; Shipston, 1995; Tian Knaus & Shipston, 1998). ACTH and glucocorticoids have been reported to exert

profound effects on the cellular excitability of neurons and neuroendocrine cells through the regulation of BK channel splicing, mRNA expression of α-, β2- and β4-subunits and protein synthesis in adrenal gland and anterior pituitary cells (McCobb & Beam, 1991; Shipston, 1995; Tian, Knaus & Shipston, 1998). Glucocorticoids regulate the pore-forming α-subunit alternative splicing of BK channels mediated by glucocorticoid and mineralocorticoid receptors (McCobb & Beam, 1991). However the cellular mechanisms are not fully understood.

1.4.2 Corticotroph electrical excitability

1.4.2.1 Action potential patterns

Secretory pituitary corticotroph cells are not only endocrine cells, but also electrically excitable cells. Electrically excitable cells with voltage-sensitive ion permeability show regenerative and propagated spontaneous electrical activity or after being stimulated (Stojilkovic, Tabak & Bertram, 2010). The resting membrane potential of isolated pituitary cells *in vitro* varies between -60 mV to -50 mV related with the activity of depolarizing and hyperpolarizing ion channels. When cell membrane potential oscillations reach the threshold, cells generate action potentials. However, the patterns of action potentials vary among pituitary cells. There are two typical patterns, one is single spike firing with frequency approximately 0.7 Hz, large amplitude more than 60 mV and narrow action potential duration with half-width less than 50 msec (Stojilkovic, Tabak & Bertram, 2010). The other pattern is termed as “pseudo-plateau bursting” consisting of periodic depolarized potentials with

superimposed small-amplitude spikes. The pseudo-plateau bursting shows a much lower firing frequency around 0.3 Hz, a significantly longer action potential duration than large and narrow spike firings. It normally lasts several seconds with smaller amplitude around 10 mV or less (Stojilkovic, Tabak & Bertram, 2010). During pseudo-plateau bursting, the cell membrane potential rarely goes above -10 mV. These two firing patterns are widely observed in various pituitary cells, and rat anterior pituitary corticotrophs show both big amplitude spikes and the pseudo-plateau bursting spontaneously (Stojilkovic, Tabak & Bertram, 2010). BK channels have been proposed as the main mediator in converting the two patterns of action potentials as discussed before.

1.4.2.2 Pituitary cell resting membrane potential

The resting membrane potential of isolated pituitary cells between -60 mV to -50 mV suggesting that in addition to the resting K^+ conductance there are depolarizing conductances active (Stojilkovic, Tabak & Bertram, 2010). When extracellular Na^+ is replaced with $NMDG^+$ cation, the resting membrane potential quickly drops to < -85 mV, which is close to the equilibrium potential for K^+. It is revealed that there is a constitutive Na^+ conductance responsible for maintaining the resting membrane potential of many pituitary cells (Sankaranarayanan & Simasko, 1996; Kwiecien *et al*., 1998). The hyperpolarization caused by the absence of extracellular Na^+ also abolished the spontaneous action potentials in pituitary cells. However, the block of TTX-sensitive Na^+ channels show no effect either on the resting membrane potentials or spontaneous action potentials. These observations reveal that TTX-

resistant Na^+ channels are responsible for the control of resting membrane potentials. No direct evidence confirms the molecular component of the TTX-resistant Na^+ (voltage-gated) channels involved in maintaining the resting membrane potential, so the Na^+ component has been named as background Na^+ (Na_b) channels in general (Simasko, 1994; Kucka *et al*., 2010).

1.4.2.3 Action potential-driven Ca^{2+} signals

During action potentials, Ca_v channels not only contribute to the cell depolarizing phase of action potentials, but also provide an efficient extracellular Ca^{2+} entry, which acts as an intracellular signal modulating cellular functions (Kuryshev, Childs & Ritchie, 1996; Guerineau *et al.*, 1991). The frequency of spontaneous action potentials impact on the dynamics of $[Ca^{2+}]_i$ and overall intracellular Ca^{2+} levels, so different pituitary cells show various patterns of Ca^{2+} signalling. Higher basal hormone releasing cells generally display higher spontaneous Ca^{2+} transients and higher $[Ca^{2+}]_i$ level and also spontaneous action potentials and depolarized cell membrane potential. While silent cells show lower $[Ca^{2+}]_i$ and a more hyperpolarized cell membrane potential. $[Ca^{2+}]_i$ level is also tightly related with the patterns of action potentials (Van Goor, Zivadinovic & Stojilkovic, 2001; Kuryshev, Childs & Ritchie, 1995a). The large amplitude spikes with short duration result in a short period of cell depolarization leading to a short time of Ca_v channels being open, which only results in elevation of $[Ca^{2+}]_i$ nanodomains, as in gonadotrophs. While in longer duration bursting action potentials, Ca_v channels stay open longer and as a consequence allow more extracellular Ca^{2+} entry. Meanwhile more nanodomains of

$[Ca^{2+}]_i$ generate and their overlap results in a global Ca^{2+} signal. Thus, bursting leads to more Ca^{2+} influx than big-amplitude single spike firings summed over time (Tomic *et al*., 1999).

Pituitary endocrine cells release hormones in the form of large dense core vesicles (LDCV) triggered by a calcium-mediated exocytosis associated with spontaneous firing of action potentials. Electrical activity has already been recorded both *in vivo* and in tissue slides of the anterior pituitary gland. Individual cells from primary cell culture preparation display asynchronous electrical activity with various firing patterns like pace-making or bursting mode. With the fluorescent monitoring of $[Ca^{2+}]i$, electrical recordings represent that single spontaneous spikes trigger transient rises in $[Ca^{2+}]i$ share the common features with stimulus-secretion. Five types of heterogeneous endocrine secretory pituitary cells would display asynchronous firing, so that the average of single cells activity represents the overall activity of each secretory type. Hypothalamic input regulates the pace of the hormone release through the secretory cells. However, the gland disconnected from the hypothalamic inputs still shows hormone release, suggesting a synchronization of cellular signals within the tissue. Homologous pituitary cells showed coupled electrical activity between cells, especially growth hormone-releasing cells. Spontaneously active endocrine cells throughout the anterior pituitary gland either act as single units or synchronized gap junction-coupled assembled. Gap junctions present in the anterior pituitary may allow both metabolic and electrical coupling between connected cells. The synchrony of spontaneously excitable pituitary cells would contribute in the basal secretion patterns shaping.

1.4.2.4 Cell excitability and hormone secretion

Electrical signals directly couple with the stimulus of hormone secretion in endocrine anterior pituitary corticotrophs. Stimulatory hypothalamic hormones and negative feedback inhibition by adrenal glucocorticoids both regulate spontaneous action potentials and Ca^{2+} influx by Ca_v channels in pituitary cells. CRH leads to cell membrane depolarization and enhances the frequency of APs through cAMP signalling pathway in rat and human tumour corticotrophs (Guerineau *et al.*, 1991; Kuryshev, Childs & Ritchie, 1995a). An additional intracellular Ca^{2+} release from endoplasmic reticulum (ER) mediated by inositol 1,4,5-trishosphate IP_3 and diacylglycerol (DAG), which are synthesised by activation of Gq/11-coupled receptors (Ozawa & Sand, 1986). Increased intracellular Ca^{2+} activates protein kinase C (PKC) and other signalling pathways to mediate ACTH release (Ozawa & Sand, 1986).

Exocytosis is evoked by stimulating priming of secretory vesicles, and then initiated by a rise of $[Ca^{2+}]_i$ totally different from constitutive exocytosis. Both Ca^{2+} entry from Ca_v channels and release from intracellular stores can trigger secretory granule release, although this step has a low Ca^{2+} affinity (Sedej *et al.*, 2004). Ca^{2+} also plays a role in priming of secretory vesicles. The removal of Ca^{2+} or blockage of L-type Ca_v channels diminishes hormone release, while the enhancement of VGCI by high K^+-induced depolarization facilitates secretion. However, these changes have no dramatic effect on basal release of LH, FSH, TSH and ACTH, which reveals that spontaneous action potentials do not couple to hormone secretion in every kind of

pituitary cells (Stojilkovic, Izumi & Catt, 1988). For neurotransmitter release from synapses, VGCI and secretory granules are co-localized, so $[Ca^{2+}]_i$ nanodomain elevation is sufficient for exocytosis. However, this spatial colocalization does not exist in endocrine cells, thus overlapping of $[Ca^{2+}]_i$ nanodomains is required to trigger hormone release. The basal level of $[Ca^{2+})_i$ and the distance between secretion sites and VGCI are both critical for the basal hormone release (Zorec, Sikdar & Mason, 1991; Zorec, 1996; Stojilkovic, 2005). In gonadotrophs, prolonged duration of action potential spikes leads to higher $[Ca^{2+}]_i$ levels that triggers LH secretion. While in somatotrophs, the change of pseudo-plateau bursting to single action potential spikes by BK channel blockers reduces $[Ca^{2+}]_i$ level (VanGoor *et al.*, 2001). Consistent with data in chromaffin cells, spikes with a larger depolarization phase result in a massive hormone secretion. So higher basal $[Ca^{2+}]_i$ level in lactotrophs and somatotrophs induces higher basal hormone release compared with gonadotrophs, and the inhibition of Ca_v channels drags the basal hormone secretion of lactotrophs and somatotrophs down to similar levels of gonadotrophs (Stanley, 1993). The secretion of GH being related to the amplitude and frequency of Ca^{2+} transients is consistent with the previous discussion. L-type Ca_v channel and K_{ir} channels both participate in the frequency of Ca^{2+} transient regulation and PRL release from lactotrophs (Mansvelder & Kits, 2000).

1.5 Approaches to identify live corticotrophs

1.5.1 A brief introduction to gene delivery systems

To investigate gene function or any particular gene modification affecting its function, a powerful tool is to introduce exogenous DNA expressed in mammalian cells, tissues or animals. There are two main categories of gene delivery systems, non-viral systems and viral systems. The non-viral systems deliver genetic material such as plasmid DNA or RNA constructs into cells by chemical and/or physical methods which are called transfection and if viral vectors are used as vehicles, it is called transduction.

1.5.1.1 Non-viral systems

Non-viral gene transfection systems deliver genetic materials into target cells mainly based on: a) physical mechanisms by creating transient pores or holes in the cell plasma membrane to allow desired genetic materials across, like electroporation using a brief high voltage electrical pulse or heat shock using a short high temperature step, both can increase the permeability of the cellular membrane for a short time (Josh, 2005). After these rapid physical stimulations, the cellular membrane recovers and traps the genetic materials inside the cell. A more direct physical (ballistic) transfection method is named “gene gun”, which “shoot” gold solid nanoparticles covered with DNA directly into the nucleus of cells (Gao, Kim & Liu, 2007).

Alternatively, approaches exploit b) endocytosis of materials such as the classic calcium phosphate coprecipitation method. In this approach, DNA is dissolved in a calcium chloride solution, and then mixed with a HEPES-buffered saline solution to produce calcium phosphate precipitates combined with DNA, which allows the DNA to bind to the cell membrane surface (Bacchetti & Graham, 1977). When cells absorb some of the precipitates, DNA is delivered with it (Josh, 2005). A specific way to improve the transfection efficiency is to use cationic lipids to make the target cells more sensitive, or by glycerol shock to give a selective pressure to cell endocytosis (Josh, 2005). Other chemical transfection reagents have the similar principle, like DEAE-Dextran as a polymeric cation, its positive charge attracts negatively charged DNA (De Smedt, Demeester & Hennink, 2000). When endocytosing Dextran cells also absorb the associated DNA. Dimethyl sulfoxide (DMSO) can enhance the transfection efficiency of certain cell types in this method (Park, Lee & Chung, 1998). c) Cellular membrane fluidity. Some non-viral biological transfection reagents like highly-branched organic compounds, dendrimers, or small membrane-bounded bodies such as liposomes are also used to deliver genes into target cells (Glomm, 2005). They package the desired DNA first, then bind to the cell membrane surface and release DNA when they fuse with cell membrane, due to the similar compounds and structure as cell membrane lipid bilayers.

However, almost all physical methods carry a risk of reducing transfection efficiency by damaging or destroying the cell membrane. Without strong selection pressure, long-term stable transgene expression is rare because the DNA resides in the cytoplasm after entry instead of integrating into the host cell genome. So transgenes

delivered by non-viral transfection methods only express transiently for a short period of time. Some chemical transfection reagents or transfection efficiency enhancing reagents are cytotoxic, so the concentration and the exposure time of these reagents have to be optimized to various cell types.

Furthermore, non-viral transfection methods only work well in some cell lines, such as the HEK293 cell line. Many cell lines can only be transfected with very low efficiency, and numerous cell lines and especially primary cultured cells cannot be transfected at all (Gao, Kim & Liu, 2007). Moreover, terminally differentiated cells like neurons can rarely be transfected by non-viral transfection methods *in vitro* and *in vivo* transfection efficiencies are also generally extremely low.

1.5.1.2 Viral delivery strategies

The low transfection efficiency of physical and chemical strategies drove the development of alternative approaches. Viruses with their particular biological properties of easily infecting animals and integrating into the host cell genome for replication have been widely applied in gene delivery. The most recently developed viral transduction systems are widely used for their advantages in high transduction efficiency, stable expression of integrated transgenes, a very wide range of cell type transduction tropism, low cytotoxicity and safety of use.

Adenoviral-based vectors were one of the first modified viral vectors shown to have high transduction efficiency in many cell lines *in vitro*. However, the fact that adenovirus do not easily integrate into the host cell genome limited their use (Russell *et al.*, 2004). In order to achieve stable transgene expression, retrovirus that can synthesise integrase to help DNA integrate into the host cell genome was designed as gene delivery vectors. Retroviral-based vectors first reverse transcribe the extrinsic RNA into DNA, import the DNA into the cell nucleus and then integrate it into the host cell genome to offer a sustained transgenic expression. Since the retrovirus-based vectors infect only dividing cells, their application is limited in transducing primary cells and terminally differentiated cells, like neurons.

Lentivirus (Lenti-, in Latin, stands for "slow"), a genus of slow viruses of the retroviral family, was found to infect non-dividing cells efficiently (Cullen, 1991). Lentivirus has been reported for its extremely high and stable transduction efficiency in a wide range of dividing cells and non-dividing cells as well. Thus, lentiviral-based vector showed a potentially superior transduction to a broad range of cell lines, tissues and animals with sustained gene expression, and it is also the first choice of animal and human gene therapy to eliminate genetic or pathological deficits *in vivo* (Josh, 2005).

1.5.2 Lentiviral three-plasmid expression system

Lentivirus is characterized with a long incubation period in its replication cycle which enables its unique ability to infect non-cycling cells (Narayan & Clements,

1989). Lentiviral-based vectors are mainly modified from human immunodeficiency virus (HIV), feline immunodeficiency virus (FIV) or simian immunodeficiency virus (SIV).

By pseudotyping with the vesicular stomatitis virus (VSV) or retroviral envelope lentiviral-based vectors offer a broad cell and tissue tropism with a significant genetic insert capacity up to 18kb in the virion (Josh, 2005). So far, lentivirus-based vector is the most efficient gene delivery system with extensive use in both *in vivo* and *in vitro*.

Commercially available lentiviral vectors are usually generated by a three-plasmid expression system which consists of a packaging vector, envelope vector and transducing vector (Figure 2.2). The packaging vector contains the cytomegalovirus (CMV) immediate early promoter driving the expression of all immunodeficiency virus functional genes required in infection, except the viral envelope gene and Vpu accessory protein (Josh, 2005). The packaging vector is constructed with gag and pol encoding group-specific antigen and viral enzymes, such as reverse transcriptase, integrase and protease, and *vif*, *tat*, *rev* and *nef* each code a single accessory or regulatory protein that are involved in the regulation of synthesis and processing of virus RNA and other replication functions (Josh, 2005). Matrix (MA) and Vpr are karyophilic proteins regulating nuclear import to the pre-integration complex, which explain how lentiviral vectors transduce non-dividing cells (Josh, 2005).

The most popular envelope vector encodes a vesicular stomatitis virus glycoprotein (VSV-G) to pseudotype the particles that gives the ability to transduce a broad range of cell lines, mammalian and nonmammalian cells, tissue and animals (Josh, 2005). The VSV-G protein is cytotoxic, so it is suggested to be transiently expressed by pVSV-G vector during packaging (Burns *et al.*, 1993). The envelope protein coat is necessary for virion transduction. After entering cells, viral particles behave like normal retrovirus. Moreover, the high structural stability of VSV-G also allows the viral particles to tolerate the ultracentrifugation required to obtain a high viral titre (Josh, 2005).

The basic transducing vector mainly contains multiple cloning sites for cDNA cloning, psi packaging sequence, reverse response element (RRE), and antibiotic resistance genes for permanent transduction selection (Josh, 2005). Any desired genes are ligated into the transducing vector through multiple cloning sites.

Furthermore, this three-plasmid system has an important advantage of improved bio-safety allowing it to be performed at biosafety level 1. Efficient transduction lentiviral particles are only produced in the presence of envelope vector. Transducing vector can only efficiently transcribe full-length vector and cytoplasmic export with the help of Tat and Rev regulatory proteins that are both encoded by the packaging vector (Gottfredsson & Bohjanen, 1997).

Lentiviral particles are produced by transient co-transfection of HEK 293T (FT) cells with the three plasmid expression system (Figure 2.5) (Josh, 2005). Crude lentiviral particles are secreted by transfected HEK 293T (FT) cells and harvested from the cell culture medium. After purification and ultracentrifugation, high titer lentiviral particles are used to transduce cell lines, tissue or inject into animals.

Lentiviral transduction efficiency is significantly improved in some cell lines by using a small cationic polymer called Polybrene. Polybrene helps viral transportation for its positive charge shields the negative charges of the cell membrane, which facilitates the viral glycoprotein fusion for further RNA injection (Josh, 2005). Polybrene also enhances the viral aggregation mechanism (Josh, 2005). However, polybrene is cytotoxic to some extent. Cells ability to tolerate is various from a concentration of 1 to 10 μg/ml.

1.5.3 High efficiency transduction *in vitro*

Lentiviral vector transduction with highly efficient infection and integration are superior to non-viral transfection methods in most cell lines, especially primary cells. Primary cultured cells for their limited dividing potential and survival time are usually difficult to transduce by non-viral vectors or even many viral vectors (Josh, 2005). Lentiviral vector is able to efficiently transduce both dividing cells and the non-dividing cells. The crucial process is the viral pre-integration complex that integrates into the host cell genomic DNA after being transported into the host cell nucleus (Josh, 2005). The gag matris nucleophilic protein (MA) of the lentiviral

vector contains a nuclear localization sequence (NLS) at its amino-terminus that may contribute to the nuclear import process in non-dividing cells (Josh, 2005). Researchers have reported that HIV-1 based lentiviral vectors quickly sheds its capsid after entry into cells, which quickly exposes the nucleoprotein complex or reverse transcription complex (RTC) (Dempsey *et al.*, 1993). Then, the RTC engages with the nuclear import machinery at several levels (Dempsey *et al.*, 1993). Integrase and the central DNA flap (is a 99-nt plus strand overhang and a cis-determinant of HIV-1 nuclear import that increases the transduction efficiency of human) are also important in the mechanism of lentiviral vector infection in non-dividing cells (Aude *et al*, 2000; Vodicka, 2001; Besik & Karin, 2007; Candela *et al*, 2011). Although the precise mechanism of how lentiviral vectors undergo nuclear import has not been elucidated completely, a considerable body of evidence has shown that lentiviral vectors could efficiently transduce non-dividing cells and integrate transgenes in transduced cells as well, like adult neurons, primary human skin fibroblasts, human peripheral blood $CD34^+$ cells, G0/G1 human hematopoietic stem cells (Goldman *et al*., 1997). For example, HIV-based lentiviral vector using the VSV-G envelope with LacZ as a reporter gene successfully transduced non-dividing airway epithelial cells to correct the cystic fibrosis defect *in vitro* (Goldman *et al*., 1997). Lentiviral vectors were also reported to deliver glia cell line-derived neurotrophic factor gene to bone marrow stromal cells to evaluate its neuroprotective effect on lactacystin-damaged PC cells when over-expressed (Goldman *et al*., 1997).

1.5.4 High efficiency transduction *in vivo*

For its highly efficient transduction, stable transgene expression and transduction of non-dividing cells, lentiviral vectors have also been widely exploited for gene therapy (Josh, 2005). After injection *in vivo*, lentiviral vector delivered transgenes can stably express up to 6 months in terminally differentiated cells like, neurons, macrophages, hematopoietic stem cells, retinal target cells, muscle and liver cells, cell types for which previous gene therapy approaches were largely unsuccessful (Josh, 2005). In hematopoietic stem cells, lentiviral vectors were shown to modify stem-cell self-renewal capacity and differentiation into mature cells in blood and the immune system (Amado & Chen, 1999). Gene therapy lentiviral vectors with tissue specific promoters could modify the defect specifically. Under the control of the rhodopsin promoter, the desired genes delivered by HIV-based lentiviral vector allowed sustained expression specifically in the photoreceptor cells of the retina, which accomplished the therapy of the inherited genetic disease, retinitis pigmentosa (Josh, 2005).

1.5.5 Safety issue and potential disadvantages

Although the lentiviral vector used in gene therapy is mainly base on HIV-1, numerous modifications have been made to the vector construct to ensure its safety in use. Replication competent lentiviral vectors do not contain any necessary HIV pathogenic genes, and cannot replicate HIV in animals and humans. The LTR promoter in the HIV genome was deleted as well, so transgenes are usually expressed under an exogenous viral or cellular promoter which is constructed in the

lentiviral transducing vector (Amado & Chen, 1999). The deletion of the LTR promoter also reduces the possibility of insertional mutagenesis after integration into the host genome, and eliminates the expression of vector RNA which minimizes the potential of replication competent lentivirus in the host cells (Josh, 2005). The important accessory gene vpr that mediates HIV infection of macrophages has also been deleted from the packaging vector, so the packaging vector is a defective HIV genome and only contains the necessary elements to produce transduction virions (Muthumani *et al.*, 2005). Furthermore, HIV-1 envelope is replaced by the VSV-G envelope to stop its infection of helper T-cells (Amado & Chen, 1999). Thus the current, commercially available, third generation lentiviral vectors are safe, efficient and are being exploited in human gene therapy trials.

Although lentivirual vectors are widely using in genome manipulation and transgenic animals for its high transduction efficiency and abroad application of cell types, it has potential disadvantages. Theoretically, the early generation lentiviral vectors were capable to maximally produce a functional genome size of 16 kb vectors particles (Kumar *et al.*, 2001). While in reality, the 16 kb vector produced viral titers are dramatically reduced by up to 1,000-fold compared with lentiviral constructs of 5-7 kb, which lead these vector particles useless in biological application (Park, 2007). The backbone of lentiviral vector is also needed to calculated, which is generally about 1.6 kb (without WPRE) or around 2.2 kb (with WPRE), so the limitation of the lentiviral vectors was roughly 13.5 kb. Due to the titer reduction, the expression of promoter-transgene larger than 4 kb showed the transgensis rates decreased due to the upper limit of the lentiviral vector packaging capacity (Kumar *et*

al., 2001; Park, 2007). Therefore, the delivery of large size of genome like more than 4 kb is very difficult to be achieved by lentiviral vectors. The most popular VSV-G pseudotyped packaging for lentiviral vectors with high efficient integration into cells from various cell species has been demonstrated fusegenic and other cellular toxicity on cell culture (Burns *et al.*, 1993). As a result, the use of alternative viral glycoproteins or using physical technique to delivery envelop-free vector may help to minimize the adverse effects on culture cells or transgenic embryo development (Burns *et al.*, 2007). Another issue of genetic mosaicism occurring through using virial constructs have been reported, which may be caused by the initial cell division happened before the process of lentiviral vector integration, or the prolonged persistence of lentiviral preintegration complex due to the long half-life of lentiviral vector (Park, 2007). Genetic mosaicism remains a potential issue in producing transgenic animals, further information is needed to determine the factors related, like the survival time frame of vectors after uncoating to better control the integration factors, or any vector-related sequences related to eliminating mosaicism through destabilizing the preintegration complexes since mosaicism are not reported in all studies (Park, 2007). The silencing of lentiviral transgene expression mediated by epigenetic modifications or promoters also remains a question of using lentivirial vectors. Also more investigations of the location of proviral integrant caused the various pattern and strength of transgene expression are needed to determine if the segregation of these integrant in transgenic animals with multiple copies leads adverse effects on the expression of transgene (Park, 2007).

1.5.6 Lentiviral-mediated labelling of primary pituitary cells

Lentiviral vectors carrying the eGFP gene were used to transduce human pituitary adenoma cells, with 67.8% of eGFP-positive cells were observed to include non-dividing tumoral cells and stroma cells, mainly fibroblasts (Josh, 2005). Using a tissue specific promoter to drive fluorescence protein expression allows specific cell labelling. Rat anterior pituitary primary cell cultures showed a different transduction efficiency from 5%-86% in different pituitary endocrine cells depending upon cellular specificity of the pituitary promoters delivered by lentiviral transduction (Josh, 2005). All anterior pituitary endocrine cells were transduced using the phosphoglycerate kinase (PGK) promoter, but none using the human growth hormone (GH) promoter (Josh, 2005). Lentiviral vectors with the α-subunit 1 human glycoprotein hormone α-subunit promoter mainly transduced thyrotroph and gonadotroph cells, while with the a-subunit 2 human glycoprotein hormone α-subunit promoter more selectively transduced PRL, GH and adrenocorticotropin (ACTH) cells (Josh, 2005).

1.5.7 Genetic manipulation of pituitary cells by lentiviral vector

In order to investigate the function of specific gene in pituitary cell, the strategies of over-expression or knock-down the gene are mainly considered. Non-viral transfection methods to deliver desired genes by electroporation, lipofectamine, calcium phosphate or poly-imine transfection methods are of low efficiency and transient in pituitary cells. In primary pituitary cells the efficiency of these methods is routinely less than 1%. A comparison among calcium phosphate ($CaPO_4$), DEAE-

dextran, lipofection, and electroporation procedures transfection methods, $CaPO_4$-mediated transfection accomplished the best transient gene expression in primary pituitary cells (Burrin & Jameson, 1989). Adenoviral vectors have been used to transduce pituitary cells *in vitro* and *in vivo*. However, severe inflammatory responses were caused by using the first generation of adenoviral vectors. Furthermore, there is a significant decrease in transgene expression 3 months after transduction (Josh, 2005). Lentiviral transduction system is proposed to carry interested gene or its siRNA into primary pituitary cells, which offer a constant over-expression or down-expression of the interested genes models for further gene function investigation.

1.6 Aims and objectives of the thesis

The anterior pituitary corticotroph is central to the regulation of the HPA axis to control the whole organism response to stress. Previous studies suggest that the pituitary corticotrophs are endocrine cells with electrical excitability. However the majority of studies examining electrical excitability are based on pituitary corticotroph cell lines or tumor models. In native pituitary corticotrophs, the ion channels regulating corticotroph electrical properties are very poorly understood and prior to this thesis there were no reports analysing native murine corticotroph electrophysiology. A major reason is because the anterior pituitary contains several hormone-secreting cell types, and these cells are similar size and shape, which makes live corticotroph identification and purification difficult.

The overall aim of this Thesis was to examine the electrophysiological properties of native murine corticotrophs under as near-physiological conditions in *vitro* as possible. The general approach taken was to express an enhanced yellow fluorescent protein (eYFP) specifically in native murine pituitary corticotrophs and then apply patch-clamp electrophysiological analysis on the identified fluorescent cells.

The objectives of the thesis:

1) To develop and exploit a lentiviral transduction system to provide labelling of live native murine corticotrophs *in vitro*. This was achieved using a minimal rat POMC (rPOMC) promoter to drive expression of eYFP specifically in corticotroph cells of the anterior pituitary *in vitro*. (Chapter 2 & 3)

2) To examine the major outward potassium conductances in metabolically intact native, labelled corticotrophs using the perforated patch-clamp approach in voltage-clamp combined with pharmacological and genetic approaches (Chapter 3)

3) To examine the spontaneous electrical firing properties of metabolically intact native, and ion channels that may control activity, in identified corticotrophs using the perforated patch-clamp mode of the whole cell recording technique in current clamp mode with pharmacological and genetic approaches (Chapter 4).

4) To characterise the effect of physiological levels of CRH and/or AVP on electrical excitability of native corticotrophs (Chapter 5)

Overall, the work in this Thesis demonstrates the utility of the lentiviral system for high efficiency identification of native murine corticotrophs *in vitro* to allow subsequent electrophysiological analysis. We reveal that murine corticotrophs display heterogeneity in spontaneous firing properties that is determined by a TTX-insensitive sodium conductance. Surprisingly, we found that TRAM-34 sensitive calcium-activated potassium channels were a dominant component of the outward potassium conductance and that, in contrast to other systems, inwardly rectifying and large-conductance calcium activated potassium channels has little functional effect on excitability.

Aspects of this work have been published (Liang *et al*., 2011).

Chapter Two:

Materials and Methods

2.1 General Materials and Reagents

2.1.1 Biochemical Reagents

General biochemical reagents used in this study were obtained from Sigma-Aldrich Company Ltd., Dorset, UK, except where stated otherwise.

2.1.2 Molecular Biology Reagents

MWG Biotech AG, Ebersberg, Germany

VH Bio Ltd, Gateshead, UK

PCR/Mutagenesis Primers

Construct sequencing

Invitrogen Ltd., Paisley, UK

UltraPure™ Agarose

SYBR® Safe DNA Gel Stain

Taq DNA Polymerase (with W-1)

pCR®II-TOPO®

pLenti6/V5 Directional TOPO® Cloning Kit

Bioline, London, UK

HyperLadder™ I

Eppendorf, Hamburg, Germany

The Perfectprep® Gel Cleanup Kit

New England Biolabs, Herts, UK

Restriction endonucleases, T4 DNA ligase

Roche, West Sussex, UK

Shrimp alkaline phosphatase

Proteinase K (recombinant, PCR Grade)

QIAGEN Ltd., West Sussex, UK

HiSpeed™ Plasmid Mini, Midi, Maxi Kit

Viagen Biotech, Inc., Los Angeles, CA, USA

Direct PCR Lysis Reagent (Ear)

2.1.3 Cell Culture Reagents

GIBCO® Invitrogen Ltd., Paisley UK

Gibco™ Dulbecco's Modified Eagles Medium (DMEM + 4.5 g/L high-glucose, + L-Glutamine, - Pyruvate)

Gibco™ Dulbecco's Modified Eagle Medium (DMEM + 4.5 g/L high-glucose, + L-Glutamine, + 25 mM HEPES, - Pyruvate)

Hank's Buffered Salt Solution (HBSS)

0.05 % Trypsin with EDTA

Foetal Bovine Serum (FBS)

Sigma-Aldrich Company Ltd., Dorset, UK

Insulin-transferrin-sodium (ITS) selenite liquid media supplement

Fibronection from bovine plasma

Albumin solution from bovine serum (BSA)

Trypsin inhibitor from Glycine max (soybean)

Deoxyribonuclease I from bovine pancreas-Type IV (DNAse I)

Aprotinin from bovine lung

Antibiotic antimycotic solution

Dimethyl sulfoxide (DMSO)

Worthington Biochemical Corporation, Lakewood, NJ, USA

Trypsin (powder)

Fermentas, York, UK

ExGen 500 in *vitro* Transfection Reagent

2.1.4 Electrophysiology Reagents

Sigma-Aldrich Company Ltd., Dorset, UK

Tetraethylammonium chloride (TEA) is used as a general and non-specific blocker of potassium channels.

Paxilline is used as a potent inhibitor of high-conductance Ca^{2+}-activated potassium (Maxi-K, BK) channels.

1-[(2-Chlorophenyl) diphenylmethyl]-1H-pyrazole (TRAM-34) is used as a potent blocker of intermediate-conductance Ca^{2+}-activated potassium (SK4) channels.

4- Aminopyridine (4-AP) is used as a potent inhibitor of A-type potassium channels.

Barium chloride ($BaCl_2$) is used as a potent a blocker of inwardly rectifying potassium (K_{ir}) channels.

N-Methyl-D-glucamine ($NMDG^+$) is a large organic molecule, unable to cross the membrane, and is used to replace Na^+ in the electrophysiology solution.

Amphotericin B from Streptomyces sp. is an antibiotic and is used to forms membrane pores, only permeable to small monovalent ions in perforated patch-clamp recording.

Bachem Distribution Services, Weil am Rhein, Germany

Corticotropin-releasing hormone (CRH), human, rat

(Arg8)-Vasopressin (AVP)

2.2 General molecular biology protocols

2.2.1 Polymerase chain reaction amplification of DNA

The standard polymerase chain reaction (PCR) is applied to amplify or sub-clone interested regions of DNA fragments. In this study, PCR was used to genotype mice (mouse BK channel and green fluorescent protein (GFP)) and to sub-clone yellow fluorescent protein (YPF) into the lentiviral transduction construct for its expression in native murine pituitary cells.

Typical 1 × PCR reaction contained 1-10 ng template DNA, 10 pmol each of forward and reverse primers, 10 × PCR reaction buffer, 1.5 mM $MgCl_2$, 10 nmol each of dATP, dCTP, dTTP, dGTP (Fermentas), and 1-2.5 U (1 U being the amount of enzyme required to incorporate 10 nmol of dNTP into acid-insoluble material in 30 minutes at 74 ℃.) of Taq DNA polymerase, all in double distilled water (ddH_2O) to a 20 µl final reaction volume. Reactions generally ran for 5 minutes at 94 ℃ to completely denature template, then 25-35 cycles of PCR amplification as denaturing at 94 ℃ for 45 seconds, annealing at the temperature appropriate 5-6 ℃ lower than the primers' calculated melting temperature (Tm) for 30 seconds and extending at 72 ℃ depending on the length of the amplicon, approximately 1 minute per kb, followed by 10 minutes at 72 ℃ after the final cycle and maintained at 4 ℃. Negative control reaction with ddH_2O replacing the template DNA was performed in parallel. All reactions were performed in GeneAmp® PCR system 2700 (Applied Biosystems). Products were analysed by agarose gel electrophoresis (Section 2.2.2) or went to restriction digestion (Section 2.2.3) directly.

2.2.2 DNA agarose gel electrophoresis

Agarose gels were composed of 1 × TBE buffer (45 mM Tris-base, 45 mM Boric acid, 2 mM EDTA, pH 8.0), 1.2-1.5 % agarose (w/v) to separate DNA fragments ranging from 7 kb - 0.5 kb and 6 kb - 0.4 kb respectively and 0.01% SYBR Safe® to visualise DNA fragments under ultraviolet (UV) illumination. DNA samples were mixed with 10 × loading dye (60% glycerol (v/v), 0.25% bromophenol blue (w/v), 33% 150 mM Tris (v/v), pH 7.6 in ddH_2O) before loading. DNA Ladder 1 was used as the molecular weight (MW) marker. Electrophoresis was performed in 1× TBE

buffer at 25 voltage/cm for 20-30 minutes related to sizes of DNA samples using a Bio-Rad model 200/2.0 power supply. Gel images were taken under UV illumination using the GeneGenius Gel Imaging System (SYNGENE).

2.2.3 DNA restriction digestion, gel purification and phosphatase treatment

DNA sequence is digested by restriction endonuclease at specific motifs producing complimentary ends of inserts and vectors allowing ligation and subsequent construct formation, or to assess DNA fragments.

1 µg DNA was digested with 1-2 U of respective restriction endonuclease in appropriate buffer and incubated at appropriate temperature. In this study, 20 µl digestion reaction was normally prepared with 1-5 µg DNA combined with 2-5 U of restriction endonuclease in ddH_2O diluted digestion buffer to a final volume of 15-25 µl. Star activity of restriction endonuclease was checked and avoided by incubating digestion reaction at appropriate temperature and duration for optimal endonuclease activity according to the manufacturer's instructions. For double endonuclease digests, a two-step digestion process was carried out to ensure the DNA was completely digested.

Digested DNA sequences were analysed by agarose gel electrophoresis (Section 2.2.2). The desired DNA fragments were cut from gels under direct UV illumination

and purified by using the Perfectprep® Gel Cleanup Kit according to the manufacturer's instructions.

To avoid self-ligation and reduce the probability of false positive ligation, 5' phosphate groups were removed from the digested end of vectors. Gel purified linearized vector DNA was dephosphorylated with Shrimp alkaline dephosphorylase at a concentration of 1 U/µg (DNA) in at 37℃ for 30 minutes followed by deactivation at 65℃ for 15 minutes.

2.2.4 Ligation of insert and vector DNA

2.2.4.1 Ligation of restricted fragments

After gel purification, the appropriate restriction endonuclease digested insert and dephosphorylated vector DNA fragment were analysed by agarose gel electrophoresis to confirm the purification and enable the approximation of the relative DNA concentrations.

Generally, three 10-15 µl ligation reactions of insert to vector were performed with varied molar ratios (3: 1, 5: 1, 7: 1, see the equation below) using T4 DNA ligase in a concentration of 40 U/reaction in 1 × T4 buffer for T4 DNA ligase topped up by ddH_2O. Negative control reaction consisting of vector DNA and T4 DNA ligase omitting the insert was performed in parallel to check self-annealing and contamination. Ligation reactions were incubated at 4℃ or 16℃ overnight before proceeding to the transformation of competent cells.

$$\frac{\text{vector (ng)} \times \text{size of insert (kb)}}{\text{size of vector (kb)}} \times \text{molar ratio of } \frac{\text{insert}}{\text{vector}} = \text{insert (ng)}$$

2.2.4.2 Ligation into TOPO vector

Fresh PCR amplicons were incubated with pCR®II-TOPO® vector at 20℃ for 5 minutes and transformed into TOPO 10 competent *E. coli* cells (Invitrogen, UK) according to the manufacturer's instructions.

2.2.5 Transformation of plasmid DNA into competent *E. coli*

A 100 µl aliquot of competent *E. coli* cells (XL 10, Strategene, USA) were taken from -80℃ and thawed on ice. After defrosting, approximately 100 ng of ligated DNA was mixed and incubated on ice for 20 minutes, followed by heat-shock at 42℃ for 45 seconds. 200 µl lysogeny broth (LB) medium was then added and incubated at 37℃ with agitation for 45 minutes for recovery. 100-200 µl cell mixture was plated onto an appropriate antibiotic (ampicillin: 100 µg/ml, kanamycin: 30 µg/ml) selective LB agar plate and incubated at 37℃ overnight.

Positive clones were screened either by PCR with specific primers or unique enzymes digestion of mini-prep DNA prepared from individual colonies.

2.2.6 Assessment of ligation transformants for plasmid amplification

The number of colonies on the control plates reflected the ligation efficiency. A large number of colonies on the control plate indicated either bacterial contained self-ligated vectors without insert or the plated was contaminated, thus the experimental plate failed.

If the control plate showing no or little background, 3-5 colonies from the experimental plated were picked, inoculated in 5 ml LB medium and incubated at 37℃ with agitation overnight for plasmid amplification. Plasmid DNA extracted via alkaline lysis (Section 2.2.7) were checked with restriction endonuclease digestion and sent for sequencing. For PCR checking, colony was picked with a sterile pipette tip and resuspended in the PCR reaction mixture directly.

2.2.7 Alkaline lysis for plasmid DNA isolation

The checked bacterial colony was picked with a sterile pipette tip, inoculated in 5 ml (miniprep), 100 ml (midiprep) or 250 ml (maxiprep) LB medium with the appropriate antibiotics (ampicillin: 100 μg/ml, kanamycin: 30 μg/ml) for plasmid selection, and incubated at 37℃ with agitation overnight (no more than 18 hours). The following day, bacterial culture was transferred to a centrifuge tube and centrifuged at 15000 × g for 5-10 minutes. LB broth was removed and the pellet was resuspended in alkaline lysis buffer. The plasmid DNA was then extracted and purified by using the QIAGEN HiSpeed™ Plasmid Mini, Midi, or Maxi Kit respectively, according to the manufacturer's instructions.

2.2.8 Bacterial glycerol stocks

1 ml bacterial culture from section 2.2.7 before centrifugation was diluted into 0.15 ml sterile glycerol, suspended and snap-frozen in the isopropanol dry ice bath prior to long-term storage at -80 ℃. Bacterial culture was recovered by inoculation into LB medium with appropriate selection antibiotic.

2.2.9 Quantitation of DNA and sequencing preparation

The quality of DNA was determined by measuring the optical absorbency of the DNA solution at 260 nm (OD_{260}) and 280 nm (OD_{280}) by spectrophotometer (Biomate3, Thermo Electron Corporation, UK). DNA sampled was 1/100 diluted by ddH_2O for measurement. The ratio of OD_{260} and OD_{280} indicates the purity of DNA samples. The ideal ratio is 1.8 indicating pure double stranded DNA, whereas values lower than 1.8 indicating protein, other nucleic acids or phenol contamination and higher than 1.8 indicating RNA contamination. The concentration of DNA was directly read from the spectrophotometer.

20 µl volume DNA (50-100 ng/µl) sample was prepared for sequencing. Primers can be order from the same company or be included at a concentration of 10 pmol/µl and 5 µl per primer. Sequencing results were analysed with Vector NTI 10.1.1 (Invitrogen).

2.3 PCR genotyping

2.3.1 Animals

Mice with the deletion of the pore exon of α–subunit of BK channel ($BK^{-/-}$) were generated as described (Sausbier, 2004). F2 generation of wild-type (WT) and $BK^{-/-}$ mice on the hybrid SV129/C57BL6 background were always used. Mice were caged in groups of 2-4 under the standard laboratory conditions (lights on at 0700 h and off at 1900 h, 21℃, with chow and tap water available). Either litter- or age-matched adult female mice (3-5 months) were randomly assigned to primary cell culture preparations every week. According to previous reports, corticotroph cells from male mice or rats displayed significantly different electrical activities from corticotrophs from female mice or rat (). To avoid the sexual variation, female mice were only used in this project. The age of mice was referred from related publication and also kept constantly to achieve comparable data. All tissue collection and cell culture preparation were performed between 0900-1100 h in accordance with accepted standards of humane animal care (United Kingdom Home Office requirements).

2.3.2 Design of primers for mice genotyping

PCR genotyping aims to classify the genotype of each individual animal by analysing the genetic difference of its DNA sequence with PCR.

In this study, genotyping PCR was performed to identify WT and $BK^{-/-}$ mice or proopiomelanocortin-green fluorescent protein (POMC-GFP) positive and negative

transgenic mice with the appropriate cycling parameters (Table 2.1) specific to the primers used, relative to the respective melting temperatures (Table 2.2).

2.3.3 Tissue digestion

Viagen DirectPCR Lysis Reagent (Ear, Viagen Biotech) was used to lyse mouse ear clips and release DNA for subsequent PCR genotyping, which contains inhibitors of PCR inhibitors found in animal tissues, thus making the DNA released compatibly for direct PCR amplification. One ear sample was digested in 120 µl lysis reagent with 25 µl proteinase K (20 mg/ml, Viagen) in a 1.2 ml eppendorf tube, which was incubated at 55 ℃ in a rotating hybridization oven for 8-12 hours to ensure complete lysis. The crude lysate was then incubated at 85 ℃ for 45 minutes to inactivate the proteinase K. Before PCR, the eppendorf tube was vortexed for 10 seconds to completely dissolve the DNA followed by centrifuging for 10 seconds to precipitate unlysed hairs.

2.3.4 PCR and DNA agarose gel electrophoresis

2 µl of the crude lysate was directly used in the PCR reaction. Negative PCR reaction control was performed with 2 µl ddH_2O in parallel to check the contamination. Amplified DNA fragments were separated in a 1.5% (w/v) agarose gel.

Figure 2.1 illustrates a representative agarose gel of PCR amplicons from genotyping reactions. The upper image (Figure 2.1 A) illustrates samples with one band around 170 bp identifying as $BK^{-/-}$ mice, samples with one band around 480 bp identifying

Table 2.1

Cycling parameters for genotyping PCR reaction

Mouse Genotypes	Forward Primer	Reverse Primer	Cycling Parameters		
			Step1	Step2	Step3
WT/BK$^{-/-}$	A and B	C	1 × 94 ℃-5 min	35 × 94 ℃-45 sec 52 ℃-30 sec 72 ℃-60 sec	1× 72 ℃-10 min 4 ℃-∞
POMC-GFP	D	E	1 × 94 ℃-5 min	25 × 94 ℃-45 sec 62 ℃-30 sec 72 ℃-60 sec	1× 72 ℃-10 min 4 ℃-∞

* Primers labels refer to Table 2.2

Table 2.2

Genotyping PCR primers

Primer	Name	Target mice	Tm (℃)	Sequence(5'- 3')
A	BK forward1	WT/ $BK^{-/-}$	59.4	TGG TCT TCT TCA TCC TCG GG
B	BK forward2	WT/ $BK^{-/-}$	57.9	AAG GGC CAT TTT GAA GAC GTC
C	BK reverse	WT/ $BK^{-/-}$	59.4	CCA GCC ACA GTG TTT GTT GG
D	POMC-GFP forward	POMC-GFP	73.5	AGG ATC CTA CCA TGG TGA GCA AGG GCG A
E	POMC-GFP reverse	POMC-GFP	61.4	CAG CTT GTG CCC CAG GAT CT

Figure 2.1
Genotyping of WT, BK$^{-/-}$ and POMC-GFP mice

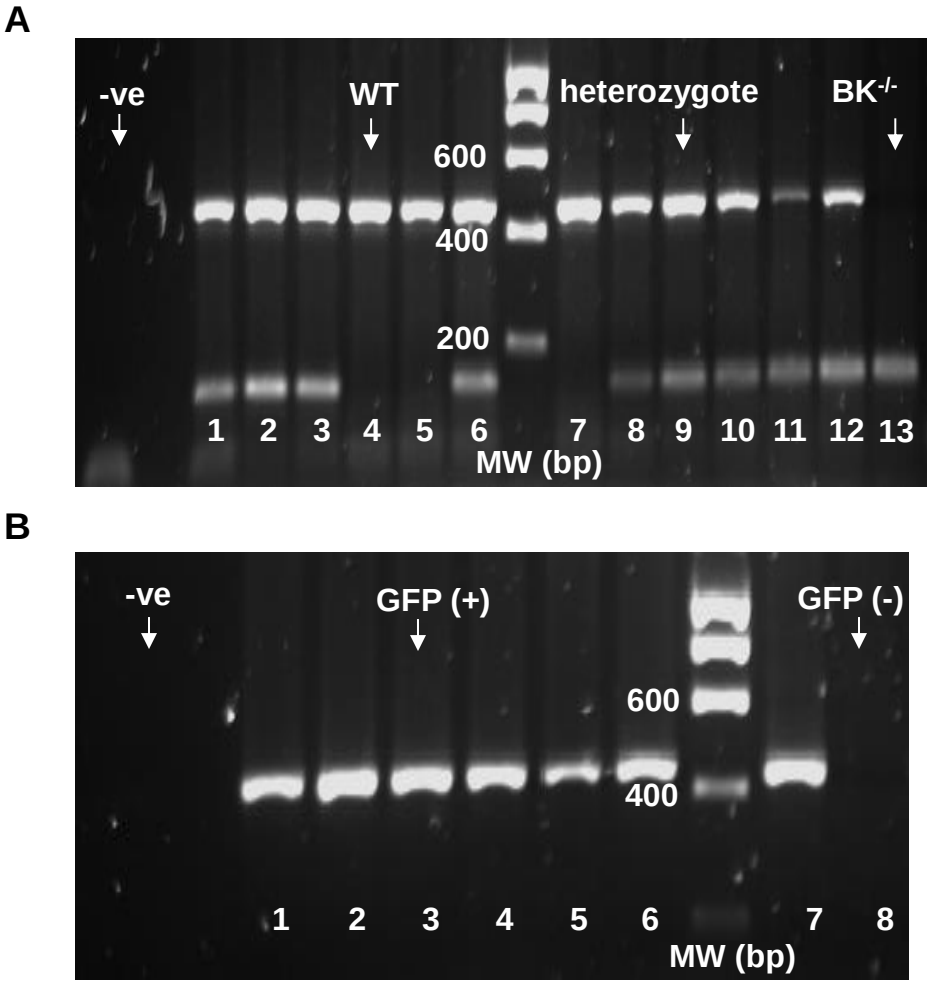

Figure 2.1 Genotyping of WT, BK$^{-/-}$ and POMC-GFP mice. Representative SYBR Safe® stained 1.5% DNA agarose gels. **A**, PCR amplicons for BK channel genotyping. A single band at around 480 bp indicates WT mice. A single band at around 170 bp indicates BK$^{-/-}$ mice and lanes with two bands indicate heterozygote (+/-) mice. **B**, the agarose gel image illustrates the samples with one band around 450 bp identified as POMC-GFP positive mice. No band indicates POMC-GFP negative mice. The molecular weight (MW) markers are 100 bp to 10 kb. –ve = negative PCR control.

as WT mice and samples with both bands identifying as heterozygotes. The molecular weight of the DNA ladder with markers from 100 bp to 10 kb is shown in the middle of the gels to identify the approximate sizes of different amplified bands.

Figure 2.1 illustrates a representative agarose gel of PCR amplicons from genotyping reactions. The upper image (Figure 2.1 A) illustrates samples with one band around 170 bp identifying as $BK^{-/-}$ mice, samples with one band around 480 bp identifying as WT mice and samples with both bands identifying as heterozygotes. The molecular weight of the DNA ladder with markers from 100 bp to 10 kb is shown in the middle of the gels to identify the approximate sizes of different amplified bands.

The bottom agarose gel image (Figure 2.1 B) illustrates samples with one band around 450 bp identifying as POMC-GFP positive mice and samples in which no band amplified identifying as POMC-GFP negative mice. The DNA ladder marker is the same as above.

2.4 Cell culture

2.4.1 Cell line

Human Embryonic Kidney (HEK) 293FT cell line was used to generate lentiviral plasmids in this study. HEK293FT cell line was derived from HEK293F cell line and stably expressed the SV40 large T antigen from the pCMVSPORT6Tag.neo plasmid (Naldini *at al.*, 1996 a). Previous studies demonstrated maximal virus production in

human 293 cells expressing SV40 large T antigen, making 293FT cell line a particularly suitable host for generating lentiviral plasmids (Naldini *at al*., 1996 b).

2.4.2 Cell culture

HEK293FT cells were cultured in Dulbecco's Modified Eagles Medium (DMEM + 4.5 g/L high-glucose, + L-Glutamine, - Pyruvate) plus 10% FCS as growth medium in a 37℃ incubator with a humidified atmosphere of 95% (v/v) air and 5% (v/v) CO_2. Cells used in this study were over a passage range from 4-25.

2.4.3 Maintenance and passage of cell lines

Cells were passaged every 2-3 days at approximately 70%-80% confluence and maintained in 75 cm^2 Greiner flasks or 125 cm^2 flasks for generating lentiviral particles. HEK293FT cells were passaged by removing old growth medium and gently rinsing twice with 3-5 ml HBSS, then 0.3-0.5 ml trypsin-EDTA was added equally to cells. The flask was incubated at 37℃ for 2-4 minutes or until most cells started to detach. Trypsinized cells were gently resuspended in 2-3 ml growth medium triturating slowly for 5-10 times. Once the cells were totally resuspended, the appropriate amount of suspension was transferred to a new sterile culture flask and new fresh growth medium was added to give a final volume of 12 ml for 75 cm^2 flask and 20 ml for 125 cm^2 flask.

2.4.4 Cell storage in liquid nitrogen and recovery

For storage, cells cultured in 2-3 125 cm^2 flasks at 80%-90% confluence were trypsinized as described in section 2.4.3, and collected into a 50 ml falcon tube by centrifugation at 200 × g for 5 minutes. Cell pellet was resuspended in the freezing medium comprising of 90% (v/v) FCS with 10% (v/v) dimethyl sulphoxide (DMSO) on ice. The ideal cell concentration for freezing is 1-3 × 10^6 per ml. Cells were aliquoted into 1 ml cryovials and frozen at -80℃ overnight, and transferred to liquid nitrogen on the next day.

To recover the frozen cells, cell stock was removed rapidly from liquid nitrogen and placed into a 37℃ water bath immediately. Cells were quickly transferred into fresh growth medium and cultured at 37℃ in 5% CO_2. Culture medium was replaced freshly after 24 hours when cells had attached to remove DMSO.

2.5 Lentiviral particle generation

2.5.1 Design and generation of lentiviral constructs

Lentiviral gene delivery system has been widely used for its extremely high transduction efficiency and the ability to integrate DNA into the host cell genome in a wide range of dividing, non-dividing cells, tissues and animals. Commercially available lentiviral gene delivery systems usually consist of a three-construct expression system which includes a transducing construct, packaging construct and envelope construct (Figure 2.2). In this study, different packaging constructs were compared. The second generation packaging construct psPAX2 (Addgene Inc.,

Figure 2.2
Lentiviral transduction system constructs

A

pLenti transducing construct

B

psPAX2 packaging construct

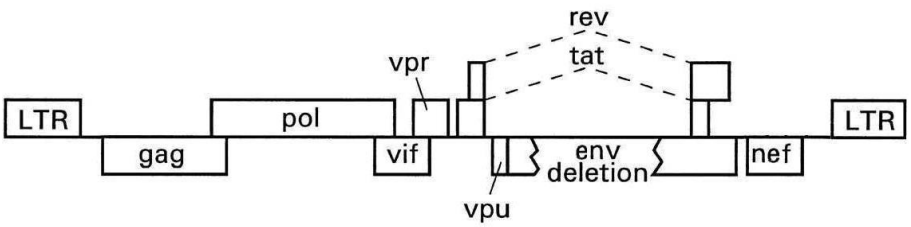

C

VSV-G envelope construct

Figure 2.2 Lentiviral transduction system constructs. Commercially available lentiviral transduction system (Invitrogen) contains three separate constructs: transducing construct, packaging construct and envelope construct. The gene to be expressed is engineered into the transducing construct.

Tronolab) gave the best transfection efficiency and used in routine lentiviral particles generation. The psPAX2 packaging construct (Figure 2.3 A) contains the cytomegalovirus (CMV) immediate early promoter driving the expression of all immunodeficiency virus functional genes required in infection, except the viral envelope gene, accessory protein *vpu* gene, HIV-1 *gag* and *pol* genes encoding group-specific antigen and viral enzymes such as reverse transcriptase, integrase and protease, *rev* gene encoding the structural proteins and the reverse transcripts, reverse response element (RRE), a region in the RNA molecule of the HIV *env* gene, providing a nuclear export signal that is essential for the export of the viral RNA out of the nucleus and the protease (PR) *orf* gene (Pro) encoding a product that cleaves the gag polyprotein precursor (Kumar *et al*., 2001). The envelope construct was obtained from pLenti6/V5 Directional TOPO® Cloning Kit (Invitrogen), encoding a vesicular stomatitis virus glycoprotein (VSV-G) (Figure 2.3 B) to pseudotype the lentiviral particles that offers a broad transduction range of cell and tissue tropism, and is also less toxicity for both inserts and mammalian cells (Farley *et al*., 2007). The high structural stability of VSV-G enables the viral particle to tolerate the ultracentrifugation required to achieve a high titer (Akkina *et al*., 1996). Transducing construct was specially designed and modified from pLenti6/V5-D-TOPO vector (Invitriogen) for this study described as below.

Enhanced yellow fluorescent protein (eYFP) is a small fluorescent protein composed of 238 amino acids, which exhibits visible bright yellow fluorescence when illuminated with UV light. EYFP has been widely used because of its low toxicity when expressed in living cells. In this study, eYFP was designed to label

Figure 2.3
Lentiviral packaging and envelope construct maps

A

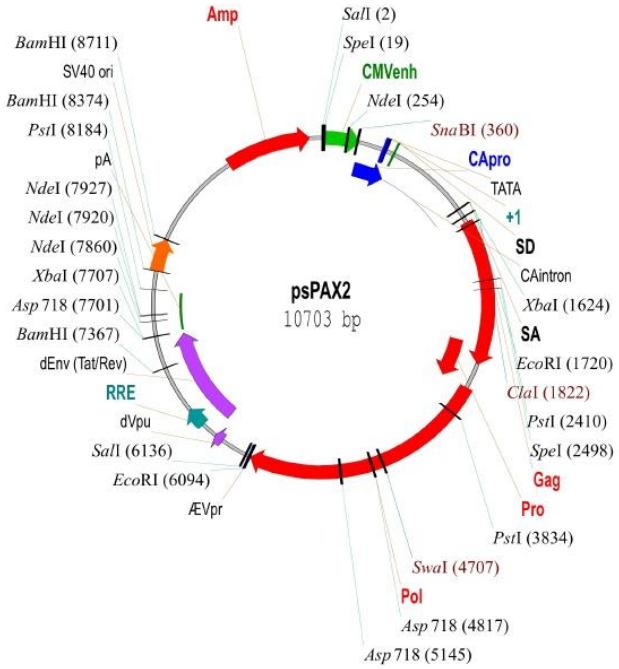

B

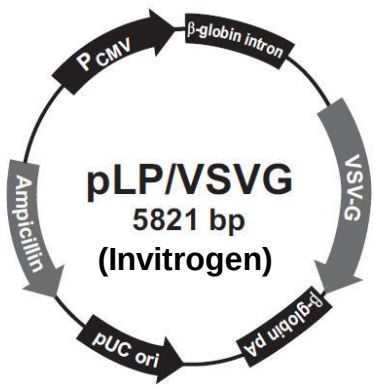

Figure 2.3 Lentiviral packaging and envelope construct maps. **A**, the psPAX2 packaging construct includes the HIV-1 *gag,* pro, *pol* genes and reverse response element (RRE) encoding the viral structural proteins and the reverse transcripts (www.addgene.org/12260/maps/). **B**, the envelope construct is obtained from pLenti6/V5 Directional TOPO® Cloning Kit (Invitrogen), encoding a vesicular stomatitis virus glycoprotein (VSV-G) to pseudotype the lentiviral particles that offers a broad transduction range of cell and tissue tropism.

corticotrophs from other cell populations in primary murine anterior pituitary cell culture with lentiviral transduction system for the further electrophysiological analysis.

EYFP gene was subcloned from pEYFP-NI vector into pLenti6/V5-D-TOPO® vector (Figure 2.4 A). However, since pEYFP-NI vector does not possess any convenient restriction sites to accommodate subsequent constructs, unique *Spe*I and *Sfu*I sites were planned to creat in pEYFP-N1 vector first. The *Spe*I site at the upstream of EYFP gene was created by amplifying pEYFP-N1 vector with primer pair

5- CCGCGTTACATAACTTACGG-3'

and 5'- CCATGGTACCGTCGACTAGTGAAT - 3'.

The *Nhe*I and *Kpn*I digested the amplicon and the vector, which were then ligated with T4 ligase. To generate the *Sfu*I site at the downstream of EYFP gene, a Site-directed Mutagenesis Kit (Strategene, USA) was used following the manufacturer's protocol. The mutagenesis primer pair used were

5'-CAAGTAAAGCGGCCGCGACTTTCGAACATAATCAGCCATACCAC-3'

and 5'-GTGGTATGGCTGATTATGTTCGAAAGTCGCGGCCGCTTTACTTG-3'.

After sequence confirmation, the mutant pEYFP vector was amplified and purified. The *Spe*I-*Sfu*I fragment from the mutant pEYFP vector was ligated into pLenti6/V5-D-TOPO® vector to get the pLenti-CMV-eYFP vector (Figure 2.4 B).

To generate the pituitary corticotroph specific eYFP expression, the minimal rat pro-opiomelanocortin (rPOMC) promoter gene was designed to replace the CMV

Figure 2.4
pLenti-POMC-eYFP construct strategy

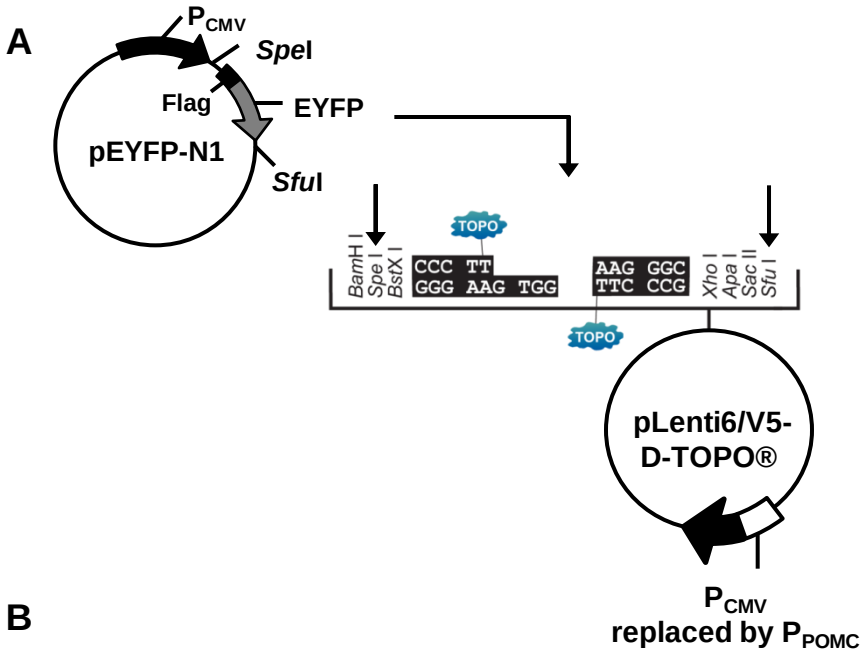

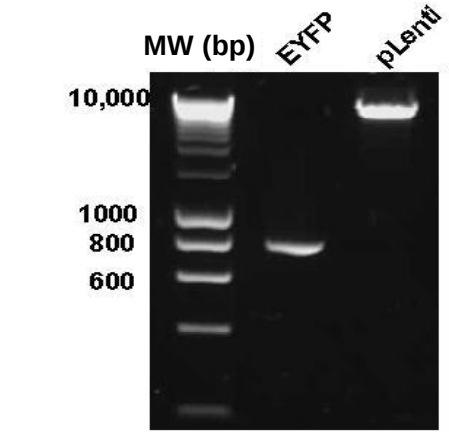

Figure 2.4 pLenti-POMC-eYFP construct strategy. A, EYFP gene from a pEYFP-NI vector was ligated into pLenti6/V5-D-TOPO® with restriction endonucleases *Sfu*I and *Spe*I. CMV promoter in pLenti6/V5-D-TOPO® vector was replaced with minimal rPOMC corticotroph specific promoter. **B**, the agarose gel image shows the *Sfu*I and *Spe*I digested pLenti6/V5-D-TOPO vector and the EYFP insert.

promoter in the pLenti-CMV-eYFP vector to drive the specific eYFP expression. The 770 bp minimal rPOMC promoter was amplified from vector pGEM TZ from Malcon J. Low (Young *et al*., 1998) with primer pair

5'- TCATATCGATGCTTCCACTTCCCTCCACAG-3'

and 5'- CTGGACTAGTTGTTCAGTGGCCTCTCTTAG-3' to create *Cla*I and *Spe*I restriction sites, respectively. *Cla*I and *Spe*I digested PCR amplicon and pLenti-CMV-eYFP vectors were ligated and transformed as described in section 2.2.5 (Figure 2.4 A).

After the construction and modification described above, pLenti-POMC-eYFP transduction construct was generated and then transfected HEK293FT cells with packaging and envelope constructs to generate corticotroph specific eYFP expression lentiviral particles.

2.5.2 Transient transfection of HEK293FT cell line

HEK293FT cells were seeded and cultured in a 125 cm^2 flask in growth medium one day before transient transfection. Cells reached approximately 70% confluence on the day of transfection. The culture medium was replaced with 14 ml fresh growth medium before transfection. 12.3 µg pLenti-POMC-eYFP construct, 9.3 µg psPAX2 packaging construct and 6.3 µg pCMV-VSVG envelope construct (pLenti-transgene : psPAX : VSV-G = 4 : 3 : 2) were diluted in 1.4 ml of 150 mM steriled NaCl solution, vortexed gently and spun down briefly. 93.3 µl of ExGen 500 was then added into the construct mixture, vortexed immediately for 10 seconds, and

incubated for 10 minutes at room temperature (RT) before dropwise addition to the cells. After 24 hours, 20 ml fresh growth medium was replaced (Figure 2.5).

2.5.3 Crude lentivirus purification and concentration

The whole 20 ml culture medium was harvested at 72 hours post-transfection. Cell debris was spun down at 5,000 rpm (Biofuge Stratos, Heraeus Instruments, UK) for 15 minutes. Supernatant was filtered through a 0.45 µm syringe filter (25 mmGD/ X, Whatman®) into a 15 ml Amicon Ultra-15 centrifugal filter device (Millipore, UK) and centrifuged at 5,000 rpm (Biofuge Stratos, Heraeus Instruments, UK) for 40-50 minutes reaching a final volume of 100-150 µl for the lentiviral particle concentration (Figure 2.5).

2.5.4 Titration of lentivirus

HEK293FT cells were seeded in a 6-well plate 24 hours before lentiviral transduction to reach a cell confluence of 50-60% by the second day for titration. Lentiviral particles in a series of volumes of 50 µl, 100 µl, 250 µl crude lentiviral particles and 2.5 µl, 5 µl, 7.5 µl concentrated lentiviral particles resuspended in 0.5 ml of fresh culture medium were added into each well to test the concentration efficiency. After 24 hours, the culture medium was refreshed. EYFP expression was checked at 72 hours post-transduction. Cells from each well were trypsined and transferred to a 650 square scaled 10 cm^2 petri dish for cell counting. 50 out of 650 squares were randomly selected under 100 x magnifications with the epi-microscope (Olympus 1 x 71, Olympus, UK) and fluorescent cells were counted. The titration of

Figure 2.5
The procedure of lentiviral particle generation

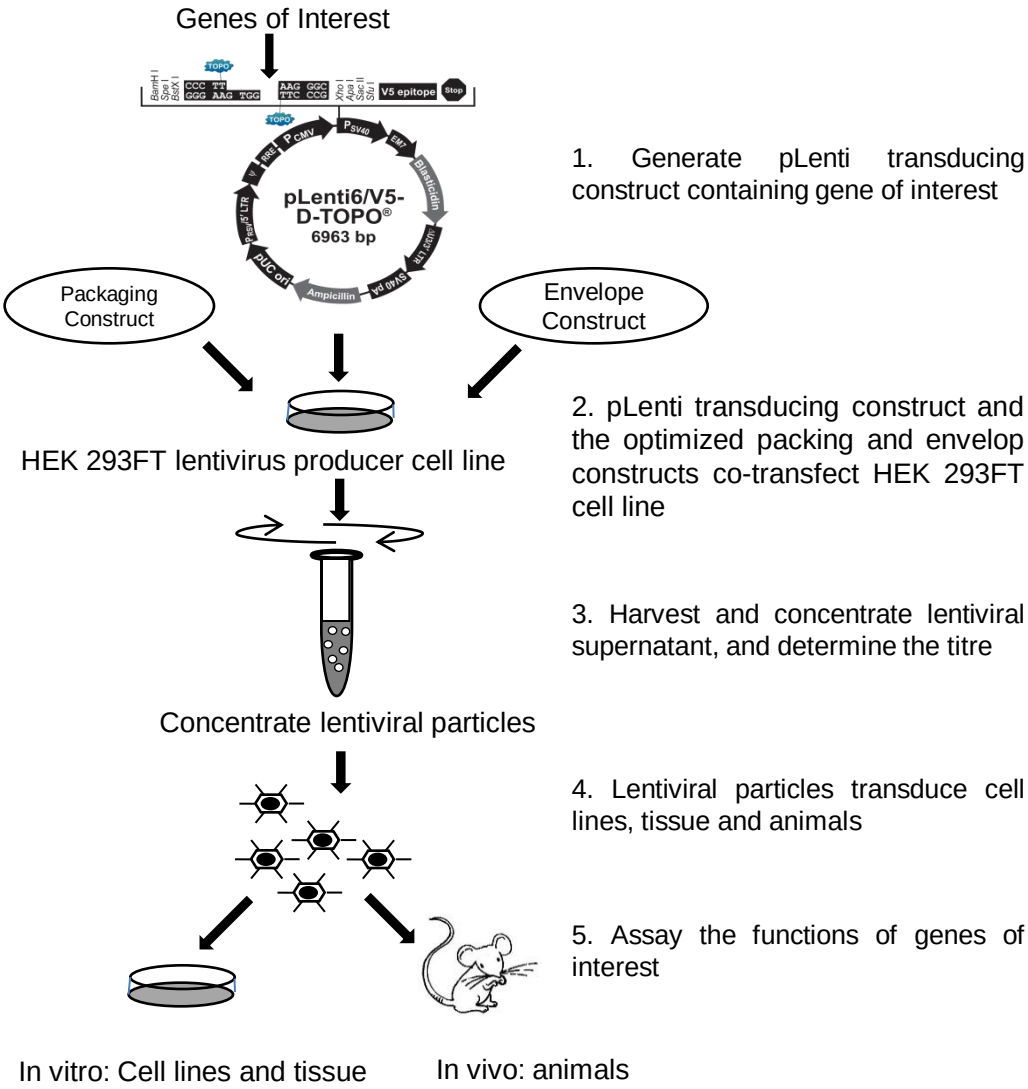

Figure 2.5 The procedure of lentiviral particle generation. pLenti transducing construct containing gene of interest was generated, and co-transfected HEK293FT cell line with packaging and envelop constructs to produce lentiviral particles. Lentiviral particles are harvested 24 hours after transfection, washed, concentrated and transduced cell lines, primary cells, tissue or animals for further analysis.

lentiviral particles was defined as transduced unit (no. of fluorescent cells) per ml of lentiviral particles (TU/ml).

The titre of lentiviral virus production was very constant among different batches. The variation in the titre of lentiviral particles was among 0.87-1.58 time. When compared the titre between the stored and freshly-harvested lentiviral particles, we found the titre reduced by 10^2-10^3 times (n = 5) after storage in 4 ℃ or -80 ℃. As a result, we freshly prepared lentiviral particles for each cell transduction.

2.6 Native murine anterior pituitary cell culture and lentiviral transduction

Native murine anterior pituitary cell culture was routinely prepared every Friday either from WT or $BK^{-/-}$ mice and transduced with fresh concentrated lentiviral particles 24 hours after preparation. Fluorescent cells were normally visible 48-72 hours post-transduction. Each batch of primary cell culture was used for 5 days electrophysiological recordings. After 5 days, the membrane of primary cells became very fragile, which made the cell-patch quite difficult to achieve. Also, even after formed cell access, the time for stable recording was very limited. As a result, we defined the time window for investigation was 2-7 days after lentiviral transduction, and prepared fresh batch of cells every week. In a small number of experiments, fluorescent corticotrophs from POMC-GFP transgenic mice were used and also prepared as above.

2.6.1 Preparation of native murine anterior pituitary cell culture

Three or four mice were killed by cervical dislocation, and bodies were removed. Pituitaries were gently removed from heads and chopped to remove the intermediate lobes. The remaining anterior pituitary lobe was chopped twice with a single edged razor blade (ASR, USA) setting 0.7 mm in both direction (rotated plate by 90 °) and placed in DMEM (+25 mM HEPES) containing 0.25% trypsin and 10 µg/ml DNAse I, and incubated at 37 ℃ for 20-25 minutes in a water bath. The tube was shaken every 5 minutes to achieve a complete and equal digestion. At the end of the digestion, after tissue pieces settled to the bottom of the tube supernatant was aspirated. 1 ml inhibitor solution (DMEM (+25 mM HEPES) containing 0.5 mg/ml lima bean trypsin inhibitor, 100 kallikrein units aprotinin (200 x dilution of Sigma stock), 10 µg/ml DNAse I) was added and the tissue bits were triturated with a 1 ml pipetman tip for about 40 times until little tissue pieces visible. The resulting suspension was filtered over a cell strainer with 70 µm nylon mesh (BD Falcon™, USA), diluted with an equal volume of culture medium (DMEM (+ 25 mM HEPES) +ITS (5 µg/ml insulin, 50 µg/ml transferrin, 30 nM sodium selenite) (ITS 100 ×, Sigma3146) + 0.3% BSA (w/v) (30% BSA, Sigma A9576) + 4.2 µg/ml fibronectin (0.1% fibronectin, Sigma F1141)) and spun in centrifugation at 100 × g for 10 minutes. The pellet was triturated in 1 ml culture medium with 1% antibiotic for 20-30 times in order to disperse single cells. 20 µl was firstly plated onto one coverslip to check how well cell dispersed. If 80% of cells stayed in single cells, and then the volume was made up to 12 ml with culture medium for plating. Cells from four anterior pituitaries were plated on 12 mm coverslips (12 mm round, Warner

Instruments) in a 6-well plate (4 coverslips per well) and incubated at 37℃ in 5% CO_2. The culture medium was refreshed every 2 days.

2.6.2 Transduction of native murine anterior pituitary cells with lentiviral particles

The cultured primary cells were replaced with non-antibiotic culture medium 6-7 hours after preparation until cells attached to the coverslips for lentiviral transduction. Cultured primary cells were transduced with lentiviral particles 24 hours after preparation. 100-150 µl freshly concentrated suspension of lentiviral particles (section 2.5.3) were diluted in 6 ml non-antibiotic culture medium for a 6-well plate. Fresh culture medium was replaced 24 hours post-transduction. Fluorescent cells were normally observed 48-72 hours post-transduction and targeted for electrophysiological analysis.

2.7 Cell imaging

ACTH antibody was used to counterstain lentiviral transduced corticotrophs to check the transduction efficiency and eYFP expression specificity.

2.7.1 Cell fixation, permeabilization and nuclear staining

Native murine pituitary cells cultured on coverslips 3-4 days after lentiviral transduction were gently washed 3 times with phosphate buffered saline (PBS) containing 1 mM Ca^{2+} and 2 mM Mg^{2+}, and then fixed with 4% paraformaldehyde in

PBS for 30 minutes at RT. To decrease the background, a quench step was done with 5 mM NH_4Cl incubation for 10 minutes at RT. Cells were then permeabilized with 0.2% (v/v) Triton X-100 in PBS (PBS-T) for 10 minutes and the cell nuclei were stained with TO-PRO-3 (Molecular Probes, USA) for 15 minutes at RT.

2.7.2 Immunohistochemistry analysis

Fixed and permeabilized cells were blocked with blocking solution (10% BSA in PBST) for 1 hour at room temperature. Primary antibody anti-ACTH (1:500 in blocking solution, Sigma, USA) was applied and incubated at 4℃ for overnight. Subsequently, cells were washed with 3 times of PBS and then incubated with Alexa 594 conjugated secondary antibody (1:500) (Molecular probes, USA) in blocking solution for 1 hour at RT. Cells were finally washed with PBS for 3 times and mounted with anti-fade Mowiol medium (Chen *et al*., 2005).

2.7.3 Confocal microscopy imaging

Mounted cells were scanned by a Zeiss LSM510 laser scanning confocal microscope equipped with a 63 x (NA 1.4) oil immersion objective lens. EYFP and Alexa 594 fluorescence were separately investigated under a 488 nm band pass filter and 543 long pass filter.

2.7.4 Lentiviral transduction efficiency and expression specificity quantification

Yellow fluorescent and Alexa 594 red fluorescent cells were randomly counted on 3 coverslips from three individual cell culture wells for each experiment, defined as eYFP and ACTH-positive cells. Five individual visual fields of every coverslip were chosen under a 100 x magnification for cell counting.

2.8 Electrophysiology: Perforated patch-clamp recording

2.8.1 Patch-clamp recording

Electrophysiology is a technique to investigate transmembrane ions movement and ion channel activities which expounds the electrical properties of live cells and tissues. Voltage-clamp recording provides the measurement of ion flow across cell membrane to be recorded as electrical current, while the membrane voltage is held at different experimental voltages using a feedback amplifier. Current-clamp recording allows the measurement of membrane potentials as well as action potentials due to various current injections by the feedback amplifier.

The crucial feature of the patch-clamp technique is the formation of tight seal between the cell plasma membrane and micropipette. A clean glass micropipette filled with appropriate electrolyte is gently pressed against a small patch of cell plasma membrane, to which the micropipette tip automatically tightly adheres by an interaction between glass and lipids of the cell membrane forming a seal with very high resistance (cell-attached) and mechanical stability providing the recording of

single channel current across the cell membrane patch. This tight seal is named as a gigaseal which means the resistance formed between glass and cell membrane should be in excess of 10^9 Ω. This high resistance is critical for reducing the electrical background noise which allows the very small electrical current flowing across the membrane to be recorded. The electrolyte within the pipette may be brought into fluid continuity with the cytoplasm by delivering a pulse of pressure to the electrolyte in order to rupture the small patch of membrane encircled by the micropipette rim (whole-cell recording). If the micropipette is pulled away from the cell under the whole-cell recording configuration, an outside-out patch recording may result. Alternatively, ionic continuity may be established by "perforating" the patch by allowing exogenous pore-forming antibiotics within the electrolyte to form pores on the membrane patch (perforated patch-clamp recording). Finally, the patch may be lifted off the cell with the intact membrane still attached to the micropipette (inside-out patch recording). In this study, I utilised perforated patch-clamp recording for the whole-cell ion channel voltage- and current-clamp studies on the native murine corticotroph cells.

2.8.2 Perforated patch-clamp recording

Perforated patch-clamp recording is designed to allow a limited ionic continuity between electrolyte and cell cytoplasm for recording metabolically intact cells. Perforated patch-clamp recording avoids the dilution and alteration of cell cytoplasm, especially for small volume cells, which provides a long and physiological stable recording condition. The method exploits the use of pore-forming antibiotics

(normally nystatin or amphotericin) that form membrane spanning pores only permeable to small monovalent ions (Figure 2.6).

For the stock preparation, 5 mg antibiotics was dissolved in 100 µl fresh DMSO. The stock solution was made freshly every week and stored in the dark at -20 ℃. Immediately prior to filling pipette stock antibiotic was thawed, and 2 µl was diluted in 500 µl of the pipette solution and dispersed by sonication (a cylindrical water bath sonicator (Special Ultrasonic cleaner Model G112SP1, Lab supplies, 29 Jefry lane, Hicksville, NY11801) for 30 seconds, with a vigorous central vortex (tank water level approximate 80% full) that popped and spurted like a geyser. The solution was sonicated in a round borosilicate glass tube (10 x 75 mm), with a maximum volume of 500 µl. Tube was placed in the centre of vortex. This solution was kept in the dark and used for up to 1 hour.

Comparing the time consume of the two antibiotics, nystatin and amphotericin, from the start to pores forming until stable access resistances, amphotericin worked more quickly to reach acceptable cell access due to a greater number of pores formed on the membrane. In further experiments, amphotericin was routinely used. The routinely uncompensated access resistances between 15-30 MΩ were achieved within 5-15 minutes after gigohm seal formation. Cells were normally stable for at least 1 hour for patch-clamp recordings.

Perforated whole-cell voltage-clamp and current-clamp recording measurements were performed at room temperature (20-24 ℃) on the primary isolated eYFP-

Figure 2.6
Perforated patch-clamp recording

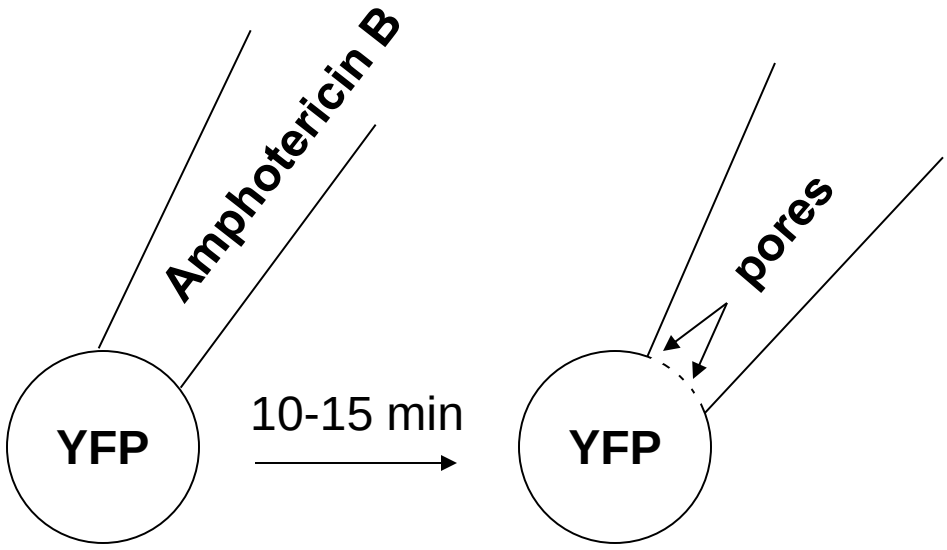

Figure 2.6 Perforated patch-clamp recording. Perforated patch-clamp recording is designed to allow a limited ionic continuity between electrolyte and cell cytoplasm for metabolically intact cells recording. Amphotericin B is used to form membrane spanning pores that are only permeable to small monovalent ions.

labelled murine corticotrophs which had been plated on the glass coverslips two days prior to use. The coverslip was placed in a perfused recording chamber situated on a fluorescent microscope (Olympus 1 x 71, Olympus, UK). The cells and patch pipettes were observed under × 40 phase contrast objective. Mechanical and hydraulic manipulators (Narishige International, Japan, model MHW-3) mounted on the microscope stage provided the control of coarse and fine movement required for patching of isolated cells. Channel activity was recorded with an Axopatch 200B patch-clamp amplifier (Axon Instruments, USA), an AD converter in the interface board (Digidata1440A, Axon Instruments, USA) and a computer for display and analysis. Glass patch pipettes (Garner Glass Company, Precision Glass Parts) with resistances from 4-5 MΩ for perforated patch-clamp recordings were mounted on mechanical and hydraulic manipulators. Recordings were made under voltage-clamp with data sampled at 10 kHZ and filtered at 2 kHZ. Current-clamp recordings were performed without any current injection allowing the recording of spontaneous action potentials. Patch-clamp data was recorded using pClamp10.1 and analysed by Clampfit 10.1 (Molecular Device).

2.8.3 Solution, drugs and hormones preparation

The standard bath solution contained (in mM): 140 NaCl, 5 KCl, 2 $CaCl_2$, 0.1 $MgCl_2$, 10 HEPES and 10 Glucose, pH 7.4 adjusted with NaOH, 300 mOsmol/1. The standard pipette solution contained (in mM): 10 NaCl, 30 KCl, 60 K_2SO_4, 1 $MgCl_2$, 10 Glucose, 10 HEPES and 50 Sucrose, pH 7.2 adjusted with KOH, 290 mOsmol/1.

A range of pharmacological blockers were applied during recordings for ion channel analysis. For stock blockers preparation, drugs were made up in the appropriate solution according to the manufacturer's instructions, aliquoted and stored at -20 ℃. For each day, a new fresh aliquot was used. Stock blockers were diluted to the working concentration with standard bath solution (Table 2.3).

CRH and AVP were applied during recordings for cell activity analysis. For stock preparation, hormones were made up in the appropriate solution according to the manufacturer's instructions, aliquoted and storied at -80 ℃. For each day, a new fresh aliquot was used. Stock hormones were diluted to the working concentration with standard bath solution with 0.2% (w/v) BSA (Table 2.3).

2.9 Data analysis

The data were expressed as means ± SEM (Standard error about the mean), n = number of independent experiments. Statistical analysis for each group was performed by standard Student's t-test or ANOVA as described in the respective figure legend. Significant differences between groups were expressed as $P < 0.01$ or $P < 0.05$.

Table 2.3

Pharmacology blockers and hormones concentrations

Blockers and Hormones	Working concentration	stock concentration (mM)	Storage temperature (℃)
TEA	1 mM	10^3	-20
Paxilline	1-10 μM	10	-20
TRAM-34	5 μM	25	-20
4-AP	1 mM	100	-20
$BaCl_2$	100 μM	100	-20
CRH	0.1 nM	0.1	-80
AVP	2 nM	1	-80

Chapter Three:

Potassium channels in native murine pituitary corticotrophs

3.1 Introduction

3.1.1. The limitation of live native corticotroph identification

Lack of routine methods to identify corticotrophs from the other anterior pituitary cells partly limited the investigation of the cell properties of native pituitary corticotrophs. Pituitary corticotrophs with small cell size and population makes the cell enrichment very difficult. Most previous labelling methods were mainly based on the corticotroph unique endocrine properties, either sensitive to its secretagogue CRH or detection of its secreted hormone ACTH. These methods either need to treat cells with chemicals with the potentials to change the cells condition, or staining cells after a large number of random recordings which is very inefficient. This chapter aims to develop a new method to identify native corticotrophs.

3.1.2. The design of lentiviral transduction system for corticotroph specific expression

Lentiviral transduction system is a highly efficient extrinsic gene delivery system, not only for cell lines and native cell transduction, but also displays strong transduction efficacy after *in vivo* injection both in experimental animals and patients that is widely used in many gene modulation and gene therapy areas. It offers a broad cell and tissue transduction tropism due to its envelope coating protein, VSV-G, which also protects lentivirus during the ultracentrifugation required for viral concentration. In addition, lentivirus belongs to the retroviral family, which enables efficient integration to exogenous gens to achieve long-term gene expression.

To allow live cell labelling, a fluorescence protein gene was chosen as the extrinsic gene integrated into the lentiviral transducing vector, for expression in target cells. A common fluorescence protein for transduced host cell expression is enhanced yellow fluorescent protein (eYFP), which is a small fluorescent protein of 238 amino acids. After expression, it exhibits visible bright yellow fluorescence when illuminated with UV light, and has been widely used due to its brightness and low cell toxicity. In my study, eYFP was used to label corticotrophs from other cell populations in murine anterior pituitary cells, which were targeted for further electrophysiological analysis.

Lentiviral vectors carrying eGFP gene have been used to transduce human pituitary adenoma cells, with 67.8% of cells being eGFP-positive (Roche *et al*., 2004). To avoid non-specific fluorescent labelling, a tissue specific promoter is needed to replace the CMV promoter to drive expression of the fluorescence protein gene. Previous studies suggested that primary cultured rat anterior pituitary cells showed a different transduction efficiency (from 5%-86%) using by lentiviral transduction (Roche *et al.*, 2004). All anterior pituitary endocrine cells were transduced using the phosphoglycerate kinase (PGK) promoter, but none using the human growth hormone (GH) promoter (Roche *et al.*, 2004). Lentiviral vectors with the α-subunit 1 human glycoprotein hormone -subunit promoter mainly transduced thyrotroph and gonadotroph cells, and when driven by the α-subunit 2 human glycoprotein hormone -subunit promoter more selectively transduced PRL, GH and adrenocorticotrophin (ACTH) cells (Roche *et al.*, 2004). In this project, the minimal rat pro-opiomelanocortin (rPOMC) gene promoter, which drives expression specifically in anterior pituitary corticotrophs, was designed to replace the CMV promoter in the

lentiviral transduced vectors (Jeannotte *et al*., 1987). Together with the high transduction efficiency, the minimal rPOMC promoter should allow the fluorescent protein gene only expressed in pituitary corticotrophs.

3.1.3 Ion channels expressed in AtT20 corticotroph cell line and rat and human corticotrophs

The major class of ion channels revealed in many types of pituitary cells and corticotrophs are potassium channels. Potassium channels exert their critical functions in cell repolarization and contribute to the downstroke of the action potential and the afterhyperpolarization phase. In the AtT20 corticotroph cell line, the dominant potassium currents are mediated by BK channels, which were revealed to be inhibited by CRH via PKA signalling pathway. They have also been implicated in the feedback regulation by glucocorticoids to decrease the ACTH secretion by preventing PKA/PKC-induced inhibition of BK channels (Shipston *et al*., 1999). In rat corticotrophs, K_{ir} channels have been recorded and suggested to maintain the resting membrane potential (Kuryshev *et al*., 1997). Apamin-sensitive Ca^{2+}-activated potassium channels (SK channels) were also reported in rat corticotrophs with functions in cell membrane hyperpolarization (Tse & Lee, 1998).

Other ion channels have been recorded in pituitary corticotrophs, including voltage-gated calcium channels which are very important in the generation of action potentials and ACTH secretion (Kuryshev, Childs & Ritchie, 1996). In this thesis, the focus is mainly on the potassium ion channels in the native murine pituitary corticotrophs.

3.2 Results

3.2.1 Identification of living native murine corticotrophs using a POMC-eYFP lentiviral reporter

In an attempt to identify living murine anterior pituitary corticotrophs in primary culture of dispersed anterior pituitary cells for subsequent investigation of their electrical properties by patch-clamp electrophysiology, we generated lentiviral constructs in which the expression of enhanced yellow fluorescent protein (eYFP) was driven by the minimal rPOMC promoter as described in methods (section 2.5.1).

Dispersed anterior pituitary cells in primary cell culture were transduced with pLenti-POMC-eYFP lentiviral particles, generated in HEK293FT cells at a titre of $> 1.24 \times 10^7$. EYFP expression could be observed within 48 hrs of transduction and this expression could be maintained in culture for more than a month. However, for the data in this thesis lentiviral-transduced cells were analysed within the first 7 days following transduction with the majority of experiments performed between days 2-5 post transduction (Figure 3.1).

To test the efficiency and specificity of pLenti-POMC-eYFP constructs we undertook immunohistochemical analysis of dispersed anterior pituitary cell cultures transduced with pLenti-POMC-eYFP by staining for ACTH that only expresses in anterior pituitary corticotrophs (Figure 3.1A). In addition, we also transduced anterior pituitary primary cell cultures with a lentiviral reporter in which eYFP

Figure 3.1
Labeling of murine corticotrophs in *vitro* using lentiviral transduction of pLenti-POMC-eYFP fluorescent reporter

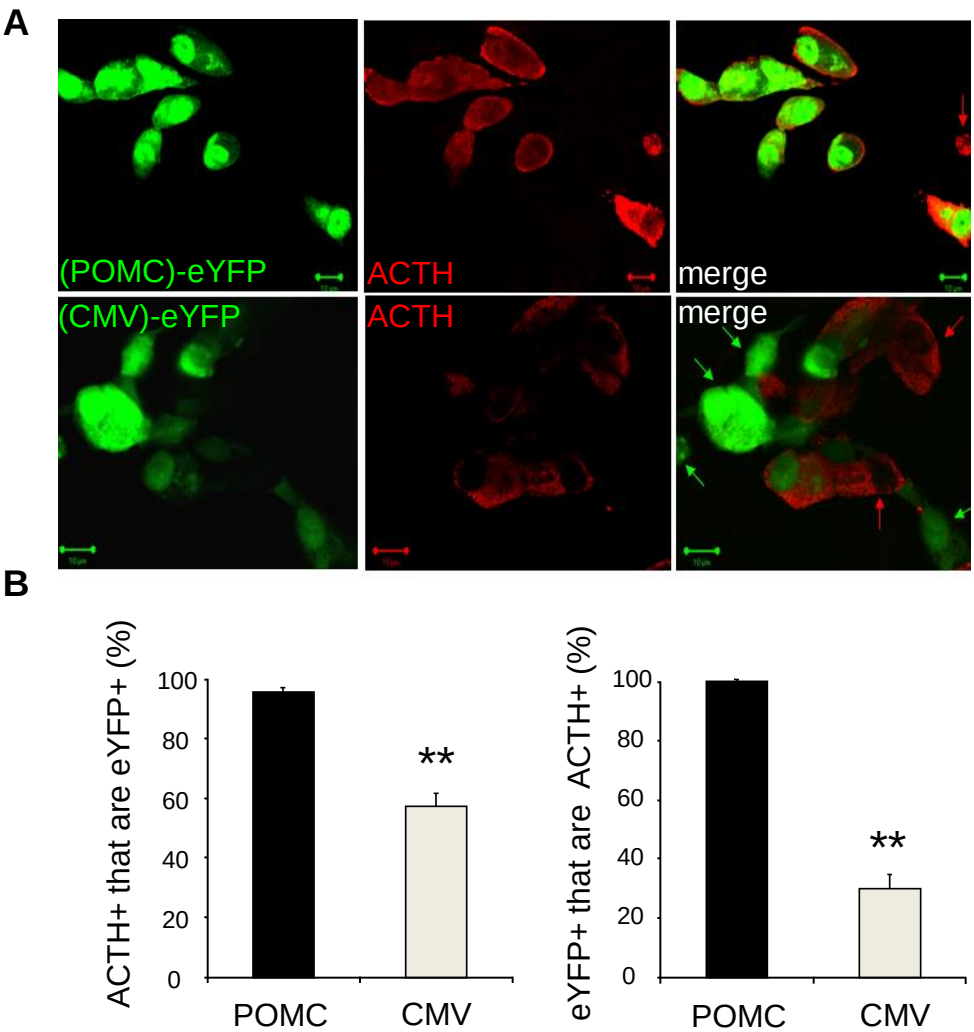

Figure 3.1 Labeling of murine corticotrophs in *vitro* using lentiviral transduction of pLenti-POMC-eYFP fluorescent reporter. A, representative confocal sections of dispersed primary anterior pituitary cells in culture 4 days after transduction with pLenti-POMC-eYFP (top panels) or pLenti-CMV-eYFP (bottom panels). The eYFP signal (left panels), ACTH immunoreactivity (middle panels) and merged images are shown. Scale bar is 10 µm. (Green arrows: eYFP-positive cells without ACTH signals. Red arrows: ACTH-positive cells without eYFP signal). **B**, quantification of percentage of cells immunoreactive for ACTH (ACTH+) that are also labelled with eYFP (eYFP+) (left panels) and eYFP (eYFP+) that are also labelled with ACTH (ACTH+) (right panels) using either pLenti-POMC-eYFP or pLenti-CMV-eYFP. All data are means ± SEM, n > 3 independent experiments (> 100 cells/experiment). ***P* < 0.01 (Student's t-test).

expression was driven by the CMV promoter, which allows gene expression in a wide range of mammalian cells.

Confocal microscopy revealed that eYFP was expressed in the nucleus and cytoplasm of anterior pituitary cells transduced with either pLenti-POMC-eYFP or pLenti-CMV constructs (Figure 3.1A left). Immunostaining for ACTH revealed robust cytoplasmic staining in a proportion of anterior pituitary cells (Figure 3.1A middle). To determine the efficiency of corticotroph labelling by the POMC-driven expression of eYFP we quantified the percentage of cells immunoreactive for ACTH that was also labelled with eYFP using the pLenti-POMC-eYFP reporter (Figure 3.1B left). More than 95% of ACTH-positive cells also expressed eYFP after transduction by pLenti-POMC-eYFP significantly greater than the proportion of ACTH-positive cells expressing eYFP driven by CMV promoter (Figure 3.1B, $P < 0.01$, Student's t-test). This suggests the efficiency of corticotroph labelling is > 95% using the pLenti-POMC-eYFP reporter. To determine the specificity of corticotroph labelling we also quantified the percentage of eYFP-positive cells that were also ACTH-positive using both pLenti-POMC-eYFP and pLenti-CMV-eYFP constructs (Figure 3.1B right). Using the pLenti-POMC-eYFP construct more than 99% of eYFP-positive cells co-labelled for ACTH. In contrast, less than 35% of eYFP cells labelled using the CMV–driven expression of eYFP displayed ACTH immunoreactivity.

Taken together these data suggest that the pLenti-POMC-eYFP transduction system allows high efficiency and specificity of corticotroph labelling in murine primary

anterior pituitary cell cultures. It allowed the routine labelling and visualisation of native live murine corticotrophs amenable for patch clamp electrophysiological investigation.

3.2.2 Whole-cell outward currents of native mouse corticotrophs

Once the eYFP expression was detectable 2 days after transduction, the expression level kept increasing and stayed stable after 3-4 days. Electrophysiological data from different days were compared, and no significant differences were found, which implied that the expression level of eYFP had no effect on the corticotroph cell excitability. We stopped use cells after 7 days of transduction was due to the cell membrane becoming fragile and the stability of patch recording being lost. The expression of eYFP controlled by the minimal rPOMC promoter in corticotrophs for cell labelling allowed enough fluorescence for detection, but with no dateable adverse effects on murine anterior pituitary corticotrophs. The establishment of the high efficiency labelling and identification of native murine corticotrophs *in vitro* allowed us to analyse the electrophysiological properties of these cells. Cells with clear fluorescent were chosen to be patched targets, no matter there were single isolated cells or cells with neighbours. No significant difference in the electrical activities were detected be tween them.

We first attempted to analyse the properties of corticotrophs using the conventional whole-cell recording technique. Recordings of total outward current in voltage-clamp were relatively stable over approximately 30 minutes of recording. However, in current-clamp spontaneous action potentials were only recorded within the first 10

seconds of going whole-cell and the membrane potential rapidly depolarized by ~40 mV resulting in abolition of firing (n = 20). ATP was added in the standard pipette solution however, no obvious improvement was observed. As a result, all subsequent data was performed using the perforated patch-clamp recording technique using amphotericin B in the patch pipette.

In the perforated patch mode, gigaseals up to 16 GΩ were obtained in more than 80% of all pLenti-POMC-eYFP construct labelled fluorescent cells patched. When stable perforated-patch recording was established, 95% of the cells had an input resistance typically greater than 3 GΩ. Cells with input resistance < 2 GΩ were discarded. In 90% of the cells uncompensated access resistances between 15-30 MΩ was achieved within 5-15 minutes of gigaseal formation. Cells were normally stable for up to 1 hour for recording. The fluorescent labelled corticotrophs recorded in the perforated patch recording mode had a cell capacitance of 3.25 ± 1.15 pF.

We first analysed the total whole-cell outward potassium currents in physiological gradients in voltage-clamp. Previous data from mouse AtT20D16:16 cell line has suggested the outward potassium conductance is dominated by large conductance calcium and voltage activated potassium channels (BK channels). Thus, we analysed the whole-cell outward currents of corticotrophs from both wild type (WT) mice and mice in which the BK channel has been genetically deleted ($BK^{-/-}$).

A standard protocol with holding potential at -80 mV stepped from -80 to 100 mV corticotrophs from both genotypes (Figure 3.2). Firstly, outward current that

Figure 3.2
Whole-cell outward currents in native murine corticotrophs

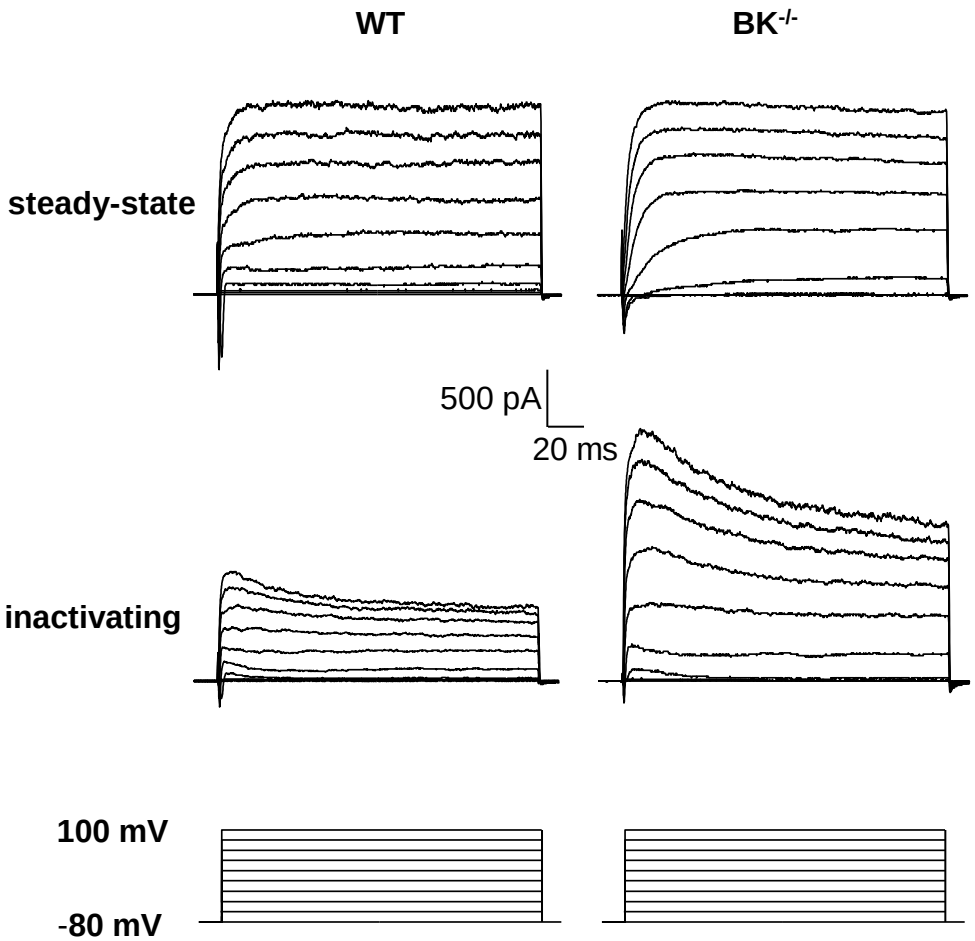

Figure 3.2 Whole-cell outward current in native murine corticotrophs. Representative voltage-clamp recording in the perforated patch-clamp mode of corticotroph whole-cell outward current traces display rapid activation and reaching steady-state plateau with little inactivating (top panel) or display marked inactivation (middle panel). Voltage protocol with a holding potential at -80 mV depolarized to +100 mV in 20 mV steps for 200 ms (bottom panel) in physiological extra- and intracellular solutions both for WT and $BK^{-/-}$ corticotrophs.

displayed rapid activation and reached a steady-state plateau at depolarised potentials that showed little inactivation during the pulse was routinely seen (Figure 3.2). In addition, outward currents that showed marked inactivation at depolarised potentials during the 200 ms pulse were also observed (Figure 3.2).

To test whether the outward potassium current of native murine corticotrophs is dominated by BK channels we compared the steady-state outward current density in corticotrophs from WT, $BK^{-/-}$ and heterozygous animals (Figure 3.3). However, measuring the steady-state current density normalised to cell capacitance at 190 ms into the depolarising pulses revealed no significant difference between the three genotypes. For example, at 100 mV the current density was 454 pA/pF in WT, 305 pA/pF in hets and 456 pA/pF in $BK^{-/-}$ corticotrophs. This suggests that the BK channel may not contribute significantly to the whole-cell outward current in native murine corticotrophs.

To determine that the relative lack of outward BK current was not a result of the lentiviral transduction we also assayed the steady-state outward current density at 190 ms into the pulses in wild-type corticotrophs from a mouse transgenic line in which GFP is constitutively expressed in corticotrophs under control of the minimal rPOMC promoter. However, the current density normalised to cell capacitance was not significantly different at any potential examined (Figure 3.4). For example, at 100 mV the current density was 345 pA/pF in pLenti-POMC-eYFP labelled corticotrophs and 398 pA/pF in corticotrophs from POMC-GFP mice.

Figure 3.3
Steady-state outward current density of labeled corticotrophs from different genotypes

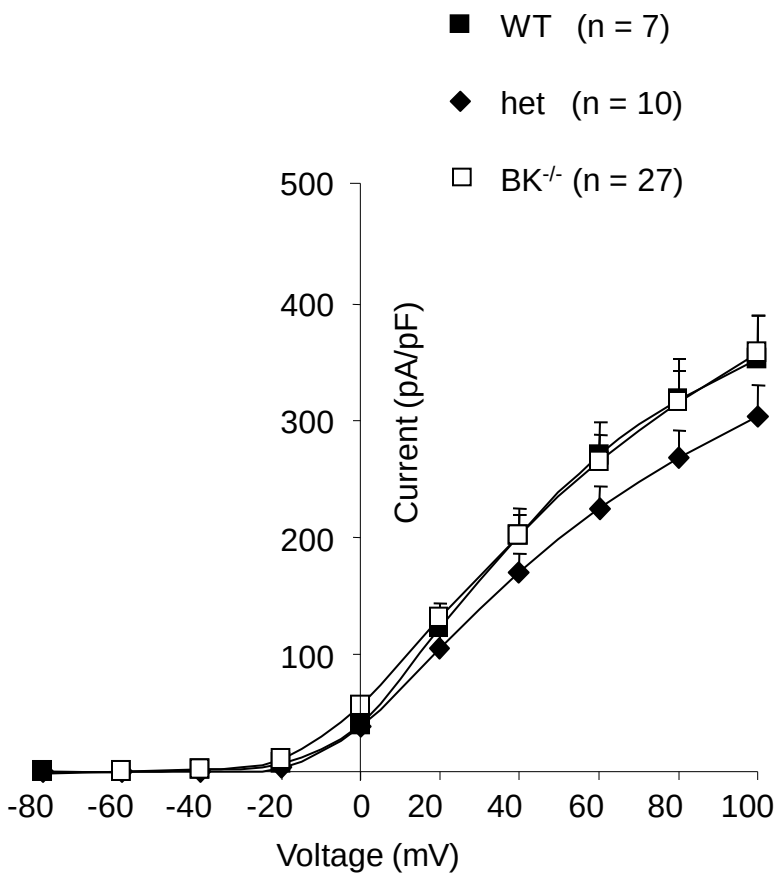

Figure 3.3 Steady-state outward current density of labeled corticotrophs from different genotypes. Current-voltage relationship of corticotrophs whole-cell outward current determined at steady-state (190 ms) from three different genotypes, WT (■, n = 7), heterozygous (◆, n = 10) and $BK^{-/-}$ (□, n = 27). The steady-state current density of labelled corticotrophs from the three genotypes was between 300-350 pA/pF at 100 mV in the *I-V* plot with no significant difference between them. All data are means ± SEM, n, no. of independent recorded cells.

Figure 3.4
Steady-state outward current density of lentiviral transduced and transgenic corticotrophs

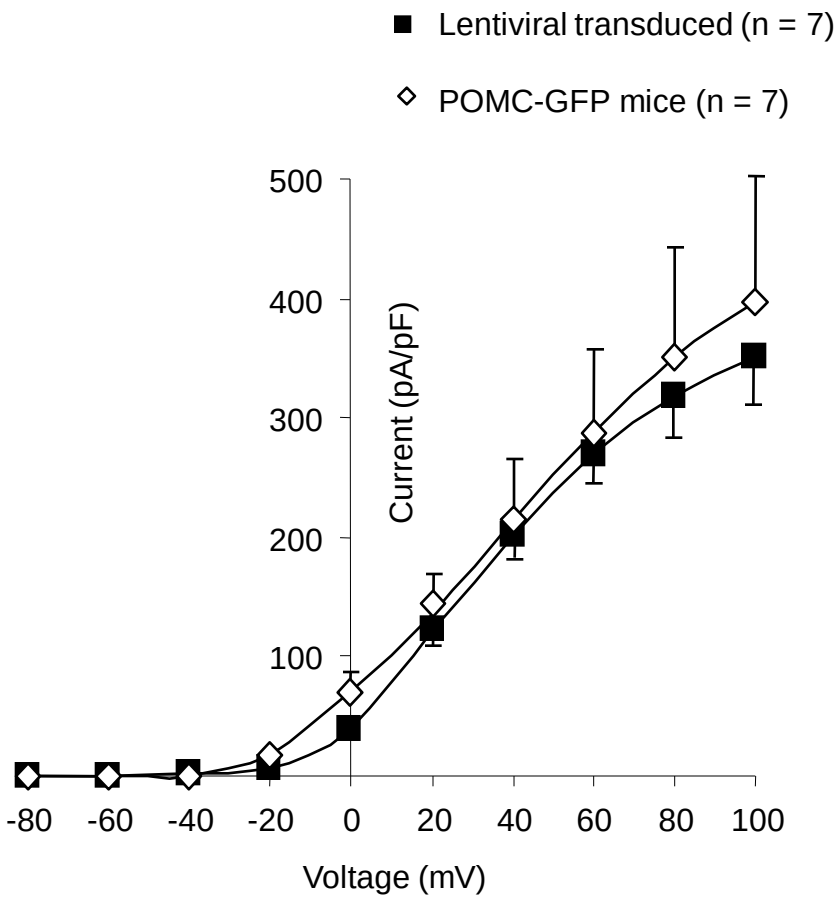

Figure 3.4 Steady-state outward current density of lentiviral transduced and transgenic corticotrophs. Current-voltage relationship of the whole-cell outward current determined at steady-state (190 ms) of pLenti-POMC-eYFP transduced corticotrophs (■, n = 7) and corticotrophs from POMC-GFP transgenic mice (◇, n = 7). The steady-state current density measured at 190 ms showed no significant difference between them. All data are means ± SEM, n, no. of independent recorded cells.

In preliminary transduce experiments FCS was used as the supplement in the medium. Considering the corticotrophs are hormone regulated cells, hormones in the serum may change the status of corticotrophs, thus FCS was replaced with ITS in the culture medium. Corticotroph cells cultured with ITS showed higher transduction efficiency suggesting serum may have a negative influence in the lentiviral transduction. In our primary cell culture assay we used a minimal serum replacement medium (insulin-transferrin-sodium, ITS) rather than foetal calf serum (FCS). This was in an attempt to avoid variability due to different levels of steroids and other hormones in serum that are known to regulate ion channel expression, including BK channels.

Thus, to determine whether culture conditions also affected outward steady-state current density we analysed current density of cells grown either in the presence of ITS or FCS (Figure 3.5). However, there was no statistically significant difference in the whole-cell outward current density at any potential examined. For example, at 100 mV the current density was 333 pA/pF in ITS treated and 247 pA/pF in FCS treated corticotrophs.

3.2.3 Pharmacological characterisation of outward potassium currents

In order to determine the potassium channels that contributed to the whole-cell outward current of native murine corticotrophs, we chose different potassium channels blockers to identify different potassium current components. Potassium

Figure 3.5
Steady-state outward current density of labeled corticotrophs in different culture conditions

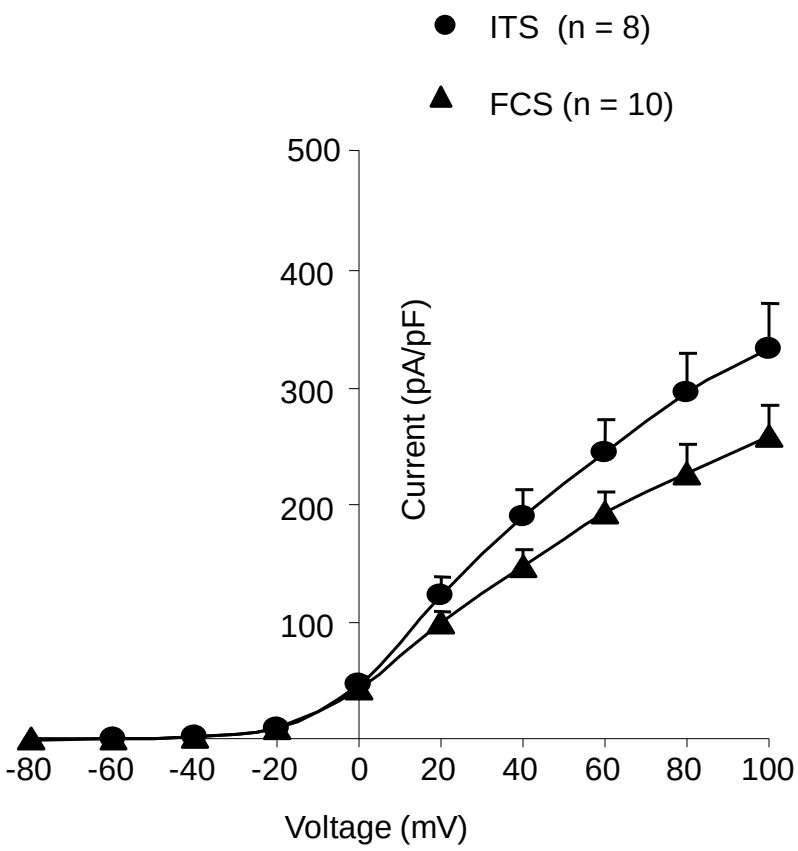

Figure 3.5 Steady-state outward current density of labeled corticotrophs in different culture conditions. Current-voltage relationship of the whole-cell outward current determined at steady-state (190 ms) of corticotrophs cultured either in the presence of ITS (●, n = 8) or FCS (▲, n = 10). The steady-state current density of lentiviral transduced corticotrophs showed no significant difference between culture conditions. All data are means ± SEM, n, no. of independent recorded cells.

channel blockers were applied to corticotrophs from WT and $BK^{-/-}$ mice to examine differences in potassium channel expression. Since pLenti-POMC-eYFP labelled corticotrophs and corticotrophs from POMC-GFP mice showed no significant difference in either the whole-cell outward current or any potassium current components, electrophysiological data from them were displayed together (Figure 3.4).

3.2.3.1 TEA-sensitive outward potassium current

TEA that blocks a wide range of potassium channels was applied to the extracellular solution bathing the native murine corticotrophs. At 1 mM TEA is relatively selective for BK channels in some systems, although may also block a range of other potassium channels. Once the whole-cell outward current was stable for over 5-10 minutes, 1mM TEA was applied to the recorded cell.

Representative traces showed that 1 mM TEA reduced the whole-cell outward current in both WT and $BK^{-/-}$ corticotrophs in 2-3 minutes after the drug was applied to the bath (Figure 3.6A). The whole-cell outward current was inhibited maximally by 1 mM TEA within 5-7 minutes after the blocker application. The steady-state whole-cell outward current was decreased by 1 mM TEA, while the inactivating component was still observed in the inhibited traces (Figure 3.6A). In the representative *I-V* plot, there was detectable current inhibition by 1 mM TEA at all depolarizing potentials examined. The steady-state current (at 190 ms) of the whole-cell outward current measured at 100 mV was blocked by around 50% by 1 mM TEA both in WT and $BK^{-/-}$ corticotrophs (Figure 3.6B). The inhibited current

Figure 3.6
TEA-sensitive outward potassium current

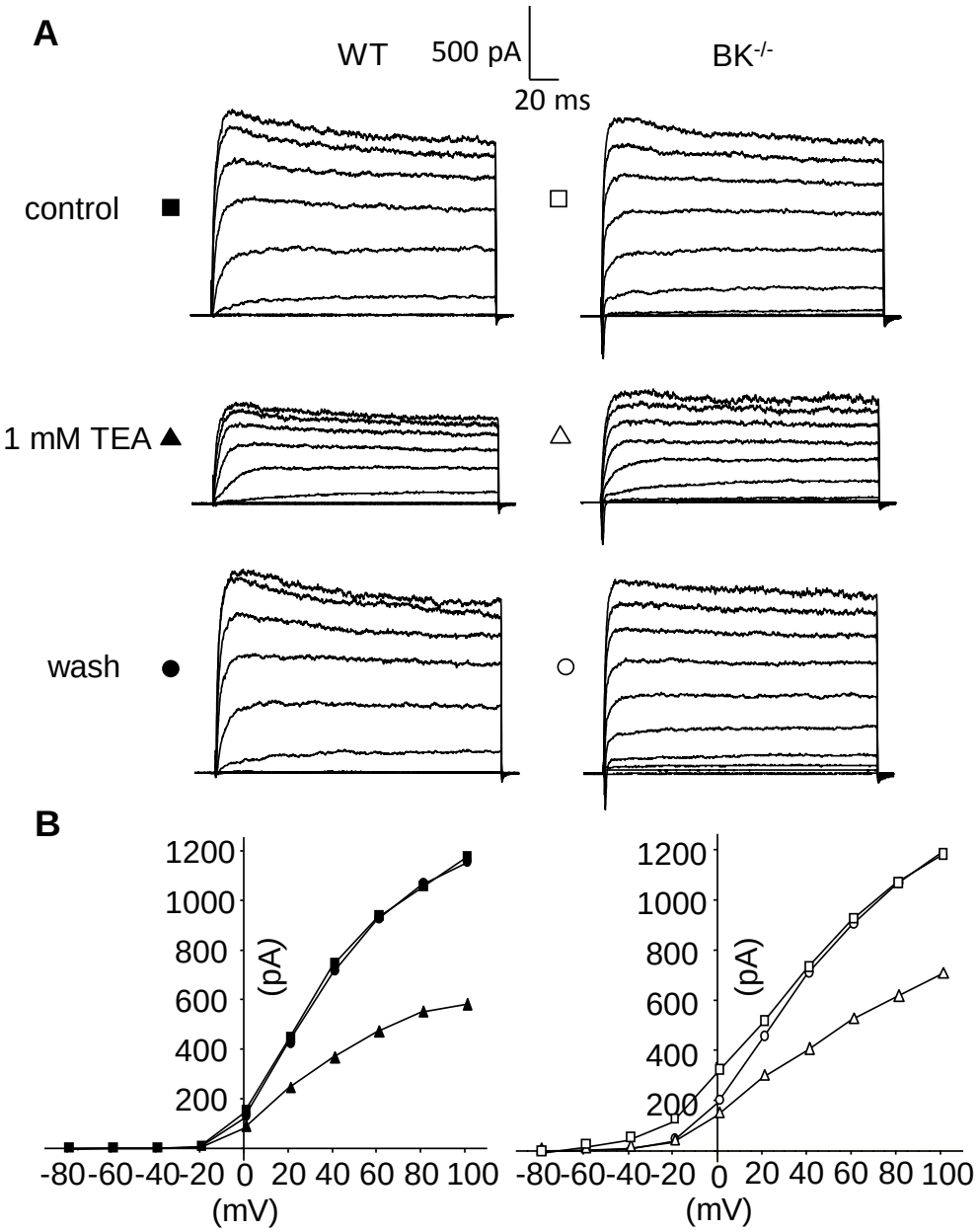

Figure 3.6 TEA-sensitive outward potassium current. **A**, representative voltage-clamp recording in perforated patch-clamp mode of a corticotroph cell depolarised from a holding potential of -80 mV to +100 mV in 20 mV steps before (cont, □), during (TEA, △) and after washout (wash, ○) exposure to 1 mM TEA (closed symbol for WT and open symbol for $BK^{-/-}$). **B**, current-voltage relationship of the whole-cell outward current from the cells as in A determined at the steady-state (190 ms). The whole-cell outward current amplitude was reduced by 50% at +100 mV for both WT and $BK^{-/-}$ corticotrophs.

returned to the control level after washing with the standard extracellular bath solution for 5-10 minutes (Figure 3.6A). In all WT (n = 12) and $BK^{-/-}$ (n = 7) corticotrophs, 1 mM TEA displayed a similar inhibition and complete washout of the whole-cell outward current. On average, 1 mM TEA blocked around 35-40% of the whole-cell outward current both in WT and $BK^{-/-}$ corticotrophs. WT and $BK^{-/-}$ corticotrophs showed no significant difference in response to 1 mM TEA inhibition (Figure 3.7).

When raising the concentration of TEA to 5 mM, only 14.9 ± 1.9% of the whole-cell outward current was left in WT cells (n = 7), and 13.4 ± 1.1% in $BK^{-/-}$ (n = 8) , and there were no further inhibition when 10 mM TEA was applied in both WT and $BK^{-/-}$ corticotrophs.

These data suggest that for both WT and $BK^{-/-}$ 35-40% of the whole-cell outward current was sensitive to 1 mM TEA. 5 mM TEA eliminated almost all the whole-cell outward current revealing that potassium channels were the main components in the murine native corticotrophs. However, as TEA is a general potassium channels blocker that is not able to identify potassium channels specifically, more specific potassium channel blockers were used in the further investigation.

3.2.3.2 Paxilline-sensitive outward current

Previous research indicated that in the mouse AtT20D16:16 cell line, the outward potassium conductance was dominated by BK channels. To test whether BK

Figure 3.7
Inhibition of outward potassium current by 1 mM TEA

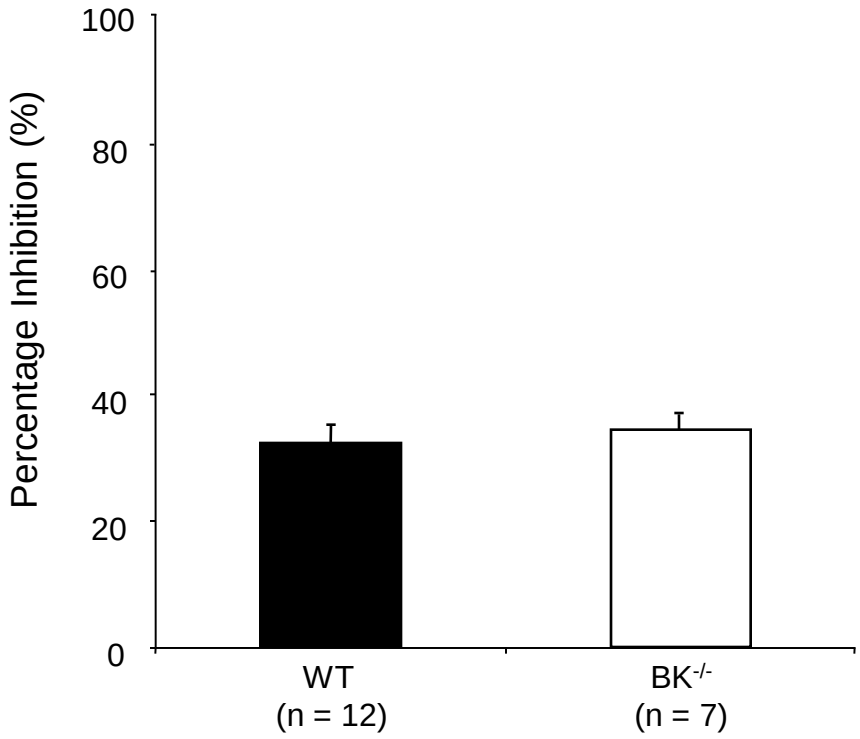

Figure 3.7 Inhibition of outward potassium current by 1 mM TEA. 1 mM TEA blocked 35-40% of the whole-cell outward steady-state current at +100 mV. There was no significant difference in current inhibition between WT and $BK^{-/-}$ corticotrophs. All data are means ± SEM, n, no. of independent recorded cells.

channels were dominant in native murine corticotrophs too, the BK channel specific blocker paxilline was used. Since WT and $BK^{-/-}$ corticotrophs did not show any significant difference in the whole-cell outward current (Figure 3.3), we attempted to investigate whether BK channels represent a small current component in WT corticotrophs or other channels compensate for BK channel deletion in $BK^{-/-}$ corticotrophs.

1 μM paxilline (prepared in 0.1% DMSO in the standard extracellular solution) was applied to the corticotroph after ensuring the cell current was stable for 5-10 minutes. Representative traces and the *I-V* plot are showed in Figure 3.8A. In 11/14 WT corticotrophs, 1 μM paxilline resulted in a small inhibition (< 5 %) at the steady-state of the whole-cell outward current measured at 100 mV (Figure 3.8A & B left). However, in 3/14 WT corticotrophs, 1 μM paxilline showed a large decrease (10-20%) of the steady-state whole-cell outward current. In $BK^{-/-}$ corticotrophs, 8/10 cells had no detectable decrease in the whole-cell outward current in the presence of 1 μM paxilline (Figure 3.8A & B right). While 2/10 cells displayed a small reduction (< 5 %) of the steady-state whole-cell outward current.

0.1 % DMSO alone in the extracellular solution was used as control to exclude the effect of DMSO on the whole-cell outward current of the corticotrophs and there was only 0.35 ± 0.32% inhibition on the whole-cell outward current by 0.1 % of DMSO in WT corticotrophs (n = 5).

Figure 3.8

Paxilline (1 µM) sensitive outward potassium current

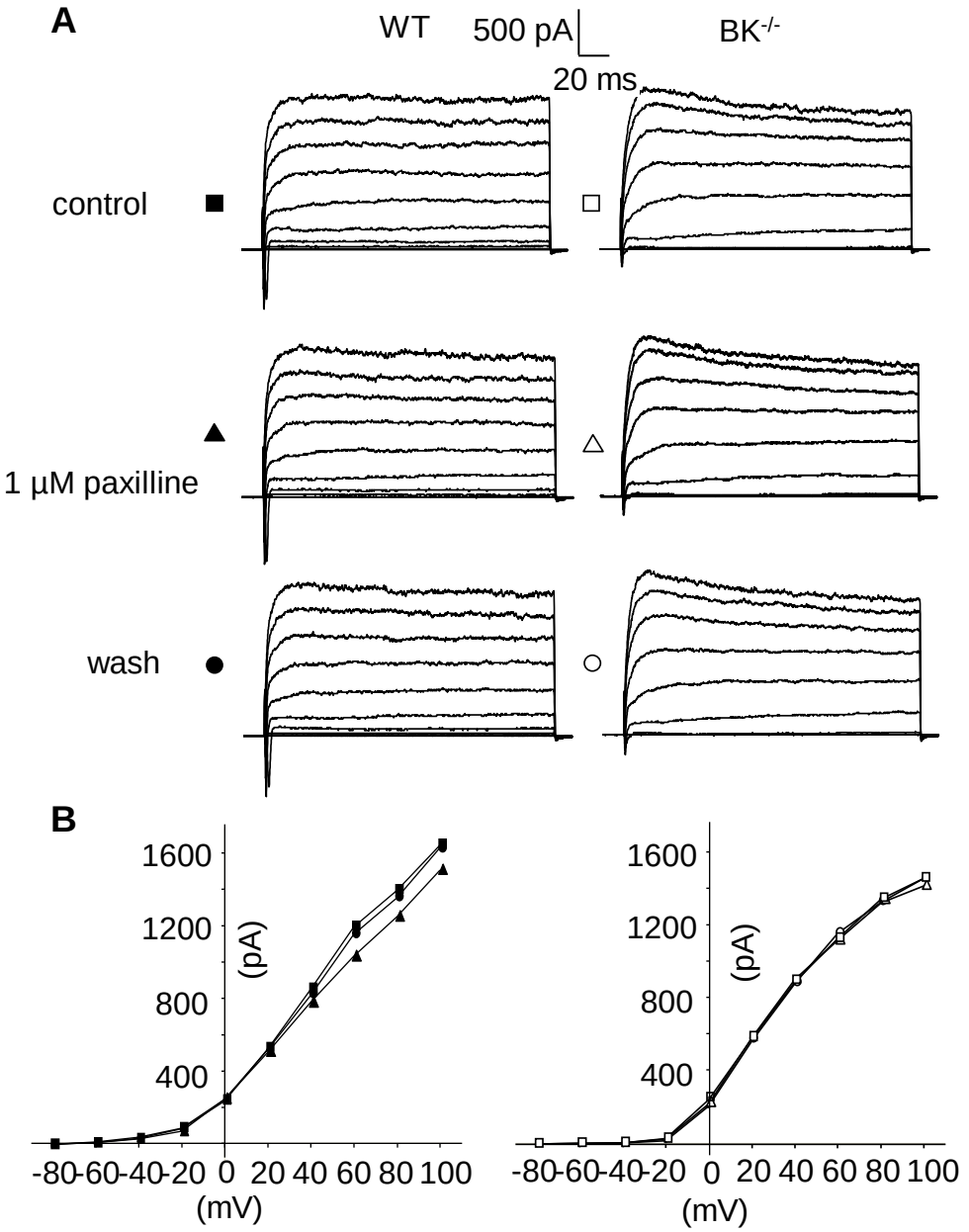

Figure 3.8 Paxilline (1 µM) sensitive outward potassium current. **A**, representative voltage-clamp recording in the perforated patch-clamp mode of a corticotroph cell depolarised from a holding potential of -80 mV to +100 mV in 20 mV step before (cont, □), during (paxilline, △) and after washout (wash, ○) exposure to 1 µM paxilline (closed symbol for WT and open symbol for $BK^{-/-}$). **B**, current-voltage relationship of the whole-cell outward current from the cells as in A determined at the steady-state (190 ms). The whole-cell outward current amplitude was blocked by less than 5% at +100 mV for the WT corticotrophs. Little inhibition was detected in $BK^{-/-}$ corticotrophs.

On average, paxilline blocked less than 10% of the whole-cell outward current in the WT corticotrophs (n = 14) and less than 5% in $BK^{-/-}$ corticotrophs (n = 10). WT and $BK^{-/-}$ corticotrophs showed no statistically significant difference in the whole-cell outward current inhibition by 1 μM paxilline (Figure 3.10).

Thus, in contrast to the mouse AtT20 cell line, BK channels only contributed a small conductance in the whole-cell current of native murine corticotrophs. Since paxilline is reported to be a specific BK channel blocker, we increased the concentration of paxilline to see if there would be a larger inhibition. When 10 μM paxilline was applied to the extracellular solution for 3-5 minutes, the steady-state whole-cell outward current was reduced by around 75% in WT corticotrophs (Figure 3.9A & B left). In the $BK^{-/-}$corticotrophs, the whole-cell outward current showed a 55% inhibition by 10 μM paxilline (Figure 3.9A & B right). In both genotypes the inhibited steady-state current component was washed out and reversed to the control current density after 10-15 minutes washout.

Extracellular solution with 1% of DMSO was performed as a control, and there was no detectable effect on the whole-cell outward current in the presence of 1% of DMSO, which demonstrated 10 μM paxilline had a marked inhibition of the corticotroph whole-cell outward current for WT and $BK^{-/-}$ mice. The percentage of inhibition was 56% of the whole-cell outward current in WT (n = 7) corticotrophs by 10 μM paxilline, and for $BK^{-/-}$ (n = 7) the corticotroph whole-cell outward current was reduced by 32% (Figure 3.10). The whole-cell outward current of WT

Figure 3.9
Paxilline (10 µM) sensitive outward potassium current

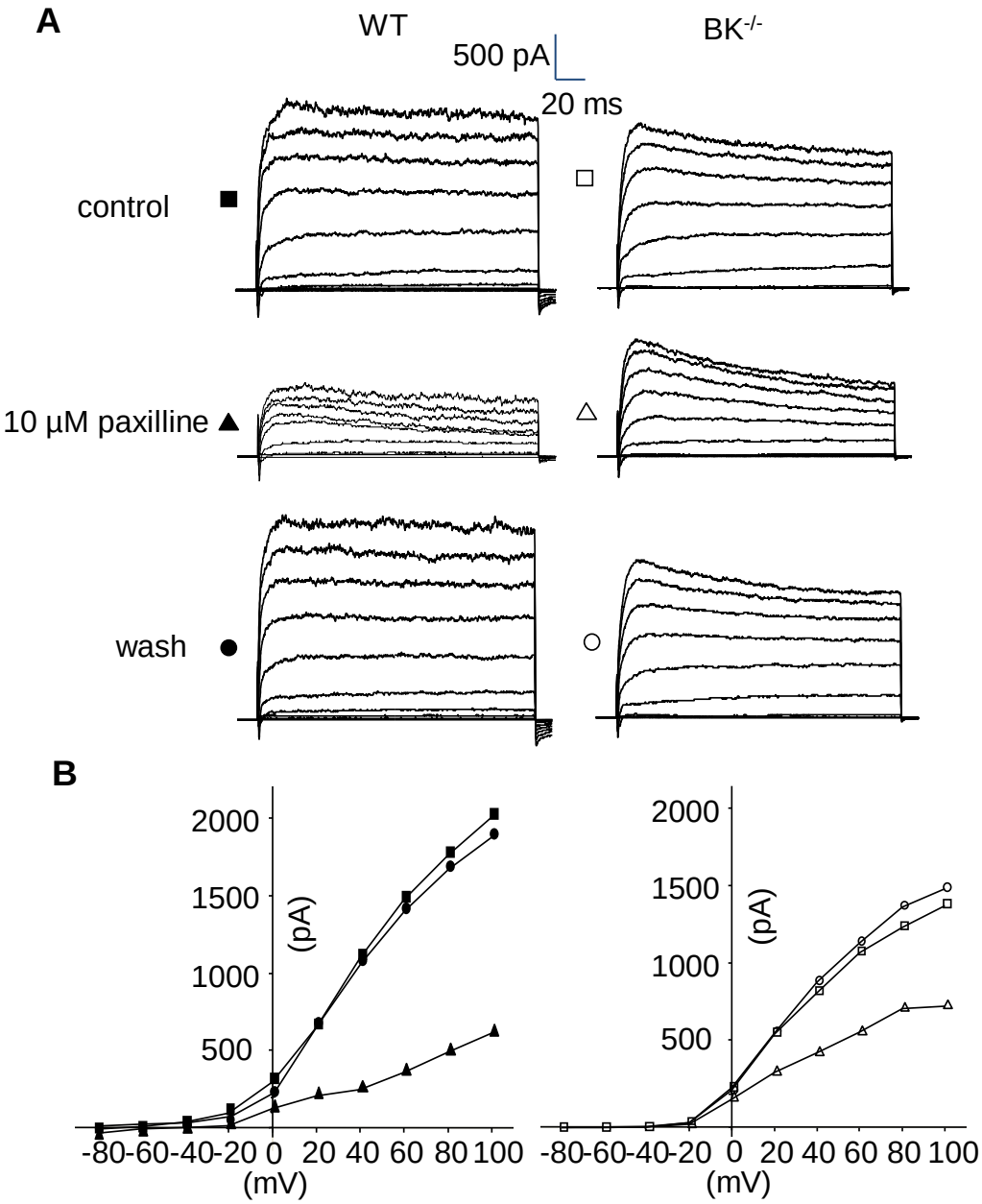

Figure3.9 Paxilline (10 µM) sensitive outward potassium current. A, in the voltage-clamp mode of perforated patch-clamp recording, representative whole-cell current traces of corticotroph depolarised from a holding potential of -80 mV to +100 mV in 20 mV steps before (cont, □), during (paxilline, △) and after washout (wash, ○) exposure to 10 µM paxilline (closed symbol for WT and open symbol for $BK^{-/-}$). **B**, current-voltage relationship of the whole-cell outward current from the cells as in A determined at the steady-state (190 ms). The WT whole-cell outward current amplitude was inhibited by 75% at 100 mV in the presence of 10 µM paxilline, and for $BK^{-/-}$ corticotrophs, the inhibition was around 50%.

Figure 3.10
Inhibition of outward potassium current by paxilline

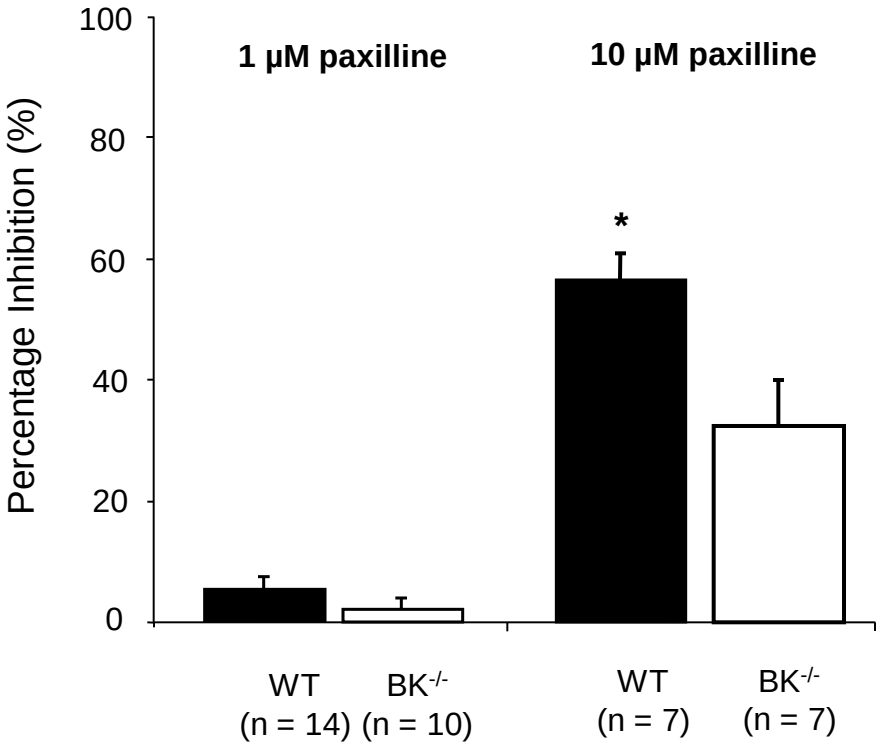

Figure 3.10 Inhibition of outward potassium current by paxilline. 1 µM paxilline blocked less than 10% of the whole-cell outward steady-state current at +100 mV averaged from WT (n = 14) corticotrophs and less than 5% for $BK^{-/-}$ (n = 10) corticotrophs. There was no significant difference in the current inhibition between WT and $BK^{-/-}$ corticotrophs. 10 µM Paxilline inhibited 56% of the whole-cell outward steady-state currents at +100 mV for WT corticotrophs (n = 7), and 32% for $BK^{-/-}$ corticotrophs (n = 7) on average. There was a significant difference in the inhibition of the whole outward steady-state (measured at 190 ms) current between WT and $BK^{-/-}$ corticotrophs in response to 10 µM paxilline. (*P < 0.05 Student's t-test). All data are means ± SEM, n, no. of independent recorded cells.

corticotrophs showed significantly larger inhibition by 10 μM paxilline than $BK^{-/-}$ corticotrophs ($P < 0.05$, Student's t-test).

Paxilline has been reported as a specific blocker for BK channels. In BK $^{-/-}$ mice, there was no BK channels expression in the corticotrophs thus these data suggest that the BK channel component was small in native murine corticotrophs. Furthermore, 10 μM paxilline displayed a marked inhibition of the whole-cell outward current in $BK^{-/-}$corticotrophs revealing that 10 μM paxilline could not be considered to block BK channels specifically. On the other hand, WT corticotrophs displayed a significant larger component sensitive to 10 μM paxilline than $BK^{-/-}$ corticotrophs. Together this suggested that not only BK channels but other channels were also blocked by 10 μM paxilline.

Compared with the relatively high expression in AtT20 corticotrophs, BK channels showed an unexpectedly small current density in the whole-cell outward current of native murine corticotrophs. We wondered whether BK channels were inhibited under our recording conditions. BK channels are also Ca^{2+}-activated potassium channels, so we designed a protocol to increase the intracellular Ca^{2+} to activate the potential BK channels in the murine corticotrophs. A two-step pulse protocol was designed to activate the voltage-gated Ca^{2+}channels (VGCCs), which allowed Ca^{2+} entry. The increased intracellular Ca^{2+} should activate the Ca^{2+}-activated potassium channels, which have been reported in other pituitary cell populations. The two-step pulse protocol differed from our standard protocol (that elicited depolarizing steps from a holding potential of -80 mV to +80 mV in 20 mV steps). In the two-step

protocol a holding potential of -80 mV was immediately followed by a 50 ms voltage-step to -10 mV, during which VGCCs should be activated to promote Ca^{2+} influx into the cell. This Ca^{2+}-influx step was immediately followed by a 100 ms depolarizing pulse to +80 mV, during which the activated BK channels were monitored. In addition, as the reversal potential for Ca^{2+} under the experimental conditions was near +80 mV, there should be minimal Ca^{2+} entry during this step. In other pituitary cell types under these conditions, in the absence of the Ca^{2+}-influx step, there was little to no change in $[Ca^{2+}]_i$, whereas in the presence of a Ca^{2+}-influx step alone or in combination with the test pulse there was a marked increase in $[Ca^{2+}]_i$, which should evoke BK channel current in WT corticotrophs.

The representative trace from the two-step Ca^{2+}-influx protocol was overlaid with the current trace at +80 mV taken from the whole-cell outward current traces examed in the standard protocol. In WT (n = 7) and $BK^{-/-}$ (n = 8) corticotrophs, the whole outward current did not show any marked increase using the two-step protocol (Figure 3.11). In the presence of 1 μM paxilline, there was 2.5 ± 2.4% inhibition using the two-step protocol comparing with the trace without a Ca^{2+}-influx step (n = 6). These data suggested no significant numbers of additional BK channels were activated in the native murine corticotrophs during the Ca^{2+} influx.

The small inhibition of the whole-cell outward current by 1 μM paxilline, no activation of BK channel by the increased intracellular Ca^{2+} and no significant difference in outward potassium current density in $BK^{-/-}$ corticotrophs compared to

Figure 3.11
Outward potassium current using a two-step pulse protocol to promote Ca^{2+} influx

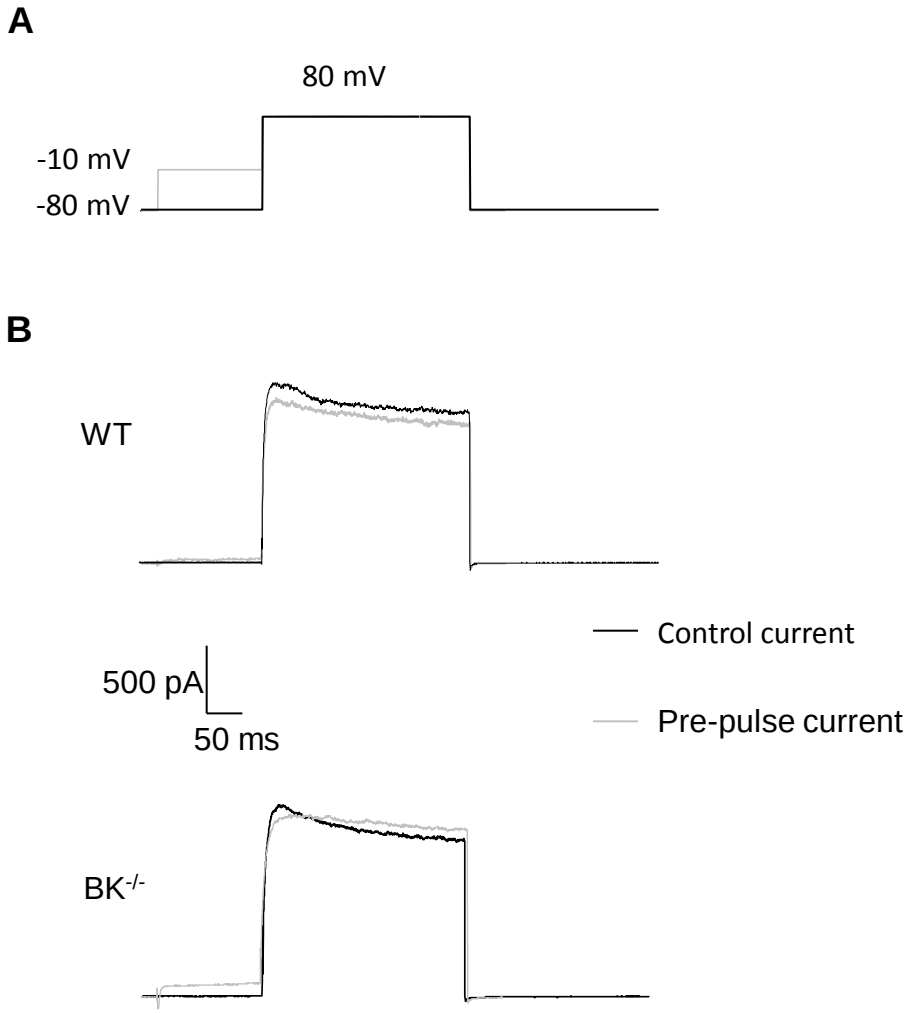

Figure 3.11 Outward potassium current using a two-step pulse protocol to promote Ca^{2+} influx. A, a two-step protocol with holding potential at -80 mV consisted of an initial 50 ms voltage-step to -10 mV and followed by one step depolarization to +80 mV was applied to the corticotrophs. **B**, representative pre-pulse current of a corticotroph in the voltage-clamp mode of perforated patch-clamp recording (black line: control current was the current trace at +80 mV from the current traces recorded under the standard protocol showing in Figure 3.2 and grey line: pre-pulse current). There was no marked increase in the pre-pulse current amplitude either for WT or $BK^{-/-}$ corticotrophs.

WT revealed BK channel was a small conductance of the whole-cell outward currents in WT native murine corticotrophs.

3.2.3.3 TRAM-34 sensitive outward current

Since BK channels had been examined that was a small current component in native murine corticotrophs, we used other specific calcium-activated potassium channel blockers. Clotrimazole is an intermediate-conductance potassium channel (SK4) blocker, and displayed a 40-50% inhibition of the whole-cell outward current both in WT and $BK^{-/-}$ corticotrophs. To eliminate the possibility that Clotrimazole might potentially inhibit other channels a more specific SK4 channel blocker TRAM-34 was applied.

Representative traces showed both WT and $BK^{-/-}$ corticotroph whole-cell outward current was inhibited in 2-3 minutes with 5 μM TRAM-34 applied to standard extracellular solution after the current was stable. TRAM-34 reduced the steady-state whole-cell outward current maximally after 5-7 minutes, while the inactivating current component was still observed in the inhibited traces (Figure 3.12A). In the representative *I-V* plot, the steady-state outward current was blocked by TRAM-34 at all depolarizing potentials (Figure 3.12B). WT corticotroph steady-state outward current measured at 100 mV was reduced by 50%, while for $BK^{-/-}$ corticotrophs the inhibition was 45% (Figure 3.12B). After standard extracellular solution washout the blocked current totally reversed (Figure 3.12A).

Figure 3.12
TRAM-34 sensitive outward potassium current

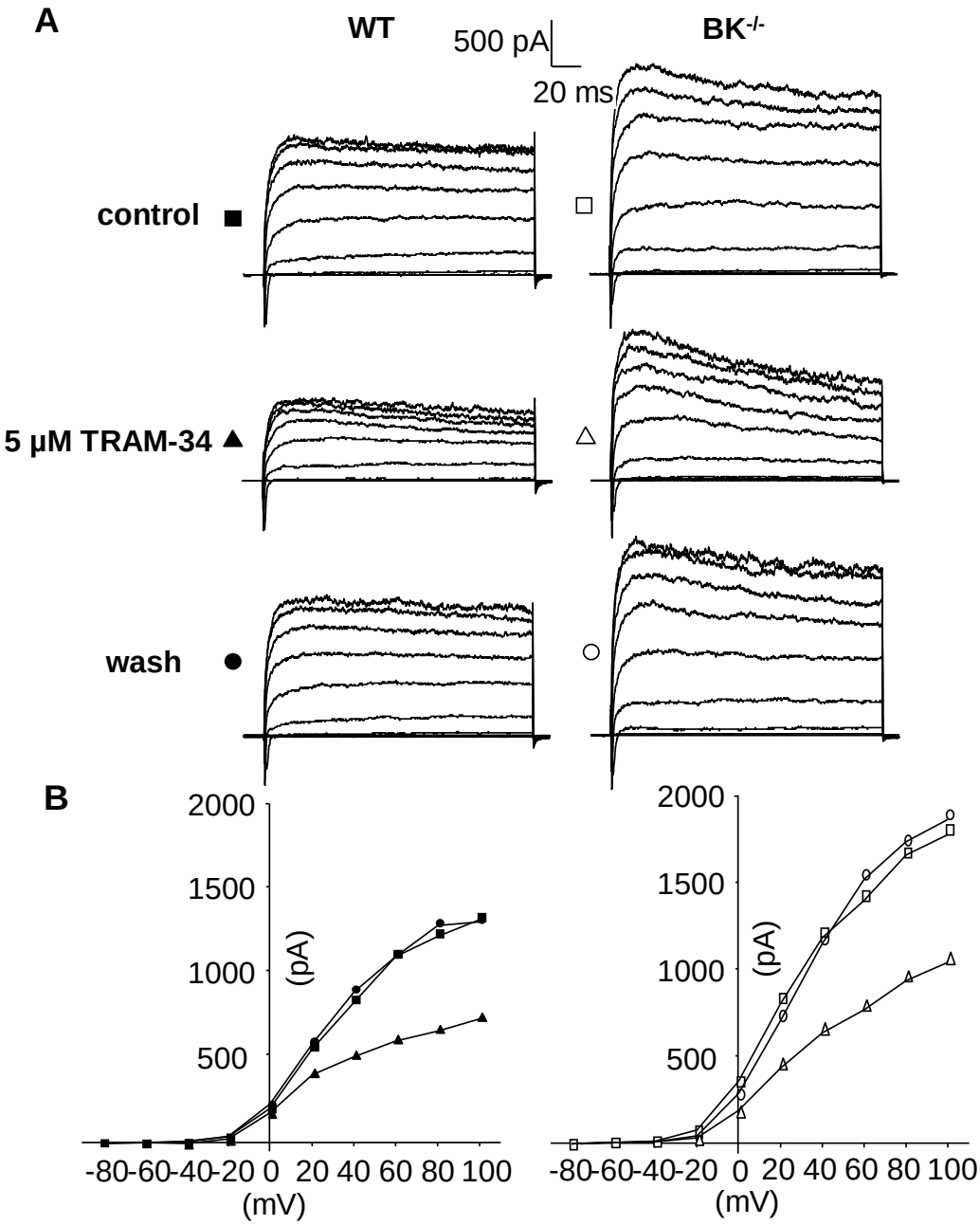

Figure 3.12 TRAM-34 sensitive outward potassium current. A, representative voltage-clamp recording in the perforated patch-clamp mode of a corticotroph depolarised from a holding potential of -80 mV to +100 mV in 20 mV steps before (cont, □), during (TRAM-34, △) and after washout (wash, ○) exposure to 5 µM TRAM-34 (closed symbol for WT and open symbol for $BK^{-/-}$). **B**, current-voltage relationship of the whole-cell outward current from the cells as in A determined at the steady-state (190 ms). The whole-cell outward current amplitude was reduced by around 45% at +100 mV for both WT and $BK^{-/-}$ corticotrophs.

Corticotrophs from WT (n = 4) and $BK^{-/-}$ (n = 5) showed similar inhibition by 5 μM TRAM-34 and recovery. On average TRAM-34 resulted an average of around 40% inhibition of WT corticotrophs steady-state whole-cell outward current measured at +100 mV and around 50% inhibition for $BK^{-/-}$ corticotrophs. WT and $BK^{-/-}$ corticotrophs did not show significant difference in the inhibition by TRAM-34 (Figure 3.13). These data suggested the 50% inhibition of the whole-cell outward current by TRAM-34 was the SK4 channel component, and SK4 channels were dominant potassium channel in native murine corticotrophs.

1mM TEA combined with 5 μM TRAM-34 blocked almost 70-80% of the steady-state whole-cell outward current. The specific inhibitor of small conductance potassium channels (SK channels) Apamin was used to identify the current amplify of SK channels in native murine corticotrophs. There was less than 5% inhibition by 1 mM Apamin indicated SK channel was a small component in native murine corticotrophs (n = 5).

3.2.3.4 4-AP sensitive outward current

In many cells, there was a marked inactivation current component shown in the whole-cell outward current traces of WT and $BK^{-/-}$ corticotrophs. In a previous publication the inactivation current component was suggested as A-type potassium current, so we selected the inhibitor of the A-type potassium channel 4-AP for the following investigation (Hille, 2001).

Figure 3.13
Inhibition of outward potassium current by TRAM-34

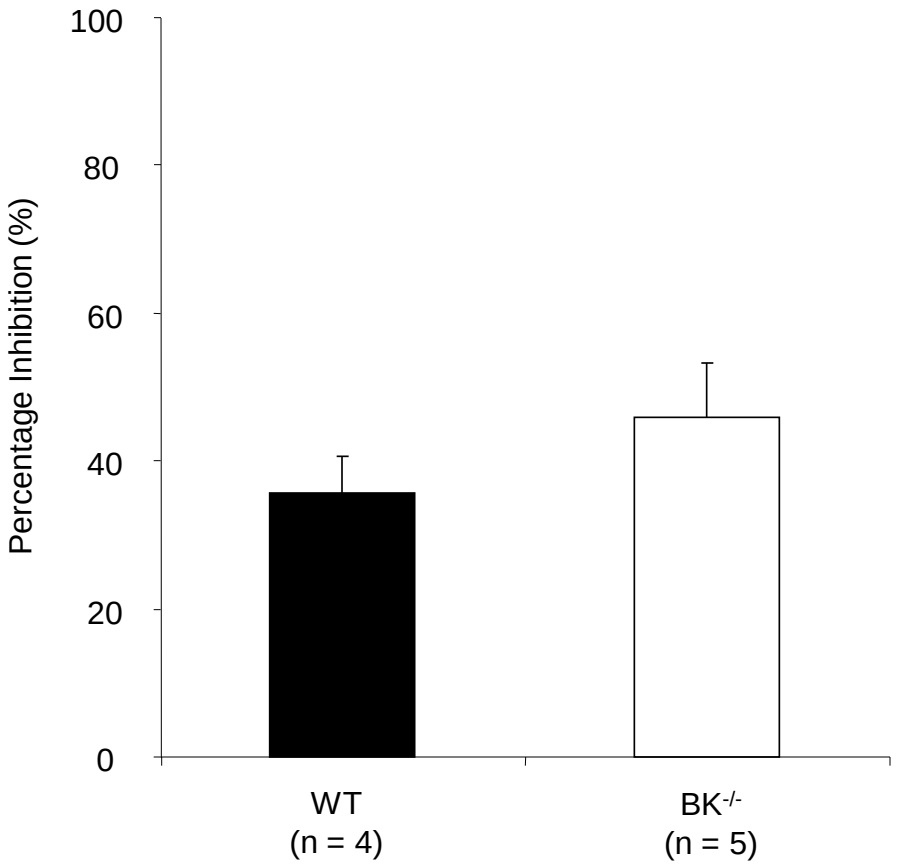

Figure 3.13 Inhibition of outward potassium current by TRAM-34. TRAM-34 blocked the whole-cell outward steady-state current of WT (n = 4) and $BK^{-/-}$ (n = 5) corticotrophs at +100 mV. There was no significant difference in the percentage inhibition between WT and $BK^{-/-}$ corticotrophs. All data are means ± SEM, n, no. of independent recorded cells.

Representative whole-cell outward current traces with a marked inactivation component of WT and $BK^{-/-}$ corticotrophs showed 1 mM 4-AP inhibited the inactivating current component dramatically and also decreased the steady-state current of the whole-cell outward current 2-3 minutes after 1 mM 4-AP was applied to the standard bath solution when the whole-cell outward was reached stable (Figure 3.14 left for WT & Figure 3.16 left for $BK^{-/-}$). The inhibition of the whole-cell outward current reached the maximum in 5-7 minutes, and the inactivation current component was lost. For the WT corticotroph, 1 mM 4-AP reduced the inactivating current amplitude by around 40% measured at the peak (measured at around 20 ms depends on where the peak was in the traces of each individual cell) and blocked the steady-state current amplitude by around 20% measured at 190 ms in the representative *I-V* plot (Figure 3.15 left). In the $BK^{-/-}$ corticotroph representative *I-V* plot, the peak whole-cell outward current was reduced by 40% and the steady-state whole-cell outward current was blocked by 20% at +100 mV (Figure 3.17 left). The inhibited whole-cell outward current started to recover 3-5 minutes after the standard extracellular solution wash and the current reversed in 10-15 minutes.

The same experiment and current trace analysis was performed on corticotrophs with whole-cell outward current without a clear inactivating current component.

Representative whole-cell outward current traces of WT and $BK^{-/-}$ corticotrophs showed 1 mM 4-AP decreased the steady-state current of the whole-cell outward current (Figure 3.14 right for WT & Figure 3.16 right for $BK^{-/-}$). In WT corticotroph representative *I-V* plot, 1 mM 4-AP inhibited 15% of the steady-state (at 190 ms)

Figure 3.14
4-AP sensitive outward potassium current

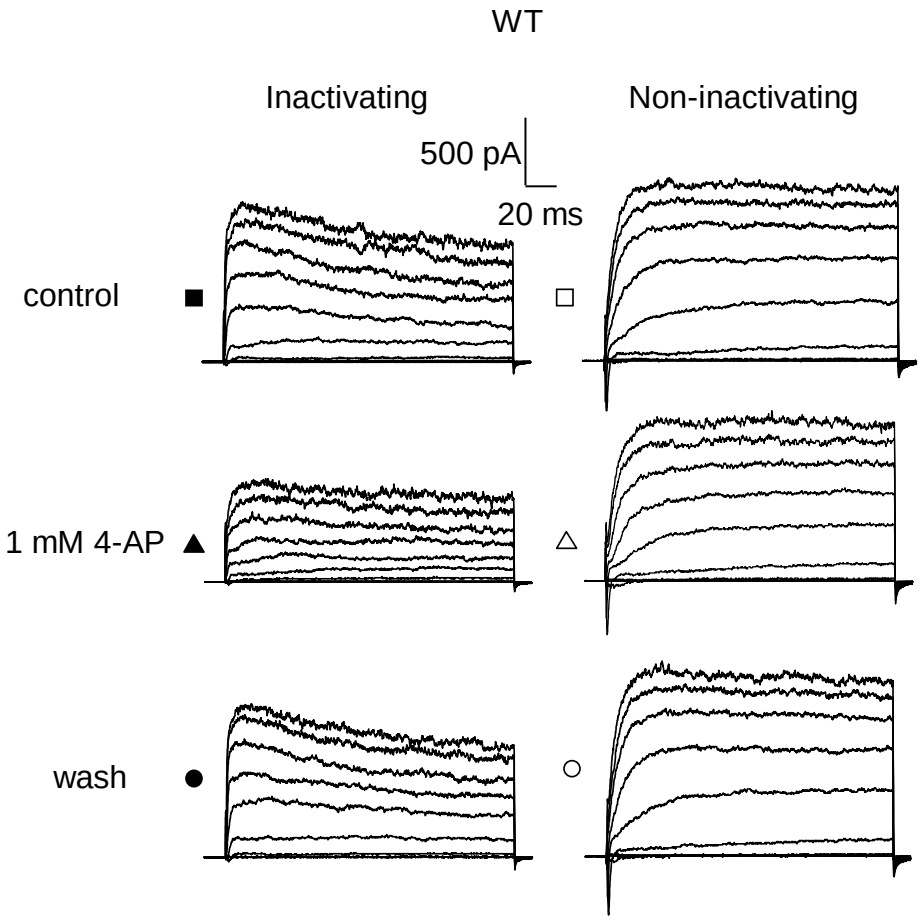

Figure 3.14 4-AP sensitive outward potassium current. Representative voltage-clamp recording in the perforated patch-clamp mode of a corticotroph depolarised from a holding potential of -80 mV to +100 mV in 20 mV steps before (cont, □), during (4-AP, △) and after washout (wash, ○) exposure to 1 mM 4-AP (closed symbol for the whole-cell current traces with a clear inactivating current component and open symbol for the whole-cell current traces without a clear inactivating current component).

Figure 3.15
Current-voltage relationship of the whole-cell outward current in the presence of 1 mM 4-AP

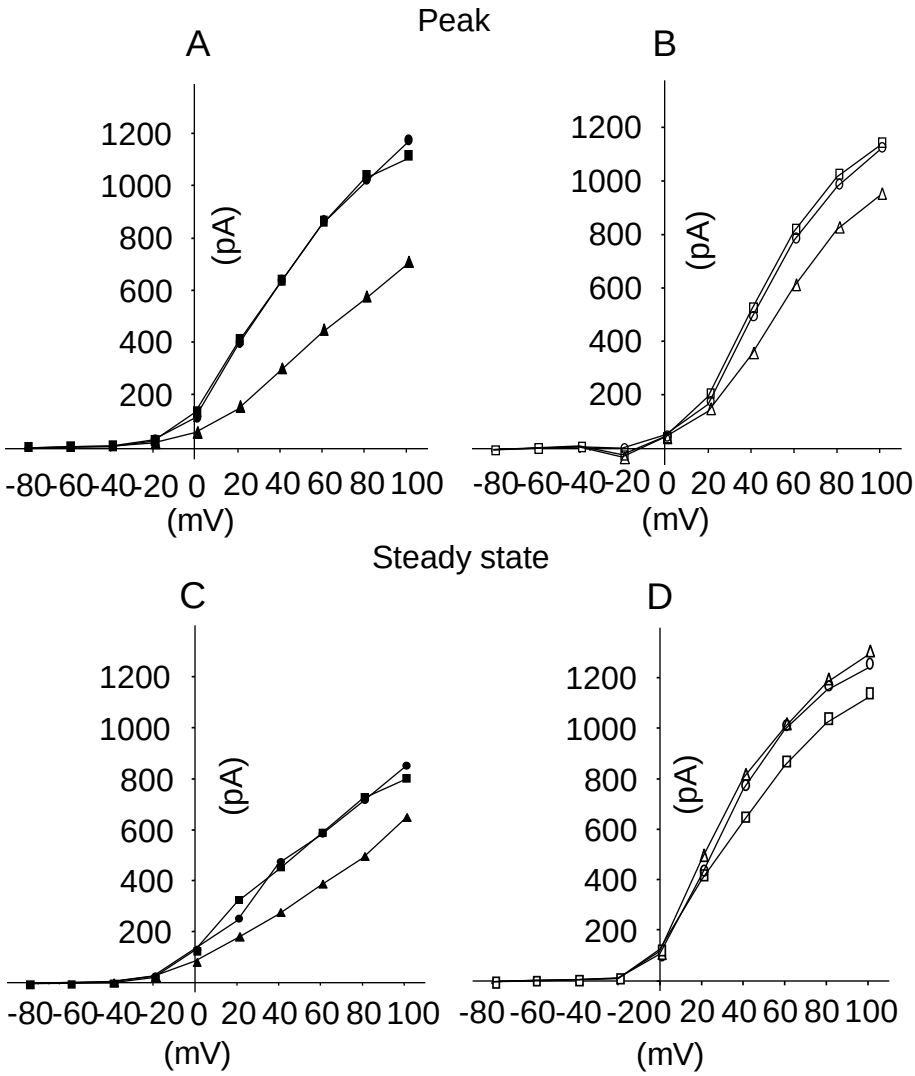

Figure 3.15 Current-voltage relationship of the whole-cell outward current in the presence of 1 mM 4-AP. Current-voltage relationship of the whole-cell outward current from WT cells as in Figure 3.14 determined at the peak (15-20 ms depended on where the peak was for each individual cell) and the steady-state (190 ms). For the whole-cell current traces with a clear inactivating current component, the peak current amplitude was reduced by around 40% at +100 mV (A), and the steady-state current amplitude was reduced by around 20% at +100 mV (C) in the presence of 4-AP. For the whole-cell current traces without a clear inactivating current component, the peak current amplitude was reduced by around 20% at +100 mV (B), and the steady-state current amplitude was reduced by around 15% at +100 mV (D) in the presence of 4-AP.

Figure 3.16
4-AP sensitive outward potassium current in $BK^{-/-}$ corticotrophs

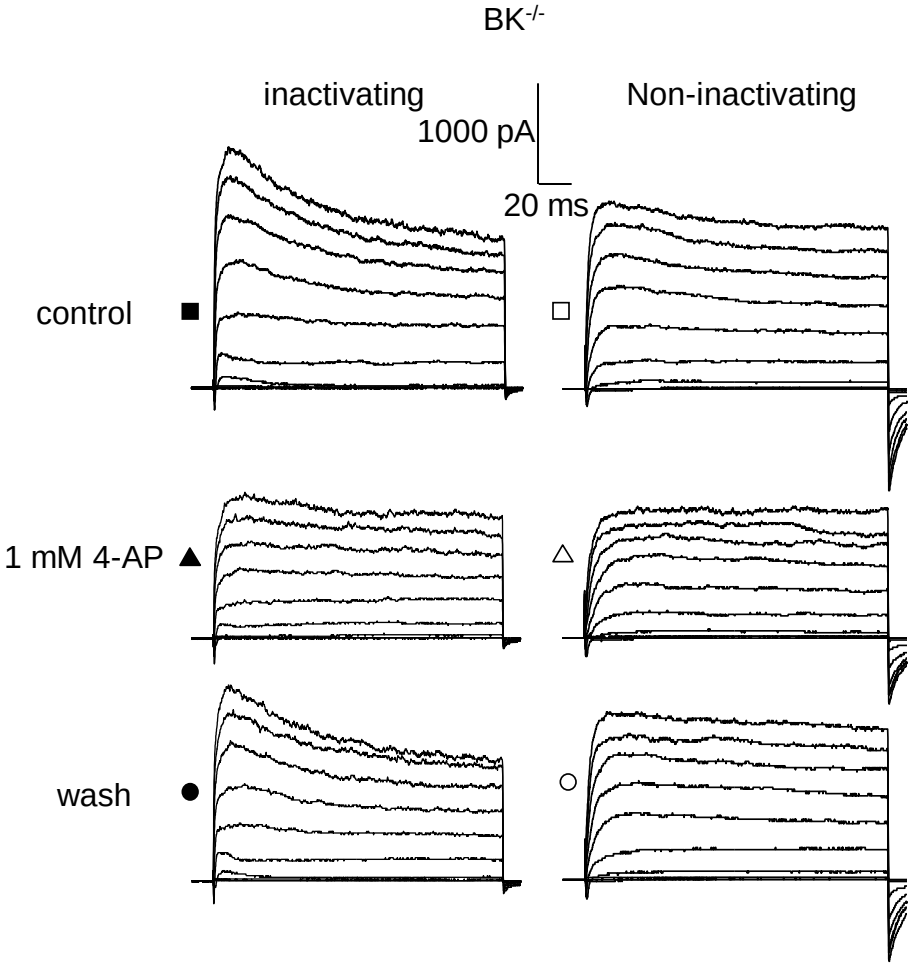

Figure 3.16 4-AP sensitive outward potassium current in $BK^{-/-}$ corticotrophs. Representative voltage-clamp recording in the perforated patch-clamp mode of a corticotroph cell depolarised from a holding potential of -80 mV to +100 mV in 20 mV steps before (cont, □), during (4-AP, △) and after washout (wash, ○) exposure to 1 mM 4-AP (closed symbol for the whole-cell current traces with a clear inactivating current component and open symbol for the whole-cell current traces without a clear inactivating current component).

whole-cell outward current, and the current amplitude measured at 20 ms (where the peak was) also showed 20% inhibition at +100 mV in the presence of 1 mM 4-AP (Figure 3.15 right). For the $BK^{-/-}$ corticotroph, there was 40% inhibition of the peak whole-cell outward current and 25% inhibition of the steady-state whole-cell outward current at +100 mV by 1 mM 4-AP shown in $BK^{-/-}$ corticotroph representative *I-V* plot (Figure 3.17 right).

Corticotrophs from WT (n = 16) and $BK^{-/-}$ (n = 6) showed a similar peak and steady-state whole-cell outward current inhibition and recovery in the presence of 1 mM 4-AP. Corticotroph whole-cell outward current with or without a clear peak current showed no significant difference in either the peak or steady-stated current inhibition by 1 mM 4-AP, so data was combined for displaying. Both for WT and $BK^{-/-}$ corticotrophs, the peak whole-cell outward current was blocked by around 40-45%. While for the steady-state whole-cell outward current, 1 mM 4-AP resulted in a 20% inhibition for WT corticotrophs and 30% inhibition for $BK^{-/-}$ corticotrophs (Figure 3.18). WT and $BK^{-/-}$ corticotroph whole-cell outward current showed no significant difference in the inhibition by 1 mM 4-AP either at peak or steady-state current. However, 1 mM 4-AP displayed a significant difference in the inhibition of the peak and the steady-state whole-cell outward current both in WT and $BK^{-/-}$ corticotrophs ($P < 0.5$, Student's t-test).

From these data, we concluded that 1 mM 4-AP blocked the peak component of the whole-cell outward current in native murine corticotrophs, although it also reduced the steady-state current. The A-type potassium channels contribute to the peak

Figure 3.17

Current-voltage relationship of the whole-cell outward current in the presence of 1 mM 4-AP in BK$^{-/-}$ corticotrophs

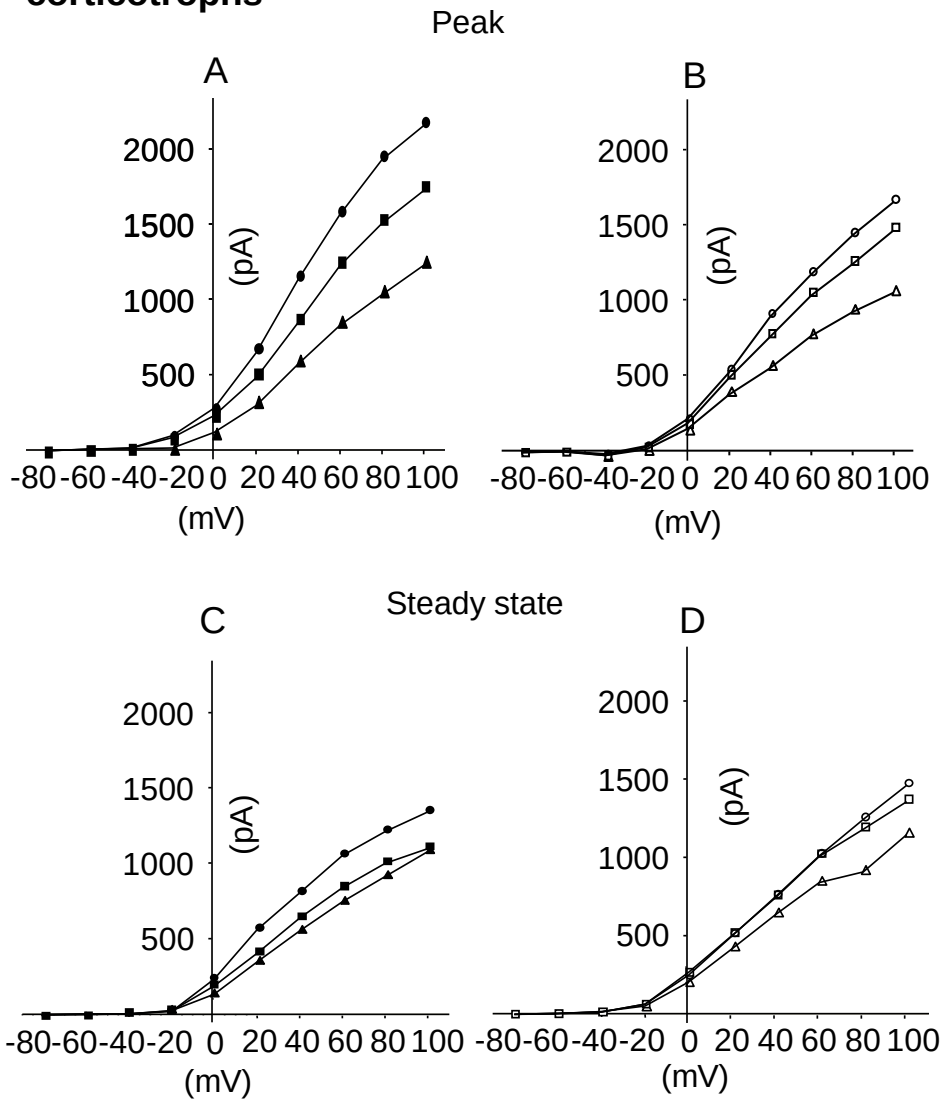

Figure 3.17 Current-voltage relationship of the whole-cell outward current in the presence of 1 mM 4-AP in BK$^{-/-}$ corticotrophs. Current-voltage relationship of the whole-cell outward current from BK$^{-/-}$ cells as in Figure 3.16 determined at the peak (15-20 ms depended on where the peak was for each individual cell) and the steady-state (190 ms). For the whole-cell current traces with a clear inactivating current component, the peak current amplitude was reduced by around 45% at +100 mV (A), and the steady-state current amplitude was reduced by around 25% at +100 mV (C) in the presence of 4-AP. For the whole-cell current traces without a clear inactivating current component, the peak current amplitude was reduced by around 40% at +100 mV (B), and the steady-state current amplitude was reduced by around 20% at +100 mV (D) in the presence of 4-AP.

Figure 3.18
Inhibition of outward potassium current by 1 mM 4-AP

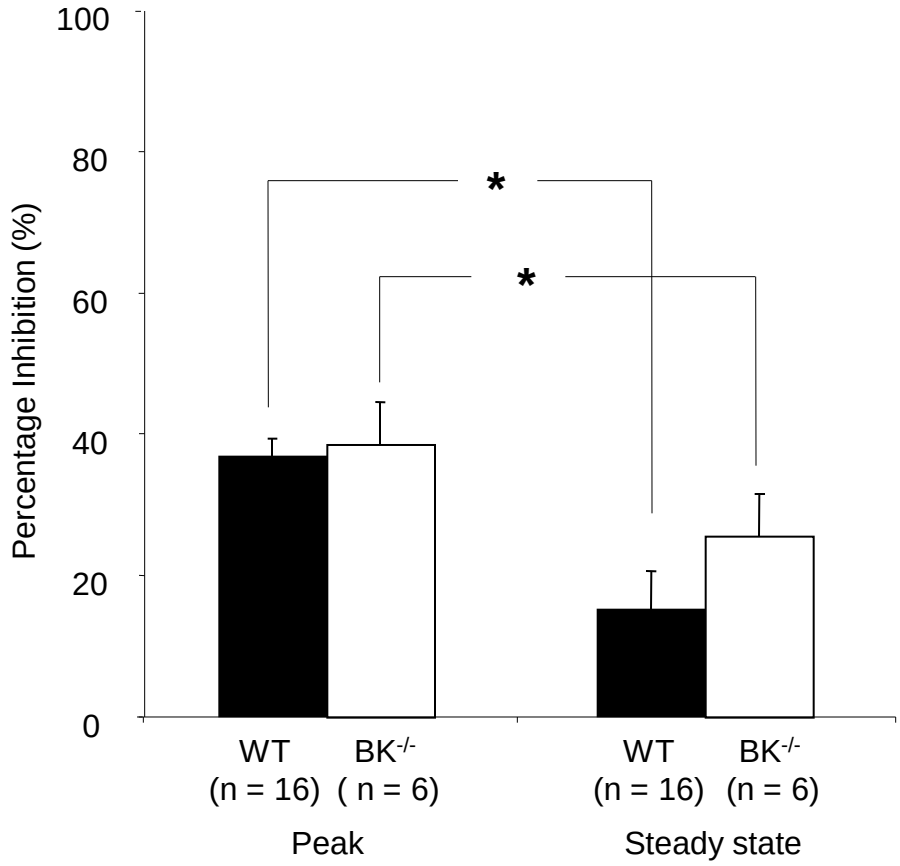

Figure 3.18 Inhibition of outward potassium current by 1 mM 4-AP. The whole outward peak current (15-20 ms) was reduced by around 40% both for WT (n = 16) and $BK^{-/-}$ (n = 6) corticotrophs, while for the whole outward steady-state current (190 ms) was decreased 20-30% by 1 mM 4-AP at 100 mV on average. There was no significant difference in the percentage inhibition between WT and $BK^{-/-}$ corticotrophs. However, 1 mM 4-AP significantly inhibited the peak current compared with the steady state current both in WT and $BK^{-/-}$. (**P* < 0.05, ANOVA with *post doc* Dunnett's test). All data are means ± SEM, n, no. of independent recorded cells.

current component of the whole-cell outward current, which suggests that the A-type potassium channel is another potassium channel component in native murine corticotrophs.

3.2.3.5 Combination of blockers

To summarize the current components in native murine corticotrophs, blockers were applied to cells one after another until all four inhibitors were applied on the cell at the same time. The four blockers were applied to the cell in the order of 1 mM TEA, 1 μM paxilline, 5 μM TRAM-34 and 1 mM 4-AP. The combined blockers reduced almost 90-95% of the whole-cell outward current for WT corticotrophs on average (n = 14) (Figure 3.19). In the combined condition, 1 mM TEA and 1 μM paxilline as the first two blockers applied to the corticotrophs showed 35% and 5% inhibition, which were similar to the blocker individual inhibition. While 5 μM TRAM-34 and 1 mM 4-AP were applied to the cell afterward, the percentage of inhibition was 40% and 25%, which were slightly smaller compared with the blocker individual inhibition. Since 1 mM TEA is a general potassium channel blocker, we explained as an overlapped inhibition between 1 mM TEA, 5 μM TRAM-34 and 1 mM 4-AP.

For $BK^{-/-}$ (n = 10), the bar chart was simply combined using the individual inhibition percentage of the four inhibitors. Compared to WT corticotroph combined inhibition experiment, the total inhibition of $BK^{-/-}$ corticotrophs whole-cell outward current was over 100% due to the overlapping inhibition of 1 mM TEA, 5 μM TRAM-34 and 1 mM 4-AP (Figure 3.19).

Figure 3.19
Inhibition of outward potassium current by combined inhibitors

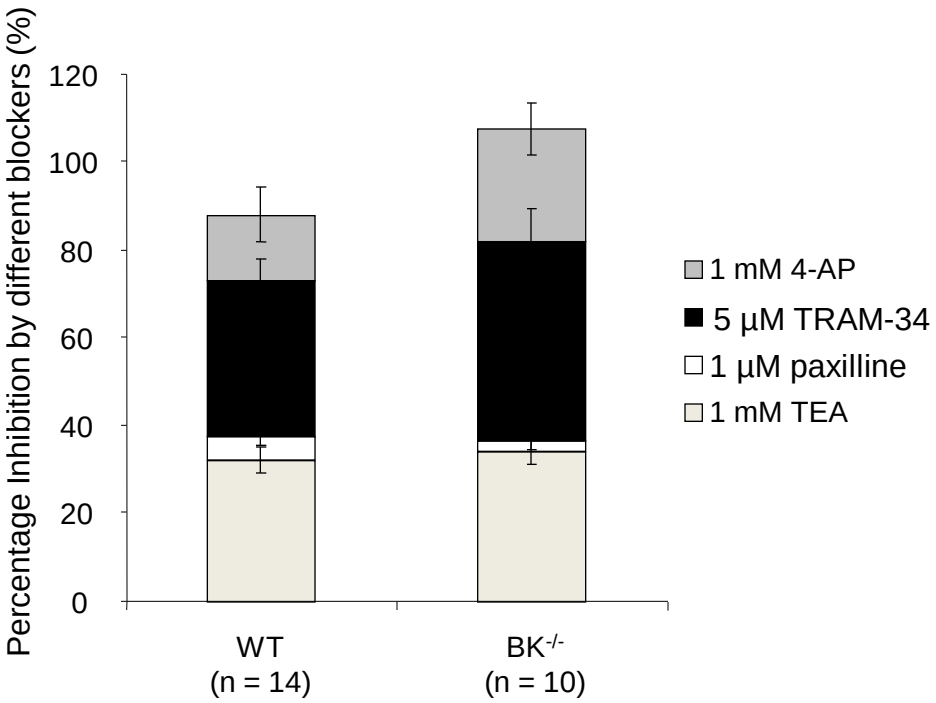

Figure 3.19 Inhibition of outward potassium current by combined inhibitors. The inhibition of the whole-cell outward current measured at steady-state (190 ms) at 100 mV by the four blockers applied to the cell in the order of 1 mM TEA, 1 µM paxilline, 5 µM TRAM-34 and 1 mM 4-AP until all four blockers were applied to the cell at the same time. The combined blockers almost abolished the whole-cell outward current of both WT (n = 14) and $BK^{-/-}$ (n = 10) corticotrophs.

In conclusion, TRAM-34 sensitive current was the main steady-state outward current and 4-AP sensitive current was the main inactivating current in the whole-cell outward current of native murine corticotrophs. These data revealed that compared to mouse AtT20 cells where BK channels dominated, SK4 channels and the A-type potassium channels were the main potassium channels in native mouse corticotrophs.

3.2.4 Pharmacological characterisation of inward currents

3.2.4.1 $BaCl_2$-sensitive K_{ir} inward current

Previous research reported that the inwardly rectifying potassium channels have been recorded in native rat corticotrophs, so we used $BaCl_2$, a relatively specific inwardly rectifying potassium channel blocker, to examine if the inwardly rectifying potassium channels also expressed in murine native corticotrophs.

Standard extracellular solution containing 5 mM TEA and 2 μM TTX was applied to corticotrophs for 10-20 minutes until most outward current and TTX sensitive current were eliminated. 100 μM $BaCl_2$ was mixed in the extracellular solution containing 5 mM TEA and 2 μM TTX and applied to the cell. The pulse protocol was modified with a holding potential at -140 mV to activate the inwardly rectifying potassium channels and depolarized in 20 mV steps to -40 mV before any significant outward current appeared.

Representative WT cell traces showed 100 μM $BaCl_2$ inhibited the early inward current of native murine corticotrophs (Figure 3.20A left). In the representative *I-V*

Figure 3.20
$BaCl_2$ sensitive inward potassium current

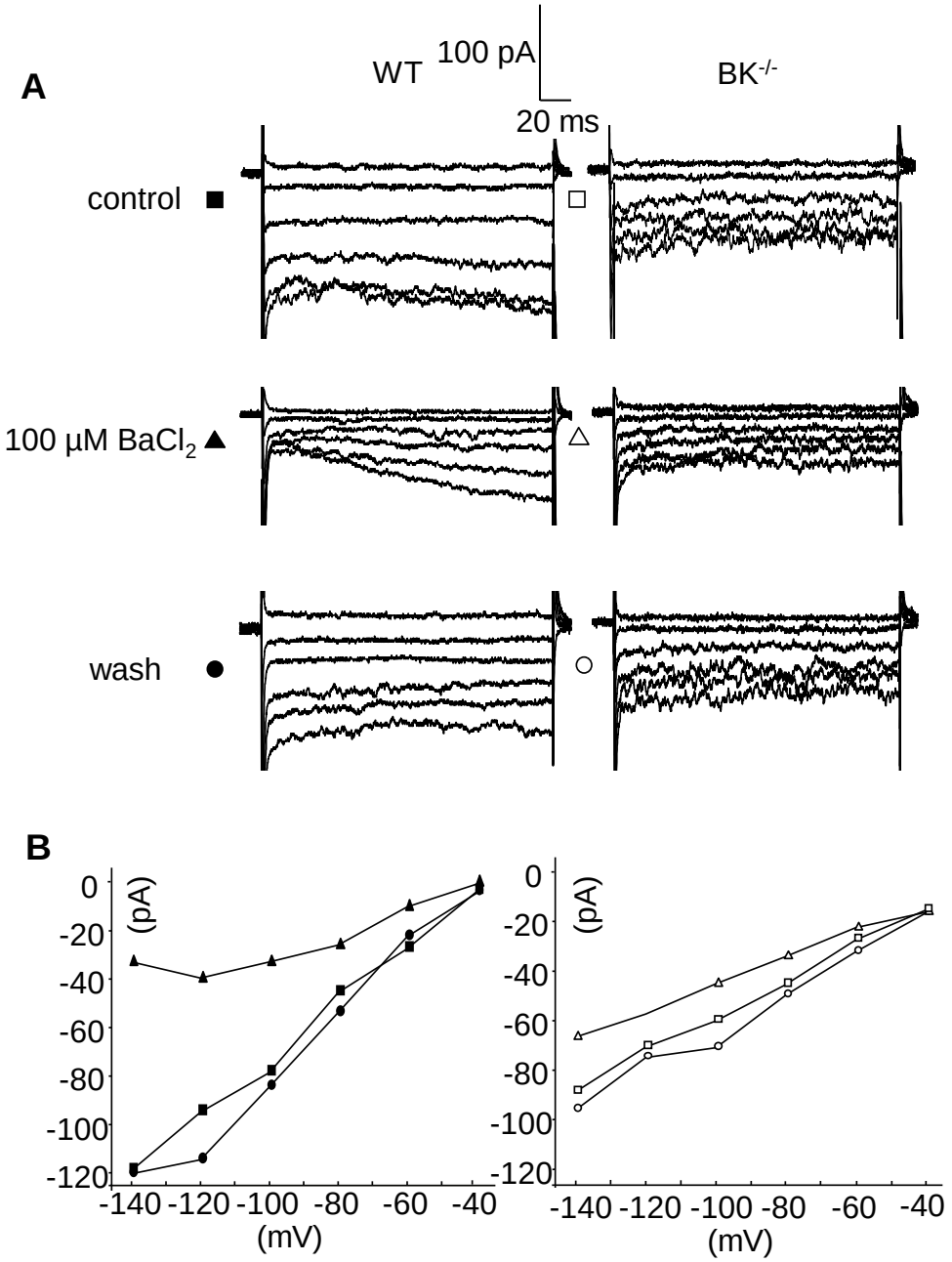

Figure 3.20 $BaCl_2$ sensitive inward potassium current. A, representative voltage-clamp recording in the perforated patch-clamp mode of a corticotroph depolarised from a holding potential of -140 mV to -40 mV in 20 mV steps before (cont, □), during ($BaCl_2$, △) and after washout (wash, ○) exposure to 100 µM $BaCl_2$ (closed symbol for WT and open symbol for $BK^{-/-}$). Traces have been truncated for clarity. **B**, current-voltage relationship of the whole-cell inward current from the cells as in A determined at 17 ms.

plot, the inward current measured at 17 ms was inhibited by 70% at -140 mV in the presence of 100 μM $BaCl_2$ (Figure 3.20B left). Inhibited current was easily washed back to control level. While for $BK^{-/-}$ 100 μM $BaCl_2$ did not show significant inhibition in the inward current of native murine corticotrophs.

μM $BaCl_2$, WT corticotrophs showed similar inhibition. 100 μM $BaCl_2$ blocked around 50% of the whole-cell inward current of WT corticotrophs, while for $BK^{-/-}$ corticotrophs, the inhibition was less than 5% (Figure 3.21). 100 μM $BaCl_2$ showed significantly stronger inhibition of K_{ir} in WT corticotrophs whole-cell inward current than $BK^{-/-}$ corticotrophs ($P < 0.05$, Student's t-test).

Data revealed that in WT corticotrophs, inwardly rectifying potassium channel were an inward current component. While in $BK^{-/-}$ cells, the expression of inwardly rectifying (Ba^{2+} sensitive) potassium channel was down-regulated, which matched the real-time PCR results of the expression level of K_{ir} channels in WT and $BK^{-/-}$ anterior pituitary tissue (MJ Shipston, unpublished).

Figure 3.21
Inhibition of inward potassium current by $BaCl_2$

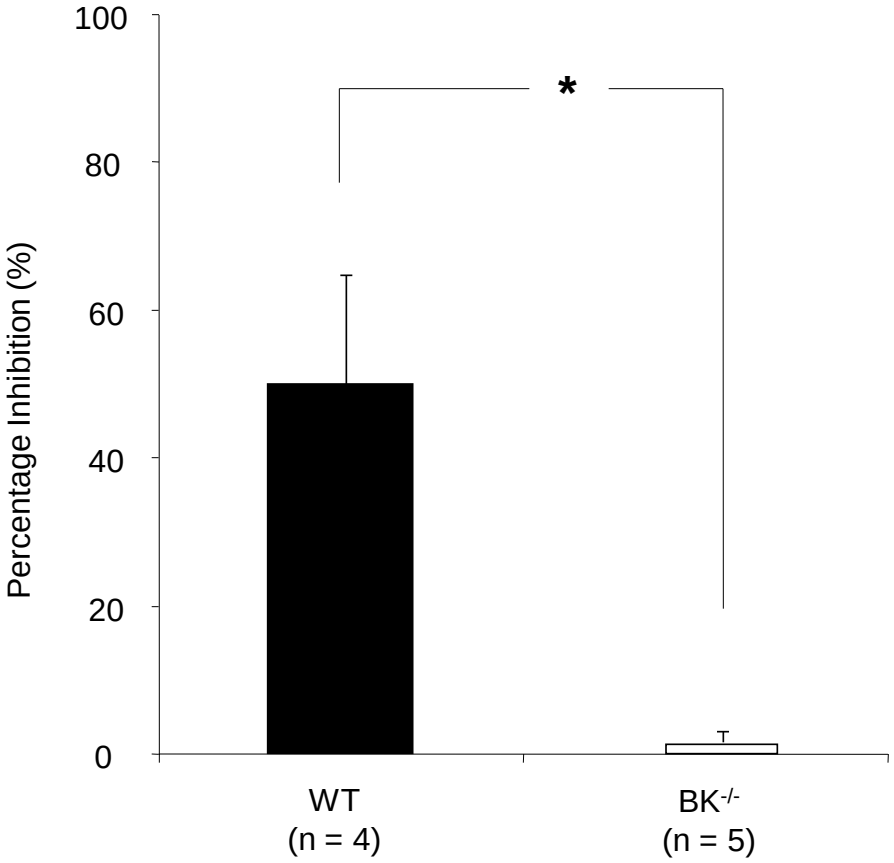

Figure 3.21 Inhibition of inward potassium current by $BaCl_2$. On average, 100 µM $BaCl_2$ blocked around 45% of the whole-cell inward current of WT (n = 4) corticotrophs at -140 mV, and for $BK^{-/-}$ (n = 4) corticotrophs the inhibition was around 2%. 100 µM $BaCl_2$ significantly inhibited more inward current in WT corticotrophs than that in $BK^{-/-}$ corticotrophs. All data are means ± SEM, n, no. of independent recorded cells.

3.3 Summary

3.3.1 Specific and high efficiency labelling of native murine corticotrophs

Since ACTH secretion is the unique endocrine property of pituitary corticotrophs, ACTH antibody staining was used as a reliable method to test the specificity of lentiviral transduced labelling using the minimal rPOMC promoter driven expression of eYFP. Although not every ACTH positive cells showed eYFP fluorescent, all eYFP fluorescent cells displayed ACTH staining confirming the recorded cells were all corticotrophs. On the hand, the percentage of eYFP positive cells is consistent with the percentage of corticotrophs in the pituitary cells. Furthermore, the percentage of corticotrophs from a mouse transgenic line in which GFP is constitutively expressed in corticotrophs under control of the minimal rPOMC promoter was also similar to the percentage of fluorescent cells transduced with lentiviral vector with eYFP driven by the minimal rPOMC promoter. In contract, pituitary cells transduced with the lentiviral vector in which eYFP expression was driven by CMV promoter, there were a high proportion of ACTH positive cells that did not express eYFP.

The initial titre of CMV or rPOMC driven lentiviral particles was various in every patch of preparation, but when applied to the primary mice pituitary culture the tire of the two different promoters driven lentiviral particles was adjusted to the same in order to compare the transduction efficiency. Although CMV promoter has been reported to drive gene expression in any cell type, the result showed in primary mice

pituitary cell culture there were some GFP negative cells. The reasons could be any, like CMV could not drive gene expression in every primary pituitary cell, or because CMV promoter is not tissue specific, which may lead its efficiency of driving gene expression too low to be detected. Even for some cell lines, like AtT20 cells, CMV promoter could not provide detectable GFP fluorescent. As a result, for the mixed primary pituitary cells, tissue specific promoter rPOMC showed a better achievement in corticotroph specific labelling.

Thus, using eYFP driven by the minimal rPOMC promoter in the lentiviral transducing vector was able to label anterior pituitary corticotroph cells efficiently and specifically.

No significant difference in the ACTH secretion level was detected between control (non-transduced) cells and POMC-eYFP labelling cells, either at basal or CRF/AVP stimulated conditions (Liang *et al*., 2011). The lentiviral labelling system was thus performed as an effective and routine approach for corticotroph identification. Lentiviral transduction system provides multiple opportunities for gene investigation and with the use of appropriate cell-specific promoters may be applicable to other pituitary cell types.

3.3.2 Perforated patch-clamp recording

To address the cell excitable properties of lentiviral transduced fluorescent corticotrophs, whole-cell mode patch-clamp technique was first applied. Whole-cell recording aims to record the whole-cell currents through multiple channels at once

over the membrane of the entire cell. When the electrode is placed on the cell membrane and the seal reaches gigohm seal, a fast and short suction is applied to rupture the membrane patch, thus providing access to the cell intracellular environment. The advantage of whole-cell patch-clamp recording is that large cell membrane opening at the tip of the patch-clamp electrode provides lower cell resistance and thus better electrical access to the cell interior. The disadvantage of this technique is that the solution volume in the electrode is larger than the intracellular environment, so the intracellular contents are slowly replaced by the electrode solution, referred to as the electrode solution dialyzing the cell intracellular contents. So the cell properties dependent on the intracellular contents will be gradually altered during the recording. The physiological recording time may be very short dependent on the time of cell being dialyzed. This limitation is revealed in the native murine corticotroph whole-cell patch-clamp recording due to their too small cell volume. In voltage-clamp recording, this situation did not affect the measurement of current components very clearly and only shortened the recording duration for 30-40 minutes compared with perforated patch-clamp mode. However, in the current-clamp recordings, the spontaneous action potentials disappeared very quickly within 10-20 seconds, which abolished the spontaneous action potentials. Even when ATP added to the electrodes, the whole-cell mode recording could not get stable spontaneous action potentials recording, which is consistent with the observation in POMC-GFP corticotrophs. (Lee & Tse 2011)

Perforated patch-clamp was applied instead for the further investigations. Perforated patch is a variation of whole-cell recording. The electrode solution used for

perforated patch contains a small amount of an antifungal or antibiotic chemical, like amphotericin-B, nystatin, or gramicidin. When gigohm seal formed, the antibiotics diffuse into the membrane patch and form small perforations in the patched membrane, providing electrical access to the intracellular environment. The big advantage of perforated patch is the pore formed by antibiotics only allows small monovalent ions to pass reducing the dialysis of the cell contents that occurs in whole-cell recordings, but there are several disadvantages. First, the cell access resistance is higher than that in whole-cell recording decreasing the electrical access to cell, which may decrease current resolution, increase recording noise, and magnify any series resistance error. Second, the time of perforation is critically related with the shapes of electrodes. Long and narrow electrodes can take a significant amount of time for the antibiotic to perforate the membrane. Thirdly, the membrane in the electrode tip may be totally ruptured during the perforations forming by the antibiotic. Perforated patch allows stable recordings and had no effect on the spontaneous action potentials, which allow the further investigation of corticotrophs cell excitability.

3.3.3 Potassium currents expressed in native murine corticotrophs

Corticotrophs from WT, hets and $BK^{-/-}$ mice were compared, and no significant difference was found in the cell capacitance, resting membrane potential or the total outward current density. This may suggest that BK channels are not the dominant potassium channels in native murine corticotrophs or the expression of other ion channels are increased in compensation. Paxilline as a pharmacological specific blocker for BK channels together with Ca^{2+} triggered pre-pulse protocol both

confirmed that BK current component was very small in native murine corticotrophs, which is inconsistent with that in AtT20 cells. In AtT20 cells, BK channels are reported as dominant potassium channels, and are the target of CRH and glucocorticoids-induced signalling pathways and play very important function in regulating the ACTH secretion. BK channels also found in other pituitary cells, like GH3 cells, gonadotrophs and somatotrophs (Lang & Ritchie, 1990; Van Goor, Li & Stojilkovic, 2001). Although paxilline is recommended as a very specific blocker, the specificity is critical with the concentration applied. 10 μM paxilline caused significant inhibition of the whole outward current even in $BK^{-/-}$ corticotrophs. According to my results, 1 μM paxilline is suggested as the specific concentration for blocking BK channels.

TEA, as the general blocker of voltage-gated potassium channels, suggested there were large potassium current components in the native murine corticotrophs. Since BK channels are not the main contributor to the outward potassium current, other voltage-gated or calcium-gated potassium channels were screened via the application of their specific channels blockers. Apamin revealed small- conductance calcium-activated potassium (SK) channels also show a small contribution to the whole outward cell current in native murine corticotrophs. SK channels have been detected in male rat corticotrophs with the role in membrane hyperpolarization activated by AVP through a transient $[Ca2^{+}]_i$ elevation from intracellular IP_3 store (Tse & Lee, 1998). SK channels are well documented in many pituitary cells, like GH cells. The expression level of SK channels in rat, mouse and ovine gonadotrophs is dependent on estradiol (Waring & Turgeon, 2006).

The percentage of inhibition by TRAM-34 revealed that intermediate-conductance calcium-activated (SK4) potassium channels are the main outward potassium channel current in native murine corticotrophs.

There are no previous reports suggesting SK4 channels are expressed in pituitary cells. According to the traces of the whole-cell outward current in some native murine corticotrophs, there was significant A-type inactivating current peaking at around 15 ms after the start of the pulse. 4-AP inhibitor confirmed that, A-type potassium channels are also expressed in the native murine corticotrophs. A-type channels show the rapid and transient activation and fast inactivation with the role in the regulation of firing frequency in cardiac and other excitable cells. A-type channels are also found widely expressed in majority of secretory pituitary cells, like GH3 mammosomatotrophs, αT3-1 gonadotrophs, frog melanotrophs, many rat pituitary cells and ovine somatotrophs (Stojilkovic Tabak & Bertram, 2001). The variability of A-type current expression in native murine corticotrophs may be due to corticotrophs being in different status, cell cycle or sub-populations.

3.3.4 K_{ir} currents have different expression levels in WT and $BK^{-/-}$ native murine corticotrophs

The only potassium current that displayed significantly different expression level between WT and $BK^{-/-}$ corticotrophs was K_{ir} current. Ba^{2+}-sensitive K_{ir} channels displayed a very small contribution to the inward current of $BK^{-/-}$ corticotrophs. K_{ir} channel have been found expressed in many endocrine pituitary cells and modulated by G protein-coupled hormone receptors (Tomic *et al.*, 2002). AtT20 corticotroph

cell lines expressed G protein coupled somatostatin and muscarinic receptor activated K_{ir} channels (Tallent, Dichter & Reisine, 1996). K_{ir} channels have also been reported in male rat corticotrophs and are suggested to contribute in maintaining resting membrane potentials. The reason why $BK^{-/-}$ corticotrophs expressed low K_{ir} channels is not clear, but the result is consistent with qRT-PCR analysis of mRNA expression for K^+ channels in pituitary tissue of WT and $BK^{-/-}$ mice. mRNA expression of Kcnj1-4,6,10,11,14 genes encoding K_{ir} channels, all revealed a significant decrease in $BK^{-/-}$ mice (MJ Shipston, unpublished).

Chapter Four:

The role of potassium channels in spontaneous action potentials of native murine pituitary corticotrophs

4.1 Introduction

Voltage-clamp recordings results of lentiviral labelled corticotrophs from chapter 3 have built up a profile of the major potassium conductances expressed in native female murine anterior pituitary corticotrophs. The pharmacological approach indicated the contribution of different potassium channel conductances to the whole-cell outward current of corticotrophs. SK4 channels and A-type potassium channels were the dominant potassium channels in corticotrophs. This chapter aims to investigate the basal electrical activity of native murine corticotrophs using current-clamp analysis of spontaneous activity in perforated patch-clamp recording mode, and to reveal the contribution of different potassium conductances indicated in chapter 3 in the regulation of corticotroph physiological properties.

Since the first endocrine pituitary cell was found to generate action potentials thirty-five years ago, all secretory anterior pituitary cells of vertebrates have been gradually revealed to be electrically excitable cells, like neurons and muscle cells (Kidokoro, 1975). Action potentials have been observed in frog, mouse, porcine, ovine and bovine endocrine pituitary cultured cells, and also *in situ* rat pituitary tissue slices (Stojilkovic, Tabak & Bertram, 2010). Male rat corticotrophs also have been reported that exhibited spontaneous action potentials (Kuryshev *et al.*, 1996). With appropriate stimulation action potentials can be initiated in corticotrophs, however, the recording of spontaneous action potentials was suggested to be dependent upon the electrophysiological patch-clamp mode used. Corticotroph cells obtained from transgenic mice with GFP over-expressed in corticotrophs driven by POMC

promoter appeared to be quiescent in the whole-cell recording mode (Lee & Tse, 2011). Similarly, previous studies on gonadotrophs also discovered that different recording modes affected the routine detection of spontaneous electrical activity. For example, in whole-cell recording mode, the majority of cells from male rats were electrically silent, whereas in perforated patch-clamp recordings most cells from female rats displayed spontaneous action potentials (Tse & Hille, 1993). In this chapter, perforated patch-clamp recordings will be used to record the lentiviral labelled corticotrophs to discover whether primary cultured murine corticotrophs display spontaneous action potentials.

In electrically excitable cells, voltage-sensitive ion channels are responsible for the generation of action potentials. The balance between the activity of depolarizing and hyperpolarizing currents generates the resting membrane potential of isolated cultured pituitary cells, which typically oscillates between -60 to -50 mV (Stojilkovic, Tabak & Bertram, 2010). Depolarizing ion channel components force the membrane potentials to reach the threshold level and trigger action potentials, while the repolarising current conductances lead the cells fall back to the resting membrane potential for the next spike. Voltage-gated Ca^{2+} channels have been revealed to exert very important roles in cell depolarization in corticotrophs, for they allow Ca^{2+} entry into the cells. Potassium channels are thought to mostly contribute to the cell repolarization and hyperpolarization depending on the activation and duration in different pituitary cells (see Introduction 1.4.1.3-1.4.1.5). The role of SK4 and A-type potassium conductances in the regulation of corticotroph excitability are the most interesting, since they are the dominate conductances in the whole-cell outward

current of murine corticotrophs. SK4 channels have not been reported previously in any corticotroph models and their functions are unknown in any pituitary cell types. A-type potassium channels have been revealed that play a role in the firing frequency regulation in cardiac and other electrically active cells (Hille, 2001). A-type current displayed a high expression level in ovine somatotrophs with a potential functional in controlling action potentials and hormone secretion (Chen *et al*., 1994). In other anterior pituitary cells, the roles of A-type K_v channels in the regulation of cell excitability are not very clear. For example, in rat lactotrophs, A-type K_v channels do not control spike generation, which may because the channels are inactivated at resting membrane potential (Sankaranarayanan & Simasko, 1998). Investigation of A-type current in the mouse corticotroph tumour cell line AtT20/D16-16 suggested a role in early glucocorticoid feedback (Pennington, Kelly & Antoni FA, 1994). In order to investigate the roles of these potassium channels in the regulation of corticotroph excitability, a pharmacological approach was used to reveal the changes in cell electrical activity when the channels were inhibited by their specific blockers.

4.2 Results

4.2.1 Spontaneous action potentials in lentiviral labelled murine native pituitary corticotrophs

After transduction with lentiviral particles, eYFP specific expression allowed the investigation of the spontaneous action potentials in native murine corticotrophs. In perforated current-clamp recording mode, with no stimulating current injection, more than 95% of lentiviral labelled pituitary corticotrophs displayed spontaneous electrical activity. In preliminary experiments, we used the conventional whole-cell recording mode, and the spontaneous action potentials were quickly abolished within less than 30 seconds. After changing to the perforated patch-clamp mode of the whole-cell configuration, the spontaneous action potentials were stable and lasted from 30 minutes to more than one hour of recording. The resting membrane potential measured in the current-clamp recording mode with 0 current applied, gave a value of -58.8 ± 1.63 mV for WT corticotrophs (n = 31) and -56.1 ± 1.87 mV for $BK^{-/-}$ corticotrophs (n = 29). The mean cell capacitance was 4.48 ± 0.38 pF for WT corticotrophs (n = 68) and 4.78 ± 0.33 pF for $BK^{-/-}$ (n = 65) corticotrophs. The input resistance for both cell types was above 4GΩ (n > 100 cells). There were no significant differences in any cell electrophysiological properties between lentiviral transduced corticotrophs and isolated corticotrophs from POMC-GFP mice, either in WT or $BK^{-/-}$ corticotrophs. The mean data was summarized from both cell resources.

Nine different patterns of action potentials were recorded in labelled corticotrophs. In any one cell, the electrical activity consisted of either one firing pattern, or

spontaneous conversion between several patterns of action potentials. The majority of cells showed repetitive large-amplitude single spikes of variable frequencies that categorised as pattern A (single spikes with significant afterhyperpolarization phase), pattern B (single spikes without afterhyperpolarization phase) (Figure 4.1 & 4.4F). Around 73% of WT cells (n = 20) displayed pattern A and/or pattern B, and for recorded $BK^{-/-}$ cells, the percentage was 82% (n = 22) (Figure 4.2). For $BK^{-/-}$ cells specifically, pattern A and B was never displayed in the same cell, while in WT cells the conversion between pattern A and B was observed in 5 of 20 cells.

Twenty single spikes of action potentials (Figure 4.3A) were randomly selected from WT cells displaying typical firing pattern A or pattern B, averaged and overlaid in Figure 4.3B with pattern A in continuous line and pattern B in dashed line (Figure 4.3B). The averaged single spike of pattern A and B was compared from measuring 6 parameters: resting membrane potential (RMP), threshold for action potential generation, spike amplitude, time to peak, spike width and afterhyperpolarization (AHP) amplitude (Figure 4.3B & 4.4). Cells showing pattern A or B had similar resting membrane potentials for both WT and $BK^{-/-}$ cells in the range of -50 to -55 mV, with no significant differences in the spike amplitude (Figure 4.4A & C). The spike threshold of pattern A (n = 3) and B (n = 4) were similar in WT cells, while in $BK^{-/-}$ cells the spike threshold of pattern A (n = 5) was significantly more depolarised than pattern B (n = 3, $P < 0.01$, Figure 4.4B). The threshold for action potential generation of pattern A in WT cells was also significantly more depolarised than that in $BK^{-/-}$ cells ($P < 0.01$, Figure 4.4B). Pattern A single spike action potentials displayed a shorter time to peak (Figure 4.4D), a more narrow spike width (Figure

Figure 4.1
Heterogeneity of spontaneous electrical activity in native murine corticotrophs

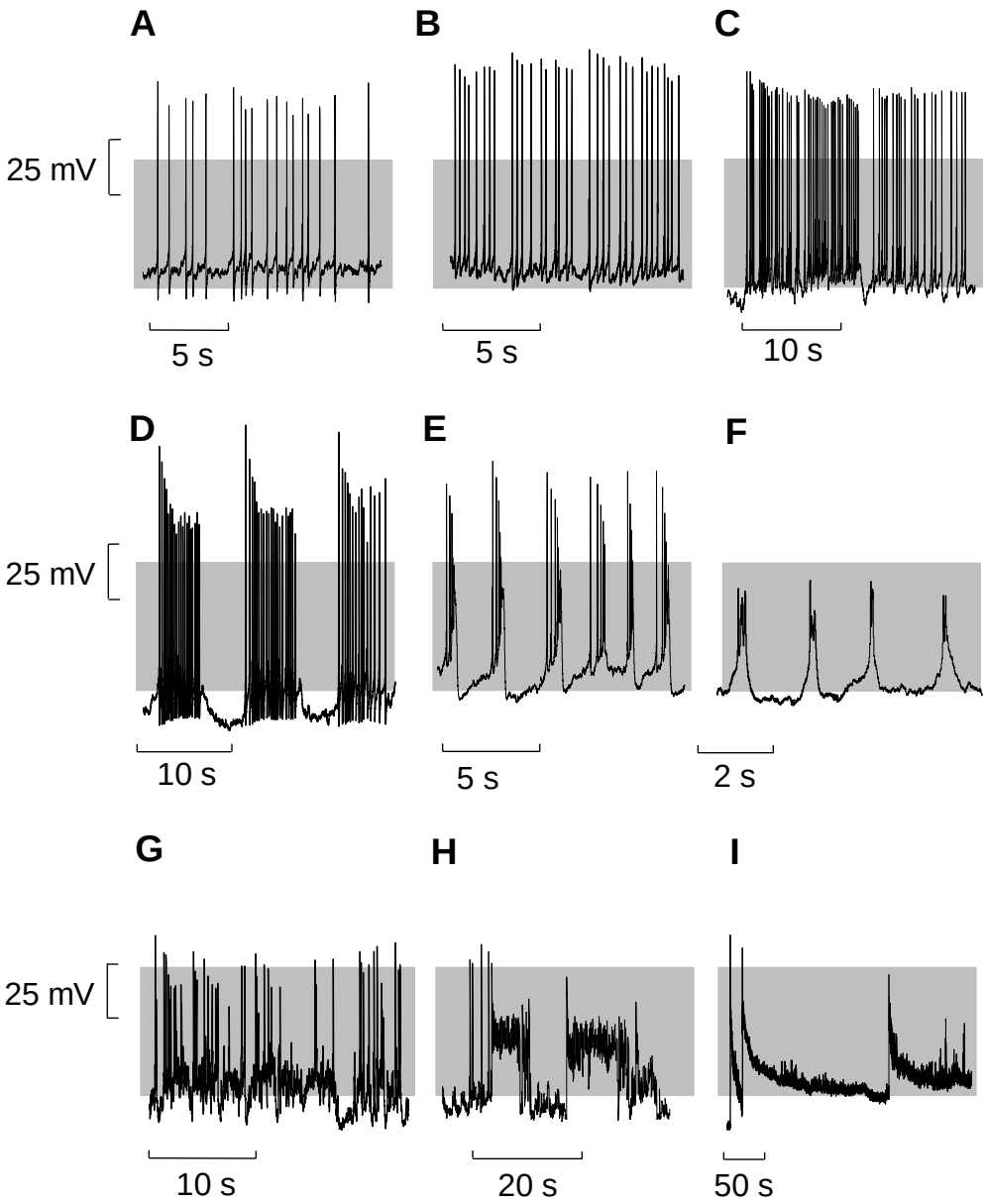

Figure 4.1 Heterogeneity of spontaneous electrical activity in native murine corticotrophs. Waveforms and firing patterns differed between cells, and individual cells could transition between firing patterns. In perforated patch-clamp recordings the majority of corticotrophs exhibited spontaneous large spikes, falling into one of two categories, as depicted in A (Type A > 30% cells) and B (Type B > 40% cells). Cells spontaneously and reversible transitioned to other firing patterns represented by panels C-H, including 'pseudo-plateau potentials' bursting behaviours. Grey shading indicates membrane potential between -50 to +10 mV.

Figure 4.2
Percentage of spontaneous firing patterns in WT and BK$^{-/-}$ corticotrophs

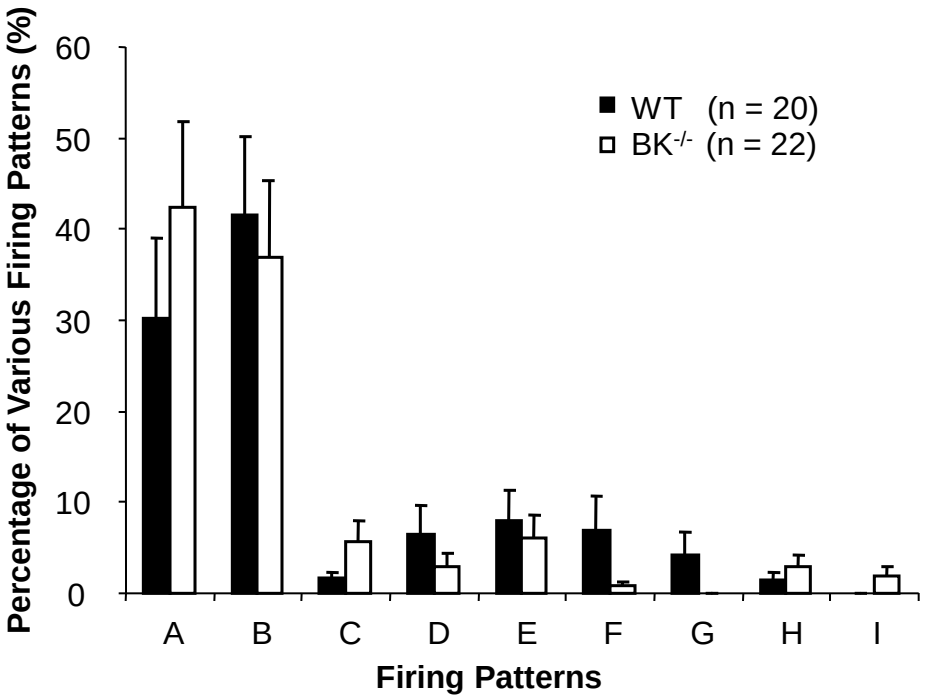

Figure 4.2 Percentage of spontaneous firing patterns in WT and BK$^{-/-}$ corticotrophs. The majority of firing patterns recorded in WT and BK$^{-/-}$ were type A and type B (see Figure 4.1). Around 30%-50% corticotrophs cells exhibited either type A or type B. Type C to type I were recorded infrequently (1%-10%) both in WT and BK$^{-/-}$ corticotrophs and there was no significant difference between genotypes.

Figure 4.3
Characterization of type A and type B action potentials

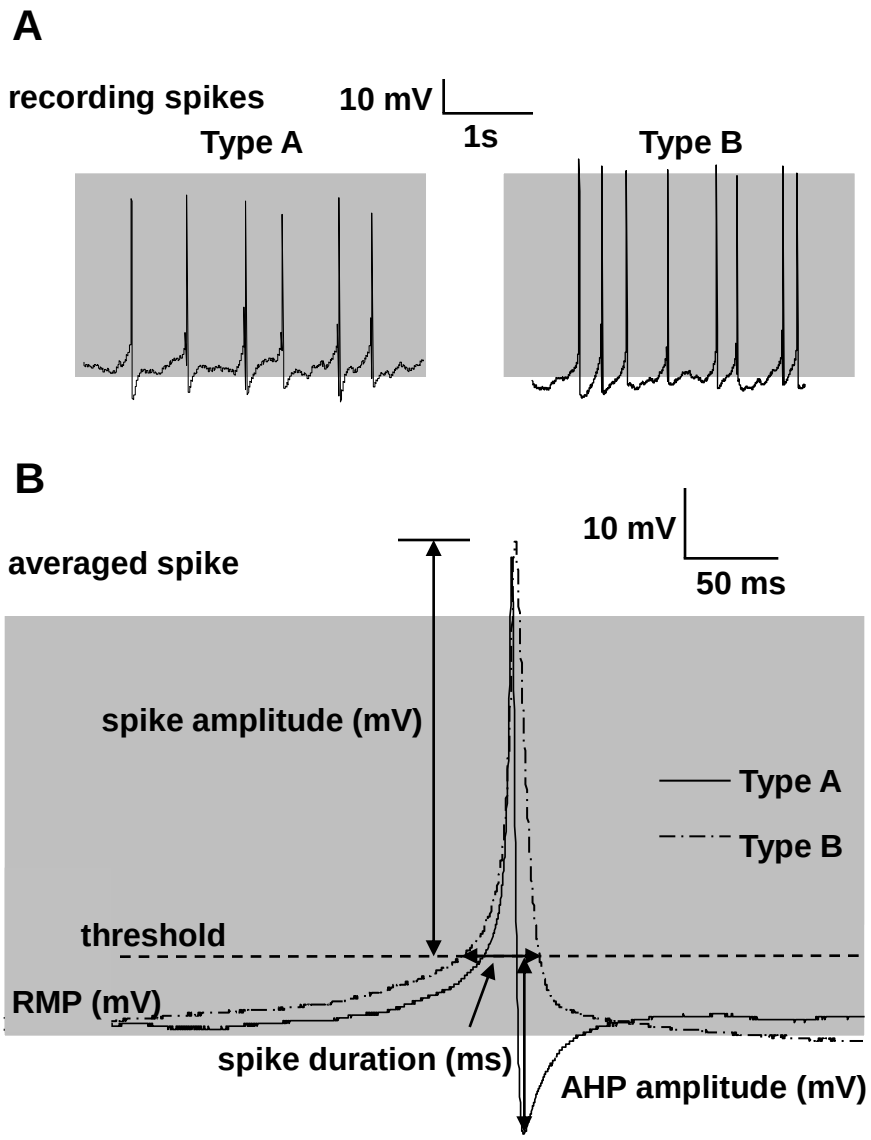

Figure 4.3 Characterization of type A and type B action potentials. A, representative recording spikes of type A and type B firings patterns. **B**, averaged spike from 20 random action potential spikes of type A (continuous line) and type B (dashed line) firing patterns. Several features of averaged type A and type B action potential waveforms are measured to be compared between them (Figure 4.4). Grey shading indicates membrane potential between -50 to +10 mV.

Figure 4.4
Characterization of type A and type B action potentials

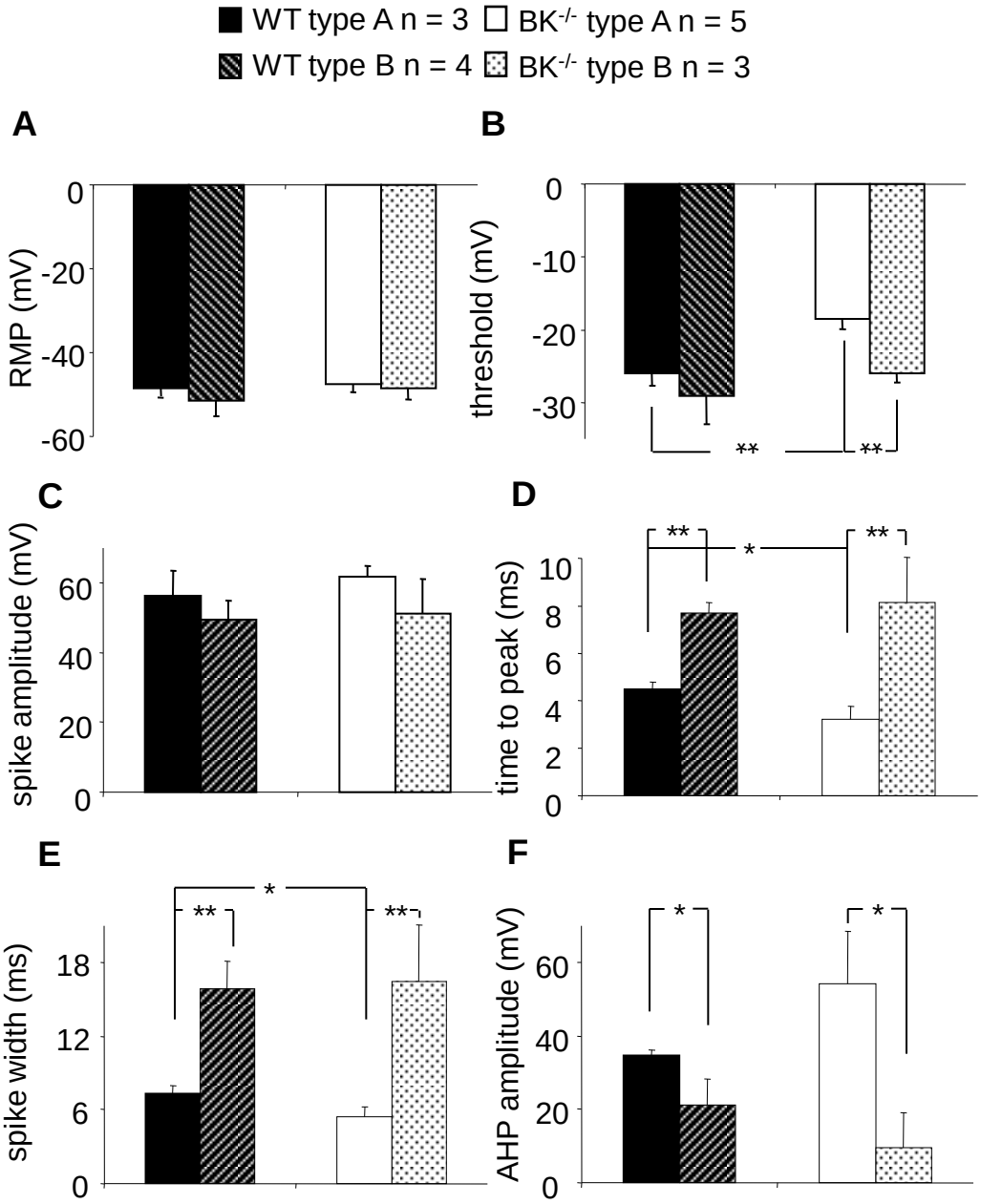

Figure 4.4 Characterization of type A and type B action potentials. Mean resting membrane potential (RMP) (A), threshold for action potential generation (B), spike amplitude (C), time to action potential peak (D), spike width (E) and afterhyperpolarization (AHP) amplitude (F) for type A and B spikes. Filled square for WT type A spike, open square for $BK^{-/-}$ type A spike, lines filled square for WT type B spike and dots filled square for $BK^{-/-}$ type B spike. $*P < 0.05$, $**P < 0.01$ (Student's t-test, ANOVA with post doc Dunnett's test). All data are means ± SEM, n, no. of independent recorded cells.

4.4E) and a bigger afterhyperpolarization amplitude (Figure 4.4F) compared to pattern B spikes both in WT and $BK^{-/-}$ corticotrophs. Pattern A single spike action potentials in WT cells displayed a longer time to peak (Figure 4.4D) and wider spike width (Figure 4.4E) compared to pattern B in $BK^{-/-}$ cells.

In addition, cells displaying pattern A and/or B spikes also showed spontaneous reversible conversion to "pseudo-plateau bursting" action potentials (Stern *et al*., 2008) with variable spike amplitudes or superimposed on periodic depolarized potentials (Figure 4.1C-G). Pattern C was considered as consisting of superimposed single spikes of pattern B on a small depolarized potential plateau from the resting membrane potentials, and the same as pattern D consisting of superimposed single spikes of pattern A (Figure 4.1). Pattern E and F were bursting action potentials initiated with a large single spike (Figure 4.1). Pattern C-F were not the dominant firing patterns, and in all examined cells 35% of WT cells showed patterns of C-F and the proportion in $BK^{-/-}$ cells was 24% (Figure 4.2). The percentage of each firing pattern represents the proportion of all cells that showed this pattern during its entire recording (Figure 4.2). Less than 5% of WT and $BK^{-/-}$ cells displayed an atypical "pseudo-plateau bursting", which started with a single-spike following either with a sustained depolarization (Figure 4.1H) or a very slow repolarization to the resting membrane potential from 10 seconds to 3 minutes (Figure 4.1I & 4.2).

In all, the nine firing patterns randomly detected in WT (n = 20) and $BK^{-/-}$ cells (n = 22) without any significant differences in any firing pattern between genotypes

(Figure 4.2). In WT cells, spontaneous transitions from pattern A to B occasionally observed, while in $BK^{-/-}$ cells pattern A and pattern B were never detected in the same cell. Pattern C to G were less often observed during recording and always occurred with pattern A and/or B. Less than 10% of WT and $BK^{-/-}$ cells only displayed "pseudo-plateau bursting" without any single spike during the recording period from 30 minutes to 1 hour. Pattern H and I were most rarely seen during recording and also occurred with pattern A and/or B rather than alone.

4.2.2 No significant effects of 1 μM paxilline on corticotroph excitability

BK channels have been reported responsible for converting single spikes to bursting activity in some types of pituitary cells with relatively high BK channels expression level (Van Goor, Li & Stojilkovic, 2001). In murine corticotrophs, the BK current component contributed little to the whole-cell outward current in voltage-clamp recordings (section 3.2.3.2). 1 μM paxilline applied to recorded cells with constant spontaneous action potentials displayed no significant change in the resting membrane potential or firing frequency in any examined cells (Figure 4.5). The percentage change in the firing frequency of WT corticotrophs was 1 ± 1.2% (firing frequency was defined as no. of spikes/min before and in the presence of paxilline) (n = 4). It is consistent that BK current did not play any significant effects on electrical activity in other pituitary cells with low expression of BK channels and also agrees with the data that firing patterns were not significantly different between the WT and $BK^{-/-}$ cell groups.

Figure 4.5
No significant effects of 1 µM paxilline on corticotroph excitability

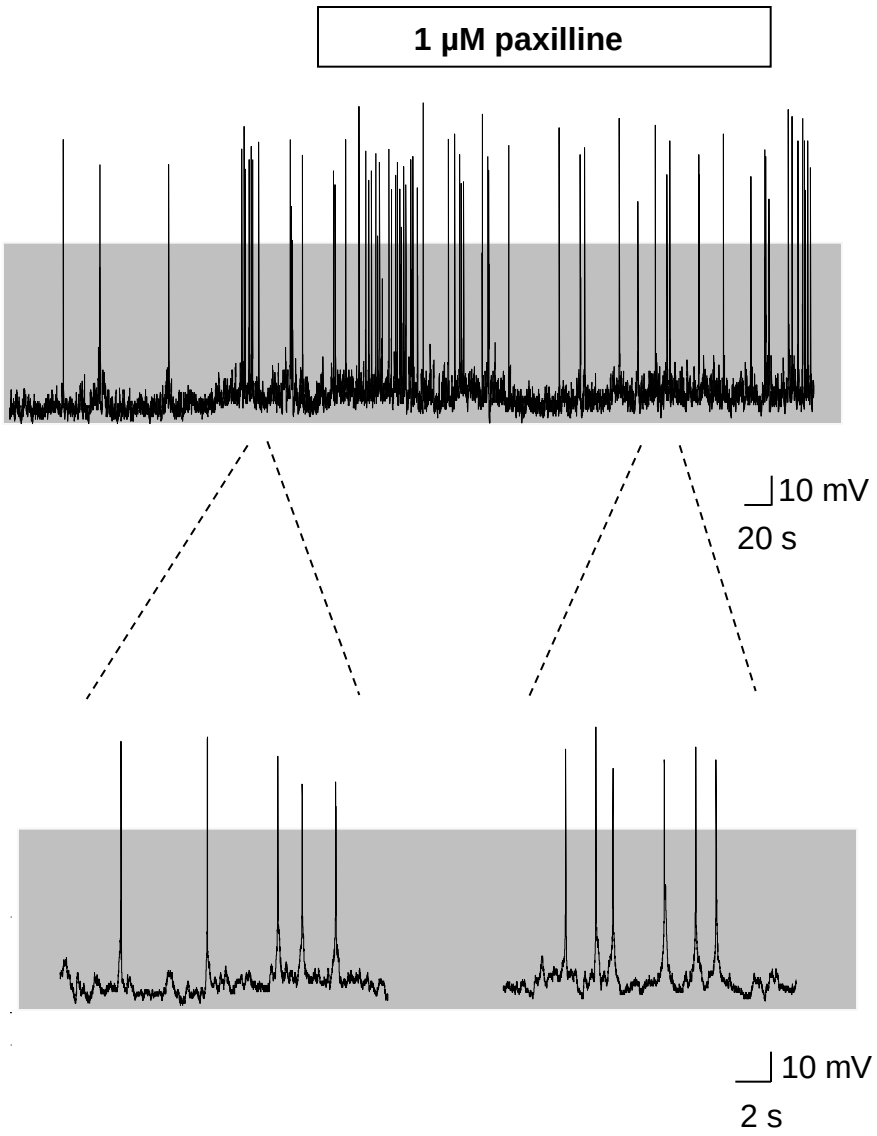

Figure 4.5 No significants effect of 1 µM paxilline on corticotroph excitability. A representative current-clamp recording of metabolically intact corticotroph cell before and during exposure to 1 µM paxilline (horizontal open bar). Grey shading indicates membrane potential between -50 to +10 mV.

4.2.3 TRAM-34 controls corticotroph excitability

In voltage-clamp recordings, a TRAM-34-sensitive potassium current was a large component in the whole-cell outward current in murine corticotrophs (section 3.2.3.3). In order to reveal its effects on corticotroph electrical activity, 5 μM TRAM-34 was applied to recorded cells showing stable spontaneous action potentials with the same concentration as used in voltage-clamp recording.

4/6 WT corticotrophs responded to 5 μM TRAM-34 with a significant increase in firing frequency with a conversion from single spikes (Figure 4.1B) to "pseudo-plateau bursting" (Figure 4.1E) without changing the resting membrane potential (Figure 4.6). The mean percentage increase in the firing frequency was 56 ± 7.2% (firing frequency was defined as no. of spikes/min before and in the presence of TRAM-34). 2/3 $BK^{-/-}$ cells exposed to TRAM-34 showed similar results, and this transition between firing patterns was rapidly reversible after washed with normal bath solution. Not every corticotroph cell showed an increase in the firing frequency when exposed to TRAM-34, which may be due to the variable expression levels of SK4 between cells or the initial firing pattern of spontaneous action potentials related with other ion channels. These studies suggested SK4 channels do not contribute to maintaining the cell resting membrane potentials, but may play a role in cell repolarization, the regulation of firing frequency and converting firing patterns in native murine corticotrophs, similar to the functions of BK channels in modulating cell activity of some other pituitary cells with a high BK channel expression level (Van Goor, Li & Stojilkovic, 2001).

Figure 4.6
TRAM-34 controls corticotroph excitability

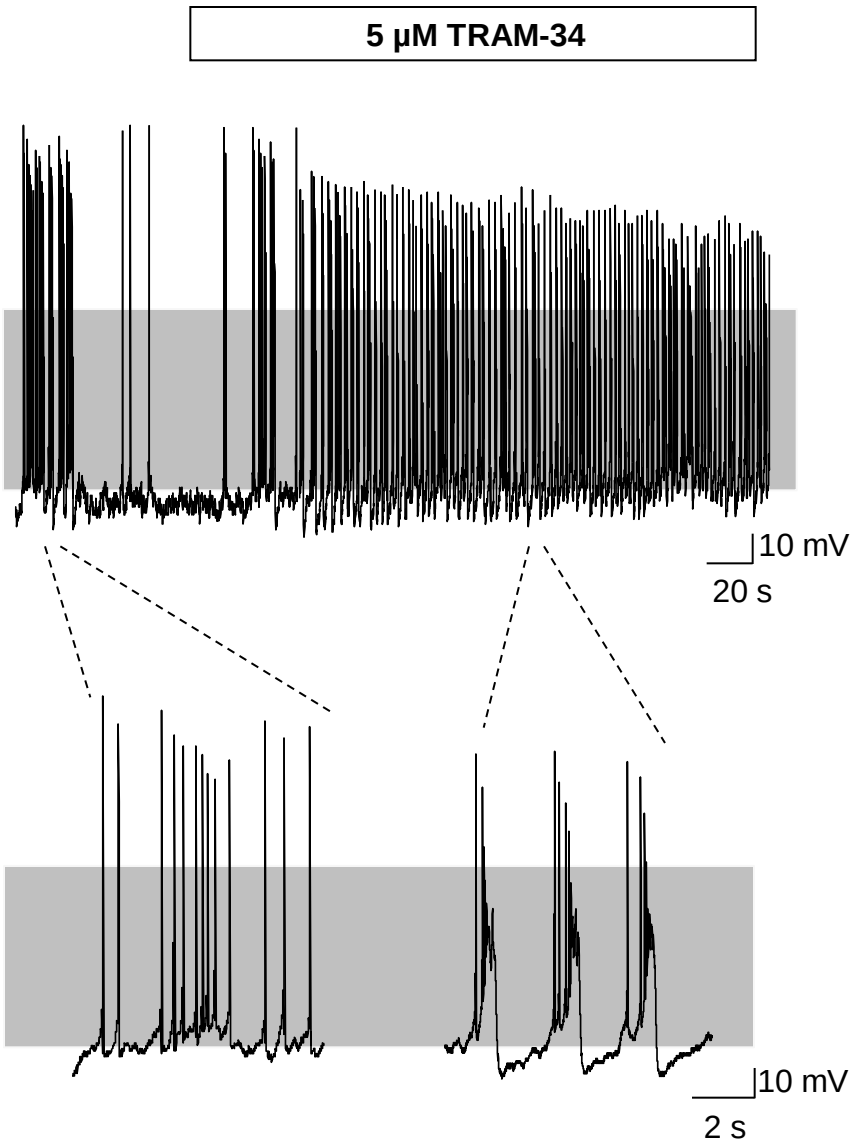

Figure 4.6 TRAM-34 controls corticotroph excitability. A representative current-clamp recording of metabolically intact corticotroph before and during exposure to 5 µM TRAM-34 (horizontal open bar). Grey shading indicates membrane potential between -50 to +10 mV. 5 µM TRAM-34 resulted in a increase in action potential frequency with a transition to a "pseudo-plateau bursting" phenotype, without any significant membrane potential depolarization.

4.2.4 The effects of 1 mM 4-AP on corticotroph excitability

4-AP sensitive current was another relatively large whole-cell outward current component in murine corticotrophs (section 3.2.3.4). We thus wondered whether it plays an important role in the control of corticotroph excitability. Stably spontaneous firing cells were exposed to 1 mM 4-AP the same concentration as applied in voltage-clamp recordings.

1/6 WT corticotrophs with single spikes showing large afterhyperpolarization (AHP) amplitude lost their AHP amplitude after the addition of 1 mM 4-AP without causing any signification changes in the resting membrane potentials or firing frequency, and the AHP inhibition was reversible with bath wash (Figure 4.7). No similar response found in the examined $BK^{-/-}$ cells (n = 7). This response was very rare in recorded corticotrophs, and it may be related with the initial firing pattern. Cells initially displaying bursting action potentials or single spikes without a large AHP amplitude showed no significant response to 1 mM 4-AP. 2/6 WT cells displayed a very small percentage firing frequency increase (less than 2%) after exposure to 1 mM 4-AP. The rare regulation of 4-AP in cell excitability was not observed in every recorded corticotroph, which may be due to the various expression levels of A-type current shown in voltage-clamp recordings.

These studies implied A-type current had no significant contribution to the frequency change of action potentials or maintaining the resting membrane potential in the majority of corticotrophs.

Figure 4.7
The effects of 1 mM 4-AP on corticotroph excitability

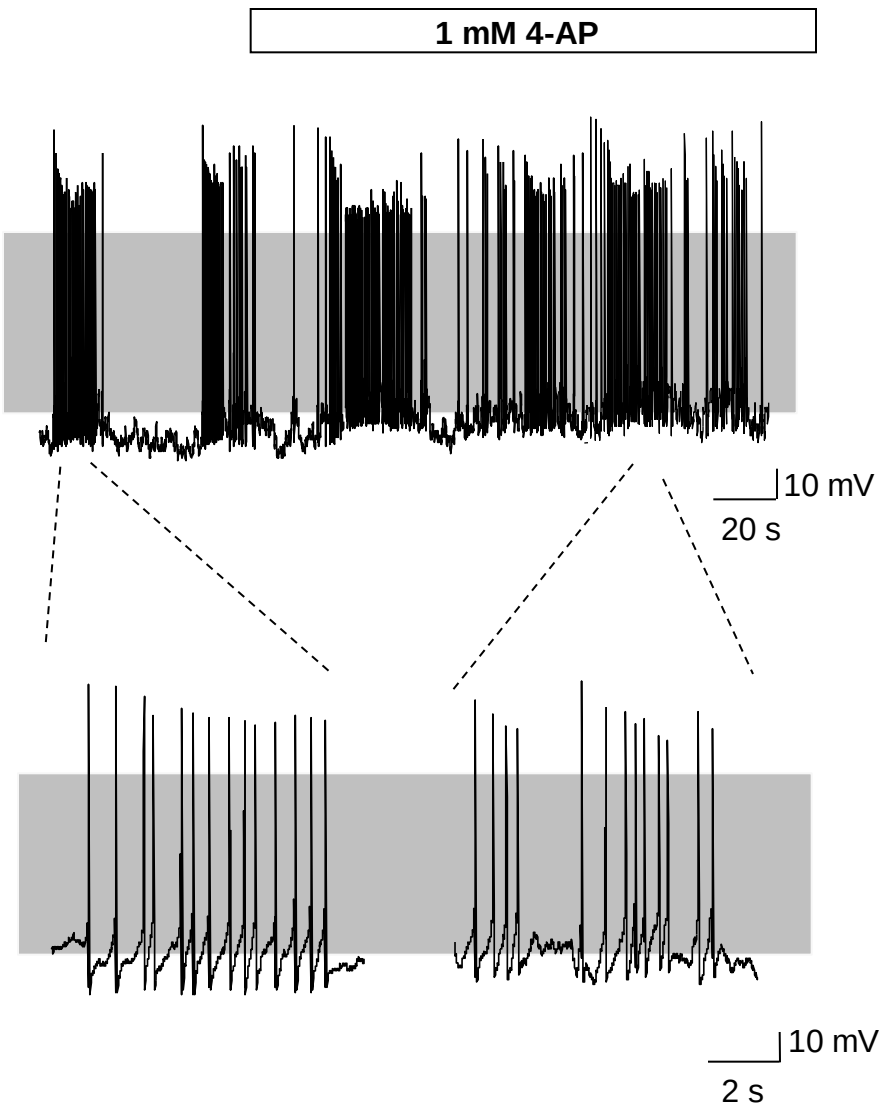

Figure 4.7 The effects of 1 mM 4-AP on corticotroph excitability. A, representative current-clamp recording of metabolically intact corticotroph before and during exposure to 1 mM 4-AP (horizontal open bar). Grey shading indicates membrane potential between -50 to +10 mV. 1 mM 4-AP resulted in a reduction of AHP amplitude without any significant membrane potential depolarization.

4.2.5 $BaCl_2$ has no significant effects on corticotroph excitability

Ba^{2+}-sensitive K_{ir} channels was the only potassium conductance that showed a significantly difference in the current density between WT and $BK^{-/-}$ corticotrophs in voltage-clamp recordings. To figure out if K_{ir} plays any role in the control of corticotroph action potentials, 100 µM $BaCl_2$ was applied to block K_{ir} potassium channels, the same concentration as used in voltage-clamp recordings.

100 µM $BaCl_2$ showed no significant effects on the frequency of action potentials or the resting membrane potentials in any examined cells from WT (n = 6) or $BK^{-/-}$ (n = 5) mice (Figure 4.8). The percentage change in the firing frequency of WT corticotrophs was 1.1 ± 0.3%, and 0.8 ± 0.5% for $BK^{-/-}$ (firing frequency was defined as no. of spikes/min before and in the presence of $BaCl_2$). Based on this observation, Ba^{2+}-sensitive K_{ir} channels have no significant role in the regulation or generation of action potentials in murine corticotrophs, which is in contrast to that reported in rat corticotrophs (Kuryshev *et al*., 1997).

Figure 4.8
$BaCl_2$ has no significant effects on corticotroph excitability

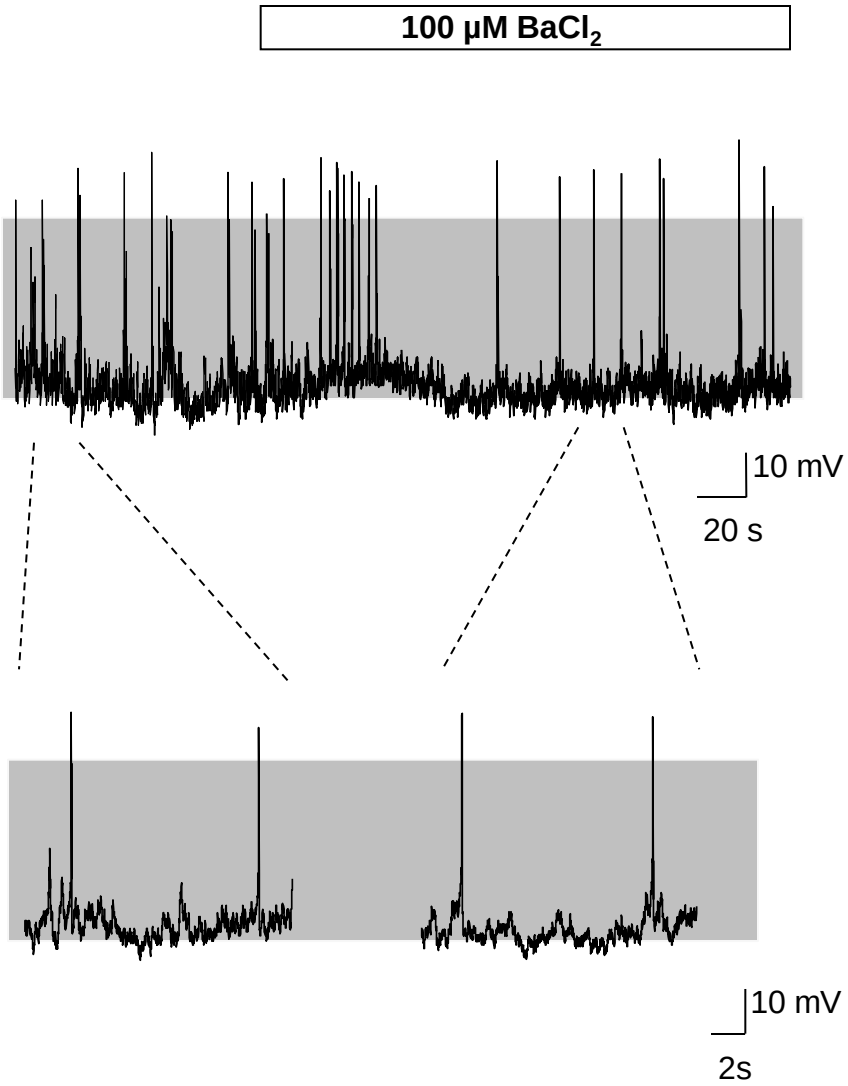

Figure 4.8 $BaCl_2$ has no significant effects on corticotroph excitability. Representative current-clamp recording of metabolically intact corticotroph before and during exposure to 100 µM $BaCl_2$ (horizontal open bar). Grey shading indicates membrane potential between -50 to +10 mV.

4.3 Summary

4.3.1 Native murine corticotrophs have spontaneous action potentials

More than 99% of recorded native murine anterior corticotrophs displayed spontaneous action potentials, which is consistent with the observation in male rat corticotrophs (Kuryshev *et al*., 1997) and other pituitary cells (Stojilkovic, Tabak & Bertram, 2010). Even in conventional whole-cell recordings, spontaneous action potentials were detectable in almost every cell, although they rapidly disappeared as the electrode solution was dialyzed the cell interior. Previous studies suggested rat and mouse corticotrophs are electrically silent (Lee & Tse, 1997; Lee & Tse, 2011), which is most likely related to the use of whole-cell recording mode, or the cell isolation method applied in these studies. Perforated patch-clamp recording allowed a stable detection of spontaneous action potentials for > 1 hour and was used routinely in the current-clamp recordings investigation of this thesis. These data suggest that both whole-cell and perforated patch-clamp recordings can detect spontaneous firings, but the time window for whole-cell recording is very narrow and spontaneous action potentials can only be observed shortly after establishing the whole-cell mode, which may be one reason previous studies missed the detection of spontaneous activity in corticotroph models.

Different from the typically regular single spike firing pattern observed in many neurons, pituitary cells have been reported to generate both single spikes and

"pseudo-plateau bursting" action potentials (Stern *et al.*, 2008). In accordance, the large majority of recorded native murine corticotrophs displayed spontaneous action potentials. However, the firing patterns and the frequency of spontaneous action potentials varied widely between cells. Spontaneous transitions between these patterns were easily observed in native murine corticotrophs similar to that found in male rat corticotrophs, melanotrophs and GH cell lines (Kuryshev, Child & Ritchie, 1996; Kuryshev *et al*., 1997; Taraskevich & Douglas, 1989; Schlegel *et al*, 1987). Single spikes were the main patterns found in both WT and $BK^{-/-}$ cells. The highly heterogeneous "pseudo plateau bursting" action potential patterns found in the native murine corticotrophs most likely reflect spontaneous oscillations in depolarising and hyperpolarising potentials with time in cells with a high cell input resistance, where small changes in currents are enough to lead to transition of the firing patterns.

4.3.2 SK4 channels regulate corticotroph cell activity

A large component of TRAM-34 sensitive outward potassium conductance was surprisingly found in native murine corticotrophs. This component was suggested to be contributed by SK4 channels, encoded by the Kcnn4 gene, which are also sensitive to clotrimazole. Clotrimazole-sensitive potassium conductances have been reported in other anterior pituitary cells, but clotrimazole may also inhibit a range of other conductances (Wu *et al*., 1999). In contrast, the concentration of TRAM-34 used here are highly selective for SK4 channels, although an effect on non-selective conductances has been reported in one study at high concentration (Schilling & Eder, 2007). Real time PCR data reveals a relatively low level of Kcnn4 mRNA expression

compared with the Kcnn1-3 genes encoding SK channels in the anterior pituitary (Liang *et al*., 2011). However, SK4 protein expression was detected that co-localised with ACTH-positive cells in the murine anterior pituitary gland using immunohistochemistry (Liang *et al*., 2011).

When TRAM-34 was applied to inhibit SK4 channels in current-clamp recordings, an increase in the frequency of action potentials was displayed, although without significant depolarization in the resting membrane potential. This suggests that SK4 channels normally limit corticotroph excitability and thus blocking them might enhance ACTH release. In support of this, genetic deletion of Kcnn4 ($Kcnn4^{-/-}$) in mice enhanced restraint stress-induced plasma ACTH levels, and the pharmacological inhibition of SK4 increased the CRH/AVP-induced ACTH secretion *in vitro* in murine corticotrophs (Liang *et al*., 2011). In humans, the non-selective inhibitor of SK4 channels, clotrimazole elevated plasma cortisol levels although this may be due to its effect on cytochrome P450 enzymes (Wojtulewski *et al*., 1980). SK4 channel inhibitors are also being developed as the drug for some diseases, such as potent immunosuppressants (Wulff *et al*., 2007). These studies suggest a role of SK4 channels also in controlling human corticotroph function and HPA-axis reactivity.

In $Kcnn4^{-/-}$ mice restraint stress-induced mRNA expression of the early immediate genes *c-fos* and *nurr*77 was enhanced in the hypothalamus compared with WT controls (Liang *et al*., 2011). These genes are markers for enhanced hypothalamic neuronal activation (Chan *et al*., 1993; Brunton *et al*., 2007). In addition, mRNA

expression of CRH/AVP in the hypothalamus and mRNA expression of CRH/AVP receptors in the anterior pituitary were both significantly increased in Kcnn4$^{-/-}$ mice. These results suggest that enhanced hypothalamic drive and increased corticotroph sensitivity to CRH/AVP may also be responsible for the stress hyperresponsiveness observed in Kcnn4$^{-/-}$ mice (Liang *et al*., 2011).

In contrast, BK$^{-/-}$ mice display a stress hyporesponsiveness even though ACTH release from the anterior pituitary is increased *in vitro*. In BK$^{-/-}$ mice, a decrease in mRNA expression of CRH in hypothalamus showed no significant effects on *nurr*77 expression in PVN neurons (Brunton *et al*., 2007). Taken together, BK channels and SK4 channels may play opposite effects on hypothalamic PVN function (Brunton *et al*., 2007). The novel role of SK4 channels in regulating corticotroph excitability and ACTH secretion *in vitro* and *in vivo* and in controlling the HPA stress axis function may be mediated both by effects at the pituitary corticotroph as well as through enhanced hypothalamic PVN neuronal excitability and drive.

4.3.3 A-type channels regulate corticotroph cell activity

The inhibition of another large component of the outward potassium current observed in native murine corticotrophs, mediated by A-type potassium channels reduced the amplitude of the afterhyperpolarization phase of action potentials in some, but not all, murine corticotrophs. This role is different from the function of A-type potassium channel current reported in the regulation of firing frequency in cardiac and other excitable tissues (Stojilkovic, Tabak & Bertram, 2010). In ovine

pituitary somatotrophs, A-type potassium channels showed a high level of expression and were suggested to regulate action potentials and hormone secretion (Mei *et al*., 1998). In rat pituitary lactotrophs, A-type potassium channels were also detected, but did not contribute to generation of action potentials (Sankaranarayanan & Simasko, 1998). Investigation of A-type current in the mouse corticotroph tumour cell line AtT20/D16-16 revealed its potential role in early glucocorticoid feedback (Pennington, Kelly & Antoni FA, 1994).

The expression level and the inactivation status of A-type potassium current may determine their role in the regulation of action potentials in pituitary cells. In rat pituitary cells, lactotrophs and gonadotrophs showed much higher expression level of A-type potassium current than somatotrophs (Van Goor, Li & Stojilkovic, 2001). Although the expression level of A-type potassium channels were relatively high in native murine corticotrophs compared with other potassium conductances, it might be only the highest expression level that reach the threshold for modulating the amplitude of the afterhyperpolarization. Meanwhile, A-type potassium channels are rapidly and transiently activated in the subthreshold range of membrane potentials and largely inactivated at the resting membrane potential of most pituitary cells, which might be another reason why it shows a variable role in generating and modulating action potentials in corticotrophs.

4.3.4 Potential function of K_{ir} channels in native murine corticotrophs

Native murine and rat corticotrophs appear to differ in the role of Ba^{2+}-sensitive K_{ir} channels in the control of spontaneous action potentials. In male rat corticotrophs, when K_{ir} channels were blocked by Ba^{2+}, cells were partially depolarized and the firing frequency increased. Furthermore, CRH was reported to inhibit K_{ir} channels leading to membrane depolarization and enhanced membrane excitability and ACTH release (Kuryshev *et al*., 1997). Thus, Ba^{2+}-sensitive K_{ir} channel conductance has been suggested to contribute to both spontaneous and CRH-induced depolarization and increase of the frequency of action potentials (Kuryshev *et al*., 1997). However, the inhibition of K_{ir} channels by 100 μM $BaCl_2$ had no significant effects on depolarization or spontaneous action potential frequency in native female murine corticotrophs in this investigation. In a modified mathematical model of murine corticotroph excitability, K_{ir} and background sodium conductances act antagonistically in the control of action potentials (Liang *et al*., 2011). The differences between rat and murine corticotrophs may reflect murine corticotrophs have a more depolarised resting membrane potential or the relative different expression levels in the two species or genders of corticotrophs. On the other side, the method used to enrich rat corticotrophs was based on the two sequential counterflow centrifugations comparing with the lentiviral labelling way that used to identity murine corticotrophs , which may changed the basal physiological condition. Further experiments on lentiviral labelled rat corticotrophs could give more information on the differences on the expression level and the function of K_{ir} channels in action potentials.

4.3.5 Potential function of BK channels in native murine corticotrophs

In the AtT20 corticotroph cell line, BK channels are reported to dominant the outward potassium current exerting a functional role in mediating the control of ACTH secretion through the inhibition of CRH (Shipston, Kelly & Antoni, 1996). However, BK channels were a small component in native murine corticotrophs and the inhibition of BK channels brought no clear effects on cell depolarization or the frequency of firing. Pharmacology data using 1 μM paxilline indicated at the resting membrane potential, BK channels contribute little conductance in the whole-cell outward current in WT corticotrophs. Paxilline is suggested as a very specific blocker for BK channels. When the concentration of paxilline increased to 10 μM, there was a notable inhibition of the outward current. Meanwhile, this dramatic inhibition was also detected in $BK^{-/-}$ mice, in which no BK channels express. However, in single channel recordings from inside-out patches exposed to 5 μM intracellular free calcium, there was a significant paxilline-sensitive component during a step pulse to +60 mV, suggesting BK channels were inactivated under normal resting membrane potential in metabolically intact murine corticotrophs (Liang *et al.*, 2011). SK4 channels have been reported to inhibit BK channels in some cells (Thompson & Begenisich, 2009). Using the lentiviral transduction system to deliver siRNA of SK4 channel gene into corticotrophs to achieve a knockdown expression level of SK4 channels may provide a way to investigate whether SK4 channels in fact inhibit BK channels in corticotrophs.

This chapter provides a summary of the roles of potassium conductances identified in voltage-clamp recordings (chapter 3) in spontaneous action potentials in native murine corticotrophs. The control of ion channels is important for corticotroph electrical activity, and they are the direct or indirect targets for hormone modulation and corticotroph physiological functions. BK channels reported having an important role in AtT20 pituitary cell lines, had little effect on the regulation of native murine corticotroph excitabilities. However, SK4 channels dominated the outward conductance in native murine corticotrophs and also exert modulation of corticotroph cell excitability. More studies to reveal the interaction between SK4 channels and BK channels are needed. Furthermore, whether CRH and AVP control SK4 or A-type potassium channels in native murine corticotrophs needs to be investigated.

Chapter Five:

Regulation of spontaneous and CRH/AVP-evoked excitability by a background sodium conductance

5.1 Introduction

In many excitable cells, TTX-sensitive voltage-gated Na^+ channels are important for action potential generation, although their role in anterior pituitary cells is not well defined (Baranauskas & Martina, 2001; Baker & Wood, 2001; Chabbert *et al.*, 2003; Hong *et al.*, 2004). In several pituitary cell types, spontaneous activity is dependent upon a TTX-resistant inward background sodium conductance, although the molecular basis of the sodium conductance is not clear (Simasko, 1994; Takano*et al*., 1996; Tomic *et al*., 2011). In this chapter, we aims to determine whether native murine corticotrophs express an inward background sodium (Na_b) conductance and investigated its role in the control of corticotroph resting membrane potential and generation of spontaneous and CRH/AVP evoked action potentials in murine corticotrophs. Na_v channels are widely express in nerve, muscle and almost all secretory pituitary cells, and even in some non-excitable cells Na_v channels can be detected at a lower expression level. The main functions of Na_v channels are to depolarize cell membrane potentials, generate the upstroke of action potentials and control the amplitude of spikes in many types of excitable cells. Based on previous studies in the AtT20 corticotroph cell line as well as rat and human corticotrophs, both TTX-sensitive and TTX-resistant voltage-gated sodium channels may be expressed in pituitary corticotrophs. We therefore expected Na_v channels would be found in the lentiviral labelled native murine corticotrophs.

CRH and AVP are the primary hormones *in vivo* that regulate corticotroph cell excitability, controlling membrane potential and action potentials frequency, which

evoke ACTH secretion from anterior pituitary corticotrophs. CRH is the most efficient secretagogue that regulates corticotroph function. AVP is also an important secretagogue in rodents, but it is a weaker stimulator of ACTH secretion. However, its synergistic effect with CRH significantly enhances the release of ACTH from pituitary corticotrophs. In this chapter, we aim to examine how the lentiviral labelled native murine pituitary corticotrophs respond to physiological levels of CRH and AVP.

Most previous investigations on the effect of CRH and AVP on corticotroph electrical excitability were based on corticotrophs sorted by the enlargement of cell volume after exposure to a high dose of CRH or in response to supraphysiological levels of the secretagogues (e.g. 10–100 nM). In this thesis, we avoided using any hormone in cell identification and examined the regulation of CRH and AVP on murine corticotroph excitability as close to near-physiological conditions by using lentiviral transduced corticotrophs expressing eYFP.

5.2 Results

5.2.1 TTX-sensitive sodium inward current

Firstly, we attempted to examine TTX-sensitive inward sodium current in native murine corticotrophs. 2 μM TTX was applied to the standard extracellular solution in cells that showed a large transient inactivating inward current. For 40 out of 50 recorded cells, the inward current began to decrease within 2-3 minutes after 2 μM TTX was applied, and was totally abolished within 5-8 minutes. The inward current quickly recovered after washout (Figure 5.1 left). In the other 20% of cells, although some inward current was inhibited, they still displayed a marked inward current even 20-30 minutes after 2μM TTX was applied (Figure 5.1 right). These data suggested that the fast inward current of native corticotrophs was largely contributed by TTX-sensitive sodium channels, although a TTX-insensitive component was also expressed.

When 2 μM TTX was applied to the cells with stable spontaneous action potentials, we detected no effects on the resting membrane potential or the firing frequency (Figure 5.2). The percentage change in the firing frequency was 2 ± 0.78% (n = 4, firing frequency was defined as no. of spikes/min before and in the presence of TTX). 2 μM TTX had no significant effects on spontaneous action potentials generation in any recorded cells. It is consistent with previous studies that low concentrations of TTX showed no clear effects on firing frequency and did not abolish spontaneous electrical activity in rat corticotrophs (Kuryshev*et al*., 1997).

Figure 5.1
TTX-sensitive and -insensitive inward current in corticotrophs

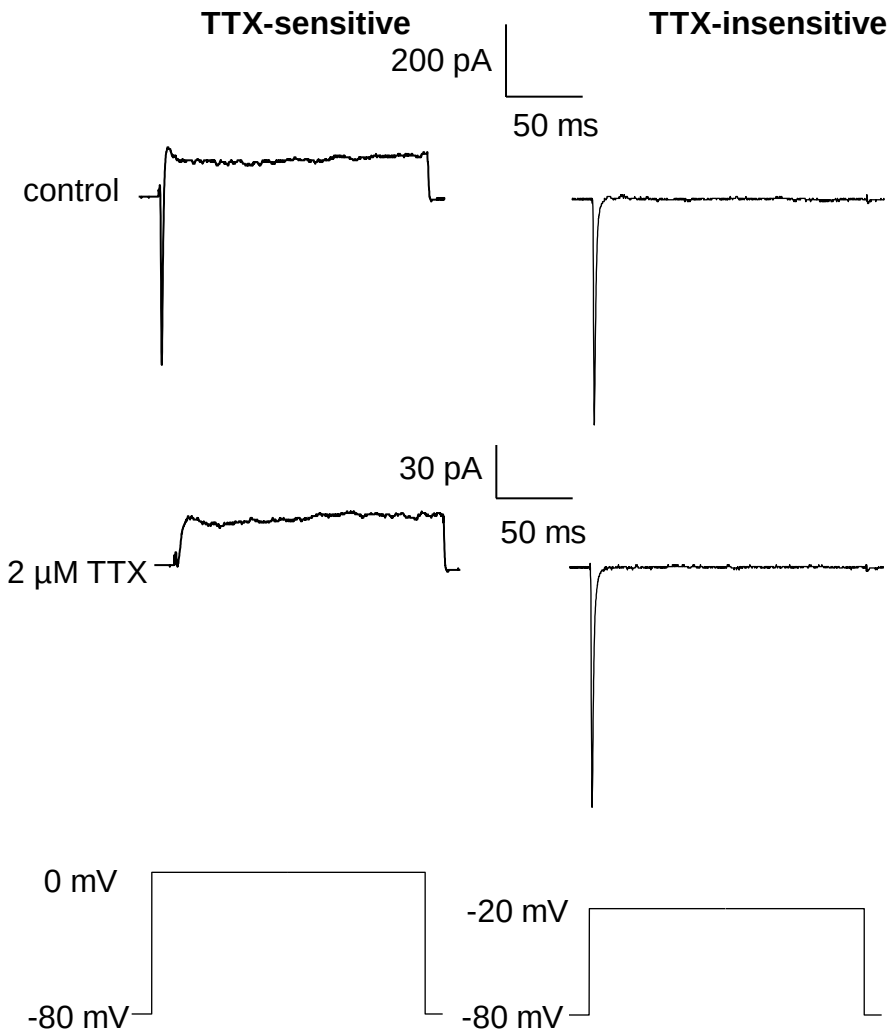

Figure 5.1 TTX-sensitive and -insensitive inward current in corticotrophs. Representative voltage-clamp recording in the perforated patch-clamp mode of a corticotroph cell depolarised from a holding potential of -80 mV to 0 mV (left) or -20 mV (right) in the presence of 2 µM TTX.

Figure 5.2
No significant effects of TTX-sensitive sodium channel on corticotroph excitability

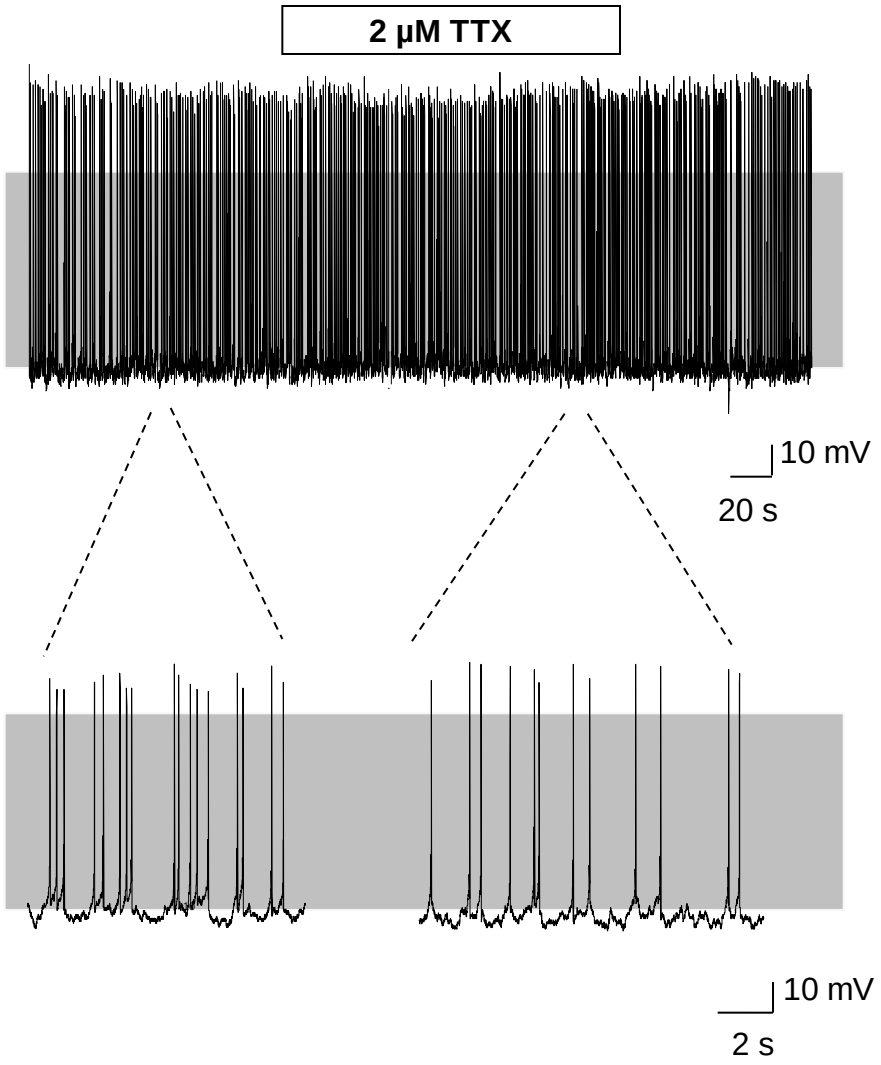

Figure 5.2 No significant effects of TTX-sensitive sodium channel on corticotroph excitability. A representative current-clamp recording of metabolically intact corticotroph before and during exposure to 2 µM TTX (horizontal open bar). Grey shading indicates membrane potential between -50 to +10 mV.

5.2.2 $NMDG^+$-sensitive current controls corticotroph resting membrane potential

In previous investigations, a TTX-insensitive inward sodium conductance was suggested to be responsible for the control of the resting membrane potential in several types of pituitary cells (Simasko, 1994; Takano *et al*., 1996; Tomic *et al*., 2011). In the extracellular solution, the extracellular Na^+ ion was replaced with the large organic cation $NMDG^+$ and applied to cells displaying spontaneous action potentials. In the presence of $NMDG^+$, the membrane potential quickly hyperpolarized and abolished the spontaneous action potential activity. This process was rapidly reversed after washout (Figure 5.3). The membrane potential hyperpolarized to near the K^+ reversal potential. Corticotrophs (n = 5) from WT showed a dramatic membrane hyperpolarization of -25 ± 7.5 mV from the resting membrane potential measured at 3 minutes after $NMDG^+$ addition, and -27 ± 6.9 mV for $BK^{-/-}$ mice (n = 5). There was no significant difference in the extent of hyperpolarization between genotypes.

In voltage-clamp recordings, the replacement of extracellular Na^+ with $NMDG^+$ resulted in the inhibition of a standing inward current, when recorded cells were held at the K^+ reversal potential (-85.6 mV) (Figure 5.4). This inhibition was similar in both WT and $BK^{-/-}$ corticotrophs. The Na^+ channel component contributing to the TTX-insensitive Na^+ component was not clear, so we termed it as background sodium ($Na_{b)}$ channel. These observations suggest that Na_b channel current

Figure 5.3
NMDG$^+$ controls corticotroph resting membrane potential

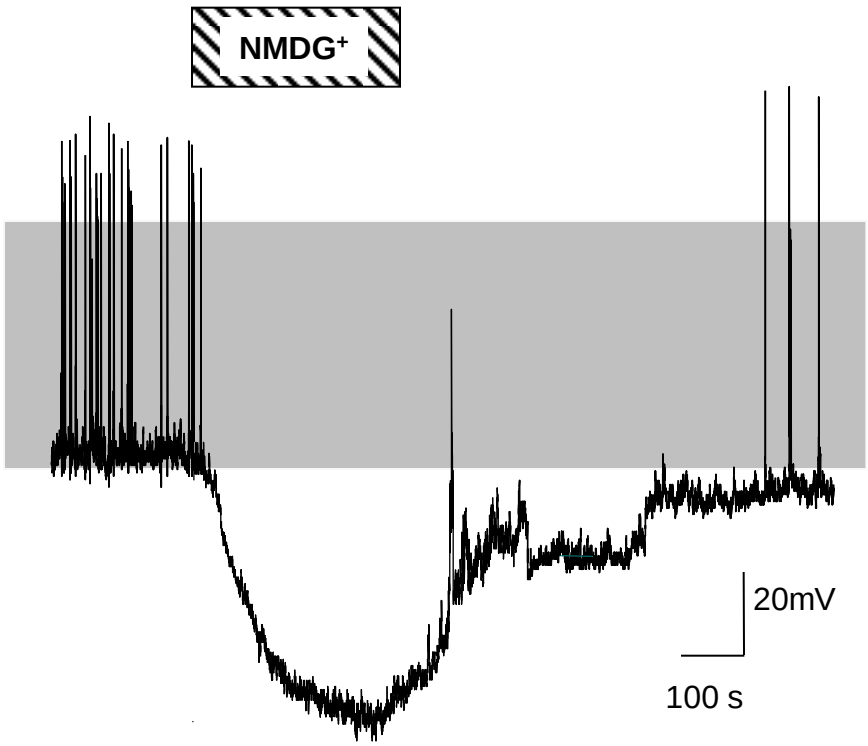

Figure 5.3 NMDG$^+$ controls corticotroph resting membrane potential. A representative current-clamp recording of metabolically intact corticotroph before and during replaced the extracellular Na^+ with $NMDG^+$ (horizontal lines filled bar), causing hyperpolarization and abolishing action potential generation.

Figure 5.4
NMDG$^+$-sensitive inward current at K$^+$ reversal potential

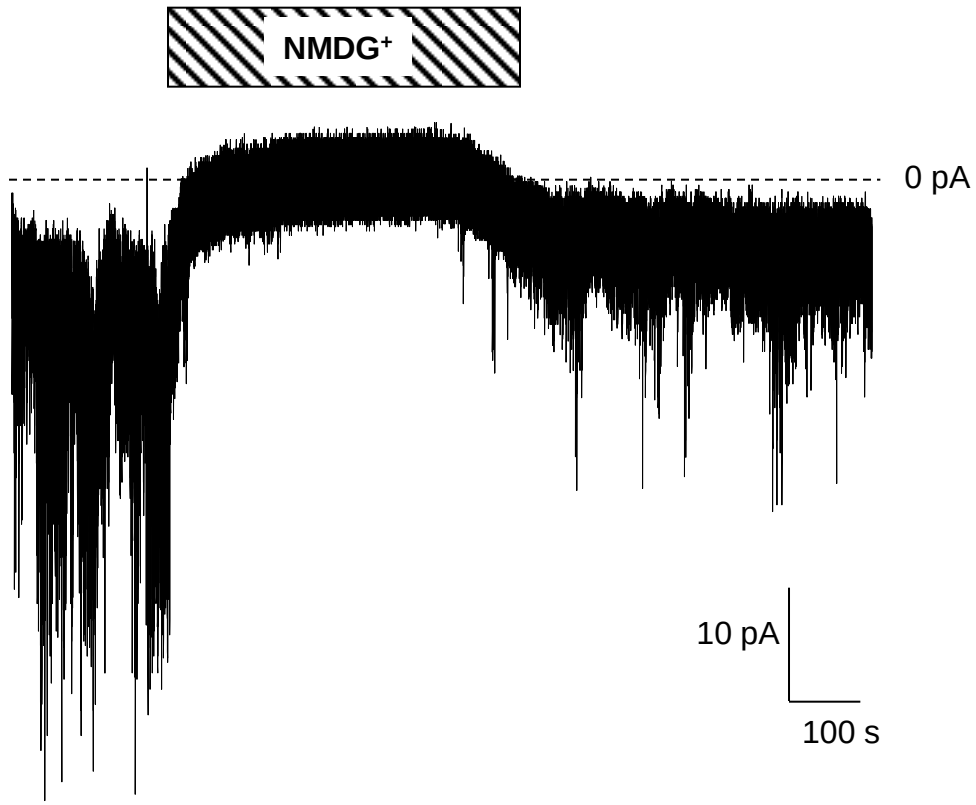

Figure 5.4 NMDG$^+$-sensitive inward current at K$^+$ reversal potential. Representative voltage-clamp trace at the K$^+$ reversal potential reveals a standing inward conductance that is eliminated during NMDG$^+$ substitution for Na$^+$ (horizontal lines filled bar).

component is responsible for maintaining the resting membrane potential of native murine corticotrophs at a depolarised potential around -55 mV.

5.2.3 The regulation of CRH/AVP in corticotroph excitability

To investigate the regulation of CRH and AVP on murine corticotrophs, we applied physiological concentrations of the combined CRH (0.1 nM) and AVP (2 nM) to spontaneously activate or silent corticotrophs. The concentrations applied are similar to the concentrations reported in the portal circulation in response to stress (Sullivan, 1995).

Cells with stable spontaneous action potentials or cells silent for over 10 minutes were exposed to combined secretagogues: 0.1nM CRH and 2nM AVP for 3 minutes. After bath application, corticotrophs displayed a rapid increase in the firing frequency associated with a sustained membrane depolarization of 14.6 ± 5.5 mV for WT corticotrophs (n = 5) from the resting membrane potential measured at 2 minutes after CRH/AVP addition. The depolarized membrane potential reached a plateau in 2-3 minutes after the stimulation. The percentage increase in the firing frequency of WT corticotrophs was 98 ± 5.2% (firing frequency was defined as no. of spikes/min before and in the presence of CRH/AVP). The membrane potential depolarization and enhanced firing frequency lasted even after secretagogues washout (Figure 5.5). The mean time of recovery back to the initial membrane potential was 20.3 ± 4.2 minutes (n = 4). Some cells only showed partial reversibility even after 1 hour bath wash. For the few silent cells recorded, CRH/AVP initiated action potentials.

Figure 5.5
Stimulation of murine corticotrophs by CRH/AVP

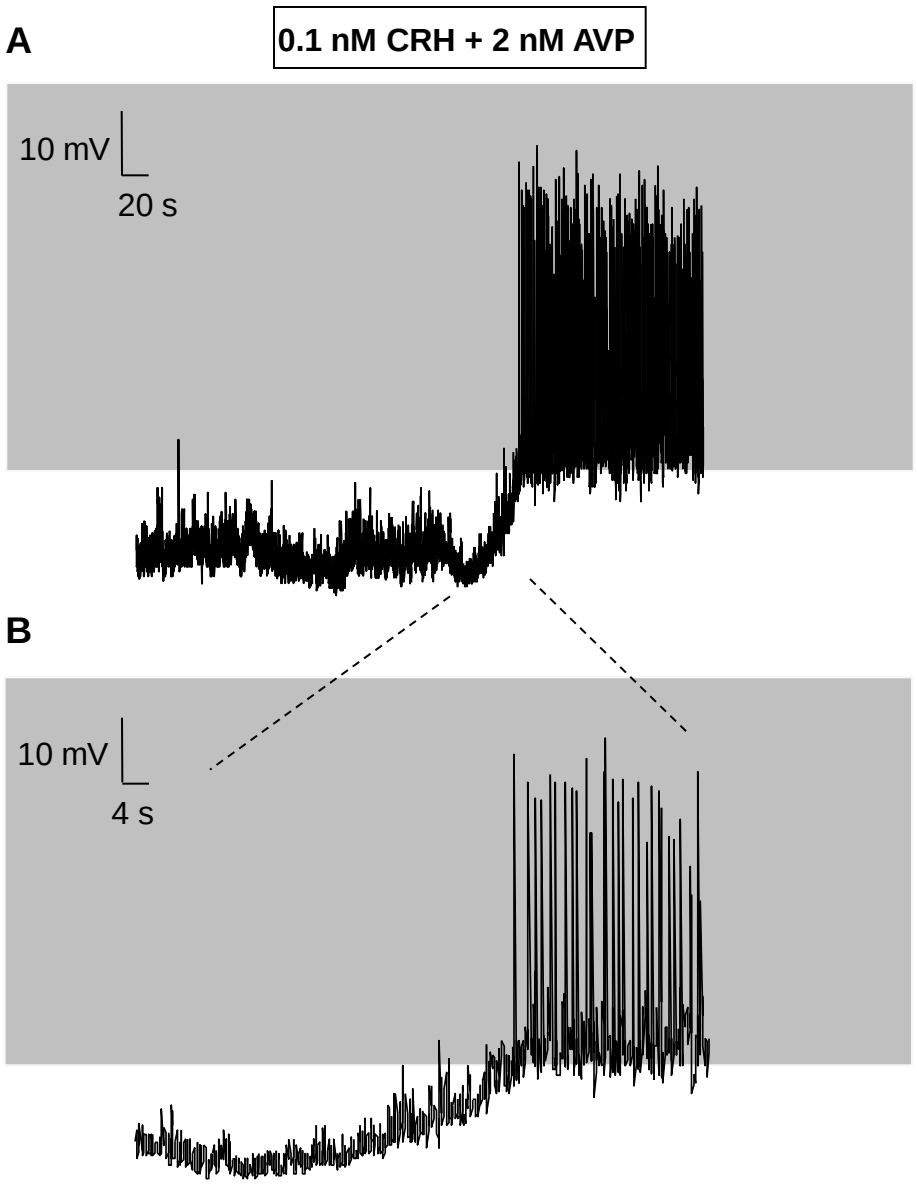

Figure 5.5 Stimulation of murine corticotrophs by CRH/AVP. **A**, representative current-clamp recording of a metabolically intact corticotroph before and during exposure to a 3 minutes pulse of 0.1 nM CRH and 2 nM AVP (horizontal open bar). **B**, expanded traces of panel A. Grey shading indicates membrane potential between -50 to +10 mV.

Corticotrophs from $BK^{-/-}$ mice showed similar responses to CRH/AVP stimulation. Cells had a mean depolarization from the resting membrane potential of 13.6 ± 6.5 mV (n = 4) measured at 2 minutes after CRH/AVP. The percentage increase in the firing frequency of $BK^{-/-}$ corticotrophs was 89 ± 7.42% (firing frequency was defined as no. of spikes/min before and in the presence of CRH/AVP). The average reversal time was 24.3 ± 4.9 minutes (n = 3) from the depolarized potential to the initial resting membrane potential after washout. Again, some $BK^{-/-}$ cells displayed incomplete recovery after wash. Full recovery only occurred both in WT and $BK^{-/-}$ cells when exposed to a brief (< 2 minutes) pulse of combined CRH/AVP. The recovered membrane potential was 90.2 ± 4.56% (n = 3) of the initial membrane potential for WT cells, and 88.9 ± 7.23% (n = 3) for $BK^{-/-}$ cells. No significant differences in the response to CRH/AVP were detected between WT and $BK^{-/-}$ cells.

5.2.4 Independent effects of CRH and AVP on corticotrophs

Among the secretagogues which trigger corticotroph ACTH secretion, CRH is the most potent. AVP is released with CRH *in vivo*, but acts as a relatively weak stimulator. In an attempt to clarify their functions in the regulation of corticotroph activity, we applied CRH or AVP independently to the recorded cells.

We applied 0.1 nM CRH alone to the stably spontaneous firing cells through bath perfusion. After exposure to 0.1 nM CRH for 3 minutes, WT corticotrophs displayed the enhanced frequency of action potentials with a concomitant membrane depolarization from the initial membrane potential of 13.3 ± 3.5 mV (n = 4)

measured at 2 minutes after CRH application. The cell response to CRH alone was consistent with that to the combined secretagogues. The cell depolarization reached the plateau in 2 minutes after the depolarization started (Figure 5.6). The percentage increase in the firing frequency of WT corticotrophs was 92 ± 5.7% (firing frequency was defined as no. of spikes/min before and in the presence of CRH). The mean time for recovery back to the resting membrane potential was 19.8 ± 4.7 minutes (n = 3). $BK^{-/-}$ corticotroph cells showed a similar response to CRH stimulation. Examined cells displayed a mean cell depolarization of 13.1 ± 5.5 mV (n = 3) measured at 2 minutes after CRH application associated with an increase in firing frequency. The percentage increase in the firing frequency of $BK^{-/-}$ corticotrophs was 99 ± 8.3% (firing frequency was defined as no. of spikes/min before and in the presence of CRH). The average recovery time was 25.3 ± 4.3 minutes (n = 3) from the depolarized potential back to the resting membrane potential. No significant difference between WT and $BK^{-/-}$ cell response to CRH stimulation was observed.

AVP is co-localized with CRH *in vivo* and co-released from the mpPVN. Although AVP alone is a weak trigger for corticotroph ACTH secretion, its main effects are synergistic with CRH significantly enhancing the effects of CRH on ACTH secretion.

In an attempt to determine the role of AVP in corticotroph electrical excitability, we applied 2 nM AVP alone to cells showing stable spontaneous action potentials. After exposed to AVP, cells initiated a fast membrane depolarization associated with an increase in firing frequency of action potentials. The percentage increase in the firing

Figure 5.6
Stimulation of murine corticotrophs by AVP and CRH separately

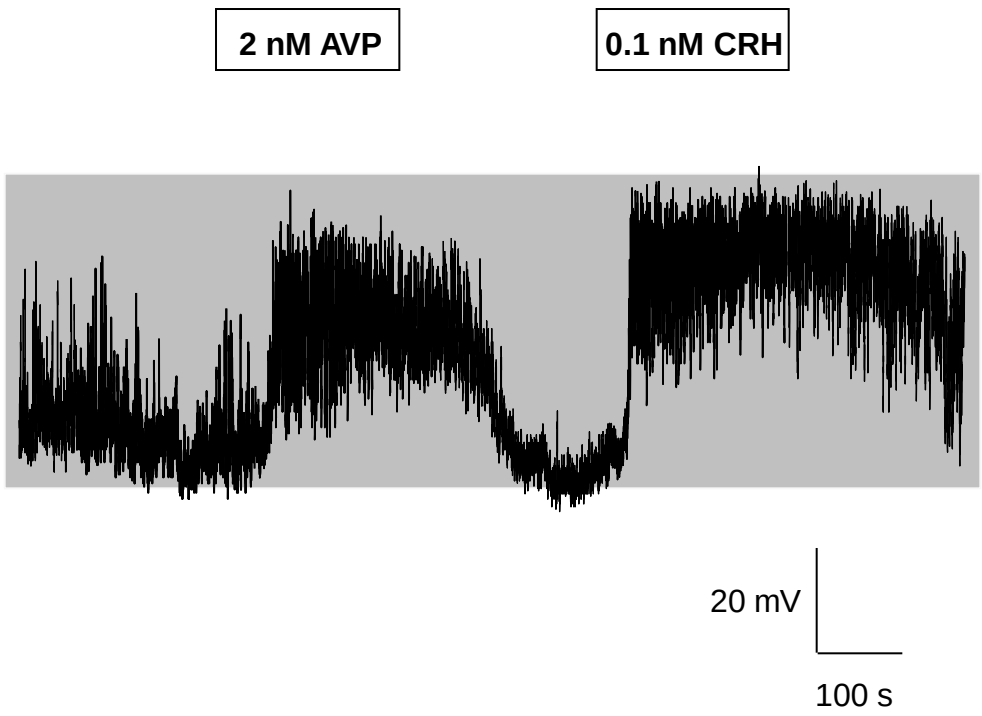

Figure 5.6 Stimulation of murine corticotrophs by AVP and CRH separately. Representative current clamp recording of a metabolically intact corticotroph before and following exposure to a 3 minute pulse of 2 nM AVP (horizontal open bar), then washout before exposure to 0.1 nM CRH (horizontal open bar). Grey shading indicates membrane potential between -50 to +10 mV.

frequency of WT corticotrophs was 93 ± 9.9% (firing frequency was defined as no. of spikes/min before and in the presence of AVP). The mean depolarized membrane potential was 6.3 ± 2.5 mV in WT corticotrophs (n = 3), which was approximately half the size of that triggered by CRH/AVP or CRH alone, measured at 2 minutes after AVP application. The membrane depolarization reached a plateau in 2 minutes after its application. The enhanced firing frequency disappeared and the depolarized membrane potential went back to the resting membrane potential after AVP washout (Figure 5.6). The mean washout time for fully recovery to the resting membrane potential was 5.3 ± 0.4 min (n = 3), which was significantly shorter than that following exposure to CRH/AVP or CRH alone ($P< 0.01$, ANOVA with post doc Dunnett's test). $BK^{-/-}$corticotrophs similarly responded to AVP alone, with the mean depolarization being 5.8 ± 1.9 mV (n = 3) measured at 2 minutes after AVP applied with a significantly increased action potential frequency. The percentage increase in the firing frequency of $BK^{-/-}$ corticotrophs was 98 ± 9.1% (firing frequency was defined as no. of spikes/min before and in the presence of AVP). The mean time for washing out the effects of AVP was 5.5 ± 0.5 min (n = 3). There was no significant difference found when comparing the response to AVP of WT and $BK^{-/-}$ cells. All examined WT and $BK^{-/-}$ cells showed a fully and relatively fast recovery after washout.

5.2.5 Rapid CRH/AVP-induced depolarization is dependent on the $NMDG^+$-sensitive current

CRH/AVP strongly depolarised the resting membrane potential and enhanced action potential frequency in murine corticotrophs. Previous analysis (section 5.2.2) showed that when the external Na^+ was replaced with $NMDG^+$, corticotrophs displayed a fast membrane hyperpolarization and the spontaneous action potentials were abolished suggesting a Na^+-dependent conductance was important for maintaining the depolarised corticotroph resting membrane potential (Figure 5.3). We thus wondered whether CRH and AVP were still able to depolarise corticotrophs in the absence of this sodium conductance and whether this sodium conductance was important for CRH/AVP-induced excitability.

Replacement of Na^+ with $NMDG^+$ prevented the CRH/AVP-induced rapid membrane depolarization or an increase in the firing frequency of spontaneous action potentials (Figure 5.7). Furthermore, CRH/AVP did not prevent the $NMDG^+$-induced cell membrane hyperpolarization. When measured at 2 minutes after CRH/AVP applied in the presence of $NMDG^+$, the mean membrane depolarization was only 2 ± 3.3 mV in WT cells (n = 5), which was significantly smaller than that detected in the physiological extracellular Na^+ solution ($P < 0.01$, Student's t-test, Figure 5.5 & 5.7). In the continued presence of CRH/AVP along with $NMDG^+$, there was a delayed and slow depolarization of 18.1 ± 2.7 mV after 12.9 ±1.7 min (n = 3) in WT corticotrophs. $BK^{-/-}$ cells showed a similar response to the CRH/AVP application in the presence of $NMDG^+$. The mean cell membrane potential depolarized less than

Figure 5.7
Effects of CRH/AVP in the presence of $NMDG^+$

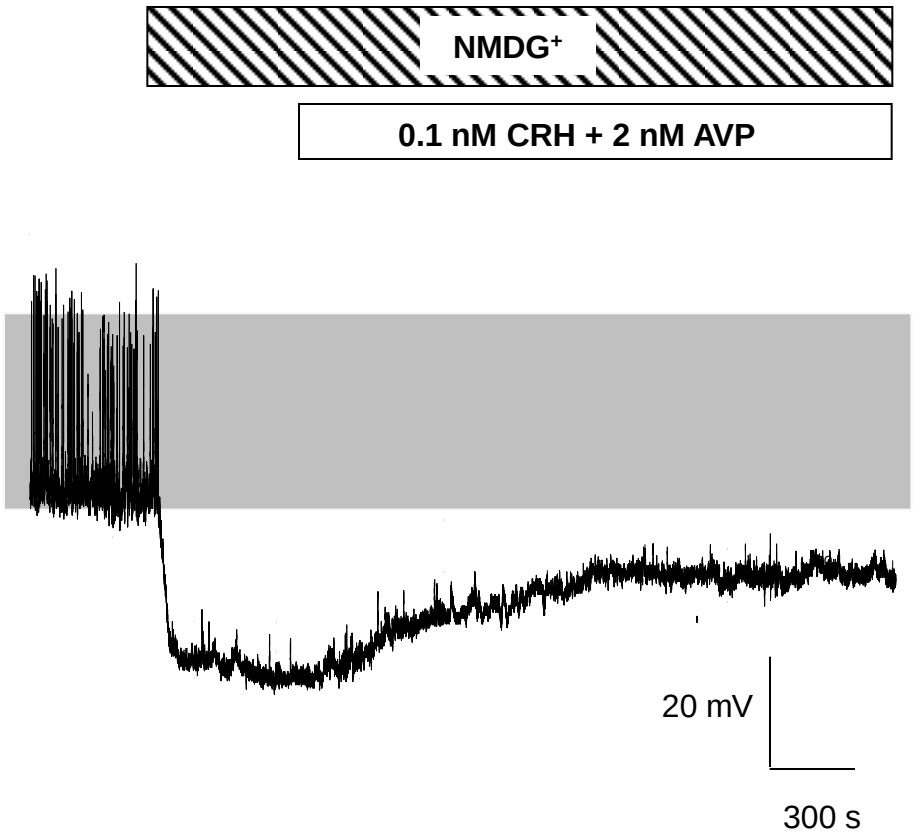

Figure 5.7 Effects of CRH/AVP in the presence of $NMDG^+$. Representative current-clamp recording of metabolically intact corticotroph cell before and during exposure to CRH/AVP (horizontal open bar) in the presence of the $NMDG^+$ solution (horizontal lines filled bar). CRH/AVP do not rapidly depolarise corticotrophs or stimulate action potential generation in Na^+-free external solution. Grey shading indicates membrane potential between -50 to +10 mV.

5 ± 0.2 mV measured at 2 minutes after CRH/AVP applied in the presence of with $NMDG^+$ (n = 3), which was significantly smaller than that detected in the physiological extracellular Na^+ solution ($P < 0.05$, Student's t-test). Furthermore, continued application of CRH/AVP in the presence of $NMDG^+$ resulted in a long term membrane depolarization at 15.1 ± 3.2 mV after 15 ± 1.7 min (n = 3) in $BK^{-/-}$ corticotrophs. No significant differences were observed between WT and $BK^{-/-}$ cells.

These data suggest that the rapid depolarisation (within 2 minutes) of resting membrane potential by CRH/AVP is dependent upon a functional TTX-insensitive background Na^+ conductance. However, with extended exposure to the secretagogues CRH/AVP could induce delayed membrane depolarisation with a much slower time course suggesting there are additional conductances involved in the long-term membrane depolarisation.

5.3 Summary

5.3.1 A background sodium conductance controls corticotroph resting membrane potential

Consistent with previous studies in rat corticotrophs, the inhibition of TTX-sensitive voltage-dependent sodium channels caused no significant effects on the generation of action potentials in murine corticotrophs (Surprenant, 1982; Kuryshev, 1997). However, the replacement of extracellular sodium ions with the large organic cation $NMDG^+$ led to a dramatic hyperpolarization of murine corticotroph resting membrane potential. In addition, a background sodium conductance was recorded at the potassium reversal potential revealing that a background sodium conductance is responsible for maintaining the resting membrane potential of murine corticotrophs. Although the molecular identify of the background sodium conductance has not been determined, the canonical transient receptor potential (TrpC) family of sodium and calcium ion channels has been suggested showing similar role in other pituitary cells (Tomic *et al.*, 2011). However, studies of the replacement of sodium ions with $NMDG^+$ in human corticotrophs derived from patients with Cushing's disease and in the murine AtT20 corticotroph cell line reported no significant effects on the resting membrane potential or electrical excitability (Mollard, 1987; Surprenant, 1982). Channels responsible for maintaining the resting membrane potential may also allow the entry of other ions expect of Na^+, and for corticotrophs from different species there may be different current components that regulate the resting membrane potential.

5.3.2 Lentiviral labelled corticotrophs respond to physiological concentrations of CRH/AVP

The concentrations of CRH and/or AVP used in the vast majority of previous studies in various pituitary corticotroph models researches were several orders of magnitude higher than physiological levels in the portal circulation (Gibbs & Vale 1982; Sheward & Fink, 1991). Together with the similar *in vitro* ACTH secretion detected in the lentiviral labelled corticotrophs to normal controls these data demonstrate that the lentiviral labelling approach does not compromise native murine corticotroph responses during the time scale of this investigation (Liang *et al*., 2011). This approach thus promises to allow an efficient method for genetic manipulation, such as knockdown with siRNA lentiviral transduction or overexpression. It also may allow identification of native corticotrophs in other species, as well as other types of pituitary cells or tissues using their respective cell-specific promoters.

The metabolically intact native murine corticotrophs labelled by the lentiviral transduction system used in this thesis were spontaneously excitable and responded to physiological concentrations of CRH/AVP with a rapid and sustained increase in the frequency of action potentials associated with a depolarisation of the membrane potential. Applying CRH or AVP independently in the same physiological concentration triggered cell depolarization and increased infiring frequency as well. The cell depolarization caused by AVP alone (2 nM) was less effective compared with CRH (0.1 nM) separately, and after wash the stimulatory effects of AVP reversed much faster. It is consistent with previous reports that AVP alone is a weak

secretagogue. For example, in male rat corticotrophs, the initial AVP-induced ACTH release was related with the elevation of $[Ca^{2+}]_i$ from IP3-sensitve stores via a GTP binding protein-coupled phosphoinositide pathway (Tse & Lee, 1998). The elevation of $[Ca^{2+}]_i$ from intracellular Ca^{2+} stores is limited which may explain that AVP induced cell depolarisation is less effective and also reversed more quickly. CRH triggered $[Ca^{2+}]_i$ elevation was dependent on Ca^{2+} entry through voltage-gated Ca^{2+} influx (VGCI), leading a more effective and sustained cell depolarization (Tse & Tse, 1998). When AVP was applied with CRH, AVP evoked an extracellular Ca^{2+} influx via L-type voltage-gated calcium channels activated by the PKC pathway as well, which enhanced the cell depolarization and duration (Tse & Lee, 1998).

Compared with the fast depolarization in response to CRH and AVP in the normal physiological solutions, the effects of CRH and AVP were limited in $NMDG^+$ extracellular solution. No rapid depolarization or increase in firing frequency was detected, which may suggest that under this condition, the fast component directly activated by CRH and AVP are inhibited. For example, Ca_v channels would be largely inactive at this hyperpolarized membrane potential in the presence of $NMDG^+$. Alternatively, the $NMDG^+$-sensitive Na_b channels might normally be one target that activated by CRH/AVP to promote rapid depolarization in the physiological extracellular solution. However, for sustained stimulation by CRH/AVP in $NMDG^+$ extracellular solution, CRH and AVP induced a delayed depolarization from the hyperpolarized membrane potential, but not enough to force the cell membrane back to the resting membrane potential or initiate action potentials. These results reveal that there are slow-response components activated by CRH and

AVP in the presence of $NMDG^+$ extracellular solution that contribute to the sustained corticotroph depolarization.

Ion channels regulated by CRH and AVP in native murine corticotroph remain to be defined. Studies about how CRH and AVP regulate specific ion conductances using voltage-clamp recordings are needed.

Chapter Six:

Summary and Conclusion

This thesis achieved three primary aims:

1) To develop an efficient method to specifically identify native murine pituitary corticotrophs for their electrophysiological characterisation.

2) To profile the major potassium and sodium conductances expressed in native murine corticotrophs and analyze their role in controlling membrane excitability.

3) To clarify whether native murine corticotrophs generate spontaneous action potentials and the effects of CRH/AVP on corticotroph electrical activity.

I developed a high efficient and cell specific lentiviral transduction system to identify native murine corticotrophs by expressing eYFP under the control of a minimal rPOMC promoter in isolated primary pituitary cell culture. This method not only allowed long-term and stable labeling, but also specified the labeling in corticotrophs. Secondly, using electrophysiological analysis of the labeled corticotrophs, I established the profile of potassium and sodium conductances expressed in murine corticotrophs. In addition, with a pharmacological approach I revealed the contributions of different conductances to corticotroph cellular excitability. Thirdly, I found native murine fluorescent corticotrophs have spontaneous action potentials with highly heterogeneous firing patterns, and corticotrophs respond to the physiological concentrations of CRH/AVP. Together, these data provide the first systematic analysis of native murine corticotroph cell electrical activity and also provide information for further investigation of corticotroph physiological properties.

6.1 Development of lentiviral transduction system for native corticotrophs identification

6.1.1 The use of lentiviral transduction system in native murine corticotrophs

Comparing with previous labeling methods, the main advantage of lentiviral transduction labeling system is to identify cells in an intact physiological way. The high transduction efficiency of lentiviral vectors ensure the fluorescent gene efficiently delivery into the native corticotrophs. Together with the lentiviral high integrative ability, the delivered gene showed stable and long-term expression providing a wide investigation time window. In addition, the design of cell specific expression allowed the fluorescent eYFP protein specifically expressed in corticotrophs. Lentiviral labeled corticotrophs displayed spontaneous action potentials and responded to physiological *in vivo* concentration of CRH/AVP. ACTH release levels from lentiviral transduced native pituitary cell culture under basal and CRH/AVP-induced conditions both showed no significant difference compared with un-transduced control groups (Liang *et al*., 2011). Altogether, rPOMC-driven lentiviral transduction system provided a highly efficient and specific way for native murine corticotrophs identification, and this labeling approach gives a stable and relatively long period for other investigations without causing any significant effects on cell physiological properties.

6.1.2 Future use of lentiviral transduction system

In this thesis, only a fluorescent reporter EYFP gene was delivered and expressed as a label for native live corticotrophs, which gave the opportunity to investigate the basic electrophysiological properties of corticotrophs. In addition, the same approach could now be used to genetically manipulate specific channel conductances. This would be a particular advantage for those channels in which the genes are known, but the pharmacology is poorly understood. The lentiviral transduction system may be used to either overexpress a channel gene of interest or knock-down the endogenous expression level of the channel by delivering the siRNA of the channel gene. In this thesis, SK4 channels were found to be highly expressed in native murine corticotrophs and controlling their spontaneous action potentials. Together with the stress-hyperresponsiveness observed in global Kcnn4$^{-/-}$ knockout mice, SK4 channels are revealed to have an important role in ACTH secretion and stress axis regulation (Liang *et al*., 2011). Using the lentiviral transduction system to knock-down SK4 channel expression level could be performed specifically in native corticotroph cells to examine their role in corticotrophs in the absence of potential other compensatory effects in the global knockout animals. Lentiviral transduction is also very reliable for *in vivo* transduction (Goldman *et al*., 1997), so the knock-down of SK4 channels could also be achieved specifically in pituitary corticotrophs *in vivo* with lentiviral carrying siRNA injection into WT animals. Conversely, expressing the SK4 channels through the lentiviral delivery of SK4 channels genes in corticotrophs in Kcnn4$^{-/-}$ knockout mice *in vivo* is also possible to establish whether the expression of SK4 only in the corticotrophs rescues the stress axis defect in the SK4$^{-/-}$ mice. Thus, lentiviral transduction system provides multiple opportunities for gene investigation

and the use of appropriate cell-specific promoters may be applicable to other pituitary cell types. For any disease caused by gene overexpression or deficiency, the lentiviral transduction system may also provide possible clinic therapy (Goldman *et al*., 1997).

6.2 Potassium conductances found in native murine corticotrophs and their roles in spontaneous action potentials

Various potassium conductances were detected in native murine corticotrophs (Figure 6.1).The majority of recorded potassium conductances have been reported in other corticotroph models or other types of pituitary cells. BK currents that showed high expression level in the AtT20 mouse corticotroph cell line displayed low expression in native murine corticotrophs, and without showing any significant role in the control of spontaneous action potentials. However, in single channel recordings from inside-out patches exposed to 5 μM intracellular free calcium, there was significantly paxilline-sensitive component during a step pulse to +60mV, suggesting BK channels were inactivated under normal resting membrane potential in metabolically intact murine corticotrophs (Liang *et al*., 2011). In contrast, SK4 channels, which have never previously identified in any pituitary cell type, dominated the outward potassium conductance in native murine corticotrophs with an important role in controlling corticotroph excitability. Together with the effects *in vivo* on ACTH and CORT secretion in the HPA axis in Kcnn4$^{-/-}$ knockout mice, SK4 channels were revealed to play a novel role in modulating ACTH secretion and stress axis function (Liang *et al*., 2011). This role may be through the effects at both levels

Figure 6.1
Ion channels in native murine pituitary corticotrophs

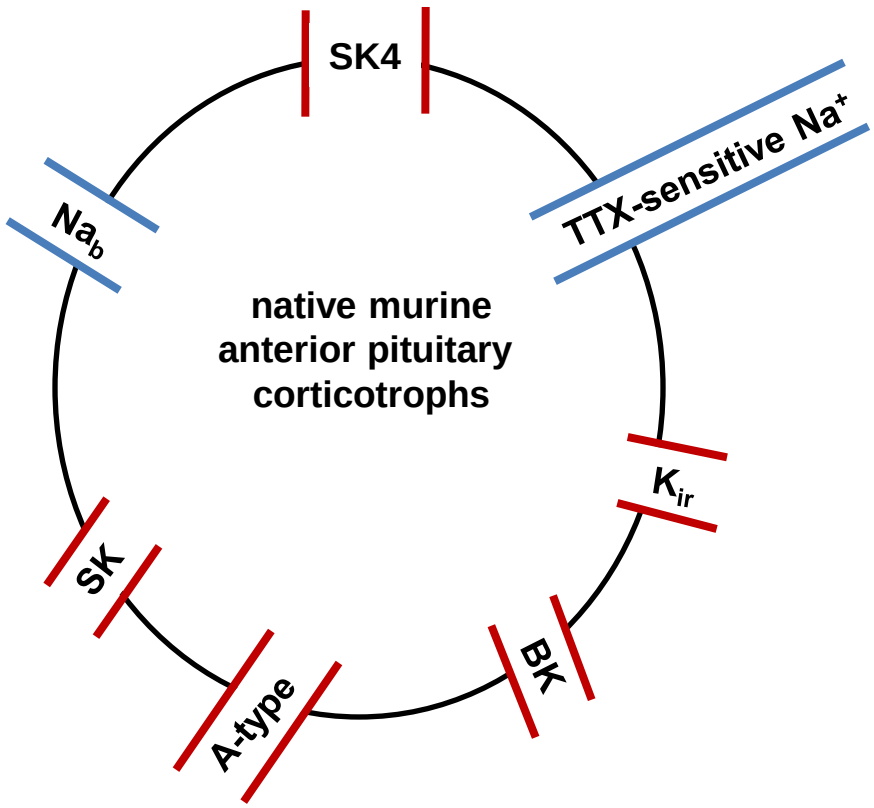

Figure 6.1 Ion channels in native murine pituitary corticotrophs. Intermediate-conductance, Ca^{2+}-activated K^+ (SK4) channel and A-type potassium channel conductances dominate the whole-cell outward current in native murine corticotrophs. High-conductance, voltage- and Ca^{2+}-activated K^+ (BK), small-conductance, Ca^{2+}-activated K^+ (SK) and inwardly rectifying K^+ (K_{ir}) channels also contribute a small component to the corticotroph whole-cell outward current. Background Na^+ (Na_b) channels maintain the corticotroph resting membrane potential, and together with TTX-sensitive Na^+ channels contribute to the inward sodium current of native murine corticotrophs.

of the pituitary corticotroph as well as the regulation of hypothalamic PVN neuronal excitability (Liang *et al.*, 2011). The 4-AP sensitive A-type potassium channel conductance was another dominant potassium current component found in native murine corticotrophs, and in some recorded cells A-type potassium channels regulated cell excitability (Figure 6.1).

The expression level of K_{ir} current conductance was significantly different between WT and $BK^{-/-}$ corticotrophs. However, inhibition of K_{ir} channels exhibited no clear effects on corticotroph excitability, although K_{ir} channels have been suggested to be important in generation of action potentials in rat corticotrophs (Kuryshev*et al.*, 1997). More studies of whether this reflects different genders of corticotrophs analysed and the activation status of K_{ir} channels are needed to examine the potential difference (Figure 6.1).

6.3 The resting membrane potential of native murine corticotrophs

The resting membrane potential of native murine corticotrophs typically ranged from -55 to -60 mV and this depolarised potential was dependent upon a background sodium conductance (Na_b), consistent with other types of pituitary cells (Sankaranarayanan & Simasko, 1996; Kwiecien*et al.*, 1998; Kucka*et al.*, 2010). Na_b is crucial in maintaining the resting membrane potential and the replacement of external sodium ions with $NMDG^+$ lead to a significant hyperpolarization and cessation of action potentials in native murine corticotrophs. The Na_b is insensitive to

TTX inhibition and the molecular identity of this background sodium component is not clear yet. One potential candidate is the sodium and calcium permeable ion channels of the transient receptor potential TrpC family that have been reported to exert a similar role in other pituitary cells (Tomic *et al*., 2011).

A TTX-sensitive fast inward sodium current component was detected in many native murine corticotrophs as well, while the inhibition of the TTX-sensitive sodium conductance caused no significant effect on the cell excitability.

6.4 Spontaneous action potentials and the response to CRH/AVP

More than 99% of recorded native murine corticotrophs showed spontaneous action potentials. The heterogeneity of firing patterns may reflect the heterogeneity of expression levels of various ion channels. Single spikes and "pseudo plateau bursting" action potentials with different firing frequency were discovered in native murine corticotrophs, similar to what observed in other types of pituitary cells. Spontaneous transitions among various firing patterns were found in native murine corticotrophs. The recording mode is crucial to record stable spontaneous action potentials. The perforated patch-clamp recording mode is required for maintaining stable cell excitability, while the whole-cell mode abolishes the spontaneous electrical activity.

Native murine corticotrophs showed responses to the *in vivo* physiological concentrations of CRH and AVP with a significant depolarization and elevation of firing frequency in spontaneously active cells, or initiating action potentials in previously silent cells. CRH or CRH and AVP together exerted prolonged effects after washout for several minutes compared with AVP alone, supporting previous suggestions that AVP is a weak secretagogue and can enhance and prolong the influence of CRH. However, we have not specified the target ion channels that CRH and AVP regulate in corticotrophs.

Taken together, this thesis exploited an efficient and specific lentiviral labeling method, which allowed electrophysiological studies to build an initial profile of ion channels and their roles in the electrical activity of native murine corticotrophs. This work will allow the analysis of corticotroph excitability to be studies in further details. Further investigations may focus on the control of ACTH secretion and its regulation by SK4 channels, the importance and molecular identity of the background sodium conductance, the exploration of ion channels regulated by CRH/AVP and the negative feedback of glucocorticoid in native murine corticotrophs.

References:

Akkina RK, Walton RM, Chen ML, Li QX, Planelles V & Chen IS. (1996). High-efficiency gene transfer into CD34+ cells with a human immunodeficiency virus type 1-based retroviral vector pseudotyped with vesicular stomatitis virus envelope glycoprotein G. *J Virol* **70(4),** 2581-2585.

Amado RG & Chen ISY. (1999). Lentiviral Vectors--the Promise of Gene Therapy Within Reach? *Science* **285(5428),** 674-676.

Armstrong CM & Hille B. (1998). Voltage-gated ion channels and electrical excitability. *Neuron* **20(3),** 371-380.

Bacchetti S & Graham FL. (1977). Transfer of the gene for thymidine kinase to thymidine kinase-deficient human cells by purified herpes simplex viral DNA. *Proc Natl Acad Sci U S A* **74(4),** 1590-1594.

Baek SC, Lin Q, Robbins PB, Fan H & Khavari PA. (2001). Sustainable systemic delivery via a single injection of lentivirus into human skin tissue. *Hum Gene Ther* **12(12),** 1551-1558.

Baker MD & Wood JN. (2001). Involvement of Na^+ channels in pain pathways. *Trends Pharmacol Sci* **22(1),** 27-31.

Becker Y & Darai G. (1995). Gene transfer by viral vectors for gene therapy. *J Mol Med (Berl)* **73(3),** 103-105.

Blomer U, Naldini L, Kafri T, Trono D, Verma IM & Gage FH. (1997). Highly efficient and sustained gene transfer in adult neurons with a lentivirus vector. *J Virol* **71(9),** 6641-6649.

Bosma MM & Hille B. (1992). Electrophysiological properties of a cell line of the gonadotrope lineage. *Endocrinology* **130(6),** 3411-3420.

Brunton PJ, Sausbier M, Wietzorrek G, Sausbier U, Knaus HG, Russell JA, Ruth P & Shipston MJ. (2007). Hypothalamic-pituitary-adrenal axis hyporesponsiveness to restraint stress in mice deficient for large-conductance calcium- and voltage-activated potassium (BK) channels. Endocrinology **148(11),** 5496-5506.

Burns JC, Friedmann T, Driever W, Burrascano M, Yee JK. Vesicular stomatitis virus G glycoprotein pseudotyped retroviral vectors: concentration to very

high titer and efficient gene transfer into mammalian and nonmammalian cells. Proc Natl Acad Sci USA 90: 8033–8037, 1993.

Burrin JM & Jameson JL. (1989). Regulation of transfected glycoprotein hormone alpha-gene expression in primary pituitary cell cultures. *Mol Endocrinol* **3(10),** 1643-1651.

Castro MG, Goya RG, Sosa YE, Rowe J, Larregina A, Morelli A & Lowenstein PR. (1997). Expression of transgenes in normal and neoplastic anterior pituitary cells using recombinant adenoviruses: long term expression, cell cycle dependency, and effects on hormone secretion. *Endocrinology* **138(5),** 2184-2194.

Catterall WA. (2000a). Structure and regulation of voltage-gated Ca^{2+} channels. *Annu Rev Cell Dev Biol* **16,** 521-555.

Catterall WA. (2000b). From ionic currents to molecular mechanisms: the structure and function of voltage-gated sodium channels. *Neuron* **26(1),** 13-25.

Catterall WA, Goldin AL & Waxman SG. (2005). International Union of Pharmacology. XLVII. Nomenclature and structure-function relationships of voltage-gated sodium channels. *Pharmacol Rev* **57(4),** 397-409.

Chabbert C, Mechaly I, Sieso V, Giraud P, Brugeaud A, Lehouelleur J, Couraud F, Valmier J & Sans A. (2003). Voltage-gated Na^{+} channel activation induces both action potentials in utricular hair cells and brain-derived neurotrophic factor release in the rat utricle during a restricted period of development. *J Physiol* **553(Pt 1),** 113-123.

Chan RK, Brown ER, Ericsson A, Kovacs KJ & Sawchenko PE. (1993). A comparison of two immediate-early genes, c-fos and NGFI-B, as markers for functional activation in stress-related neuroendocrine circuitry. *J Neurosci* **13(12),** 5126-5138.

Chatterjee O, Taylor LA, Ahmed S, Nagaraj S, Hall JJ, Finckbeiner SM, Chan PS, Suda N, King JT, Zeeman ML & McCobb DP. (2009). Social stress alters expression of large conductance calcium-activated potassium channel subunits in mouse adrenal medulla and pituitary glands. *J Neuroendocrinol* **21(3),** 167-176.

Chen C, Heyward P, Zhang J, Wu D & Clarke IJ. (1994). Voltage-dependent potassium currents in ovine somatotrophs and their function in growth hormone secretion. *Neuroendocrinology* **59(1),** 1-9.

Chen L, Tian L, MacDonald SH, McClafferty H, Hammond MS, Huibant JM, Ruth P, Knaus HG & Shipston MJ. (2005). Functionally diverse complement of large conductance calcium- and voltage-activated potassium channel (BK) alpha-subunits generated from a single site of splicing. *J Biol Chem* **280(39),** 33599-33609.

Childs GV, Lloyd JM, Rougeau D & Unabia G. (1988). Enrichment of corticotropes by counterflow centrifugation. *Endocrinology* **123(6),** 2885-2895.

Childs GV, Marchetti C & Brown AM. (1987). Involvement of sodium channels and two types of calcium channels in the regulation of adrenocorticotropin release. *Endocrinology* **120(5),** 2059-2069.

Connor TJ & Leonard BE. (1998). Depression, stress and immunological activation: the role of cytokines in depressive disorders. *Life Sci* **62(7),** 583-606.

Cordier G, Cozon G, Greenland T, Rocher F, Guiguen F, Guerret S, Brune J & Mornex JF. (1990). In vivo activation of alveolar macrophages in ovine lentivirus infection. *Clin Immunol Immunopathol* **55(3),** 355-367.

Cullen BR. (1991). Human immunodeficiency virus as a prototypic complex retrovirus. *J Virol* **65(3),** 1053-1056.

Davis HE, Rosinski M, Morgan JR & Yarmush ML. (2004). Charged polymers modulate retrovirus transduction via membrane charge neutralization and virus aggregation. *Biophys J* **86(2),** 1234-1242.

De Smedt SC, Demeester J & Hennink WE. (2000). Cationic polymer based gene delivery systems. *Pharm Res* **17(2),** 113-126.

Dempsey M; Haggerty S; Gulizia J; Bukrinsky M; Stevenson M; University of Nebraska Medical Center O. (1993). HIV-1 replication in non-dividing cells. *Abstr Gen Meet Am Soc Microbiol.* **93(444)**.

Deora AA, Diaz F, Schreiner R & Rodriguez-Boulan E. (2007). Efficient electroporation of DNA and protein into confluent and differentiated epithelial cells in culture. *Traffic* **8(10),** 1304-1312.

Desgranges C, Campan M, Gadeau AP, Guerineau N, Mollard P & Razaka G. (1991). Influence of 8-(N,N-diethylamino)octyl-3,4,5-trimethoxybenzoate (TMB-8) on cell cycle progression and proliferation of cultured arterial smooth muscle cells. *Biochem Pharmacol* **41(6-7),** 1045-1054.

Dittgen T, Nimmerjahn A, Komai S, Licznerski P, Waters J, Margrie TW, Helmchen F, Denk W, Brecht M & Osten P. (2004). Lentivirus-based genetic manipulations of cortical neurons and their optical and electrophysiological monitoring in vivo. *Proceedings of the National Academy of Sciences* **101(52),** 18206-18211.

Dubinsky JM & Oxford GS. (1985). Dual modulation of K channels by thyrotropin-releasing hormone in clonal pituitary cells. *Proc Natl Acad Sci U S A* **82(12),** 4282-4286.

Fakler B & Adelman JP. (2008). Control of K(Ca) channels by calcium nano/microdomains. *Neuron* **59(6),** 873-881.

Felgner PL, Gadek TR, Holm M, Roman R, Chan HW, Wenz M, Northrop JP, Ringold GM & Danielsen M. (1987). Lipofection: a highly efficient, lipid-mediated DNA-transfection procedure. *Proc Natl Acad Sci U S A* **84(21),** 7413-7417.

Fouchier RA, Meyer BE, Simon JH, Fischer U & Malim MH. (1997). HIV-1 infection of non-dividing cells: evidence that the amino-terminal basic region of the viral matrix protein is important for Gag processing but not for post-entry nuclear import. *EMBO J* **16(15),** 4531-4539.

Freed EO. (2001). HIV-1 replication. *Somat Cell Mol Genet* **26(1-6),** 13-33.

Gagner JP & Drouin J. (1987). Tissue-specific regulation of pituitary proopiomelanocortin gene transcription by corticotropin-releasing hormone, 3',5'-cyclic adenosine monophosphate, and glucocorticoids. *Mol Endocrinol* **1(10),** 677-682.

Gallay P, Swingler S, Aiken C & Trono D. (1995). HIV-1 infection of nondividing cells: C-terminal tyrosine phosphorylation of the viral matrix protein is a key regulator. *Cell* **80(3),** 379-388.

Gao X, Kim KS & Liu D. (2007). Nonviral gene delivery: what we know and what is next. *AAPS J* **9(1),** E92-104.

Gibbs DM & Vale W. (1982). Presence of corticotropin releasing factor-like immunoreactivity in hypophysial portal blood. *Endocrinology* **111(4),** 1418-1420.

Glomm WR. (2005). Functionalized Gold Nanoparticles for Applications in Bionanotechnology. *Journal of Dispersion Science and Technology* **26(3),** 389-414.

Goldman MJ, Lee PS, Yang JS & Wilson JM. (1997). Lentiviral vectors for gene therapy of cystic fibrosis. *Hum Gene Ther* **8(18),** 2261-2268.

Gottfredsson M & Bohjanen PR. (1997). Human immunodeficiency virus type I as a target for gene therapy. *Front Biosci* **2,** d619-634.

Goujon C, Jarrosson-Wuilleme L, Bernaud J, Rigal D, Darlix JL & Cimarelli A. (2003). Heterologous human immunodeficiency virus type 1 lentiviral vectors packaging a simian immunodeficiency virus-derived genome display a specific postentry transduction defect in dendritic cells. *J Virol* **77(17),** 9295-9304.

Grosjean F, Jordan M & Wurm F (2005). *Analyzing Calcium Phosphate Transfection of Adherent CHO Cells Using Microscopic Live Imaging, Animal Cell Technology Meets Genomics*. In Analyzing Calcium Phosphate Transfection of Adherent CHO Cells Using Microscopic Live Imaging, Animal Cell Technology Meets Genomics Eds Gòdia F & Fussenegger M pp. 159-161. Springer Netherlands.

Guerineau N, Corcuff JB, Tabarin A & Mollard P. (1991). Spontaneous and corticotropin-releasing factor-induced cytosolic calcium transients in corticotrophs. *Endocrinology* **129(1),** 409-420.

Gutman GA, Chandy KG, Grissmer S, Lazdunski M, McKinnon D, Pardo LA, Robertson GA, Rudy B, Sanguinetti MC, Stuhmer W & Wang X. (2005). International Union of Pharmacology. LIII. Nomenclature and molecular relationships of voltage-gated potassium channels. *Pharmacol Rev* **57(4),** 473-508.

Hatzinger M. (2000). Neuropeptides and the hypothalamic-pituitary-adrenocortical (HPA) system: review of recent research strategies in depression. *World J Biol Psychiatry* **1(2),** 105-111.

Heyward PM, Chen C & Clarke IJ. (1995). Inward membrane currents and electrophysiological responses to GnRH in ovine gonadotropes. *Neuroendocrinology* **61(6),** 609-621.

Hille B. (2001). Ion Channels of Excitable Membranes, 3rd Edition. Sinauer Associates: Sunderland, MA.

Hong S, Morrow TJ, Paulson PE, Isom LL & Wiley JW. (2004). Early painful diabetic neuropathy is associated with differential changes in tetrodotoxin-sensitive and -resistant sodium channels in dorsal root ganglion neurons in the rat. *J Biol Chem* **279(28),** 29341-29350.

Hou S, Heinemann SH & Hoshi T. (2009). Modulation of BKCa channel gating by endogenous signaling molecules. *Physiology (Bethesda)* **24,** 26-35.

Isom LL. (2001). Sodium channel beta subunits: anything but auxiliary. *Neuroscientist* **7(1),** 42-54.

Jeannotte L, Trifiro MA, Plante RK, Chamberland M & Drouin J. (1987). Tissue-specific activity of the pro-opiomelanocortin gene promoter. *Mol Cell Biol* **7(11),** 4058-4064.

Jessop DS. (1999). Review: Central non-glucocorticoid inhibitors of the hypothalamo-pituitary-adrenal axis. *J Endocrinol* **160(2),** 169-180.

Jones IR. (2002). Work Stress. The Making of a Modern Epidemic. *International Journal of Epidemiology* **31(6),** 1282-1283.

Josh P Roberts (2005). Insertional Mutagenesis from a Viral Vector. *The Scientist*, 19:20

Kaczorowski GJ, Knaus HG, Leonard RJ, McManus OB & Garcia ML. (1996). High-conductance calcium-activated potassium channels; structure, pharmacology, and function. *J Bioenerg Biomembr* **28(3),** 255-267.

Kalpana GV. (1999). Retroviral vectors for liver-directed gene therapy. *Semin Liver Dis* **19(1),** 27-37.

Kidokoro Y. (1975). Spontaneous calcium action potentials in a clonal pituitary cell line and their relationship to prolactin secretion. *Nature* **258(5537),** 741-742.

Kucka M, Kretschmannova K, Murano T, Wu CP, Zemkova H, Ambudkar SV & Stojilkovic SS. (2010). Dependence of multidrug resistance protein-mediated cyclic nucleotide efflux on the background sodium conductance. *Mol Pharmacol* **77(2),** 270-279.

Kudielka BM & Kirschbaum C. (2005). Sex differences in HPA axis responses to stress: a review. *Biol Psychol* **69(1),** 113-132.

Kumar M, Keller B, Makalou N & Sutton RE. (2001). Systematic determination of the packaging limit of lentiviral vectors. *Hum Gene Ther* **12(15),** 1893-1905.

Kuryshev YA, Childs GV & Ritchie AK. (1995a). Three high threshold calcium channel subtypes in rat corticotropes. *Endocrinology* **136(9),** 3916-3924.

Kuryshev YA, Childs GV & Ritchie AK. (1995b). Corticotropin-releasing hormone stimulation of Ca^{2+} entry in corticotropes is partially dependent on protein kinase A. *Endocrinology* **136(9),** 3925-3935.

Kuryshev YA, Childs GV & Ritchie AK. (1996). Corticotropin-releasing hormone stimulates Ca^{2+} entry through L- and P-type Ca^{2+} channels in rat corticotropes. *Endocrinology* **137(6),** 2269-2277.

Kuryshev YA, Haak L, Childs GV & Ritchie AK. (1997). Corticotropin releasing hormone inhibits an inwardly rectifying potassium current in rat corticotropes. *J Physiol* **502 (Pt 2),** 265-279.

Kwiecien R, Robert C, Cannon R, Vigues S, Arnoux A, Kordon C & Hammond C. (1998). Endogenous pacemaker activity of rat tumour somatotrophs. *J Physiol* **508 (Pt 3),** 883-905.

Lai Z, Han I, Zirzow G, Brady RO & Reiser J. (2000). Intercellular delivery of a herpes simplex virus VP22 fusion protein from cells infected with lentiviral vectors. *Proc Natl Acad Sci U S A* **97(21),** 11297-11302.

Lang DG & Ritchie AK. (1990). Tetraethylammonium blockade of apamin-sensitive and insensitive Ca^{2+}-activated K^{+} channels in a pituitary cell line. *J Physiol* **425,** 117-132.

Latorre R, Oberhauser A, Labarca P & Alvarez O. (1989). Varieties of calcium-activated potassium channels. *Annu Rev Physiol* **51,** 385-399.

LeBeau AP, Robson AB, McKinnon AE, Donald RA & Sneyd J. (1997). Generation of action potentials in a mathematical model of corticotrophs. *Biophys J* **73(3),** 1263-1275.

Lee AK, Smart JL, Rubinstein M, Low MJ & Tse A. (2011). Reciprocal regulation of TREK-1 channels by arachidonic acid and CRH in mouse corticotropes. *Endocrinology* **152(5),** 1901-1910.

Lee AK & Tse A. (1997). Mechanism underlying corticotropin-releasing hormone (CRH) triggered cytosolic Ca^{2+} rise in identified rat corticotrophs. *J Physiol* **504 (Pt 2),** 367-378.

Lee AK & Tse A. (2001). Endocytosis in identified rat corticotrophs. *J Physiol* **533(Pt 2),** 389-405.

Lee AL, Ogle WO & Sapolsky RM. (2002). Stress and depression: possible links to neuron death in the hippocampus. *Bipolar Disorders* **4(2),** 117-128.

Liang Z, Chen L, McClafferty H, Lukowski R, MacGregor D, King JT, Rizzi S, Sausbier M, McCobb DP, Knaus HG, Ruth P & Shipston MJ. (2011). Control of hypothalamic-pituitary-adrenal stress axis activity by the intermediate conductance calcium-activated potassium channel, SK4. *J Physiol* **589(Pt 24),** 5965-5986.

Lightman SL, Wiles CC, Atkinson HC, Henley DE, Russell GM, Leendertz JA, McKenna MA, Spiga F, Wood SA, Conway-Campbell BL. (2008). The significance of glucocorticoid pulsatility. *Eur J Pharmacol* **583(2-3)**:255-62.

Lim MC, Shipston MJ & Antoni FA. (1998). Depolarization counteracts glucocorticoid inhibition of adenohypophysical corticotroph cells. *Br J Pharmacol* **124(8),** 1735-1743.

Lledo PM, Guerineau N, Mollard P, Vincent JD & Israel JM. (1991). Physiological characterization of two functional states in subpopulations of prolactin cells from lactating rats. *J Physiol* **437,** 477-494.

Maffie J & Rudy B. (2008). Weighing the evidence for a ternary protein complex mediating A-type K^+ currents in neurons. *J Physiol* **586(Pt 23),** 5609-5623.

Mansvelder HD & Kits KS. (2000). All classes of calcium channel couple with equal efficiency to exocytosis in rat melanotropes, inducing linear stimulus-secretion coupling. *J Physiol* **526 Pt 2,** 327-339.

Marchetti C, Childs GV & Brown AM. (1987). Membrane currents of identified isolated rat corticotropes and gonadotropes. *Am J Physiol* **252(3 Pt 1),** E340-346.

McCobb DP & Beam KG. (1991). Action potential waveform voltage-clamp commands reveal striking differences in calcium entry via low and high voltage-activated calcium channels. *Neuron* **7(1),** 119-127.

McEwen BS. (2008). Central effects of stress hormones in health and disease: Understanding the protective and damaging effects of stress and stress mediators. *Eur J Pharmacol* **583(2-3),** 174-185.

Mehier-Humbert S, Bettinger T, Yan F & Guy RH. (2005). Plasma membrane poration induced by ultrasound exposure: implication for drug delivery. *J Control Release* **104(1),** 213-222.

Mei YA, Soriani O, Castel H, Vaudry H & Cazin L. (1998). Adenosine potentiates the delayed-rectifier potassium conductance but has no effect on the hyperpolarization-activated Ih current in frog melanotrophs. *Brain Res* **793(1-2),** 271-278.

Miskin J, Chipchase D, Rohll J, Beard G, Wardell T, Angell D, Roehl H, Jolly D, Kingsman S & Mitrophanous K. (2006). A replication competent lentivirus (RCL) assay for equine infectious anaemia virus (EIAV)-based lentiviral vectors. *Gene Ther* **13(3),** 196-205.

Miyoshi H, Takahashi M, Gage FH & Verma IM. (1997). Stable and efficient gene transfer into the retina using an HIV-based lentiviral vector. *Proc Natl Acad Sci U S A* **94(19),** 10319-10323.

Mollard P, Guerineau N, Chiavaroli C, Schlegel W & Cooper DM. (1991). Adenosine A1 receptor-induced inhibition of Ca^{2+} transients linked to action potentials in clonal pituitary cells. *Eur J Pharmacol* **206(4),** 271-277.

Mollard P, Vacher P, Guerin J, Rogawski MA & Dufy B. (1987). Electrical properties of cultured human adrenocorticotropin-secreting adenoma cells: effects of high K^+, corticotropin-releasing factor, and angiotensin II. *Endocrinology* **121(1),** 395-405.

Muthumani K, Hwang DS, Choo AY, Mayilvahanan S, Dayes NS, Thieu KP & Weiner DB. (2005). HIV-1 Vpr inhibits the maturation and activation of macrophages and dendritic cells in vitro. *International Immunology* **17(2),** 103-116.

Naldini L, Blomer U, Gage FH, Trono D & Verma IM. (1996). Efficient transfer, integration, and sustained long-term expression of the transgene in adult rat brains injected with a lentiviral vector. *Proc Natl Acad Sci U S A* **93(21),** 11382-11388.

Naldini L, Blomer U, Gallay P, Ory D, Mulligan R, Gage FH, Verma IM & Trono D. (1996). In vivo gene delivery and stable transduction of nondividing cells by a lentiviral vector. *Science* **272(5259),** 263-267.

Narayan O & Clements JE. (1989). Biology and pathogenesis of lentiviruses. *J Gen Virol* **70 (Pt 7),** 1617-1639.

Ouyang J & Alway SE. (2004). Transgene expression in hypertrophied and aged skeletal muscle in vivo by lentivirus delivery. *J Gene Med* **6(3),** 278-287.

Ozawa S & Sand O. (1986). Electrophysiology of excitable endocrine cells. *Physiol Rev* **66(4),** 887-952.

Park A (2009). *Fat bellied monkeys suggest why stress sucks.* In Fat bellied monkeys suggest why stress sucks.

Park F. (2007). Lentiviral vectors: are they the future of animal transgenesis? *Physiol Genomics* **31(2),** 159-73

Park J, Lee K & Chung I. (1998). Improved propagation of human rotavirus from cell cultures of rhesus monkey kidney cells using medium supplemented with DEAE-dextran, dimethyl sulfoxide and cholesterol. *Biotechnology Techniques* **12(1),** 7-10.

Pennington AJ, Kelly JS & Antoni FA. (1994). Selective enhancement of an A type potassium current by dexamethasone in a corticotroph cell line. *J Neuroendocrinol* **6(3),** 305-315.

Petersen OH & Maruyama Y. (1984). Calcium-activated potassium channels and their role in secretion. *Nature* **307(5953),** 693-696.

Piguet V & Trono D. (1999). The Nef protein of primate lentiviruses. *Rev Med Virol* **9(2),** 111-120.

Pongs O. (1992). Molecular biology of voltage-dependent potassium channels. *Physiol Rev* **72(4 Suppl),** S69-88.

Pongs O, Leicher T, Berger M, Roeper J, Bahring R, Wray D, Giese KP, Silva AJ & Storm JF. (1999). Functional and molecular aspects of voltage-gated K^+ channel beta subunits. *Ann N Y Acad Sci* **868,** 344-355.

Reiser J, Harmison G, Kluepfel-Stahl S, Brady RO, Karlsson S & Schubert M. (1996). Transduction of nondividing cells using pseudotyped defective high-titer HIV type 1 particles. *Proceedings of the National Academy of Sciences* **93(26),** 15266-15271.

Roberts JP. (2005). Insertional Mutagenesis from a Viral Vector. *The Scientist* **19(9),** 2.

Roche C, Zamora AJ, Taieb D, Lavaque E, Rasolonjanahary R, Dufour H, Bagnis C, Enjalbert A & Barlier A. (2004). Lentiviral vectors efficiently transduce human gonadotroph and somatotroph adenomas in vitro. Targeted expression of transgene by pituitary hormone promoters. *J Endocrinol* **183(1),** 217-233.

Russell RA, Vassaux G, Martin-Duque P & McClure MO. (2004). Transient foamy virus vector production by adenovirus vectors. *Gene Ther* **11(3),** 310-316.

Sankaranarayanan S & Simasko SM. (1996). A role for a background sodium current in spontaneous action potentials and secretion from rat lactotrophs. *Am J Physiol* **271(6 Pt 1),** C1927-1934.

Sankaranarayanan S & Simasko SM. (1998). Potassium channel blockers have minimal effect on repolarization of spontaneous action potentials in rat pituitary lactotropes. *Neuroendocrinology* **68(5)**, 297-311.

Sarabdjitsingh RA, Conway-Campbell BL, Leggett JD, Waite EJ, Meijer OC, de Kloet ER, Lightman SL. (2010). Responsiveness varies over the ultradian glucocorticoid cycle in a brain-region-specific manner. *Endocrinology* **151(11)**:5369-79.

Sausbier M, Hu H, Arntz C, Feil S, Kamm S, Adelsberger H, Sausbier U, Sailer CA, Feil R, Hofmann F, Korth M, Shipston MJ, Knaus HG, Wolfer DP, Pedroarena CM, Storm JF & Ruth P. (2004). Cerebellar ataxia and Purkinje cell dysfunction caused by Ca^{2+}-activated K^{+} channel deficiency. *Proc Natl Acad Sci U S A* **101(25),** 9474-9478.

Scheff JD, Calvano SE, Lowry SF, Androulakis IP. (2012). Transcriptional implications of ultradian glucocorticoid secretion in homeostasis and in the acute stress response. *Physiol. Genomics* **44(2)**:121-9.

Schilling T & Eder C. (2007). TRAM-34 inhibits nonselective cation channels. *Pflugers Arch* **454(4),** 559-563.

Schlegel W, Winiger BP, Mollard P, Vacher P, Wuarin F, Zahnd GR, Wollheim CB & Dufy B. (1987). Oscillations of cytosolic Ca^{2+} in pituitary cells due to action potentials. *Nature* **329(6141),** 719-721.

Schwarz JR & Bauer CK. (2004). Functions of erg K^{+} channels in excitable cells. *J Cell Mol Med* **8(1),** 22-30.

Sedej S, Tsujimoto T, Zorec R & Rupnik M. (2004). Voltage-activated Ca^{2+} channels and their role in the endocrine function of the pituitary gland in newborn and adult mice. *J Physiol* **555(Pt 3),** 769-782.

Selye H (1956). The stress of life. McGraw-Hill, New York.

Sheward WJ & Fink G. (1991). Effects of corticosterone on the secretion of corticotrophin-releasing factor, arginine vasopressin and oxytocin into hypophysial portal blood in long-term hypophysectomized rats. *J Endocrinol* **129(1),** 91-98.

Shipston MJ. (1995). Mechanism(s) of early glucocorticoid inhibition of adrenocorticotropin secretion from anterior pituitary corticotropes. *Trends Endocrinol Metab* **6(8),** 261-266.

Shipston MJ & Armstrong DL. (1996). Activation of protein kinase C inhibits calcium-activated potassium channels in rat pituitary tumour cells. *J Physiol* **493 (Pt 3),** 665-672.

Shipston MJ, Duncan RR, Clark AG, Antoni FA & Tian L. (1999). Molecular components of large conductance calcium-activated potassium (BK) channels in mouse pituitary corticotropes. *Mol Endocrinol* **13(10),** 1728-1737.

Shipston MJ, Kelly JS & Antoni FA. (1996). Glucocorticoids block protein kinase A inhibition of calcium-activated potassium channels. *J Biol Chem* **271(16),** 9197-9200.

Shorten PR, Robson AB, McKinnon AE & Wall DJ. (2000). CRH-induced electrical activity and calcium signalling in pituitary corticotrophs. *J Theor Biol* **206(3),** 395-405.

Simasko SM. (1994). A background sodium conductance is necessary for spontaneous depolarizations in rat pituitary cell line GH3. *Am J Physiol* **266(3 Pt 1),** C709-719.

Slominski A, Wortsman J, Luger T, Paus R & Solomon S. (2000). Corticotropin releasing hormone and proopiomelanocortin involvement in the cutaneous response to stress. *Physiol Rev* **80(3),** 979-1020.

Smith AE. (1995). Viral vectors in gene therapy. *Annu Rev Microbiol* **49,** 807-838.

Stanfield PR, Nakajima S & Nakajima Y. (2002). Constitutively active and G-protein coupled inward rectifier K^+ channels: Kir2.0 and Kir3.0. *Rev Physiol Biochem Pharmacol* **145,** 47-179.

Stanley EF. (1993). Single calcium channels and acetylcholine release at a presynaptic nerve terminal. *Neuron* **11(6),** 1007-1011.

Stern JV, Osinga HM, LeBeau A & Sherman A. (2008). Resetting behavior in a model of bursting in secretory pituitary cells: distinguishing plateaus from pseudo-plateaus. *Bull Math Biol* **70(1),** 68-88.

Stojilkovic SS. (2005). Ca^{2+}-regulated exocytosis and SNARE function. *Trends Endocrinol Metab* **16(3),** 81-83.

Stojilkovic SS, Izumi S & Catt KJ. (1988). Participation of voltage-sensitive calcium channels in pituitary hormone release. *J Biol Chem* **263(26),** 13054-13061.

Stojilkovic SS, Tabak J & Bertram R. (2010). Ion channels and signaling in the pituitary gland. *Endocr Rev* **31(6),** 845-915.

Stojilkovic SS, Zemkova H & Van Goor F. (2005). Biophysical basis of pituitary cell type-specific Ca^{2+} signaling-secretion coupling. *Trends Endocrinol Metab* **16(4),** 152-159.

Stutzin A, Stojilkovic SS, Catt KJ & Rojas E. (1989). Characteristics of two types of calcium channels in rat pituitary gonadotrophs. *Am J Physiol* **257(5 Pt 1),** C865-874.

Su YR, Wang J, Wu JJ, Chen Y & Jiang YP. (2007). Overexpression of lentivirus-mediated glial cell line-derived neurotrophic factor in bone marrow stromal cells and its neuroprotection for the PC12 cells damaged by lactacystin. *Neurosci Bull* **23(2),** 67-74.

Suda T, Tozawa F, Yamada M, Ushiyama T, Tomori N, Sumitomo T, Nakagami Y, Demura H & Shizume K. (1988). Effects of corticotropin-releasing hormone and dexamethasone on proopiomelanocortin messenger RNA level in human corticotroph adenoma cells in vitro. *J Clin Invest* **82(1),** 110-114.

Sullivan JP. (1995). Psychopharmacology: The fourth generation of progress. F. E. Bloom, D. J. Kupfer, eds., Raven Press, Ltd., New York, 1995, xlii + 2,002 pages, $175. *Drug Development Research* **35(3),** 185-188.

Surprenant A. (1982). Correlation between electrical activity and ACTH/beta-endorphin secretion in mouse pituitary tumor cells. *J Cell Biol* **95(2 Pt 1),** 559-566.

Suzuki K, Sawa Y, Kaneda Y, Ichikawa H, Shirakura R & Matsuda H. (1997). In vivo gene transfection with heat shock protein 70 enhances myocardial tolerance to ischemia-reperfusion injury in rat. *J Clin Invest* **99(7),** 1645-1650.

Takano K, Yasufuku-Takano J, Teramoto A & Fujita T. (1996). Corticotropin-releasing hormone excites adrenocorticotropin-secreting human pituitary adenoma cells by activating a nonselective cation current. *J Clin Invest* **98(9),** 2033-2041.

Tallent M, Dichter MA & Reisine T. (1996). Evidence that a novel somatostatin receptor couples to an inward rectifier potassium current in AtT-20 cells. *Neuroscience* **73(3),** 855-864.

Taraskevich PS & Douglas WW. (1989). Effects of BAY K 8644 on Ca-channel currents and electrical activity in mouse melanotrophs. *Brain Res* **491(1),** 102-108.

Thompson J & Begenisich T. (2009). Mechanistic details of BK channel inhibition by the intermediate conductance, Ca^{2+}-activated K channel. *Channels (Austin)* **3(3),** 194-204.

Tian L, Knaus HG & Shipston MJ. (1998). Glucocorticoid regulation of calcium-activated potassium channels mediated by serine/threonine protein phosphatase. *J Biol Chem* **273(22),** 13531-13536.

Tian L, Philp JA & Shipston MJ. (1999). Glucocorticoid block of protein kinase C signalling in mouse pituitary corticotroph AtT20 D16:16 cells. *J Physiol* **516 (Pt 3),** 757-768.

Tomic M, Koshimizu T, Yuan D, Andric SA, Zivadinovic D & Stojilkovic SS. (1999). Characterization of a plasma membrane calcium oscillator in rat pituitary somatotrophs. *J Biol Chem* **274(50),** 35693-35702.

Tomic M, Kucka M, Kretschmannova K, Li S, Nesterova M, Stratakis CA & Stojilkovic SS. (2011). Role of nonselective cation channels in spontaneous and protein kinase A-stimulated calcium signaling in pituitary cells. *Am J Physiol Endocrinol Metab* **301(2),** E370-379.

Tomic M, Van Goor F, He ML, Zivadinovic D & Stojilkovic SS. (2002). Ca($^{2+}$)-mobilizing endothelin-A receptors inhibit voltage-gated Ca($^{2+}$) influx through G(i/o) signaling pathway in pituitary lactotrophs. *Mol Pharmacol* **61(6),** 1329-1339.

Tsaneva-Atanasova K, Sherman A, van Goor F & Stojilkovic SS. (2007). Mechanism of spontaneous and receptor-controlled electrical activity in pituitary somatotrophs: experiments and theory. *J Neurophysiol* **98(1),** 131-144.

Tse A & Hille B. (1993). Role of voltage-gated Na^+ and Ca^{2+} channels in gonadotropin-releasing hormone-induced membrane potential changes in identified rat gonadotropes. *Endocrinology* **132(4),** 1475-1481.

Tse A & Lee AK. (1998). Arginine vasopressin triggers intracellular calcium release, a calcium-activated potassium current and exocytosis in identified rat corticotropes. *Endocrinology* **139(5),** 2246-2252.

Tse A & Lee AK. (2000). Voltage-gated Ca^{2+} channels and intracellular Ca^{2+} release regulate exocytosis in identified rat corticotrophs. *J Physiol* **528 Pt 1,** 79-90.

Tse A & Tse FW. (1998). alpha-adrenergic stimulation of cytosolic Ca^{2+} oscillations and exocytosis in identified rat corticotrophs. *J Physiol* **512 (Pt 2),** 385-393.

Tse A, Tse FW & Hille B. (1995). Modulation of Ca^{2+} oscillation and apamin-sensitive, Ca^{2+}-activated K^+ current in rat gonadotropes. *Pflugers Arch* **430(5),** 645-652.

Uchida N, Sutton RE, Friera AM, He D, Reitsma MJ, Chang WC, Veres G, Scollay R & Weissman IL. (1998). HIV, but not murine leukemia virus, vectors mediate high efficiency gene transfer into freshly isolated G0/G1 human hematopoietic stem cells. *Proceedings of the National Academy of Sciences* **95(20),** 11939-11944.

Van Goor F, Li YX & Stojilkovic SS. (2001). Paradoxical role of large-conductance calcium-activated K^+ (BK) channels in controlling action potential-driven Ca^{2+} entry in anterior pituitary cells. *J Neurosci* **21(16),** 5902-5915.

Van Goor F, Zivadinovic D, Martinez-Fuentes AJ & Stojilkovic SS. (2001). Dependence of pituitary hormone secretion on the pattern of spontaneous voltage-gated calcium influx. Cell type-specific action potential secretion coupling. *J Biol Chem* **276(36),** 33840-33846.

Van Goor F, Zivadinovic D & Stojilkovic SS. (2001). Differential expression of ionic channels in rat anterior pituitary cells. *Mol Endocrinol* **15(7),** 1222-1236.

Vodicka MA. (2001). Determinants for Lentiviral Infection of Non-Dividing Cells. *Somat Cell Mol Genet* **26(1),** 35-49.

Waring DW & Turgeon JL. (2006). Estradiol inhibition of voltage-activated and gonadotropin-releasing hormone-induced currents in mouse gonadotrophs. *Endocrinology* **147(12),** 5798-5805.

Wasungu L & Hoekstra D. (2006). Cationic lipids, lipoplexes and intracellular delivery of genes. *J Control Release* **116(2),** 255-264.

Wei AD, Gutman GA, Aldrich R, Chandy KG, Grissmer S & Wulff H. (2005). International Union of Pharmacology. LII. Nomenclature and molecular relationships of calcium-activated potassium channels. *Pharmacol Rev* **57(4),** 463-472.

Wen S, Schwarz JR, Niculescu D, Dinu C, Bauer CK, Hirdes W & Boehm U. (2008). Functional characterization of genetically labeled gonadotropes. *Endocrinology* **149(6)**, 2701-2711.

Windle RJ, Wood SA, Shanks N, Lightman SL, Ingram CD. (1998). Ultradian Rhythm of Basal Corticosterone Release in the Female Rat: Dynamic Interaction with the Response to Acute Stress. *Endocrinology* **139 (2)**, 443-450

Wojtulewski JA, Gow PJ, Walter J, Grahame R, Gibson T, Panayi GS & Mason J. (1980). Clotrimazole in rheumatoid arthritis. *Ann Rheum Dis* **39(5),** 469-472.

Wu SN, Li HF, Jan CR & Shen AY. (1999). Inhibition of Ca^{2+}-activated K^{+} current by clotrimazole in rat anterior pituitary GH3 cells. *Neuropharmacology* **38(7),** 979-989.

Wulff H, Miller MJ, Hansel W, Grissmer S, Cahalan MD & Chandy KG. (2000). Design of a potent and selective inhibitor of the intermediate-conductance

Ca^{2+}-activated K^+ channel, IKCa1: a potential immunosuppressant. *Proc Natl Acad Sci U S A* **97(14),** 8151-8156.

Wulfsen I, Hauber HP, Schiemann D, Bauer CK & Schwarz JR. (2000). Expression of mRNA for voltage-dependent and inward-rectifying K channels in GH3/B6 cells and rat pituitary. *J Neuroendocrinol* **12(3),** 263-272.

Yang SH, Agca Y, Cheng PH, Yang JJ, Agca C, Chan AW. Enhanced transgenesis by intracytoplasmic injection of envelope-free lentivirus. Genesis **45**: 177–183, 2007

Yang SK, Wang K, Parkington H & Chen C. (2008). Involvement of tetrodotoxin-resistant Na^+ current and protein kinase C in the action of growth hormone (GH)-releasing hormone on primary cultured somatotropes from GH-green fluorescent protein transgenic mice. *Endocrinology* **149(9),** 4726-4735.

Yau HJ, Baranauskas G & Martina M. (2010). Flufenamic acid decreases neuronal excitability through modulation of voltage-gated sodium channel gating. *J Physiol* **588(Pt 20),** 3869-3882.

Yellen G. (2002). The voltage-gated potassium channels and their relatives. *Nature* **419(6902),** 35-42.

Young JI, Otero V, Cerdan MG, Falzone TL, Chan EC, Low MJ & Rubinstein M. (1998). Authentic cell-specific and developmentally regulated expression of pro-opiomelanocortin genomic fragments in hypothalamic and hindbrain neurons of transgenic mice. *J Neurosci* **18(17),** 6631-6640.

Yu FH & Catterall WA. (2003). Overview of the voltage-gated sodium channel family. *Genome Biol* **4(3),** 207.

Zorec R. (1996). Calcium signaling and secretion in pituitary cells. *Trends Endocrinol Metab* **7(10),** 384-388.

Zorec R, Sikdar SK & Mason WT. (1991). Increased cytosolic calcium stimulates exocytosis in bovine lactotrophs. Direct evidence from changes in membrane capacitance. *J Gen Physiol* **97(3),** 473-497.

Publications:

J Physiol 589.24 (2011) pp 5965–5986

The Journal of Physiology

Control of hypothalamic–pituitary–adrenal stress axis activity by the intermediate conductance calcium-activated potassium channel, SK4

Zhi Liang[1], Lie Chen[1], Heather McClafferty[1], Robert Lukowski[2], Duncan MacGregor[1], Jonathan T. King[3], Sandra Rizzi[4], Matthias Sausbier[2], David P. McCobb[3], Hans-Guenther Knaus[4], Peter Ruth[2] and Michael J. Shipston[1]

[1] *Centre for Integrative Physiology, Hugh Robson Building, College of Medicine and Veterinary Medicine, University of Edinburgh, Edinburgh EH89XD, Scotland, UK*

[2] *Pharmacology and Toxicology, Institute of Pharmacy, University of Tübingen, 72076 Tübingen, Germany*

[3] *Neurobiology and Behaviour, Cornell University, Ithaca, NY, USA*

[4] *Division of Molecular and Cellular Pharmacology, Medical University Innsbruck, Innsbruck A-6020, Austria*

Non-technical summary Our ability to respond to stress is critically dependent upon the release of the stress hormone adrenocorticotrophic hormone (ACTH) from corticotroph cells of the anterior pituitary gland. ACTH release is controlled by the electrical properties of corticotrophs that are determined by the movement of ions through channel pores in the plasma membrane. We show that a calcium-activated potassium ion channel called SK4 is expressed in corticotrophs and regulates ACTH release. We provide evidence of how SK4 channels control corticotroph function, which is essential for understanding homeostasis and for treating stress-related disorders.

Abstract The anterior pituitary corticotroph is a major control point for the regulation of the hypothalamic–pituitary–adrenal (HPA) axis and the neuroendocrine response to stress. Although corticotrophs are known to be electrically excitable, ion channels controlling the electrical properties of corticotrophs are poorly understood. Here, we exploited a lentiviral transduction system to allow the unequivocal identification of live murine corticotrophs in culture. We demonstrate that corticotrophs display highly heterogeneous spontaneous action-potential firing patterns and their resting membrane potential is modulated by a background sodium conductance. Physiological concentrations of corticotrophin-releasing hormone (CRH) and arginine vasopressin (AVP) cause a depolarization of corticotrophs, leading to a sustained increase in action potential firing. A major component of the outward potassium conductance was mediated via intermediate conductance calcium-activated (SK4) potassium channels. Inhibition of SK4 channels with TRAM-34 resulted in an increase in corticotroph excitability and exaggerated CRH/AVP-stimulated ACTH secretion *in vitro*. In accordance with a physiological role for SK4 channels *in vivo*, restraint stress-induced plasma ACTH and corticosterone concentrations were significantly enhanced in gene-targeted mice lacking SK4 channels ($Kcnn4^{-/-}$). In addition, $Kcnn4^{-/-}$ mutant mice displayed enhanced hypothalamic c-fos and nur77 mRNA expression following restraint, suggesting increased neuronal activation. Thus, stress hyperresponsiveness observed in $Kcnn4^{-/-}$ mice results from enhanced secretagogue-induced ACTH output from anterior pituitary corticotrophs and may also involve increased hypothalamic drive, thereby suggesting an important role for SK4 channels in HPA axis function.

DOI: 10.1113/jphysiol.2011.219378

(Received 24 August 2011; accepted after revision 28 October 2011; first published online 31 October 2011)
Corresponding author M. J. Shipston: Centre for Integrative Physiology, Hugh Robson Building, University of Edinburgh, Edinburgh, Scotland, UK. Email: mike.shipston@ed.ac.uk

Abbreviations ACTH, adrenocorticotrophin hormone; AVP, arginine vasopressin; BK, large conductance calcium- and voltage-activated potassium channel; c-*fos* cellular FBJ murine osteosarcoma viral oncogene homologue; CRH, corticotrophin releasing hormone; eYFP, enhanced yellow fluorescent protein; GR, glucocorticoid receptor; HPA, hypothalamic–pituitary–adrenal; MR, mineralocorticoid receptor; *nurr*77, nerve growth factor inducible gene-B; POMC, proopiomelanocortin; PVN, paraventricular nucleus of the hypothalamus.

Introduction

The ability to respond to external stressors as well as perturbations of the internal environment is essential to the long term survival and healthy ageing of organisms. The hypothalamic–pituitary–adrenal axis (HPA axis) represents the major neuroendocrine response to stress, by coordinating appropriate responses to sensory input. Stressors ultimately activate hypothalamic neuroendocrine neurones in the paraventricular nucleus, releasing corticotrophin releasing hormone (CRH) and arginine vasopressin (AVP) into the portal circulation. CRH and AVP act on the anterior pituitary corticotrophs to stimulate release of adrenocorticotrophin hormone (ACTH). ACTH is released into the systemic circulation to control release of the powerful glucocorticoid hormones (cortisol in man, corticosterone in rodents) from the adrenal gland. Glucocorticoids in turn feedback at multiple levels of the HPA axis to terminate the stress response. Acute activation of the HPA axis is required for stress adaptation, but prolonged and/or excessive levels of stress hormones, in particular glucocorticoids, may predispose to major metabolic, immune, cardiovascular and affective disorders (Antoni, 1986; Dallman *et al.* 1987; Sapolsky *et al.* 2000; McEwen & Wingfield, 2003).

The anterior pituitary corticotroph represents a major 'hub' in the control of the HPA axis function, integrating efferent signals from the brain with feedback control from circulating steroid hormones to coordinate ACTH release. Stimulatory (e.g. CRH and AVP) and inhibitory factors controlling ACTH output from pituitary corticotrophs are well characterised. Furthermore, it is now well established that anterior pituitary corticotrophs in many species are electrically excitable, as are other cells of the anterior pituitary gland (Stojilkovic *et al.* 2010). However, ion channels and mechanisms controlling corticotroph excitability and its coupling to calcium-dependent ACTH secretion in corticotrophs remain poorly understood (Kuryshev *et al.* 1997; Lee & Tse, 1997). Considerable insight has been gained from a variety of tumour models, including variants of the mouse anterior pituitary cell line AtT20 (Surprenant, 1982; Pennington *et al.* 1994; Shipston *et al.* 1996) and cells from human pituitary corticotroph tumours (Mollard *et al.* 1987; Takano *et al.* 1996). However, the extent to which ionic mechanisms in these models truly reflect corticotroph function remains unclear. In part, this is a result of the major challenge of unequivocally distinguishing live corticotrophs from the variety of different anterior pituitary cell populations.

To address these issues several previous identification/labelling approaches have been exploited, including: (i) biotinylated CRH peptides to label corticotrophs (Childs *et al.* 1987), (ii) purification of corticotrophs following volume expansion in response to high doses of CRH by centrifugal elutriation (Ritchie *et al.* 1996; Kuryshev *et al.* 1997), (iii) identification based on ACTH release detected by haemolytic plaque assay (Lee & Tse, 1997), and (iv) *post hoc* staining of fixed cells for ACTH immunoreactivity or responsiveness to CRH or AVP (Brunton *et al.* 2007). Finally, a recent study has exploited transgenic mice constitutively expressing green fluorescent protein (GFP) under the control of the proopiomelanocortin (POMC; the precursor for ACTH synthesis) promoter (Lee *et al.* 2011), although analysis of spontaneous activity was not studied. Such studies have implicated a number of different ion channels and mechanisms in controlling corticotroph electrical excitability. However, in most cases analysis was performed with supramaximal concentrations of CRH or AVP several orders of magnitude greater than those reported in the portal circulation (Gibbs & Vale, 1982; Sheward & Fink, 1991). The difficulty in routine identification of living corticotrophs has precluded the systematic analysis of the spontaneous electrical excitability of these cells in the absence of secretagogues.

In this report, we have applied a highly efficient and selective labelling approach using lentiviral mediated transduction of primary murine pituitary cells *in vitro* with a fluorescent (enhanced yellow fluorescent protein; eYFP) construct driven by a minimal POMC promoter. Using this approach, we have characterised the electrical properties of unstimulated and secretagogue-evoked murine corticotrophs in metabolically intact cells that are responsive to physiological concentrations of CRH and AVP. Importantly, our studies reveal a novel role for intermediate conductance calcium-activated potassium (SK4)

channels in corticotroph function, and reveal that mice genetically deficient for the channel display stress hyperresponsiveness.

Methods

Ethical approval

All experiments and tissue collection were performed between 08.00 h and 11.00 h and performed in accordance with accepted standards of humane animal care, UK Home Office requirements and the German legislation on protection of animals.

Lentiviral transduction of primary corticotrophs

Generation of POMC-eYFP lentiviral reporter. The POMC-eYFP lentiviral vector was constructed in the pLenti6/V5-D-TOPO vector. To facilitate subcloning steps we first generated new *Spe*I and *Sfu*I restriction sites flanking eYFP in the pEYFP-N1 vector. The subsequent *Spe*I and *Sfu*I restriction fragment containing eYFP from the mutant pEYFP-NI vector was then ligated into the pLenti6/V5-D-TOPO vector (Invitrogen) generating a construct (pLenti-CMV-eYFP) in which eYFP expression is driven by the CMV promoter. To generate a construct for expression restricted to POMC-expressing cells we amplified the rat minimal POMC promoter (−707 to +64 bp, a generous gift from Prof. Malcolm Low (University of Michigan Medical School); Hammer *et al.* 1990) from the pGEM TZ vector using forward and reverse primers (5′-TCATATCGATGCTTCCACTTCCCTCCACAG-3′ and 5′-CTGGACTAGTTGTTCAGTGGCCTCTCTTAG-3′) engineered to create *Cla*I and *Spe*I restriction sites, respectively. Amplicons were cloned into the pCRII-TOPO vector and the *Cla*I and *Spe*I fragment was ligated into the pLenti-CMV-eYFP construct to generate the pLenti-pomc-eYFP (available to academic laboratories on request) construct in which the minimal POMC promoter replaces the CMV promoter. To generate lentiviral particles the pLenti-CMV-eYFP or pLenti-pomc-eYFP plasmids were co-transfected with the psPAX2 packing plasmid (a generous gift from Prof. D. Trono, EPFL, Lausanne) and the pLP/VSVG envelope plasmid (Invitrogen) into HEK293FT cells. HEK293FT cells were seeded and cultured in a area correct, 75 cm^2 flask in growth medium 1 day before transient transfection at approximately 70% confluency. Before transfection, culture medium was replaced with fresh growth medium and the respective plenti6-POMC-eYFP, pLenti6-CMV-eYFP, psPAX2 and pLP/VSVG plasmids at a 4:3:2 ratio using ExGen 500 transfection reagent (Fermentas). After 24 h, the medium was replaced with 20 ml fresh growth medium, and the cells were harvested at 72 h post-transfection. The collected medium was spun at 4860 *g* for 15 min and the supernatant filtered through a 0.45 μm syringe filter (25 mmGD/X, Whatman) into a 15 ml Amicon Ultra-15 centrifugal filter device (Millipore, UK) and concentrated by spinning at 4860 *g* for 40–50 min. Lentivirus titre was determined using HEK293FT cells and defined as transduced Unit/ml lentiviral particles (TU ml^{-1}).

Transduction of primary murine anterior pituitary cells *in vitro*. Three to four female mice (mixed sv129/Bl6 background age range 2–5 months) were killed by cervical dislocation and the pituitaries were rapidly removed; the outer edges of the anterior lobes of the gland were removed to ensure no contamination from the intermediate lobe (which contains POMC-expressing melanotrophs). The anterior pituitary lobes were chopped with a single edged razor blade mounted on a McIlwain chopper (setting 0.7 mm) in both directions (rotated plate by 90 deg) and placed in Dulbecco's modified Eagle's medium (DMEM; Invitrogen) containing 25 mM Hepes, 0.25% trypsin and 10 μg ml^{-1} DNAse I, and incubated at 37°C for 20–25 min in a water bath. The tube was shaken every 5 min to achieve a complete and equal digestion. At the end of the digestion, tissue pieces settled to the bottom of the tube, and supernatant was aspirated. One millilitre of inhibitor solution (DMEM containing 0.5 mg ml^{-1} lima bean trypsin inhibitor, 100 kallikrein units aprotinin (200 × dilution of Sigma stock), 10 μg ml^{-1} DNAse I) was added and the tissue bits were triturated with a 1 ml Pipetman tip (Gilson) for approximately 40 times. The resulting suspension was filtered over a cell strainer with 70 μm nylon mesh (BD Biosciences (Franklin Lakes, NJ, USA)), diluted with an equal volume of culture medium (DMEM containing 25 mM Hepes, 5 μg ml^{-1} insulin, 50 μg ml^{-1} transferrin, 30 nM sodium selenite, 0.3% BSA (w/v), 4.2 μg ml^{-1} fibronectin and spun in a centrifuge at 100 *g* for 10 min. The pellet was triturated in 1 ml culture medium with 1% antibiotic/mycotic solution (Sigma), in order to disperse single cells. Cells from three to four anterior pituitaries were plated on 24 × 12 mm coverslips in a 6-well plate (4 coverslips per well) and incubated at 37°C in 5% CO_2. Pituitary cells were transduced 24 h after plating in antibiotic free culture medium. The culture medium was replaced with fresh medium 24 h post-transduction, culture medium was changed every 2 days, and fluorescent cells were typically used 48–72 h post-transduction.

Immunohistochemical co-labelling of transduced primary cells for ACTH. Primary mouse pituitary cells cultured on poly-D-lysine coated glass coverslips 2–4 days after lentiviral transduction were gently washed 3 times with phosphate buffered saline (PBS) containing 2 mM

$CaCl_2$ and 1 mM $MgCl_2$, and then fixed with 4% paraformaldehyde in PBS for 30 min at room temperature (RT). Following a quench step with 50 mM NH_4Cl for 10 min at RT, cells were washed, permeabilised with 0.3% (v/v) Triton X-100 in PBS (PBS-T) for 10 min and blocked with blocking solution (3% BSA in PBS-T) for 1 h at RT. Primary anti-ACTH antibody (1:500 in blocking solution, Sigma-Aldrich) was applied and incubated at 4°C overnight. Subsequently, cells were washed 3 times with PBS, rinsed in dH_2O and then incubated with Alexa-594 conjugated secondary antibody (1:1000) (Invitrogen, USA) in blocking solution for 1 h at RT. Cells were finally washed with PBS 3 times and mounted with Mowiol 4-88 mounting medium(Calbiochem, Damstadt, Germany)containing 1,4-diazabizyclo[2.2.2]octane (DABCO, Sigma) as antifade. Cells were imaged using a Zeiss LSM510 laser scanning confocal microscope equipped with a 63× (NA 1.4) oil immersion objective lens in multitracking mode.

Animals

Experiments with lentiviral-transduced cells were performed using virgin female mice (age range 2–5 months) on a mixed sv129/C57Bl6 background. In a limited number of experiments (predominantly to confirm aspects of pharmacological characterisation of potassium conductances) recordings were also performed using transgenic mice expressing GFP under control of the POMC promoter in a C57Bl6 background (a generous gift from Prof. J. Friedman (The Rockefeller University, NY, USA); Pinto *et al.* 2004). No significant differences in potassium conductances were observed between lentiviral transduced and transgenic corticotrophs (for example 1 μM clotrimazole inhibition of outward current was 38.4 ± 2.4 ($n = 5$) and 41.1 ± 3.8% ($n = 4$), respectively). Mice lacking the pore exon of the Kcnn4 channel α-subunit ($Kcnn4^{-/-}$), were generated previously (Sausbier *et al.* 2006). Wild-type (WT) and $Kcnn4^{-/-}$ mice on the hybrid SV129/C57BL6 background were used. Litter- and age-matched (F2 hybrid) adult female mice (age range 2–5 months, generated from F1 hybrid parents) were randomly assigned to each experimental condition. Mice were caged in groups of two to four under standard laboratory conditions (lights on at 07.00 h, lights off at 19.00 h, 21°C, with chow and tap water available *ad libitum*).

Electrophysiology

The perforated patch clamp configuration of the whole-cell recording technique was used for all whole cell current- and voltage-clamp recordings. Amphotericin was used at a final pipette concentration of 200 μg ml^{-1} with uncompensated access resistances between 15 and 30 MΩ, routinely achieved within 5–15 min of giga-ohm seal formation and stable for up to 1 h. The standard bath solution contained (in mM): 140 NaCl, 5 KCl, 2 $CaCl_2$, 0.1 $MgCl_2$, 10 Hepes and 10 glucose; pH 7.4 adjusted with NaOH, 300 mosmol l^{-1}. The standard pipette solution contained (in mM): 10 NaCl, 30 KCl, 60 K_2SO_4, 1 $MgCl_2$, 10 glucose, 10 Hepes and 50 sucrose; pH 7.2 adjusted with KOH, 290 mosmol l^{-1}. Cells were perfused using a gravity-driven perfusion system with flow rates <1.5 ml min^{-1} to minimise flow-induced artefacts.

Electrophysiological measurements in the inside-out configuration were made on corticotrophs from POMC-GFP transgenic mice. Experiments were conducted at 20–22°C. Patch electrodes (3–5 MΩ) were pulled from borosilicate glass (World Precision Instruments, Sarasota, FL, USA) and coated with silicone elastomer (Sylgard 184, Dow Corning). Data were collected using a List EPC-9 patch clamp amplifier, Bessel filtered at 10 kHz, and stored on a Power Macintosh G3 using Pulse 8.5 software (Heka Electronik, Lambrecht/Pfalz, Germany). Offline analysis was conducted with custom software written for Igor Pro (WaveMetrics, Inc., Lake Oswego, OR, USA). For inside-out patches, symmetrical K^+ solutions were used to eliminate potassium driving force and allow DC offset to be cancelled at 0 mV. The pipette and bath saline solutions contained (in mM): 160 KCl, 10 Hepes, 1 $MgCl_2$, 1 HEDTA, 0.188 $CaCl_2$, pH adjusted to 7.2 with KOH to obtain approximately 5 μM free [Ca^{2+}]. The free [Ca^{2+}] was calculated with MAXCHELATOR software (WEBMAXC v2.1; Bers *et al.* 1994). Zero-Ca^{2+} solution contained an additional 5 mM EGTA (Sigma). Paxilline (Sigma) was dissolved in 100% DMSO and stored at −20°C until the day of experiment, when it was diluted at least 1000× before use. The osmolarity of the saline solutions was measured by a dew point osmometer and adjusted to 300 mosmol l^{-1}.

Double immunofluorescence histochemistry of pituitary sections

Adult wild-type and $Kcnn4^{-/-}$ mice were deeply anaesthetized with 150 mg (kg body weight)$^{-1}$ thiopental (25 mg ml^{-1}; Sandoz) and immediately perfused via the left cardiac ventricle with PBS (pH 7.4) for 1 min, followed by ice-cold 4% paraformaldehyde in PBS for 10 min (approximately 45 ml) and PBS for 1 min. Pituitary glands were dissected and transferred into 20% sucrose in PBS for 18 h at 4°C. Thereafter, pituitary glands were snap frozen in prechilled (−70°C) isopentane (Merck) for 90 s and stored at −70°C. Sections of 10 μm were cut using

a cryostat and transferred onto polylysine coated slides and stored at −20°C for up to 8 weeks. Pituitary glands sections of 10 μm were washed twice in Tris-buffered saline (TBS; pH 7.4) for 5 min and permeabilized in 0.2% Triton X-100 in TBS (TBS-T) for 10 min. Slices were pre-incubated in 2% normal goat serum, 2% bovine serum albumin and 0.2% milk powder in TBS-T for 1 h at room temperature and incubated overnight with rabbit polyclonal anti-SK4 whole serum (Abcam Inc., Cambridge, MA, USA; no. 83740) diluted 1:1000 in 1% BSA in TBS-T. Sections were washed 10 min with TBS-T and incubated with mouse monoclonal anti-ACTH antibody, clone 02A3 (Dako, Carpenteria, CA, USA) diluted in 1% BSA in TBS-T 1:100 for 2 h at room temperature. Sections were washed with TBS-T for 30 min and incubated with secondary antibodies goat anti-rabbit Alexa-488 and goat anti-mouse Alexa-594 (both Invitrogen, nos A-11034 and A-11032) diluted 1:1000 in 2% BSA in TBS-T for 1 h at room temperature. Sections were washed with TBS-T for 10 min followed by TBS for 20 min. Nuclei were stained using 0.5 μg ml^{-1} DAPI (Sigma-Aldrich) for 5 min. Afterwards, sections were washed with TBS and mounted in *p*-phenylenediamine-glycerol to prevent photobleaching. The sections were coverslipped and sealed with nail polish. The slides were stored in a dark box at 4°C for up to 72 h with stable signal to noise ratio. Images were taken using a Zeiss Axioplan 2 imaging system equipped with Apotome stepper, Axiocam camera system and AxioVision 4.8 software.

Restraint stress protocol, tissue collection and plasma ACTH and corticosterone measurements

Restraint stress was used as a mixed physical and psychological stressor (Pacak & Palkovits, 2001). Mice were randomly assigned to one of two experimental groups assayed in parallel: control, non-stressed (basal) and restraint for 30 min (restraint). For restraint, mice were placed individually in a clear plastic restraint tube (CH Technologies (USA) Inc., Westwood, NJ, USA) of internal diameter 31 mm with a variable pusher, adjusted based on animal size. Mice were decapitated and trunk blood collected in chilled Eppendorf tubes containing 5 μl of 5% EDTA. Brains were rapidly isolated in ice-cold Hanks' buffered salt solution (HBSS, Invitrogen) and 1 mm coronal sections cut using a fresh razor blade. Hypothalamic blocks were then prepared by cutting along the top of the third ventricle and diagonally towards the ventral aspect to either side of the major hypothalamic nuclei, and then bisected in a sagittal plane. Anterior pituitary glands were sectioned on ice to produce two anterior lobes, removing the posterior and intermediate lobes, and individual adrenal glands were trimmed of fat. One half of each tissue or individual adrenal gland was stored at 4°C in RNAlater (Ambion Inc., Austin, TX, USA) overnight to ensure tissue penetration and then frozen at −80°C until use. Blood samples were chilled on ice and centrifuged at 1000 *g* for 10 min, and plasma was separated and stored at −80°C until subsequent radioimmunoassay for ACTH and corticosterone. Plasma ACTH and corticosterone concentrations were determined by radioimmunoassay using commercially available kits (MP Biomedicals, Solon, OH, USA). ACTH was measured in unextracted plasma samples using a two-site immunoradiometric assay (Hodgkinson *et al.* 1984). Corticosterone was measured in unextracted plasma (diluted 1:200 in assay buffer) using a double antibody radioimmunoassay with ^{125}I-labelled corticosterone as the tracer (Keith *et al.* 1978). Sensitivities were 5 pg ml^{-1} and 0.5 ng ml^{-1} and the intra-assay variation <8% and <6%, for the ACTH and corticosterone assays, respectively.

qRT-PCR

Tissue samples stored at −80°C in RNAlater were rapidly thawed at room temperature, weighed, and disrupted through a 21G needle using ∼20 strokes for hypothalamus and pituitary and ∼40 strokes for adrenal glands. RNA was then purified using RNeasy Mini Kit (Qiagen) or High Pure RNA Tissue Kit (Roche Applied Science) as per the manufacturer's instructions. RNA concentrations were determined using a Nanodrop (Thermo Scientific). cDNA was synthesised using Transcriptor High Fidelity cDNA Synthesis Kit (Roche Applied Science) using ∼2 μg of RNA. Reactions were primed with a 1:2 ratio mix of oligo-dT and random hexamers and incubated at 50°C for 30 min before inactivation at 85°C for 5 min. Control cDNA syntheses were performed in parallel including no reverse transcriptase enzyme control and no template RNA control.

qRT-PCR was performed on an Applied Biosystems Prism 7000 real-time PCR machine using SYBR Green JumpStart Taq Ready Mix (Sigma) in a 25 μl total volume reaction. Reactions were performed in triplicate with cycling as follows: 50°C for 2 min, 95°C for 10 min then 40 cycles of 95°C for 15 s and 60°C for 1 min under standard cycling conditions. PCR controls (no template, no enzyme, no primer, etc.) and template from cDNA synthesis controls were performed in parallel. mRNA expression was quantified relative to β-actin using the $\Delta\Delta C_t$ method (Livak & Schmittgen, 2001; Yuan *et al.* 2006; Bustin *et al.* 2009). Commercially available qRT-PCR primers were used (Qiagen) except for Kcnn1–4 that were designed and validated in-house with the following sequences:

Kcnn1 fwd CATCAgCCTgTCCACTgTCATCTTg; Kcnn1 rev gTCgTCggCACCATTgTCCAC; Kcnn2 fwd

ATCTTCggCATgTTCggCATCg; Kcnn2 rev ATCgTggAg AgACTgATAAggCATTTC; Kcnn3 fwd gCTTgTCCATCC TggTCTgTTgC; Kcnn3 rev ATggCggTAgAgTTgg CTgAAgTg; Kcnn4 fwd ggTTCTgCACgCTgAgATgTTg; Kcnn4 rev AAggCAgTggACAgggTgATC

Single cell RT-PCR

The cellular contents of single, fluorescently labelled corticotrophs that had been maintained in culture for 4 days were aspirated into RNAse free borosilicate patch-pipettes containing 7 μl of RNAse-free water. Aspirant was immediately transferred to an Eppendorf tube for cDNA synthesis using Sensiscript reverse transcriptase (Qiagen), RNasin ribonuclease inhibitor (Promega, Madison, WI, USA) and a mix of random and poly-dT primers in a final volume of 20 μl at 37°C for 1 h. For single cell PCR analysis, a two-stage PCR amplification strategy was used. Firstly, 2.5 μl of cDNA generated from the single cell aspirate was used in a 25 μl reaction using the SYBR Green JumpStart Taq Ready Mix and primers as for qRT-PCR. Samples were heated to 50°C for 2 min followed by 10 min at 95°C before performing 40 cycles at 95°C for 15 s and 60°C for 1 min standard cycling conditions on an ABI 7000. An aliquot (2.5 μl) of the first round amplification was then diluted into a new 25 μl PCR reaction and subjected to a further 10 amplification cycles using the conditions above. Multiple negative controls including control cell aspirants for which no reverse transcriptase was added (no-RT), aspiration of extracellular medium adjacent to intact cells (bath) and PCR controls were run in parallel with no detectable amplicon under identical conditions. Amplicons from the end-point PCR analysis were run on a 2% agarose gel and visualised using RedSafe (iNtRON Biotechnology, Kyungki-Do Korea). The predicted amplicon size (bp) for each primer set was: Kcnn1 = 94, Kcnn2 = 119, Kcnn3 = 75, Kcnn4 = 93, Kcnma1 = 106, Pomc = 99.

ACTH secretion *in vitro*

ACTH secretion *in vitro* was evaluated using dispersed anterior pituitary cells in static incubation assays. Dispersed anterior pituitary cells were prepared and transduced with lentivirus as above and plated in 96-well cluster dishes. Forty-eight to seventy-two hours post-transduction, cells were washed in Dulbecco's modified Eagle's medium (Invitrogen) containing 25 mM Hepes (Sigma-Aldrich) and 0.1% bovine serum albumin (BSA; Sigma-Aldrich) (DMEM-BSA), incubated for 2 h at 37°C in a water bath. Cells were then exposed to vehicle (basal) or 0.1 nM CRH + 2 nM AVP in the presence or absence of the respective ion channel inhibitor for 30 min. Plates were then placed on ice and the supernatant removed, spun briefly at 100 *g*, snap frozen on dry ice and stored at −70°C until radioimmunoassay. ACTH was determined, in duplicate, using a commercial radioimmunoassay kit (ACTH kit RK-001–21, Phoenix Pharmaceuticals Inc., Belmont, CA, USA) following appropriate dilution in radioimmunoassay buffer.

Corticotroph action potential model

The model is adapted from the original corticotroph action potential model from LeBeau *et al.* (1997), incorporating some of the adaptations made by Shorten *et al.* (2000). The original model simulates membrane potential using a set of Hodgkin–Huxley-type equations representing L-type and T-type voltage sensitive Ca^{2+} currents, a delayed rectifier (K-DR), a Ca^{2+} activated K^+ current (K-Ca), and a leak current representing the remaining ionic currents. It does not include a voltage-activated sodium conductance. It includes a basic representation of intracellular Ca^{2+}, sufficient to model the calcium-activated channels, assuming uniform spatial distribution of Ca^{2+}. We have developed the Le Beau model by adding a voltage sensitive A-type K^+ current (K-A) and replacing the leak current with a background, non-selective predominantly conducting Na^+ current (NS-Na) and an inward rectifying K^+ current (K-IR). The modelled K-A current is based on Tabak *et al.* (2007) and the NS-Na current is based on the formulation of Tsaneva-Atanasova *et al.* (2007). Our K-IR current uses a different formulation from Shorten *et al.* (2000), based instead on the somatotroph model of Tsaneva-Atanasova *et al.* (2007). In each case we have used their parameter values as a base and then adjusting to match our own recordings, looking at the detailed form of the action potentials. We have also added some Gaussian noise to the model's membrane potential, in order to more closely compare with the irregular recorded data. The noise is generated using an Ornstein–Uhlenbeck process (essentially integration step size scaled Gaussian noise with exponential decay), controlled by amplitude and decay parameters, o_A and o_d.

Parameters controlling calcium- and voltage-dependent time courses were shifted in order to match the time scale of our observed action potentials. The action potentials in the LeBeau model are very much slower, on a scale of ∼100 ms compared to our *in vitro* action potentials of ∼20 ms. To shorten these we increased the Ca^{2+} buffering factor from 0.01 to 0.2, reduced the Ca^{2+} exchange time constant from 500 ms to 110 ms, and shifted the voltage dependence of Ca^{2+} channel (L-type and T-type) gating in the negative direction (LeBeau *et al.* 1997).

Model equations for K-IR, NS-Na and K-A. The K-IR current is described by:

$$I_{\mathrm{K-IR}} = g_{\mathrm{K_{IR}}} K_{\mathrm{IR}_\infty} \Phi_K$$

where Φ_K is the K^+ driving force described in LeBeau *et al.* (1997) and the steady state activation $K_{IR,\infty}$ is described:

$$K_{IR\infty} = \frac{\alpha_{IR}}{\alpha_{IR} + \beta_{IR}}$$

$$\alpha_{IR} = \frac{0.1}{1 + exp(0.06(V_m - V_{IR} - 200)}$$

$$\beta_{IR} = \frac{3\exp[0.0002(V_m - V_{K_{IR}} + 100)] + \exp[0.1(V_m - V_{K_{IR}} - 10)]}{1 + \exp[-0.5(V_m - V_{K_{IR}})]}$$

The non-selective predominantly Na^+-conducting current (NS-Na) uses a very simple form:

$$I_{NSNa} = g_{NSNa}(V_m - V_{NSNa})$$

The fast-inactivating, voltage sensitive A-type K^+ current is described by:

$$I_A = g_A m_{A_\infty} h_A \Phi_K$$

with steady state activation $m_{A,\infty}$ and inactivation $h_{A,\infty}$ is described:

$$m_{A_\infty} = \frac{1}{1 + \exp[(V_{m_A} - V_m)/k_{m_A}]}$$

$$\frac{dh_A}{dt} = \frac{h_{A\infty}(V) - h_A}{\tau_{h_A}}$$

$$h_{A_\infty}(V) = \frac{1}{1 + \exp[(V_{h_A} - V)/k_{h_A}]}$$

Adding these currents to the LeBeau *et al.* (1997) model and removing the leak current gives the new membrane potential (V) equation:

$$\frac{dV}{dt} = \frac{(I_{Ca-L} + I_{Ca-T} + I_{K-DR} + I_{K-Ca} + I_{K-IR} + I_A + I_{NSNa}) + \text{noise}}{c_m}$$

The equations were integrated with the Runge–Kutta method, using a 0.1 ms step size.

Statistics

All data are expressed as means ± SEM with n = number of individual experiments or cells. Data were analysed using a parametric one-way ANOVA with *post hoc* Dunnett's test or non-parametric Kruskal–Wallis test as appropriate using Igor Pro v6.0 (Wavemetrics) or GraphPad Prism 5 (GraphPad Software Inc., La Jolla, CA, USA) with significant differences between groups defined at $^*P < 0.05$ or $^{**}P < 0.01$.

Reagents

Salts and biochemical reagents for electrophysiological analysis, including channel inhibitors, were from Sigma-Aldrich Co. (Poole, UK) and of the highest analytical grade unless specified otherwise in the methods. CRH and AVP were from Bachem Ltd (Weil am Rhein, Germany). Cell culture media including DMEM, HBSS, PBS and fetal calf serum were from Gibco Invitrogen Ltd (Paisley, UK)

Results

Labelling of corticotrophs *in vitro* using a lentiviral-driven POMC-eYFP reporter

To allow specific labelling of corticotrophs *in vitro* for patch clamp electrophysiological analysis we expressed eYFP under the control of a minimal POMC promoter using lentivirus-mediated cell transduction of isolated anterior pituitary cells *in vitro* (Fig. 1*A*). Using the minimal POMC promoter greater than 95% of corticotrophs that were immunohistochemically identified as ACTH-expressing cells from the murine anterior pituitary gland expressed the eYFP reporter. In contrast, using the constitutive CMV promoter less than 30% of the ACTH positive cells expressed eYFP (Fig. 1*B*) demonstrating the efficiency of lentiviral-mediated expression of eYFP in corticotrophs. The specificity of the minimal POMC-promoter driven expression of eYFP for ACTH positive cells was greater than 99.5% (Fig. 1*C*), presenting an ideal approach for the unequivocal identification of living murine anterior pituitary corticotrophs. Importantly, lentiviral mediated-transduction of corticotrophs with eYFP did not compromise basal or secretagogue-induced ACTH secretion, as measured by RIA (Fig. 1*D*), indicating that corticotroph viability and function were not compromised by our identification approach.

Murine corticotrophs are spontaneously active with heterogeneous firing patterns

The specific labelling of corticotrophs with eYFP allowed us to examine the spontaneous electrical activity of naive cells. Preliminary experiments using conventional whole cell recording resulted in a rapid (within a few minutes) cessation of spontaneous firing, and thus all subsequent analyses were performed using the perforated patch-clamp version of the whole-cell recording technique. Under these conditions of metabolically intact cells more than 95% of all cells displayed spontaneous electrical excitability that was maintained for the duration (typically >30 min) of the recording. The mean cell capacitance was 4.56 ± 0.32 pF,

mean resting membrane potential -55.0 ± 1.7 mV, and typical input resistance >3 GΩ ($n > 100$ cells).

The high input resistance of these cells would imply that small fluctuations in membrane current would have a significant impact on membrane potential. Accordingly, there was very considerable variability in action potential firing patterns between cells even from the same batch of cells recorded on the same day (Fig. 2). Furthermore, similar heterogeneity was also observed in corticotrophs isolated from POMC-GFP mice in current clamp using the perforated patch mode of recording (not shown). Previous studies analysing spontaneous action potentials in corticotrophs are conflicting. For example, rat corticotrophs are reported to be either spontaneously active (Kuryshev *et al.* 1997) or electrically silent (Lee & Tse, 1997). This might reflect either the recording conditions (perforated patch *vs.* whole-cell respectively) or cell isolation procedure used. Indeed, we found that in pilot studies conventional whole-cell approaches led to rapid run-down of spontaneous activity. This is in agreement with a recent study (Lee *et al.* 2011) using whole-cell recording from corticotrophs isolated from transgenic mice overexpressing GFP under control of the POMC promoter, in which corticotrophs appear to be predominantly electrically silent.

The majority of cells in our perforated-patch clamp studies displayed large amplitude single action potential spikes of variable frequency (Fig. 2*A* and *B*). Analysis of single spikes from different corticotrophs revealed a bimodal distribution in the amplitude of the after-hyperpolarisation following the spike (Fig. 3*A* and *B*). We thus categorised single spikes as either type A (Fig. 2*A*), in which the AHP was >25 mV, or type B (Fig. 2*B*) with AHP amplitude <20 mV. The proportion of cells displaying type A spikes was similar to that displaying type B spikes (~40%). Cells displaying type A or B spikes typically had similar resting membrane potentials in the range of -50 mV with no significant differences in spike threshold or spike amplitude (Fig. 3*A*, *C*, *D* and *F*). In addition, the mean cell capacitance (type A: 4.58 ± 0.31 pF, type B: 4.55 ± 0.38 pF) or input resistance (type A: 5.28 ± 0.51 GΩ, type B 5.25 ± 0.43 GΩ) of cells that displayed type A or type B spikes was not significantly different. However, type B spikes displayed a slower time

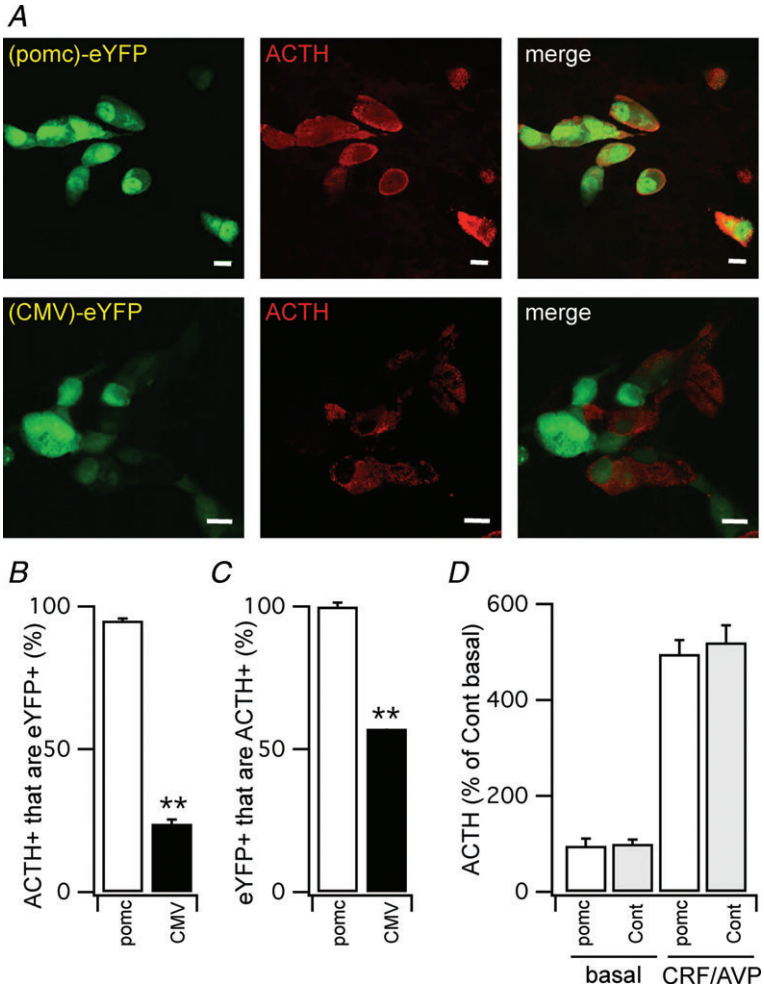

Figure 1. Labelling of murine corticotrophs *in vitro* using lentiviral transduction of a POMC-eYFP fluorescent reporter
A, representative confocal sections of dispersed anterior pituitary cells in primary culture 4 days following transduction with pomc-eYFP (top panels) or CMV-eYFP (bottom panels). The eYFP signal (left panels), ACTH immunoreactivity (middle panels) and merged images are shown. Scale bar is 10 μm. *B*, quantification of percentage of cells immunoreactive for ACTH (ACTH+) that are also labelled with eYFP (eYFP+) using either the POMC- or CMV- promoter lentiviral constructs. *C*, quantification of percentage of cells labelled with eYFP (eYFP+) that are also immunoreactive for ACTH (ACTH+) and that are also using either the POMC- or CMV-promoter lentiviral constructs. *D*, ACTH release from control (Cont) and POMC-eYFP (POMC) transduced cultures under basal and stimulated (CRH/AVP, 0.1 and 2 nM respectively) expressed as a percentage of the basal release in control (non-transduced) cultures. All data are means ± SEM, $n > 3$ independent experiments.

to peak (Fig. 3*E*), increased spike width (Fig. 3*G*) as well as a smaller afterhyperpolarisation amplitude (Fig. 3*H*) compared to type A spikes.

While cells rarely spontaneously converted between type A and type B action potentials, spike frequency during recordings varied considerably, ranging from <0.1 Hz to several hertz. Furthermore, cells with type A or B spikes also displayed spontaneous, reversible transitions to 'pseudo-plateau bursting modes', in which action potentials, of variable amplitude may be superimposed on periodic depolarized potentials (e.g. Fig. 2*C*–*H*) as described in other anterior pituitary cells (Tabak *et al.* 2007; Tsaneva-Atanasova *et al.* 2007). In a low proportion (<5%) of cells 'pseudo-plateau bursts' were observed during recordings (∼30 min) devoid of single spike events.

Exposure of corticotrophs to a brief pulse (3 min) of the combined secretagogues CRH and AVP (at 0.1 nM and 2 nM respectively, concentrations approximating those released into the portal circulation in response to stress; Gibbs & Vale, 1982; Sheward & Fink, 1991) resulted in a rapid increase in the frequency of action potential firing, with a concomitant steady depolarisation from rest of 14.6 ± 5.5 mV ($n = 5$), measured at 2 min after CRH/AVP application (Fig. 4*A*–*C*). The membrane

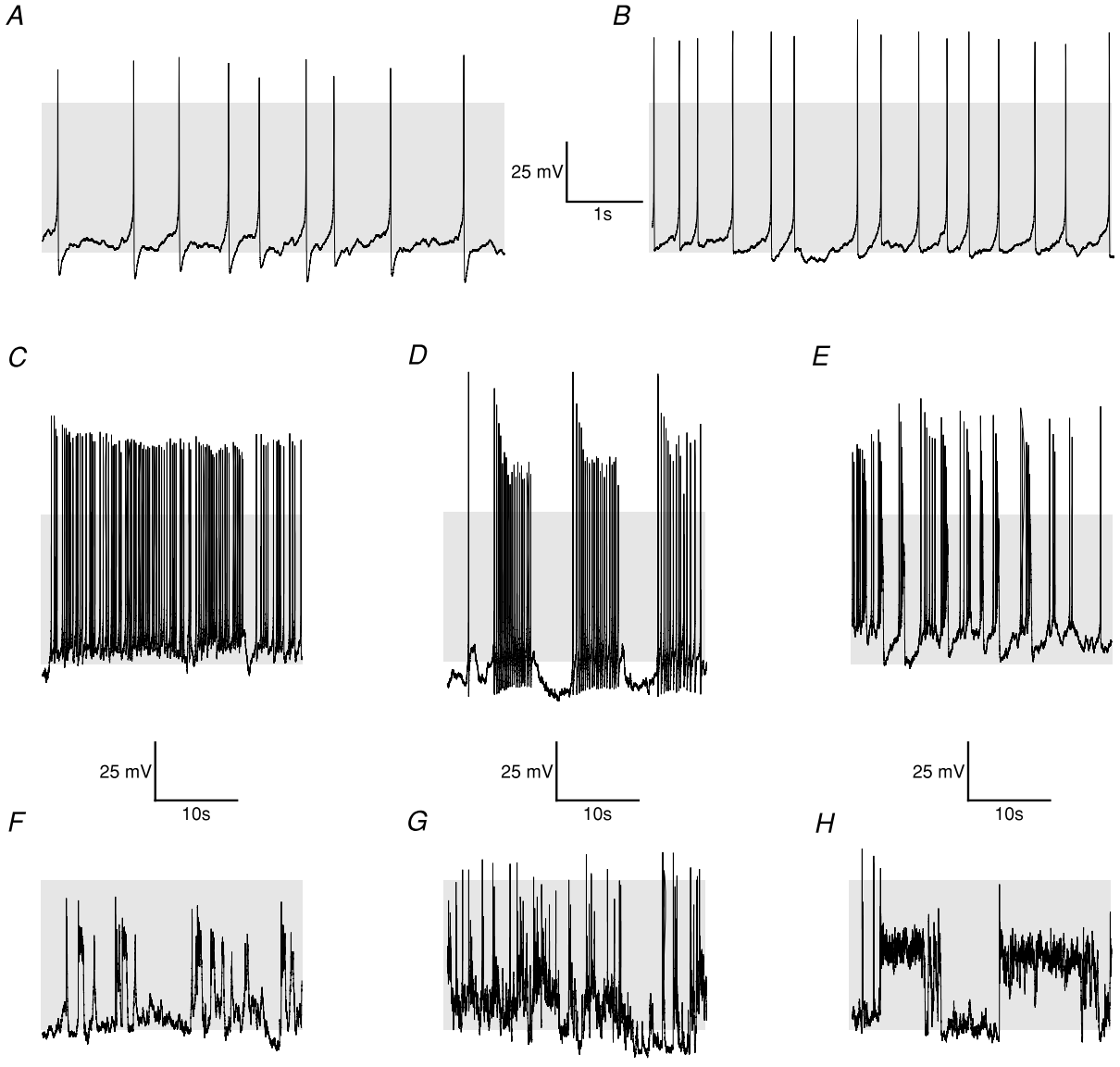

Figure 2. Heterogeneity of spontaneous electrical activity in murine corticotrophs
Waveforms and firing patterns differed widely between cells, and individual cells could transition between firing patterns. In perforated-patch clamp recordings the majority of cells exhibited spontaneous tall spikes, falling into one of two categories, as depicted in *A* (Type A; >30% of cells) and *B* (type B; >40% of cells). Detailed differences between these waveform types are elaborated upon in Fig. 3. Cells spontaneously and reversibly transitioned to other firing patterns represented by panels *C*–*H*, including 'pseudo-plateau potential' bursting behaviours. Grey shading indicates membrane potential between −50 and +10 mV.

depolarisation and increase in action potential frequency were maintained upon washout of the secretagogues. The mean time to full recovery to the preceding (unstimulated) membrane potential was 20.3 ± 4.2 min ($n = 4$).

A background sodium conductance controls resting membrane potential

In a proportion of cells we could detect TTX-sensitive fast inactivating inward currents; however current amplitude was highly variable. TTX modified the amplitude of the tallest spike events but had no significant effect on spikes that did not reach above 0 mV (data not shown). On the whole, TTX (1–2 μM) did not typically alter the probability or frequency of spike generation in these cells, in agreement with previous studies in rat corticotrophs (Kuryshev *et al.* 1997).

In several pituitary types, spontaneous activity is dependent on a non-voltage gated (and TTX-insensitive) inward sodium conductance (Simasko, 1994; Takano *et al.* 1996; Tomic *et al.* 2011). In our studies, replacement of external Na^+ ions with the large impermeant organic cation *N*-methyl-D-glucamine ($NMDG^+$) was accompanied by a rapid and reversible hyperpolarisation of the membrane potential resulting in cessation of spontaneous action potential firing (Fig. 5*A*). In voltage clamp recordings, in which cells were held at the potassium reversal potential, replacement of external Na^+ with $NMDG^+$ resulted in inhibition of a standing inward current (Fig. 5*B*). This suggests that a background inward sodium conductance maintains the resting membrane potential of murine corticotrophs in a relatively (∼−55 mV) depolarised state. As removal of extracellular Na^+ prevents any inward sodium conductance, we cannot, however, exclude that other voltage-dependent, TTX-insensitive sodium conductances also contribute to the rising phase of spontaneous action potentials.

Replacement of external Na^+ with $NMDG^+$ also prevented the rapid CRH/AVP-induced depolarisation of the cell and increases in CRH/AVP-stimulated action potential firing. At 2 min following addition of CRH/AVP, in the continued presence of NMDG, the mean

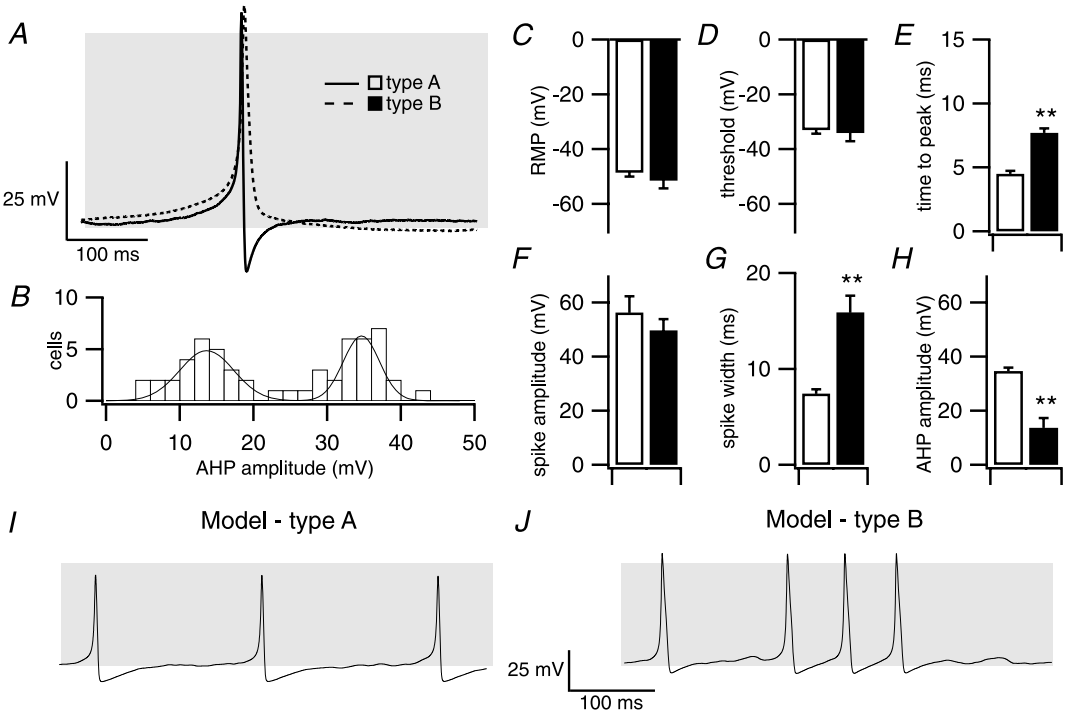

Figure 3. Characterisation of type A and type B action potentials.
Several features of type A and type B action potential waveforms differed concurrently between cells. *A*, averaged traces from type A (continuous line, open square) and type B (dashed line, filled square) action potentials as in Fig. 2. *B*, histogram of afterhyperpolarisation (AHP) amplitude from single spikes demonstrates a bimodal distribution. Spikes with an AHP amplitude >25 mV were defined as type A spikes. *C–H*, mean resting membrane potential (*C*), threshold for action potential generation (*D*), time to action potential peak (*E*), spike amplitude (*F*), spike width (*G*) and afterhyperpolarisation amplitude (*H*) for type A and B spikes. *I* and *J*, modelling of type A (*I*) and type B (*J*) action potentials using a revised formulation of a corticotroph action potential model that incorporates additional conductances identified in this study. Grey shading indicates membrane potential between −50 and +10 mV. Data are means ± SEM, $n = 19$ per group. $^{**}P < 0.01$, ANOVA with *post hoc* Dunnett's test compared to type A spikes.

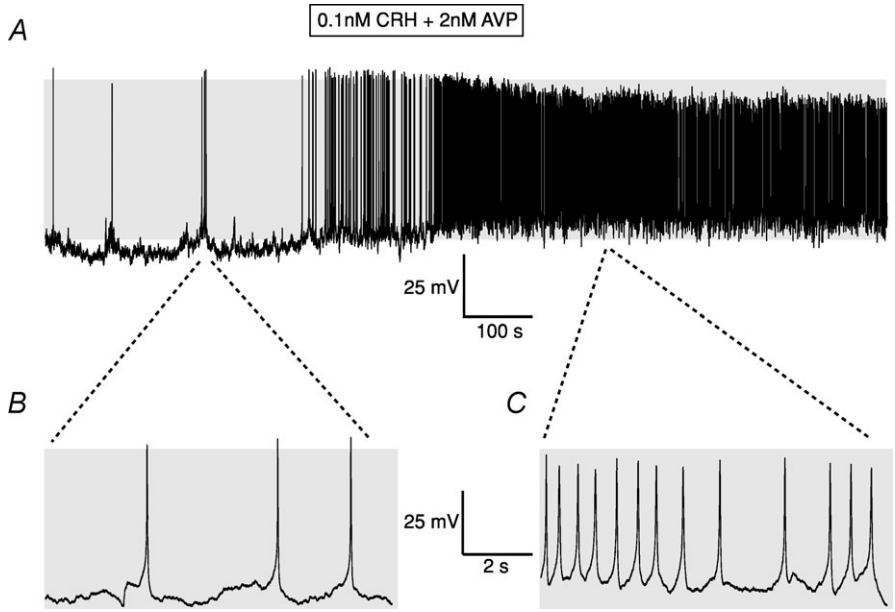

Figure 4. Stimulation of murine corticotrophs by CRH/AVP
A, representative current clamp recording of a metabolically intact corticotroph before and following exposure to a 3 min pulse of 0.1 nM CRH and 2 nM AVP. *B* and *C*, expanded traces before application of CRH/AVP (*B*) and immediately following washout of secretagogue (*C*). Grey shading indicates membrane potential between −50 and +10 mV.

depolarisation was only 2 ± 3 mV, $n = 5$, significantly smaller than that observed in physiological extracellular Na^+ solutions (Fig. 5*C*). In the continued presence of NMDG and CRH/AVP there was, however, a significantly delayed depolarisation, peaking to 18.1 ± 2.7 mV after 12.9 ± 1.7 min. The identity of this CRH/AVP-regulated conductance is unknown. However, the time course suggests it may contribute to the sustained depolarisation

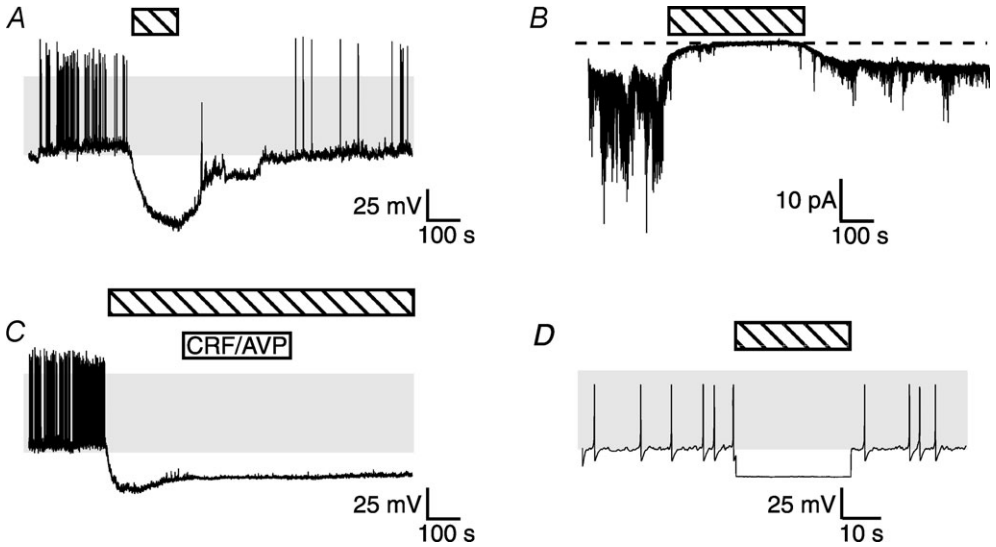

Figure 5. A background sodium conductance contributes to resting membrane potential
Effects of substitution of external Na^+ with the impermeant ion $NMDG^+$, indicated by the horizontal hatched bar, during perforated patch recordings. TTX at 2 μM is present throughout. *A*, $NMDG^+$ substitution for Na^+ causes hyperpolarization and cessation of action potential generation. *B*, voltage clamp at the K^+ reversal potential reveals a standing inward conductance that is eliminated during $NMDG^+$ substitution. *C*, CRH/AVP does not rapidly depolarise corticotrophs or stimulate action potential generation in Na^+-free external solutions. *D*, in the mathematical model of a corticotroph, elimination of the background Na^+ conductance simulates the recording shown in *A*.

and increase of action potential firing upon washout of CRH/AVP under physiological conditions.

Modelling spontaneous activity of murine corticotrophs

In previous models of corticotroph excitability (LeBeau *et al.* 1997; Shorten *et al.* 2000), some key aspects of action potential properties and bursting were studied that do not accurately predict the observed resting membrane potential of murine corticotrophs or the variability in duration of action potential waveform. For example, mean resting potential is at or below −70 mV in these models, potentials rarely reached in murine corticotrophs. This is likely to reflect that current models do not include the NMDG-sensitive background sodium conductance that maintains the resting membrane potential of murine corticotrophs around −55 mV. We thus modified the LeBeau model to incorporate a sodium-dependent non-selective inward conductance (NS-Na) with additional conductances (including an inactivating A-type conductance (K-A) and inwardly rectifying conductance (K-IR), based on our analysis of potassium conductances in murine corticotrophs as below). In our revised model, the K-IR and NS-Na currents act against each other to control the cell's resting membrane potential and excitability. To simulate our recordings their conductances were balanced against each other and we introduced Gaussian noise to simulate the variability in firing patterns. In the model, too much K-IR prevents firing, and too much NS-Na prevents the cell from repolarising, maintaining a high plateau potential. We could thus simulate typical resting membrane potentials in murine corticotrophs (range −60 to −50 mV), with concomitant action potential firing, by increasing NS-Na and then increasing K-IR in parallel to preserve firing activity. Under these conditions, the shift from type A to type B action potentials could be accurately modelled by reducing both the A-type and calcium-sensitive potassium channel conductances (Fig. 3*I* and *J*). Furthermore, in agreement with our electrophysiological recordings from spontaneously active cells, inhibition of the inward sodium conductance (NS-Na) resulted in cell membrane hyperpolarisation and cessation of action potential firing (Fig. 5*D*).

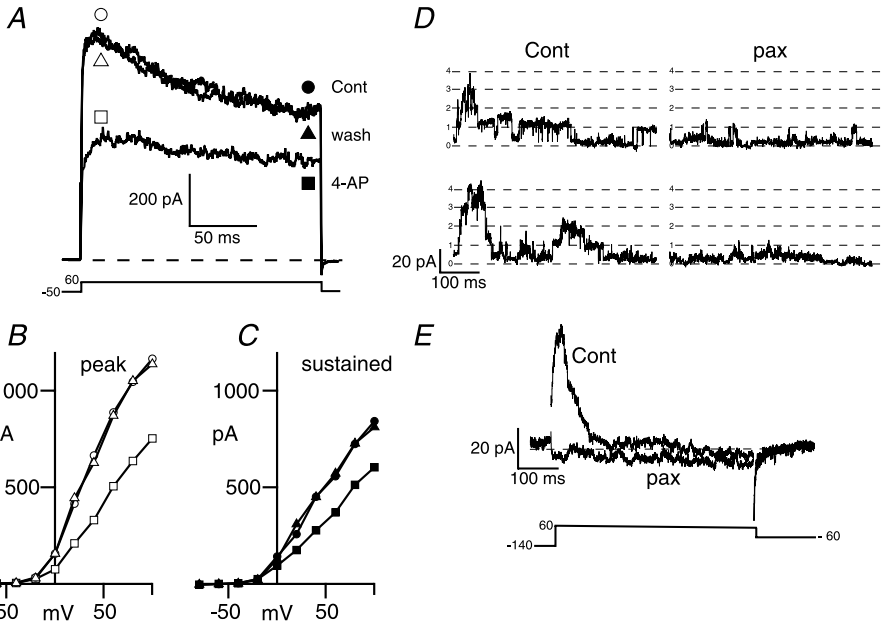

Figure 6. A-type voltage-gated potassium channels and large conductance calcium-activated potassium (BK) channels are expressed in corticotrophs.
A, representative voltage-clamp recording of a metabolically intact corticotroph displaying significant inactivating outward current when depolarised from a holding potential of −50 mV to +60 mV before (cont, circles) during (4-AP, squares) and after washout (wash, triangles) with 4-aminopyridine (4-AP, 1 mM) an inhibitor of A-type potassium channels. *B* and *C*, current–voltage relationship for the cell in *A* determined at the peak outward current shown by the open symbols in *A* (*B*) or during the sustained phase (180–200 ms into pulse) shown by the filled symbols in *A* (*C*). *D*, single channel recordings from inside-out membrane patches exposed to 5 μM intracellular free calcium determined during a step pulse to +60 mV before (Cont) and after application of the specific BK channel inhibitor paxilline (pax, 1 μM). *E*, ensemble average traces in the presence and absence of paxilline from 15 recordings as in *D*.

Murine corticotrophs express multiple potassium channels

Murine corticotrophs display large outward currents at positive potentials under the perforated patch conditions used with inactivating and non-inactivating components dominating in different cells (compare, for example, Fig. 6*A* and Fig. 7*A*). To investigate the contribution of different potassium conductances we took a pharmacological approach and analysed the effects of various potassium channel inhibitors on the outward current.

Previous studies in murine AtT20 D16:16, as well as rat, corticotrophs have reported an A-type inactivating potassium conductance sensitive to 4-aminopyridine (4-AP) (Pennington *et al.* 1994; Lee & Tse, 1997). At 1 mM, 4-AP is relatively selective for A-type potassium channels. At this concentration it inhibited the peak outward current (Fig. 6*B*) during the pulse by 36.7 ± 2.8% ($n = 16$, determined at +40 mV) whereas the sustained current (Fig. 6*C*) was only reduced by 15.1 ± 6.0% ($n = 16$). Raising 4-AP to 10 mM resulted in an inhibition of sustained and peak outward potassium current by 73.1 ± 2.8% ($n = 5$) and 75.3 ± 3.1% ($n = 5$), respectively.

Application of 1 mM TEA inhibited the outward sustained current by 31.9 ± 4.6% ($n = 6$). This concentration is relatively selective for large conductance calcium activated potassium channels in some systems. However, application of 1 μM paxilline, the specific BK channel inhibitor, blocked only a small and variable proportion of the outward sustained current (mean 11.5 ± 2.3%, range 5–28%, $n = 14$) and 18.3 ± 3.2% ($n = 14$) of the peak current, suggesting a relatively modest contribution of BK channels to the outward current under the recording conditions used. In inside-out patch recordings, in the presence of 5 μM intracellular free calcium, a step depolarisation to +60 mV, from a holding potential of −140 mV, revealed activation of large conductance (~300 pS) BK channels, at the start

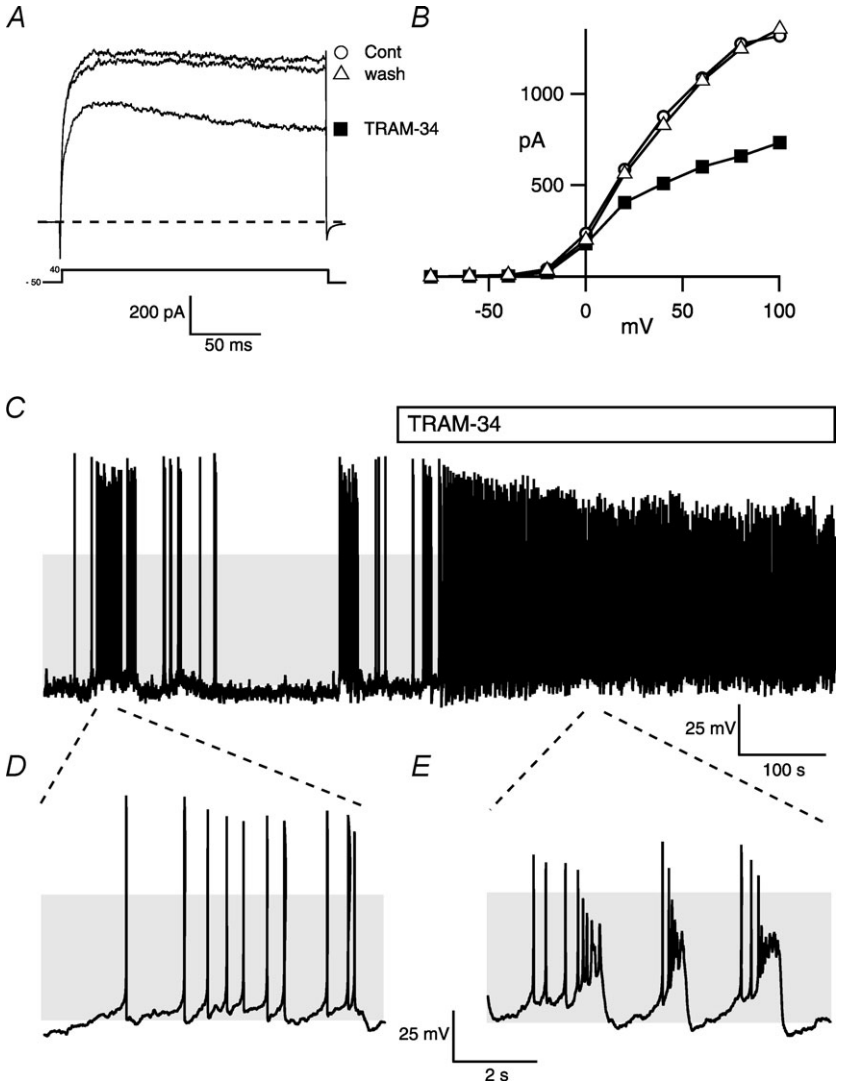

Figure 7. TRAM-34 sensitive intermediate conductance calcium-activated potassium channels (SK4) control corticotroph excitability
A, representative voltage-clamp recording of a metabolically intact corticotroph depolarised from a holding potential of −50 mV to + 40 mV before (cont, open circle) during (TRAM-34, filled square) and after washout (wash, open triangle) of the specific inhibitor of intermediate conductance calcium activated potassium (SK4) channels, TRAM-34 (1 μM). *B*, current–voltage relationship of the whole cell outward current from the cell in *A*. *C–E*, representative current-clamp recording of a metabolically intact corticotroph before and during exposure to TRAM-34 (*C*), with expanded traces before (*D*), and during exposure to TRAM-34 (*E*). Grey shading indicates membrane potential between −50 and +10 mV.

of the pulse that inactivated (t_{half} of 51.5 ± 6.0 ms over the time course of the pulse (Fig. 6*D*). Paxilline (1 μM) blocked 89.4% of this current, as determined from ensemble averages from 15 individual sweeps (Fig. 6*D* and *E*). Furthermore, BK channel activity was essentially abolished under these conditions upon perfusion of a nominally (EGTA buffered) calcium free intracellular solution to the intracellular face of the patch (not shown). Thus, while BK channels are expressed in murine corticotrophs their contribution to the outward current is modest under normal resting membrane conditions in metabolically intact corticotrophs.

To test whether other calcium-activated potassium conductances are expressed in murine corticotrophs we first examined the effect of 500 nM apamin. Apamin blocks a variety of small conductance calcium-activated potassium (SK) channels that are reported to be activated by AVP in rat corticotrophs (Tse & Lee, 1998). In 8/9 cells application of apamin elicited a small but significant (mean inhibition was 11.3 ± 8.4%, $n = 9$, $P < 0.05$ Student's paired *t* test) inhibition of the sustained outward current. In contrast, 1 μM clotrimazole, at a concentration that blocks intermediate conductance calcium-activated (SK4) potassium channels, inhibited the sustained outward current by 39.8 ± 3.5% ($n = 9$). However, at concentrations above 1 μM clotrimazole has been reported to be non-selective for SK4 channels (Wulff *et al.* 2000); thus we examined the effect of the selective SK4 inhibitor 1-[(2-chlorophenyl)diphenylmethyl]-1*H*-pyrazole (TRAM-34; Fig. 7*A* and *B*). TRAM-34 inhibited the sustained outward current, determined at +40 mV, by 37.6 ± 3.8% ($n = 5$), a value similar to that observed with clotrimazole.

Taken together these data demonstrate that murine corticotrophs express multiple outward potassium conductances and that in perforated patch recordings the calcium-activated intermediate conductance potassium channel, sensitive to TRAM-34, mediates a significant proportion of the outward current.

Murine corticotrophs also express an inwardly rectifying potassium conductance (Fig. 8*A*) that is blocked more than 50% by 100 μM external Ba^{2+}, as previously reported in rat corticotrophs (Kuryshev *et al.* 1997). In corticotrophs from male rats, the Ba^{2+}-sensitive inwardly rectifying potassium conductance has been implicated in controlling both spontaneous and CRH-induced corticotroph depolarisation and enhanced action potential frequency. However, 100 μM Ba^{2+} had no significant effect on murine corticotroph depolarisation or action potential frequency in any cell (6/6) examined (Fig. 8*B*).

Intermediate conductance calcium-activated potassium channels regulate corticotroph excitability and ACTH secretion *in vitro*

Since a large component of the outward potassium current was carried via the TRAM-34 sensitive current in murine corticotrophs, we further analysed whether SK4 channels control corticotroph excitability and/or ACTH secretion. In 4/6 corticotrophs, exposure to TRAM-34 resulted in a significant increase (4.7 ± 1.8-fold, $n = 4$ determined from the 2 min immediately preceding and following TRAM-34 exposure) in action potential frequency that was typically associated with a transition to a pseudo-plateau bursting phenotype (Fig. 7*C*–*E*). In the presence of TRAM-34 the duration of the plateau burst, the number of spikes per burst and interspike interval across the spontaneous bursts were highly variable even in the same cell as well as between responding cells. Furthermore, in contrast to the effect of CRH/AVP, the change in action potential frequency and 'pseudo-plateau bursting' seen with TRAM-34 was not associated with a significant and sustained depolarisation of the resting membrane potential. In the four cells that responded with an

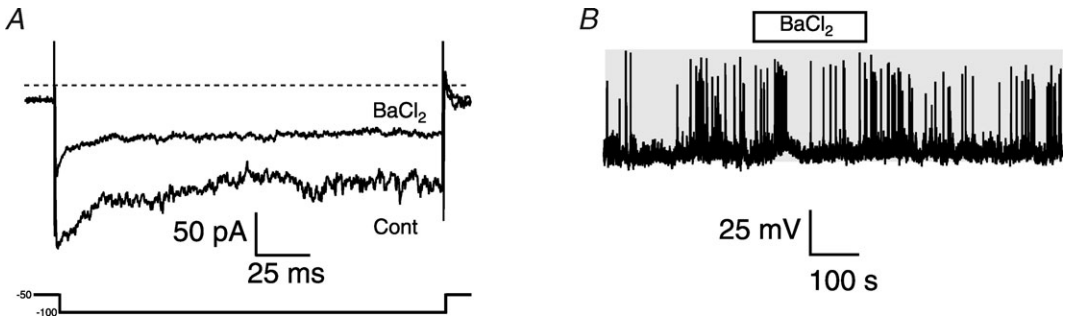

Figure 8. Barium-sensitive inwardly rectifying potassium conductance does not control action potential generation in murine corticotrophs
A, representative voltage-clamp recording of a metabolically intact corticotroph in the presence of elevated (20 mM) extracellular potassium and step hyperpolarised from −50 mV to −100 mV before (Cont) and after addition of 100 μM $BaCl_2$ to the bath. *B*, current-clamp recording of corticotroph in physiological extracellular solution exposed to 100 μM $BaCl_2$ (horizontal open bar). Note lack of Ba^{2+} on firing. Grey shading indicates membrane potential between −50 and +10 mV.

increase in activity following exposure to TRAM-34 the mean resting membrane potential increased by only 1.7 ± 2.1 mV compared to the pretreatment control period.

To examine whether SK4 channels affect ACTH secretion *in vitro*, we assayed basal and CRH/AVP stimulated ACTH release in static cultures in the presence and absence of clotrimazole or TRAM-34. Both clotrimazole and TRAM-34 alone induced a small, but significant ($P < 0.05$, Kruskal–Wallis with *post hoc* Dunnett's test) increase in basal ACTH output and induced a small potentiation of CRH/AVP stimulated ACTH release *in vitro*. A 30 min exposure to 0.1 nM CRH and 2 nM AVP stimulated basal ACTH release in static cultures 4.1 ± 0.3-fold ($n = 6$). TRAM-34 (1 μM) alone had a small but significant effect (Kruskal-Wallis with *post hoc* Dunnett's test, $P < 0.05$) increasing ACTH release to 1.4 ± 0.2 fold above basal levels. In the presence of TRAM-34 the effect of CRH and AVP was significantly potentiated compared to the effect CRH and AVP alone (to 5.2 ± 0.4-fold above basal levels in the absence of TRAM-34). As TRAM-34 potentiated rather than reduced the CRH/AVP-induced release of ACTH, this suggests that CRH/AVP does not regulate corticotroph excitability by inhibiting the TRAM-34 sensitive SK4 channels *per se*. Taken together these data support a role for SK4 channels as negative regulators of corticotroph excitability and ACTH secretion and point to a role for these channels in determining corticotroph and stress axis function.

Stress hyperresponsiveness in mice deficient for Kcnn4

To address whether SK4 channels play an important role in corticotroph function *in vivo* we examined the stress response in female mice lacking the SK4 channel (Kcnn4) (Sausbier *et al.* 2006). If SK4 channels play a significant role in ACTH release from the corticotroph *in vivo* we would predict that mice deficient for SK4 would display an exaggerated ACTH and corticosterone (CORT) release in response to an acute stress, i.e. a stress hyperresponsive phenotype in accordance with the exaggerated release of ACTH from corticotrophs *in vitro*. In mice with a global deletion of the pore exon of the Kcnn4 gene encoding SK4 channels (Kcnn4$^{-/-}$ mice) basal release of ACTH was not significantly different from wild-type (WT) age and litter matched female mice (Fig. 9*A*). Thirty minutes of restraint resulted in robust stimulation of plasma ACTH levels in WT by more than 3-fold. However, stress-induced plasma ACTH levels were significantly enhanced in Kcnn4$^{-/-}$ mice compared to WT controls, resulting in a more than 4-fold increase in plasma ACTH levels following restraint (Fig. 9*A*). These stress-induced changes in plasma ACTH were paralleled by changes in plasma CORT (Fig. 9*B*). Again, no significant difference in basal CORT levels was observed between genotypes. However, restraint stress-induced plasma CORT levels were significantly higher in Kcnn4$^{-/-}$ mice than in WT. Thus, both the ACTH and CORT response to restraint stress, but not basal output, are significantly enhanced in mice deficient for the Kcnn4 gene encoding the SK4 channel. This suggests that SK4 channels are more important for damping stress responses than for inhibiting basal HPA-axis function.

These data are in agreement with the *in vitro* effects of SK4 inhibition on evoked ACTH release, suggesting that the stress hyperesponsiveness observed in the Kcnn4$^{-/-}$ mice results, in part at least, from the loss of SK4 channels from corticotrophs. However, to examine whether Kcnn4 deletion may additionally exert effects at other levels of the HPA axis, or through additional mechanisms at the level of the anterior pituitary corticotroph, we used qRT-PCR to test for changes in gene expression in key HPA components in WT and Kcnn4$^{-/-}$ mice under basal and restraint stress conditions.

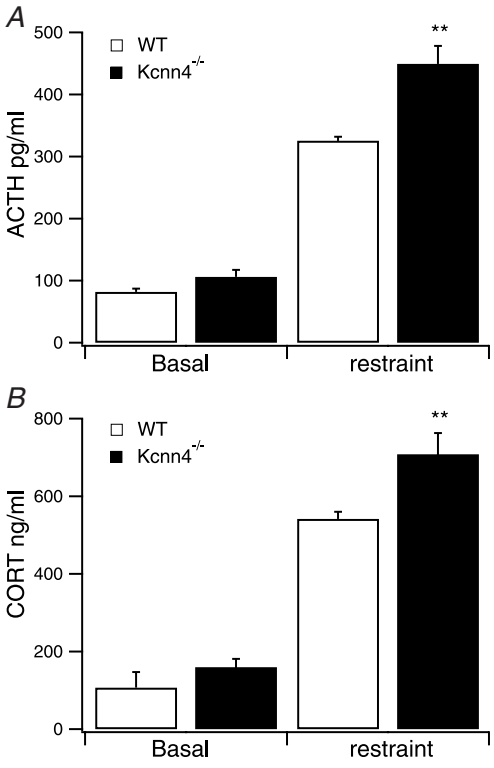

Figure 9. Enhanced restraint stress-induced plasma ACTH and corticosterone concentration in Kcnn4$^{-/-}$ knockout mice
A and *B*, plasma ACTH (*A*) and corticosterone (CORT) (*B*) concentrations under resting conditions (basal) and following 30 min of restraint stress (restraint) in wild-type (WT, open bar) and mice genetically deficient for the gene (Kcnn4) encoding SK4 channels (Kcnn4$^{-/-}$, filed bar). Data are means ± SEM, $n = 7$/group. $^{**}P < 0.01$, ANOVA with *post hoc* Dunnett's test compared to WT.

First, we examined tissue mRNA expression of Kcnn4 to confirm that Kcnn4 is expressed in the anterior pituitary and determine whether Kcnn4 is also expressed in the hypothalamus and adrenal gland. Kcnn4 mRNA was expressed in the hypothalamus, anterior pituitary and adrenal gland (Fig. 10*A*). However, mRNA levels were at least an order of magnitude below the mRNA expression for the related genes (Kcnn1–3) encoding small conductance calcium activated potassium channels (SK1–3). As expected, a qRT-PCR approach that was based on sequences, which have not been deleted in construction of the Kcnn4$^{-/-}$ mice resulted in a significant reduction (by approximately an order of magnitude) of Kcnn4 mRNA detected in all analysed tissues from the Kcnn4$^{-/-}$ mice. Importantly, knockout of Kcnn4 did not significantly affect mRNA expression of the related small conductance calcium activated channels SK1–3 in the hypothalamus, pituitary or adrenal (Fig. 10*A*). To verify that mRNA encoding for SK4 channels was expressed in corticotrophs we undertook single cell PCR.

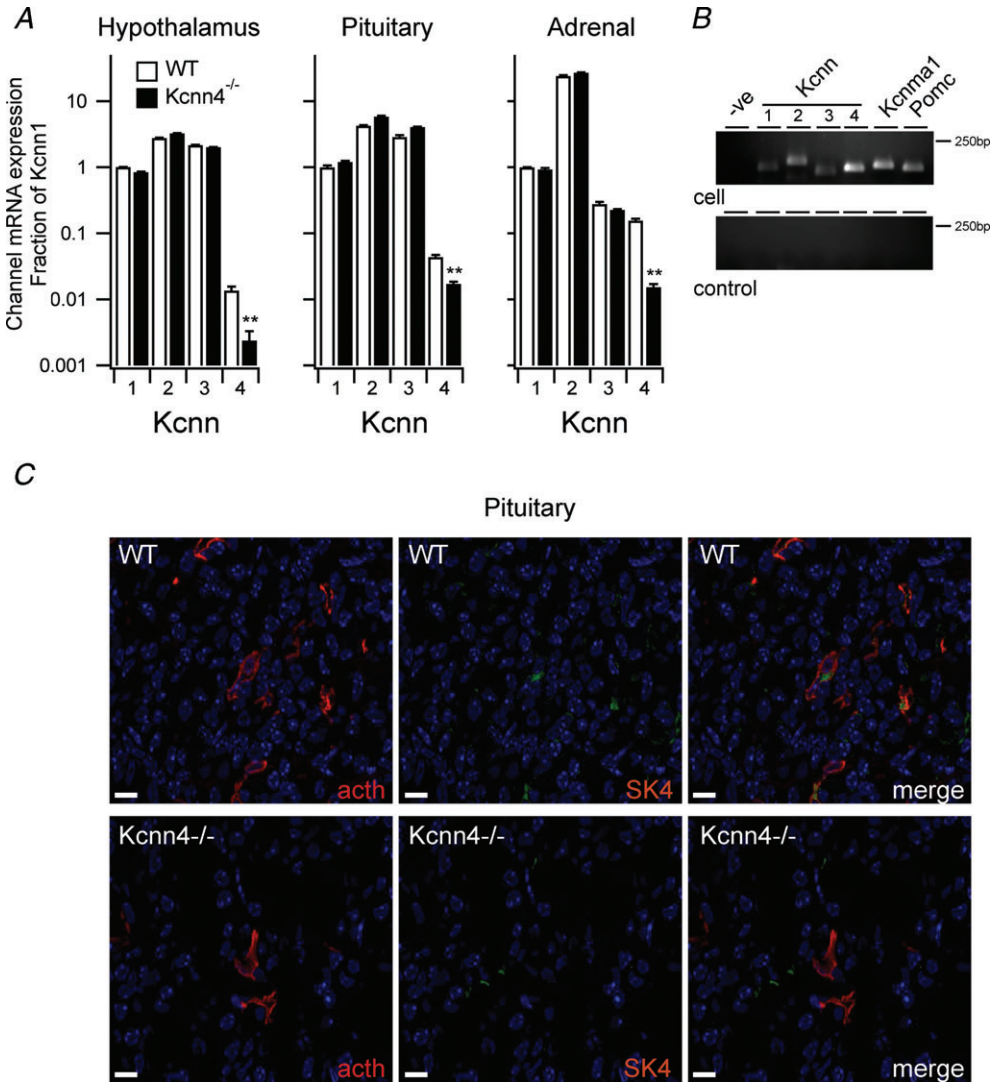

Figure 10. Expression of SK4 in HPA axis and anterior pituitary corticotrophs
A, mRNA expression encoding for SK4 channels (Kcnn4) and the related small conductance calcium-activated potassium channels SK1–3 (Kcnn1 to 3) determined by qRT-PCR in hypothalamus, anterior pituitary and adrenal gland from wild-type (WT, open bar) and Kcnn4 knockout mice (Kcnn4$^{-/-}$, filled bar). For each tissue, data are expressed as a fraction of the mRNA expression for Kcnn1. Data are means ± SEM, $n = 7$. $^{**}P < 0.01$, Kruskal–Wallis with *post hoc* Dunnett's test compared to WT. *B*, PCR amplicons from end-point single cell RT-PCR analysis from a fluorescently labelled corticotroph (cell) and negative sampling control (control) using primers to amplify Kcnn1–4, Kcnma1 and Pomc mRNA. –ve indicates PCR control. *C*, representative fluorescence images of anterior pituitary sections from wild-type (WT, top panels) and SK4 knockout (Kcnn4$^{-/-}$, bottom panels) mice probed for ACTH (left panels, red), and SK4 (middle panels, green) immunoreactivity with merged images shown at the right. Scale bars are 10 μm.

mRNA encoding for SK4 channels, as well as mRNA encoding small (SK1–3) and large (BK) conductance calcium-activated potassium channels, were detectable in cellular aspirates from single, fluorescently labelled corticotrophs positive for POMC mRNA (Fig. 10*B*). To examine whether SK4 protein is detectable in corticotrophs of the anterior pituitary we undertook dual-labelling immunohistochemistry in sections of the murine pituitary gland. Low levels of SK4 expression were detectable in wild-type animals (Fig. 10*C*), and quantitative distribution analysis demonstrated that $87.5 \pm 9.3\%$ of all ACTH-positive cells also expressed SK4 immunoreactivity. Conversely, $83.5 \pm 7.7\%$ of SK4-positive pituitary cells were also ACTH-positive. Therefore, the majority of SK4 expression in the anterior pituitary occurs in corticotrophs. While robust ACTH immunoreactivity was still evident, only non-specific background staining was detectable for SK4 in Kcnn4$^{-/-}$ mice.

To address whether global deletion of Kcnn4 function may result in additional stress hyperresponsiveness through enhanced excitation at the level of the hypothalamus we first examined the mRNA expression levels of the two early-immediate genes (c-*fos* and *nurr*77) as markers of hypothalamic activation (Chan *et al.* 1993; Brunton *et al.* 2007) in WT and Kcnn4$^{-/-}$ mice under control and restraint stress conditions (Fig. 11*A*). Control levels of c-*fos* mRNA expresssion were not significantly different between genotypes. Restraint stress induced a robust increase in c-*fos* mRNA expression in WT and Kcnn4$^{-/-}$ mice, as expected. However the increase in expression was significantly enhanced in the knockout. For *nurr*77 there was a small but significant increase in basal mRNA expression in the Kcnn4$^{-/-}$ mice compared to WT, an effect that was also maintained under stress conditions (Fig. 11*A*). Kcnn4$^{-/-}$ mice also displayed a significant increase in expression of both CRH and AVP mRNA. Under basal conditions, CRH mRNA expression in Kcnn4$^{-/-}$ mice was 2-fold higher than WT basal, and similar to that observed after 30 min restraint in WT mice. CRH mRNA levels in Kcnn4$^{-/-}$ mice were further increased following restraint, suggesting that CRH mRNA expression was not maximal, but remained sensitive to stress inputs. For AVP mRNA expression, basal levels in Kcnn4$^{-/-}$ mice were again higher than in WT basal, and similar to those seen after restraint in WT. However, no further increase in AVP mRNA expression was observed following restraint in Kcnn4$^{-/-}$ mice. This suggests that either AVP mRNA levels are maximally stimulated under basal conditions, or that stress-induced regulation of AVP mRNA levels is attenuated in the Kcnn4$^{-/-}$ mice.

Although there was a small (<40%) increase in mineralocorticoid receptor (MR) mRNA expression (Fig. 11*A*) no significant changes in glucocorticoid receptor (GR) mRNA expression were observed between genotypes under control or stress conditions. This suggests that the stress-induced negative feedback circuitry is largely unaffected. Taken together, these data suggest that enhanced stress-induced activation of the hypothalamus, as well as elevated expression of the major ACTH secretagogues, CRH and AVP, may contribute to the stress hyperresponsiveness observed in the Kcnn4$^{-/-}$ mice.

We next asked whether additional mechanisms might contribute to the stress hyperresponsive phenotype at the level of the anterior pituitary. Kcnn4$^{-/-}$ mice displayed a significantly elevated expression of mRNA for the G-protein coupled receptors for AVP (AVPR1b) and CRH (CRHR1) respectively in the anterior pituitary. This suggests that increased CRH and AVP receptor density may, in part, contribute to the enhanced evoked ACTH output in Kcnn4$^{-/-}$ corticotrophs *in vivo* and *in vitro*. There was no significant difference in POMC mRNA expression between genotypes under basal conditions (Fig. 11*B*) although levels after stress were modestly increased in the Kcnn4$^{-/-}$ mice. As for the hypothalamus, a small (∼40%), but significant, increase in MR, but not GR, mRNA expression was observed. Whether such modest increases in MR abundance at hypothalamic and/or pituitary levels could contribute to stress hypersensitivity is not known.

Although the plasma CORT responses in Kcnn4$^{-/-}$ mice followed the changes in plasma ACTH, suggesting that adrenal function *per se* was not compromised, we examined whether significant changes in adrenal function may contribute to the stress hyperresponsive phenotype in the Kcnn4$^{-/-}$ mice (Fig. 11*C*). No significant changes in mRNA expression for the ACTH receptor, MR or GR were observed under control or stress conditions. Furthermore, no significant changes were observed in mRNA expression of the two major enzymes required for CORT biosynthesis in the adrenal gland: cytochrome P450 side chain cleaving enzyme (Cyp11a1) required for synthesis of pregnenolone from cholesterol, and 3-β-hydroxysteroid dehydrogenase/Δ-5–4 isomerase (Hsd3b2), required for conversion of pregnenolone to progesterone.

Taken together these data suggest that SK4 channels may contribute to HPA axis function at multiple levels, including the anterior pituitary corticotroph and hypothalamic neural circuitry.

Discussion

In this paper we present a highly specific and efficient approach for labelling murine anterior pituitary corticotrophs using a lentiviral driven fluorescent eYFP reporter. This has allowed the first systematic analysis of the spontaneous and stimulated electrophysiological properties of murine corticotrophs. Importantly, our

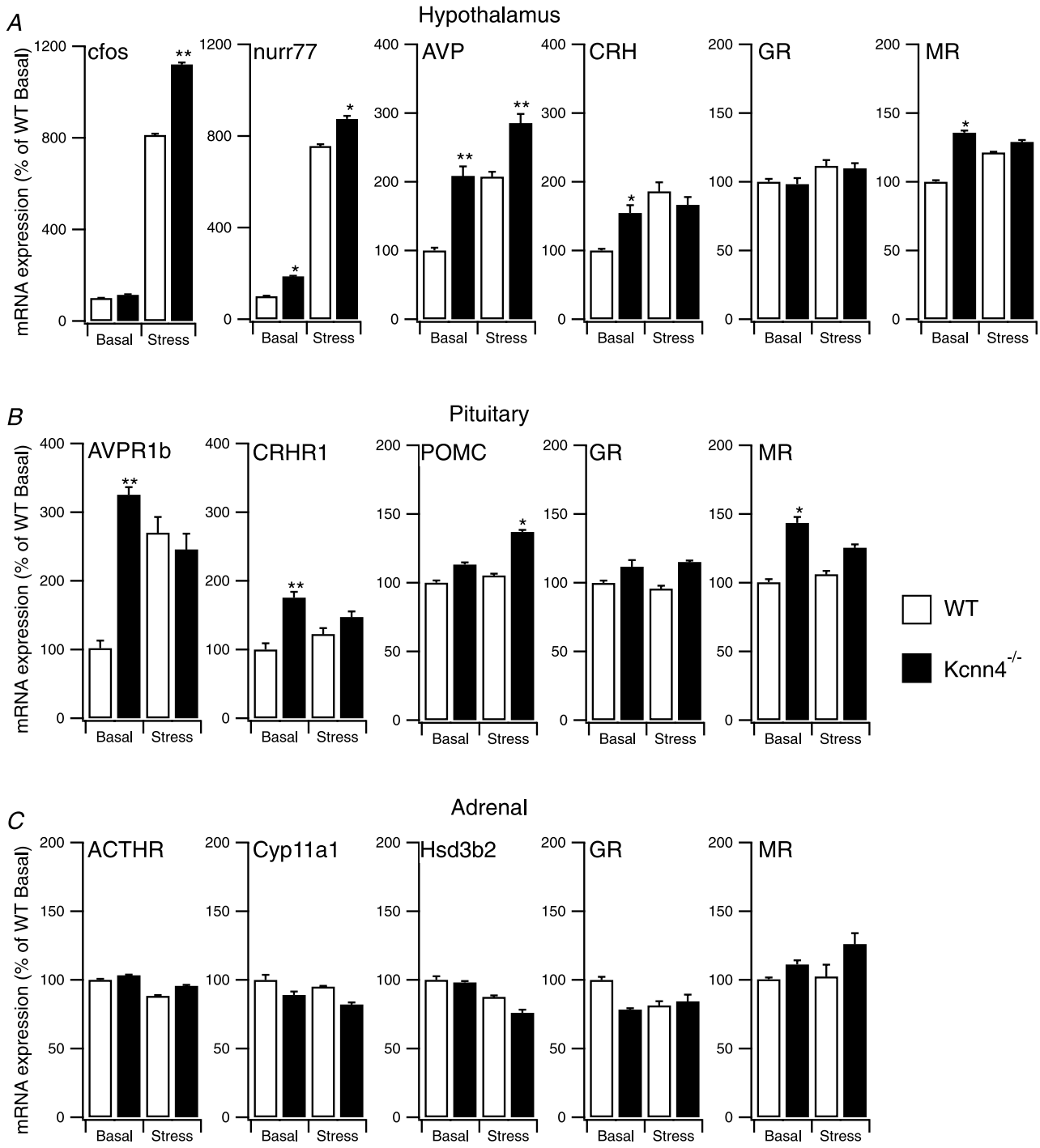

Figure 11. Enhanced hypothalamic activation and increased CRH and AVP mRNA expression in Kcnn4$^{-/-}$ mice

A–*C*, mRNA expression of selected genes in hypothalamus (*A*), anterior pituitary (*B*) or adrenal gland (*C*). mRNA expression was determined by qRT-PCR, under resting conditions (Basal) and following 30 min of restraint stress (Stress), from wild-type (WT, open bar) and SK4 knockout mice (Kcnn4$^{-/-}$, filled bar). mRNA expression was determined for: the markers of neural activation c-*fos* and *nurr*77; the peptides CRH and AVP; glucocorticoid (GR) and mineralocorticoid (MR) receptors; the G-protein coupled receptors for AVP (AVPR1b) and CRH (CRHR1); proopioiomelanocortin (POMC); the ACTH receptor (ACTHR); and the two major rate limiting enzymes in the corticosterone biosynthesis pathway, cytochrome P450 side chain cleaving enzyme (Cyp11a1) and 3-β-hydroxysteroid dehydrogenase/Δ-5–4 isomerase (Hsd3b2). Data are expressed as a percentage of the respective WT basal value (100%) with means ± SEM, $n = 7$. *$P < 0.05$ and **$P < 0.01$, Kruskal–Wallis with *post hoc* Dunnett's test compared to respective WT basal or WT restraint stress mRNA expression.

studies reveal a novel role for intermediate conductance calcium-activated potassium (SK4) channels in corticotroph function and demonstrate that mice deficient for this channel display stress hyperresponsiveness, at least in part, due to exaggerated CRH/AVP-evoked ACTH release from corticotrophs.

Specific and high efficiency labelling of murine corticotrophs

By exploiting lentiviral-mediated transduction of murine corticotrophs using eYFP driven by a minimal POMC promoter we have been able to label anterior pituitary corticotroph cells with >95% efficiency and >99% specificity without compromising corticotroph function. Perforated patch clamp recordings of labelled cells revealed that the large majority of murine corticotrophs tested displayed spontaneous electrical activity, and that frequency and patterns of spontaneous action potentials varied widely between cells. In the majority of cells, spontaneous activity was dominated by single action potential spikes. Single spikes displayed a bimodal distribution in the amplitude of the after-hyperpolarisation (AHP) following the spike. We thus classified spikes as either type A or type B where type A spikes had the larger AHP amplitude (>25 mV). In individual cells, single spikes rarely transitioned between the type A and type B phenotype. However, cells spontaneously transitioned from type A or type B spikes to more complex 'pseudo-plateau bursting modes' during recordings, reflecting spontaneous fluctuations in depolarising and hyperpolarising conductances with time. A major challenge for the future will be to determine whether such heterogeneity in corticotroph spontaneous activity exists in the intact pituitary and, more importantly, understand the relationship between different action potential firing patterns and the control of both 'basal' and stimulated ACTH secretion.

Importantly, metabolically intact murine corticotrophs used in our studies were spontaneously active and responded to physiological (low or subnanomolar) concentrations of CRH and AVP with a rapid and sustained increase in action potential firing and an associated depolarisation of the membrane potential. The vast majority of previous studies in various models have typically used CRH and/or AVP concentrations several orders of magnitude (typically 10–100 nM CRH, 20–100 nM AVP) higher than physiological levels in the portal circulation (Gibbs & Vale, 1982; Sheward & Fink, 1991).

A number of different transgenic mouse lines expressing fluorescent proteins under control of the POMC promoter, including that used in aspects of our study (Pinto *et al.* 2004), have very recently begun to be exploited to understand corticotroph regulation (Lee *et al.* 2011) and development (Budry *et al.* 2011) although the electrical or secretory properties of corticotrophs from these transgenic models have not been explored. Our lentiviral-labelling approach should complement these models and, in addition, allow rapid genetic manipulation (e.g. knockdown and/or overexpression of multiple genes) as well as interrogation of corticotrophs in other species in which transgenic models are not readily available.

A background sodium conductance controls resting membrane potential

In accordance with most previous studies in corticotrophs, inhibition of low micromolar tetrodotoxin (TTX)-sensitive voltage-dependent sodium channels had no consistent effect on generation of spontaneous action potentials (Surprenant, 1982; Kuryshev *et al.* 1997). However, replacement of extracellular Na^+ ions with the large organic cation $NMDG^+$ resulted in a robust hyperpolarisation of the cell membrane potential and cessation of spontaneous action potentials. Furthermore, a background Na^+ conductance was recorded at the potassium reversal potential, suggesting that a background Na^+ conductance is import in setting the resting membrane potential of murine corticotrophs. CRH has been reported to activate a non-selective cation current in human corticotrophs derived from both an ACTH-secreting adenoma as well as from non-adenoma tissue (Takano *et al.* 1996). This conductance was blocked by the large cation tetramethylammonium (TMA^+) but supported by lithium ions. These are characteristics shared with cAMP-activated non-selective cation conductances that also maintain a depolarised resting membrane potential of many other pituitary cell types, from both rat and mouse (Tomic *et al.* 2011). Although the molecular identity of this conductance has not been determined, recent pharmacological data support the role for members of the canonical transient receptor potential (TrpC) family of sodium and calcium permeable ion channels (Tomic *et al.* 2011). However, in human corticotrophs derived from patients with Cushing's disease (Mollard *et al.* 1987), and in the murine AtT20 corticotroph cell line (Surprenant, 1982), replacement of sodium with large organic blockers is reported to have no significant effect on resting membrane potential or electrical excitability. Whether murine corticotrophs represent a closer model to normal human corticotrophs, or whether these differences might result from distinct recording or isolation approaches, or perhaps differences in sex of corticotrophs analysed remains to be examined.

Murine and rat corticotrophs appear to differ in the contribution of inwardly rectifying potassium channels to the control of spontaneous electrical activity. While

we observed robust Ba^{2+}-sensitive inwardly rectifying conductances in female murine corticotrophs used in these studies, inhibition of these conductances with Ba^{2+} had no significant effects on spontaneous activity, unlike the effects reported in male rat corticotrophs (Kuryshev *et al.* 1997). For example, in male rat corticotrophs 100 μM Ba^{2+} depolarised the membrane potential by ∼6 mV from a mean resting membrane potential ∼−60 mV (Kuryshev *et al.* 1997). Our modelling studies suggest that the inwardly rectifying potassium conductance and non-selective sodium conductance act antagonistically to control action potential firing. The observed differences in rat *vs.* murine corticotrophs may reflect the more depolarised resting potential of the murine corticotrophs and/or differences in the relative expression or rectification properties of these channels between the two species, or sexes, of corticotroph.

Intermediate conductance calcium activated channels control corticotroph function *in vivo* and *in vitro*

Surprisingly, a large component of the outward potassium conductance of murine corticotrophs was mediated by a TRAM-34- and clotrimazole-sensitive conductance, indicative of the intermediate calcium activated potassium (SK4) channel encoded by the Kcnn4 gene. Although clotrimazole has been reported to regulate potassium conductances in other anterior pituitary cells (Wu *et al.* 1999), clotrimazole may inhibit a variety of channels. At the concentrations used here, TRAM-34 is reputed to be highly selective for SK4 channels (Wulff *et al.* 2000, 2007) (although one report has suggested effects on other conductances; Schilling & Eder, 2007). Kcnn4 mRNA was expressed at low levels relative to other Kcnn1–3 genes encoding the small conductance calcium-activated potassium channels in the anterior pituitary. However, we could detect SK4 protein expression co-localised with ACTH positive cells in the murine anterior pituitary gland. Inhibition of SK4 channels with TRAM-34 resulted in an increased frequency of action potentials in corticotrophs, although this was not associated with a significant depolarisation in resting membrane potential of the cell like that routinely observed with CRH/AVP. TRAM-34 potentiated CRH/AVP-stimulated ACTH secretion *in vitro*, and genetic deletion of functional SK4 channels resulted in enhanced stress-evoked plasma ACTH levels *in vivo*. Taken together, these data suggest that CRH/AVP does not stimulate ACTH release through inhibition of SK4 channels *per se*, even though SK4 channels are regulated for example by reversible protein phosphorylation (Gerlach *et al.* 2000). In humans, the SK4 channel inhibitor clotrimazole is widely reported to elevate plasma cortisol levels (Wojtulewski *et al.* 1980), although this may result in part from the effects of clotrimazole on cytochrome P450 enzymes. SK4 inhibitors are being developed as treatments for a range of disorders, including as potent immunosuppressants (Wulff *et al.* 2007). Clearly, if SK4 channels also play a role in controlling human corticotroph function, parallel changes in HPA-axis reactivity must be considered. Speculatively, concurrently elevated cortisol levels could contribute to the immunosuppressant effects of the drugs.

The above data clearly point to a significant role of SK4 channels in controlling corticotroph function; however we also observed changes in stress-induced hypothalamic excitability and drive. In these studies, we used restraint stress as a mixed physical and psychological stressor that activates multiple higher brain centres (Pacak & Palkovits, 2001) ultimately converging on the CRH and/or AVP expressing neurones in the paraventricular nucleus (PVN) of the hypothalamus. To examine whether the stress hyperresponsiveness of the $Kcnn4^{-/-}$ mice may also result from changes at the hypothalamic level, we examined mRNA expression for the immediate early genes c-*fos* and *nurr*77, markers for enhanced hypothalamic neuronal activation (Chan *et al.* 1993; Brunton *et al.* 2007). Restraint stress-induced c-*fos* mRNA and *nurr*77 mRNA expression were elevated in the $Kcnn4^{-/-}$ mice compared to WT controls. In addition, CRH and AVP mRNA expression in the hypothalamus were significantly elevated in $Kcnn4^{-/-}$ mice. If these translate to increases in CRH and AVP peptide content and release, they should result in an enhanced drive to the anterior pituitary corticotroph. We also observed a significant increase in CRH and AVP receptor mRNA expression in the anterior pituitary of $Kcnn4^{-/-}$ mice. POMC mRNA expression did not differ from control mice. Taken together, these data suggest that increased hypothalamic drive, as well as increased corticotroph sensitivity to CRH and AVP, may also contribute to the stress hyperresponsiveness observed in $Kcnn4^{-/-}$ mice. The enhanced activation of hypothalamic PVN CRH and AVP neurones may result from either changes in intrinsic excitability of the neurones *per se* or through changes to the afferent inputs. Intriguingly, mice deficient for BK channels show a decrease in hypothalamic CRH mRNA expression, without significant effects on *nurr*77 expression in PVN neurones. This suggests that large- and intermediate-conductance calcium activated potassium channels exert opposite effects on hypothalamic PVN function (Brunton *et al.* 2007).

The increased hypothalamic drive observed in the $Kcnn4^{-/-}$ mice might result from deletion of SK4 channels from hypothalamic PVN neurones, or their inputs, *per se*. However, the HPA axis is controlled by complex feed-forward as well as feedback mechanisms operating at multiple levels of the axis (Sapolsky *et al.* 2000). Thus, the changes in the hypothalamus could potentially be secondary, positive feedforward responses to elevations in ACTH and CORT output resulting from SK4 channel loss

from pituitary corticotrophs. In support of this, Kcnn4 mRNA in the hypothalamus (as well as whole brain) is expressed at very low levels (at least an order of magnitude lower) compared to other calcium-activated potassium channels. Moreover, as SK4 channels play a role in a wide variety of physiological processes in the CNS and in the periphery, ranging from control of T-cell and microglial activation, cell proliferation, to vasodilatation and epithelial ion transport (Kaushal *et al.* 2007; Wulff *et al.* 2007; Köhler & Ruth, 2010), a global deletion of Kcnn4 may affect other homeostatic mechanisms that influence HPA axis function and compromise allostasis (McEwen & Wingfield, 2003).

In conclusion, we have exploited a high efficiency lentiviral-mediated transduction system to allow the routine identification and first systematic analysis of the electrophysiological properties of murine corticotrophs. Our data reveal a novel role for intermediate conductance calcium-activated potassium (SK4) channels in controlling corticotroph excitability and ACTH secretion *in vitro* and *in vivo*. Furthermore, our data also suggest that SK4 channels may play additional roles in controlling stress axis function through the control of hypothalamic PVN neuronal excitability and drive.

References

Antoni FA (1986). Hypothalamic control of adrenocorticotropin secretion: advances since the discovery of 41-residue corticotropin-releasing factor. *Endocr Rev* **7**, 351–378.

Bers DM, Patton CW & Nuccitelli R (1994). A practical guide to the preparation of Ca^{2+} buffers. *Methods Cell Biol* **40**, 3–29.

Brunton PJ, Sausbier M, Wietzorrek G, Sausbier U, Knaus H-G, Russell JA, Ruth P & Shipston MJ (2007). Hypothalamic-pituitary-adrenal axis hyporesponsiveness to restraint stress in mice deficient for large-conductance calcium- and voltage-activated potassium (BK) channels. *Endocrinology* **148**, 5496–5506.

Budry L, Lafont C, el Yandouzi T, Chauvet N, Conejero G, Drouin J & Mollard P (2011) Related pituitary cell lineages develop into interdigitted 3D cell networks. *Proc Natl Acad Sci U S A* 108, 12515–12520

Bustin SA, Benes V, Garson JA, Hellemans J, Huggett J, Kubista M, Mueller R, Nolan T, Pfaffl MW, Shipley GL, Vandesompele J & Wittwer CT (2009). The MIQE guidelines: minimum information for publication of quantitative real-time PCR experiments. *Clin Chem* **55**, 611–622.

Chan RKW, Brown ER, Ericsson A, Kovacs KJ & Sawchenko PE (1993). A comparison of 2 immediate-early genes, C-Fos and Ngfi-B, as markers for functional activation in stress-related neuroendocrine circuitry. *J Neurosci* **13**, 5126–5138.

Childs GV, Marchetti C & Brown AM (1987). Involvement of sodium channels and two types of calcium channels in the regulation of adrenocorticotropin release. *Endocrinology* **120**, 2059–2069.

Dallman MF, Akana SF, Cascio CS, Darlington DN, Jacobson L & Levin N (1987). Regulation of ACTH secretion: variations on a theme of B. *Rec Prog Hormo Res* **43**, 113–173.

Gerlach AC, Gangopadhyay NN & Devor DC (2000). Kinase-dependent regulation of the intermediate conductance, calcium-dependent potassium channel, hIK1. *J Biol Chem* **275**, 585–598.

Gibbs DM & Vale W (1982). Presence of corticotropin releasing factor-like immunoreactivity in hypophysial portal blood. *Endocrinology* **111**, 1418–1420.

Hammer GD, Fairchild-Huntress V & Low MJ (1990). Pituitary-specific and hormonally regulated gene expression directed by the rat proopiomelanocortin promoter in transgenic mice. *Mol Endocrinol* **4**, 1689–1697.

Hodgkinson SC, Allolio B, Landon J & Lowry PJ (1984). Development of a non-extracted 2-site immunoradiometric assay for corticotropin utilizing extreme amino-terminally and carboxy-terminally directed antibodies. *Biochem J* **218**, 703–711.

Kaushal V, Koeberle PD, Wang Y & Schlichter LC (2007). The Ca^{2+}-activated K^+ channel KCNN4/KCa3.1 contributes to microglia activation and nitric oxide-dependent neurodegeneration. *J Neurosci* **27**, 234–244.

Keith LD, Winslow JR & Reynolds RW (1978). A general procedure for estimation of corticosteroid response in individual rats. *Steroids* **31**, 523–531.

Köhler R & Ruth P (2010). Endothelial dysfunction and blood pressure alterations in K^+-channel transgenic mice. *Pflugers Arch* ***459****, 969–976.*

Kuryshev YA, Haak L, Childs GV & Ritchie AK (1997). Corticotropin releasing hormone inhibits an inwardly rectifying potassium current in rat corticotropes. *J Physiol* **502**, 265–279.

LeBeau AP, Robson AB, McKinnon AE, Donald RA & Sneyd J (1997). Generation of action potentials in a mathematical model of corticotrophs. *Biophys J* **73**, 1263–1275.

Lee AK, Smart JL, Rubinstein M, Low MJ & Tse A (2011). Reciprocal regulation of TREK-1 channels by arachidonic acid and CRH in mouse corticotropes. *Endocrinology* **152**, 1901–1910.

Lee AK & Tse A (1997). Mechanism underlying corticotropin-releasing hormone (CRH) triggered cytosolic Ca^{2+} rise in identified rat corticotrophs. *J Physiol* **504**, 367–378.

Livak KJ & Schmittgen TD (2001). Analysis of relative gene expression data using real-time quantitative PCR and the $2^{-\Delta\Delta CT}$ method. *Methods* **25**, 402–408.

McEwen BS & Wingfield JC (2003). The concept of allostasis in biology and biomedicine. *Horm Behav* **43**, 2–15.

Mollard P, Vacher P, Guerin J, Rogawski MA & Dufy B (1987). Electrical properties of cultured human adrenocorticotropin-secreting adenoma cells: effects of high K^+, corticotropin-releasing factor, and angiotensin II. *Endocrinology* **121**, 395–405.

Pacak K & Palkovits M (2001). Stressor specificity of central neuroendocrine responses: Implications for stress-related disorders. *Endocr Rev* **22**, 502–548.

Pennington AJ, Kelly JS & Antoni FA (1994). Selective enhancement of an A type potassium current by dexamethasone in a corticotroph cell line. *J Neuroendocrinol* **6**, 305–315.

Pinto S, Roseberry AG, Liu H, Diano S, Shanabrough M, Cai X, Friedman JM & Horvath TL (2004). Rapid rewiring of arcuate nucleus feeding circuits by leptin. *Science* **304**, 110–115.

Ritchie AK, Kuryshev YA & Childs GV (1996). Corticotropin-releasing hormone and calcium signaling in corticotropes. *Trends Endocrinol Metab* **7**, 365–369.

Sapolsky RM, Romero LM & Munck AU (2000). How do glucocorticoids influence stress responses? Integrating permissive, suppressive, stimulatory and preparative actions. *Endocr Rev* **21**, 55–89

Sausbier M, Matos JE, Sausbier U, Beranek G, Arntz C, Neuhuber W, Ruth P & Leipziger J (2006). Distal colonic K^+ secretion occurs via BK channels. *J Am Soc Nephrol* **17**, 1275–1282.

Schilling T & Eder C (2007). TRAM-34 inhibits nonselective cation channels. *Pflugers Arch* **454**, 559–563.

Sheward WJ & Fink G (1991). Effects of corticosterone on the secretion of corticotrophin-releasing factor, arginine vasopressin and oxytocin into hypophysial portal blood in long-term hypophysectomized rats. *J Endocrinol* **129**, 91–98.

Shipston MJ, Kelly JS & Antoni FA (1996). Glucocorticoids block protein kinase a inhibition of calcium-activated potassium channels. *J Biol Chem* **271**, 9197–9200.

Shorten PR, Robson AB, McKinnon AE & Wall DJ (2000). CRH-induced electrical activity and calcium signalling in pituitary corticotrophs. *J Theor Biol* **206**, 395–405.

Simasko SM (1994). A background sodium conductance is necessary for spontaneous depolarizations in rat pituitary cell line GH3. *Am J Physiol Cell Physiol* **266**, C709–C719.

Stojilkovic SS, Tabak J & Bertram R (2010). Ion channels and signaling in the pituitary gland. *Endocr Rev* **31**, 845–915.

Surprenant A (1982). Correlation between electrical activity and ACTH/β-endorphin secretion in mouse pituitary tumor cells. *J Cell Biol* **95**, 559–566.

Tabak J, Toporikova N, Freeman ME & Bertram R (2007). Low dose of dopamine may stimulate prolactin secretion by increasing fast potassium currents. *J Comput Neurosci* **22**, 211–222.

Takano K, Yasufuku-Takano J, Teramoto A & Fujita T (1996). Corticotropin-releasing hormone excites adrenocorticotropin-secreting human pituitary adenoma cells by activating a nonselective cation current. *J Clin Invest* **98**, 2033–2041.

Tomic M, Kucka M, Kretshmannova K, Li S, Nesterova M, Stratakis CA & Stojilkovic SS (2011). Role of non-selective cation channels in spontaneous and protein kinase A stimulated calcium signalling in pituitary cells. *Am J Physiol Endocrinol Metab* **301**, E370–379.

Tsaneva-Atanasova K, Sherman A, van Goor F & Stojilkovic SS (2007). Mechanism of spontaneous and receptor-controlled electrical activity in pituitary somatotrophs: experiments and theory. *J Neurophysiol* **98**, 131–144.

Tse A & Lee AK (1998). Arginine vasopressin triggers intracellular calcium release, a calcium-activated potassium current and exocytosis in identified rat corticotropes. *Endocrinology* **139**, 2246–2252.

Wojtulewski JA, Gow PJ, Walter J, Grahame R, Gibson T, Panayi GS & Mason J (1980). Clotrimazole in rheumatoid arthritis. *Ann Rheum Dis* **39**, 469–472.

Wu S-N, Li HF, Jan CR & Shen AY (1999). Inhibition of Ca^{2+}-activated K^+ current by clotrimazole in rat anterior pituitary GH3 cells. *Neuropharmacology* **38**, 979–989.

Wulff H, Kolski-Andreaco A, Sankaranarayanan A, Sabatier J-M & Shakkottai V (2007). Modulators of small- and intermediate-conductance calcium-activated potassium channels and their therapeutic indications. *Curr Med Chem* **14**, 1437–1457.

Wulff H, Miller MJ, Hansel W, Grissmer S, Cahalan MD & Chandy KG (2000). Design of a potent and selective inhibitor of the intermediate-conductance Ca^{2+}-activated K^+ channel, IKCa1: a potential immunosuppressant. *Proc Natl Acad Sci U S A* **97**, 8151–8156.

Yuan JS, Reed A, Chen F & Stewart CN (2006). Statistical analysis of real-time PCR data. *BMC Bioinformatics* **7**, 85.

Author contributions

Z.L. performed and analysed the majority of voltage- and current-clamp electrophysiological recordings; L.C. developed and validated the lentiviral pomc-eYFP reporters; H.McC., performed and analysed the qRT-PCR experiments; D.MacG., developed the corticotroph H-H model; D.McC. and J.K. performed and analysed electrophysiological recordings and pharmacological analysis; R.L. and M.J.S. conducted the *in vivo* stress experiments; S.R. and H.G.K performed the immuno-histochemical analysis of SK4 protein expression; M.S. and P.R. generated the Kcnn4 knockout mice; M.J.S. conceived the study, analysed and interpreted results and wrote the manuscript. All authors contributed to critical review and revision of the final manuscript.

Acknowledgements

We are grateful to Prof. M. Low for the generous gift of the minimal rat pomc promoter construct; Prof. J. Friedman for the Pomc-GFP expressing mice line; Prof. D. Trono for the psPAX2 packing plasmid, and to Dr Trudi Gillespie in the IMPACT imaging facility, Centre for Integrative Physiology for assistance in fluorescence and confocal microscopy. We thank Clement Kabagema-Bilan for technical assistance in animal maintenance and *in vivo* assays. The work was supported by a Wellcome Trust programme grant to H.G.K., P.R. and M.J.S. Z.L. was in receipt of a China PhD scholarship.